A THESIS SUBMITTED FOR THE DEGREE

DOCTOR OF PHILOSOPHY IN

MOLECULAR SCIENCES

QUANTUM YIELDS AND TRANSIENT SPECIES

IN THE PHOTOCHEMICAL DECOMPOSITION

OF ARENEDIAZONIUM SALTS

By

DAVID ROBERT PAYNE

To the best of my knowledge the work submitted

in this thesis is entirely original

(September, 1978)

To my parents Betty and Robert

ABSTRACT:

The structure of 4-morpholinobenzenediazonium tetra-
fluoroborate has been determined by X-ray crystallography.
Interatomic distances and angles in the ring indicate
considerable distortion when compared with that in the
$C_6H_5N_2^+$ ion. The distribution of π electrons closely
resembles that of similarly substituted nitrobenzenes. An
electronic ground state considerably quinoidal in character
has been proposed to explain these observations.

Photodecomposition quantum yields for simple meta-
and para-substituted arenediazonium salts and a large
number of commercially important ones (mostly 2,5-dialkoxy
derivatives with a 4-morpholino or 4-tolylthio group) have
been determined in 0.05 mol dm^{-3} sulphuric acid, ethanol
(0.05 mol dm^{-3} in sulphuric acid) and in a cellulose acetate
film. Determinations were made at 293 K using monochromatic
light of wavelength 313, 380, 401 and 439 nm. Where possible
attempts have been made to correlate the observed quantum
yield with the electronic effects of substituent groups on
the benzene ring. Quantum yields for simple meta- and para-
substituted arenediazonium salts determined in solution can
be correlated with appropriate Hammett σ constant. A series
of arenediazonium salts all gave $\phi \sim 0.32$ when determined
in a cellulose acetate film.

Photodecomposition in aqueous acid proceeds exclusively
by carbonium ion formation while in ethanol both this

mechanism and a radical chain reaction operate in parallel. In solution, the radical pathway can be suppressed by the addition of oxygen and acid to the medium. Complexation of arenediazonium salts with 18-crown-6 retards thermal and photodecomposition.

Electron spin resonance spectra of irradiated arenediazonium salts ($\lambda > 300$ nm) in cellulose acetate film (and certain other media) at 77 K display signals corresponding to aryl radicals and hydrogen atoms. Additionally, arenediazonium salts containing a para-dialkylamino group give three broad signals at ca. 80 ca. 150 and ca. 440 mT, and the species responsible has been assigned to the aryl cation, Ar^+. The preferred electronic configuration of para-dialkyamino aryl cations is that of a ground state triplet i.e. $(\pi)^5(sp^2)^1$.

Attempts to record the ultra-violet/visible spectra of aryl cations by matrix isolation and laser flash photolysis have been unsuccessful.

The majority of the work described in this thesis has reached the stage of publication, viz

(i) Electron Spin Resonance of Ground-state Triplet
    Aryl Cations in the Photolysis of Substituted
    Arenediazonium Salts at 77 K
    by
    A. Cox, T.J. Kemp, D.R.Payne, M.C.R.Symons, D.M.Allen
    and P.Pinot de Moira, J.C.S. Chem.Comm.,(1976)p.693,

(ii) The Photolysis of Arenediazonium Salts in Solutions

and Films: Quantum Efficiencies and Reactive

Intermediates

by

A.Cox, T.J.Kemp, D.R.Payne and P.Pinot de Moira

J. Photo. Sci., (1977), 25, 208

(iii)Electron Spin Resonance of Ground State Triplet

Aryl Cations Substituted at the 4-position by

Dialkylamino Groups

by

A.Cox, T.J.Kemp, D.R.Payne, M.C.R.Symons and

P.Pinot de Moira accepted by J.Amer.Chem.Soc.

for publication

(iv) A Crystallographic Examination of the Ring-Bonding

in a 4-dialkylaminobenzenediazonium Cation

by

N.W.Alcock, T.Greenough, D.M.Hirst, T.J.Kemp and

D.R.Payne in progress.

ACKNOWLEDGEMENTS

CONTENTS

CHAPTER I

INTRODUCTION

1.1. HISTORICAL BACKGROUND TO ARENEDIAZONIUM SALTS

Few chemists attempt to isolate arenediazonium salts from the acidic solutions in which they have been prepared because of their unpredictable and potentially explosive nature when dried and handled in the crystalline state. However, careful matching (as regards size and redox behaviour) of suitable anions with the diazonium cation enables many arenediazonium salts to be precipitated and handled with comparative ease provided that precautions are taken against detonation by shock.

Arenediazonium salts have been widely used as intermediates in organic synthesis by virtue of the ready and specific replacement of the $-N_2^+$ moiety. Economically they are essential to the dyeline process being the basic component of a very inexpensive and extremely reliable reprographic method.

Griess[1] prepared the first arenediazonium salts by passing nitrous fumes into a solution of picramic acid. Griess inadvertently discovered the route to arenediazonium salts whilst trying to convert the amino group of picramic acid to a hydroxyl one. His supposition that the alcoholic, rather than an aqueous medium, was important in deriving the new class of compounds was without foundation; nevertheless suitable conditions for the diazotisation reaction had been found. The almost quantitative conversion of many aromatic amines to arenediazonium salts probably accounts for Griess' thoroughness in characterising the diazotisation reaction.

1.2. ELECTROPHILIC AROMATIC SUBSTITUTION REACTIONS OF ARENEDIAZONIUM SALTS

Arenediazonium salts are well known as electrophilic reagents, forming azo compounds with aromatic amines and phenols, the addition being described as diazo or azo coupling. Commercially, azo compounds are of considerable importance since many of them are brightly coloured, and consequently they are employed as dyes in the textile industry and imaging agents in reprographic systems.

Simple azo compounds like 4-aminoazobenzene (a basic dye formed from aniline) and 4-hydroxyazobenzene (an acidic dye formed from phenol) are of little economic importance. Structurally more complex azo dyes like Bismark Brown (a tetra-azo compound made by the action of nitrous acid on meta-phenylene diamine) and Chrysoidine (a diazonium salt coupled to meta-phenylene diamine) are still manufactured in large quantities for the dyeing of paper and leather.

The mechanism of the coupling reaction has been derived mainly from kinetic evidence. Rates of reaction have been determined by following the decrease of the arenediazonium salt concentration (by polarography[2]) or by monitoring the formation of azo dye (by colorimetry[3]). Kinetically the rate is given by

$$\frac{d(Az)}{dt} = k(D)(C) \tag{1}$$

where

Az = concentration of azo dye

D = arenediazonium salt

C = coupling component

k = rate constant

The rate of coupling is dependent on pH, most of the reactions having an optimum pH.[2] Substituent groups[4] also affect the rate of coupling and their effect may be readily interpreted within the context of normal Hammett σ relationships.

1.3. STRUCTURAL ASPECTS OF ARENEDIAZONIUM SALTS

Benzenediazonium salts are typically represented by structure (I) with the positive charge located on the α nitrogen atom (II).

$$Ar-N_2^+X^-$$

(I)

$$Ar-\overset{+}{N} \equiv NX^-$$

(II)
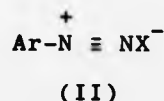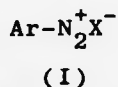
where X^- is any one of a large number of anions such as (i) BF_4^- and PF_6^- (for organic solvent-soluble diazonium salts) and (ii) Cl^-, HSO_4^-, $ZnCl_4^{2-}$ and $HgCl_4^{2-}$ (for water-soluble diazonium salts).

X-ray diffraction analysis of benzenediazonium chloride crystals has shown that the anion is at a distance of 3.5Å[5] from the N_2^+ group and slightly closer to the terminal nitrogen atom, which suggests that both nitrogen atoms bear some of the positive charge[6] (Fig. 1). The effective radii of the anion

Figure (1)

Schematic representation of the benzenediazonium chloride crystal lattice according to X-ray diffraction data.
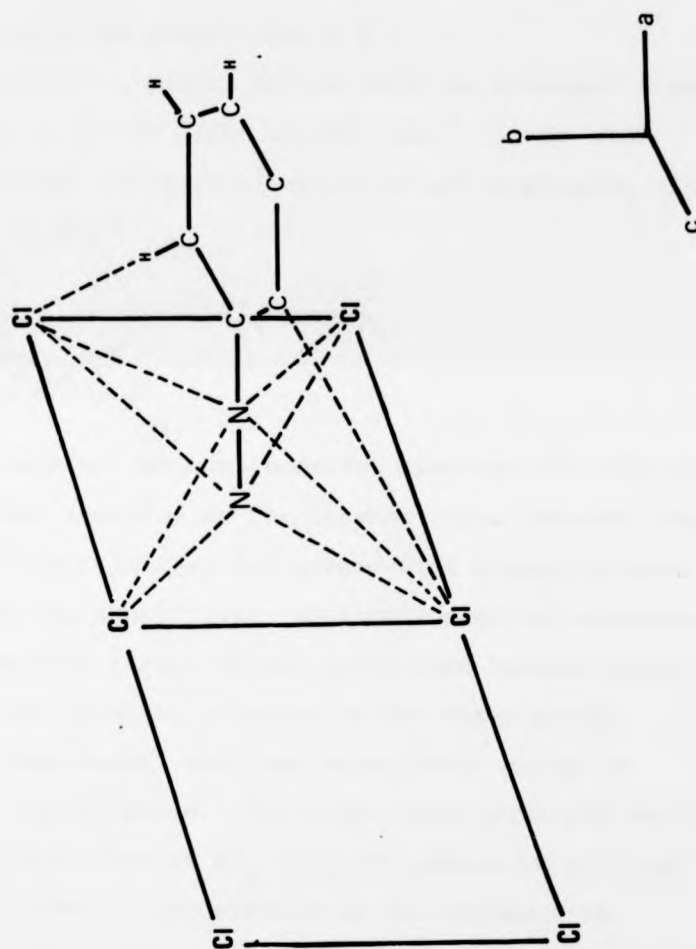
and the two nitrogen atoms slightly overlap, but this is sufficient to allow some degree of covalency in the $N---X^-$ bond whilst remaining essentially ionic in nature to an extent dependent upon the properties of X^-.

The carbon ring is a planar system with the nitrogen atoms linearly distributed in the plane of the ring.[7] It is also subject to some slight distortion[8] which is not surprising
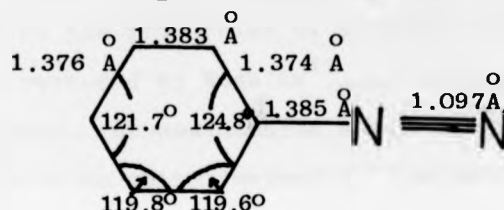
(II)

since it contains one of the most powerful electron withdrawing groups known[9]), when compared to the unsubstituted benzene ring. Simple Hückel MO[10] calculations for substituted arenediazonium salts suggest that the substitution of strong electron-donating groups has a pronounced effect on the total bond length between the α carbon and the terminal nitrogen of the diazo group.

Nmr studies have shown[6] that any substituent group is always a donor to the N_2^+ group. The electron-withdrawing ability of N_2^+ is roughly twice that of NO_2 (with σ values of 1.91 and 0.78 respectively);this is illustrated by the decrease in π-electron density at carbon atoms ortho to the diazo group in the following compound:

(III)
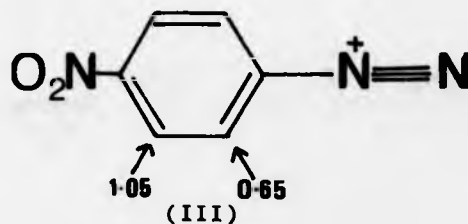
Of the three bonds between the two sp-hybridised nitrogen
atoms, one π-bond effectively overlaps with the π-orbital of
the aromatic ring. As a result, the aromatic ring is conjugated
both with any other substituents and with the terminal nitrogen
atom.

Many of the properties of arenediazonium salts in solution
have been reviewed by Koshits[11] and only a brief outline is
intended here. Arenediazonium salts of strong acids are generally
considered to be fully ionised at concentrations $> 10^{-4}$ mol dm^{-3},[12]
whilst those of weak acids usually convert to covalent forms (IV)
and (V), but can be regenerated by the addition of strong acid.

$$C_6H_5\overset{+}{N}\equiv N:CN^- \underset{H^+}{\overset{OH^-}{\rightleftharpoons}} \quad C_6H_5\underset{\cdot\cdot}{N}=\underset{\cdot\cdot}{N}^{CN} + C_6H_5\underset{\cdot\cdot}{N}=\underset{\cdot\cdot}{N}_{CN} \tag{2}$$

$$(IV) \qquad\qquad (V)$$
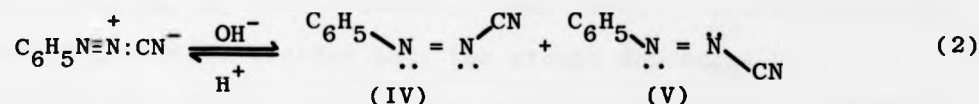
The covalent forms are sometimes significant in the reactions of
diazonium salts, since they offer a convenient pathway for the
formation of free radicals, e.g.

$$C_6H_5-N=N-CN \longrightarrow C_6H_5\cdot + N_2 + \cdot CN \tag{3}$$
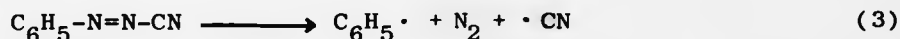
Hydroxide ion also adds reversibly to form covalent diazonium
compounds, e.g. the benzenediazonium cation gives benzenediazotic
acid (VI).

$$C_6H_5\overset{+}{N}\equiv N+O\overline{H} \underset{H_3O^+}{\rightleftharpoons} \quad C_6H_5\underset{\cdot\cdot}{N}=\underset{\cdot\cdot}{N}^{OH} + C_6H_5\underset{\cdot\cdot}{N}=\overset{\cdot}{N}_{OH} \tag{4}$$

$$(VI)$$
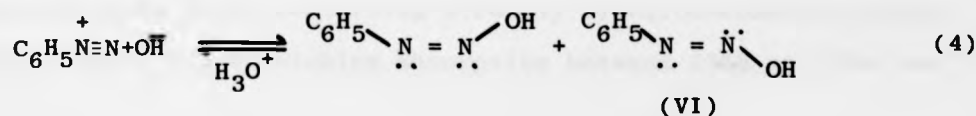
The diazotic acids are unstable in neutral or acid solution with respect to the parent diazonium salt, but in basic solution they form stable diazotate salts.

$$C_6H_5N=N-OH_4 + NaOH \rightarrow [C_6H_5N \text{---} N \text{---} O]^- Na^+ + H_2O \qquad (5)$$

1.4. INFRA-RED SPECTRAL ANALYSIS OF ARENEDIAZONIUM SALTS (INCLUDING A CRITIQUE OF CURRENT IDEAS)

The infra-red spectra of arenediazonium cations exhibit two major absorption bands associated with the presence of a N_2^+ group, viz. one at 1300-1400 cm^{-1} arising from aryl C-N stretching, and the other at 2155-2305 cm^{-1} due to N ≡ N stretching,[13,14] the latter band having been studied in some detail. N ≡ N stretching frequencies can be divided into two groups depending upon the nature of the substituent present in the benzene ring. Electron-withdrawing and weakly electron-donating groups (νN ≡ N 2305-2240 cm^{-1}) have a slight effect on the two triple-bonded nitrogen atoms, such that the ground state of the salt is best represented as a resonance hybrid of structures (VII) and (VIII).

(VII)   (VIII)
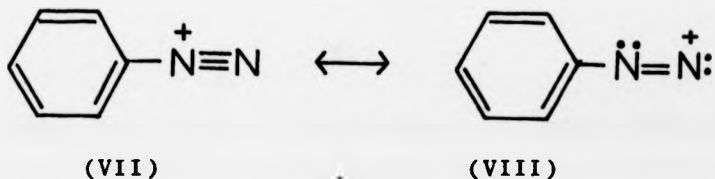
Arenediazonium salts containing strongly electron-donating groups display the N ≡ N stretching absorption between 2155 and 2240 cm^{-1}.

The pronounced shift to longer wavelengths indicates a much larger contribution of structures (IX) and (X) to the hybrid.

$$X-\langle \rangle = \overset{+}{N} = \bar{N} \quad \longleftrightarrow \quad \overset{+}{X} = \langle \rangle = \overset{+}{N} = \overset{..}{\underset{..}{N}} : \qquad (7)$$

(IX)   (X)
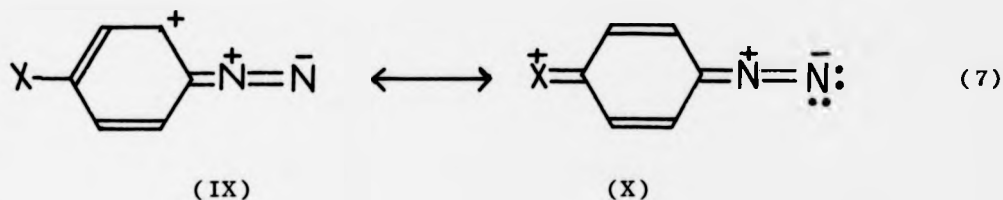
Recently Tabei and Ito[15] have claimed some correlation between Hammett σ values for the substituents involved with both ν(C-N) *and* ν(N≡N)[16] but the validity of the relationship they derived is doubtful. Thus, they noted a break in this linear correlation with those examples involving strongly electron-donating groups, which they ascribed to the contribution of (XI) to the hybrid.

$$: \bar{X} = \langle \rangle = \overset{+}{N} = \overset{+}{N} :$$

(XI)
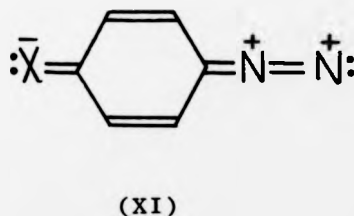
In an attempt to clarify the situation, we have collected similar data[17,6] (Fig. 2) for comparison. Our findings substantiate those of Tabei and Ito. In addition, the perturbing effect of the counter-ion cannot be ignored in agreement with the views of Koshits.[6] From inspection of Fig. 2, it is clearly evident that the data for $HgCl_2$ and Cl^- salts refer to two distinct situations.

Figure (2)

Plot of diazonium group stretching frequency
(ν N≡N) against Hammett σ constant for the
corresponding para-substituent

  ● data of Porai Koshits[6] (as chloride salt)

  ✳ data of Tabei and Ito[15] (as mercurous

                                chloride salt)

  ⊕ data of Kazitsyna et al.[17] (as chloride

                                salt)

  ⊙ data of Kazitsyna et al.[17] (as mercurous

                                chloride salt)
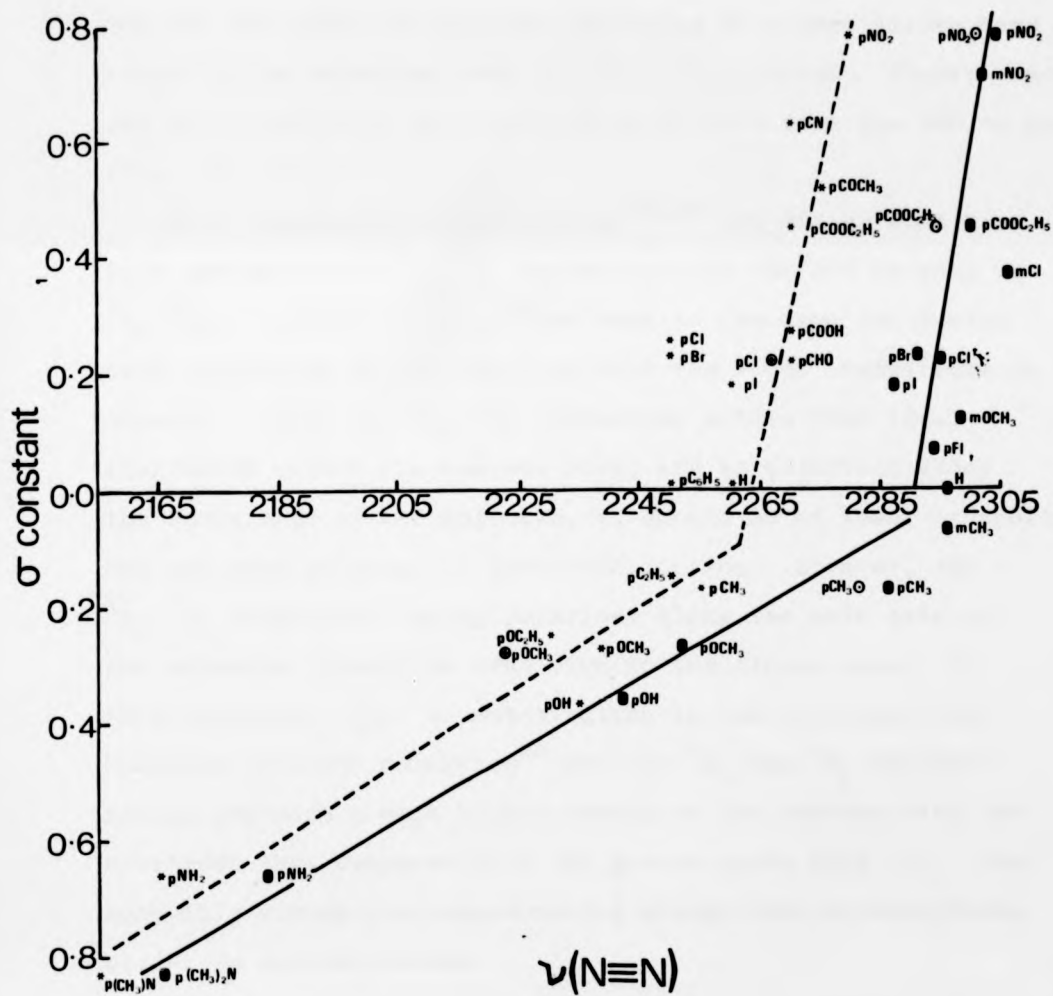
1.5   ULTRA-VIOLET SPECTRA OF ARENEDIAZONIUM SALTS

The ultra-violet spectrum of the benzenediazonium cation shows a strong absorbtion band at 263 nm with a shoulder at ca. 300 nm, and there is also the beginning of a very strong band below 220 nm extending into the far ultra-violet. Fluorescence[18] and phosphorescence have been observed only from the 300 nm band (Fig. 3).

From theoretical calculations,[16,19] the 263 nm band has been assigned to a $^1A_1-^1A_1$ transition and the 300 nm band to $^1A_1-^1B_1$. Schulte-Frohlinde[65] has come to the same conclusion from comparison of the spectrum with the known transitions in styrene. Since the $^1A_1-^1B_1$ transition arises from local excitation within the benzene ring, and is polarised along the short axis of the molecule, it should be of lower intensity and not much affected by para-substitution. However, the $^1A_1-^1A_1$ transition, being polarised along the main axis of the molecule, should be sensitive to the dipole moment in this direction, i.e. to substitution in the para-position. Computed electron densities[20] for the $^1A_1$ and $^1B_1$ excited states indicate a much higher demand on the benzene ring for electrons when compared with the ground state (Fig. 4). Consequently strong electron-donating groups have a stabilising effect on excited states.

Figure (3)

Jablonski diagram for benzenediazoniom

tetrafluoroborate
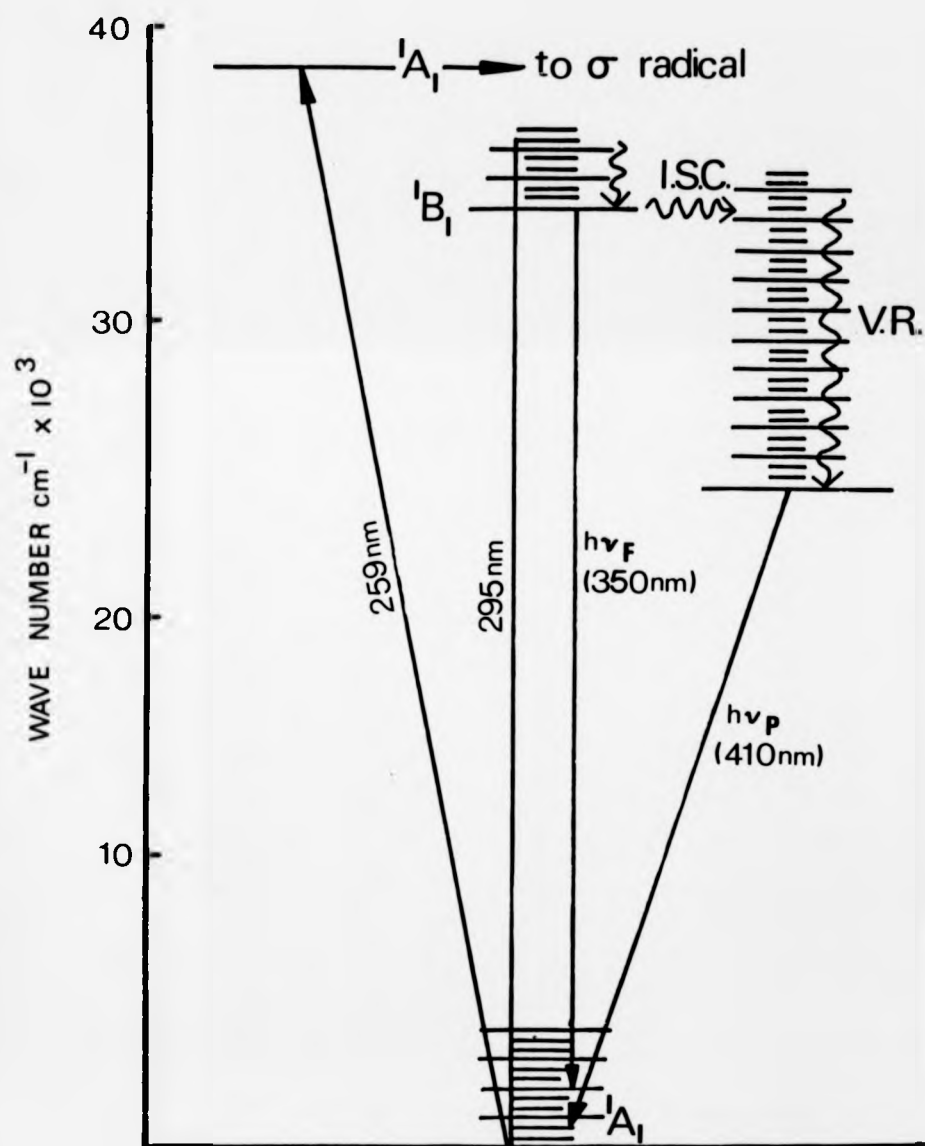
Figure (4)

Charge densities in the benzenediazonium cation
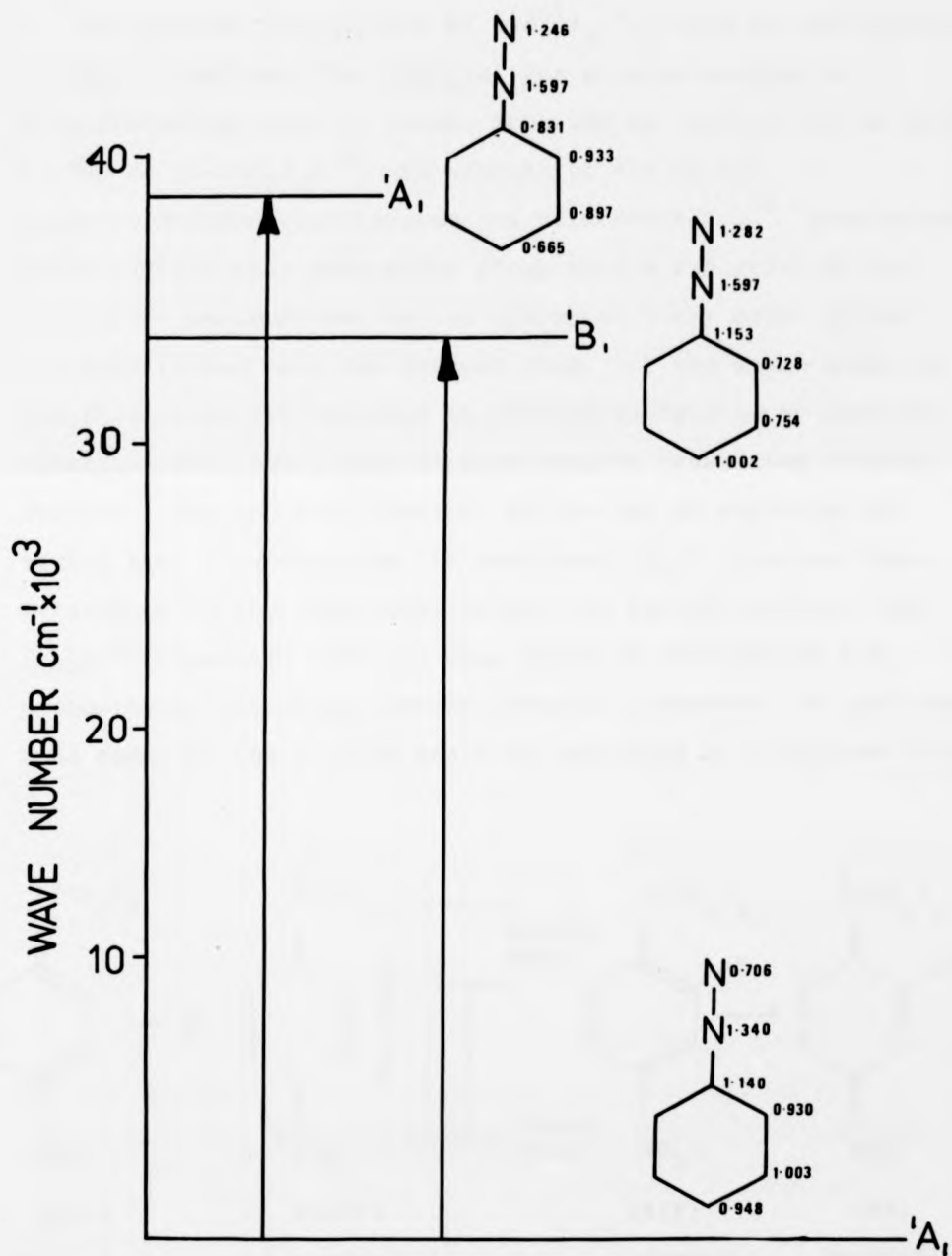
The extreme sensitivity of the $^1A_1$-$^1A_1$ band to substitution is clearly evident; for example, for a cross-section of arenediazonium salts it ranges from 260 nm (p-NO$_2$) 313 nm (p-OCH$_3$) to 380 nm [p-(CH$_3$)$_2$N][21] and extends to 434 nm for 2-pyrrolidinobenzenediazonium tetrafluoroborate.[22] Arenediazonium salts containing a para-amino group show a red shift in the absorption maximum when either alkoxy or bulky alkyl groups are substituted into the benzene ring. If the amino group of 4-N,N- dimethylnitrobenzene is sterically twisted by similar substitutions, the lowest singlet-singlet transition is blue shifted. The opposing spectral shifts may be explained by taking into consideration the contribution of quinoidal type structures to the respective ground and excited states. Cox et.al.[23] suggested that the blue shift of substituted 4-N, N-dimethylnitrobenzenes arises from the increased C-N (aryl-amino) bond order in the excited state as indicated by structure (XIII)

| (XII) | (XIII) | (XIV) | (XV) |
| Ground state | Excited state | Ground state | Excited state |
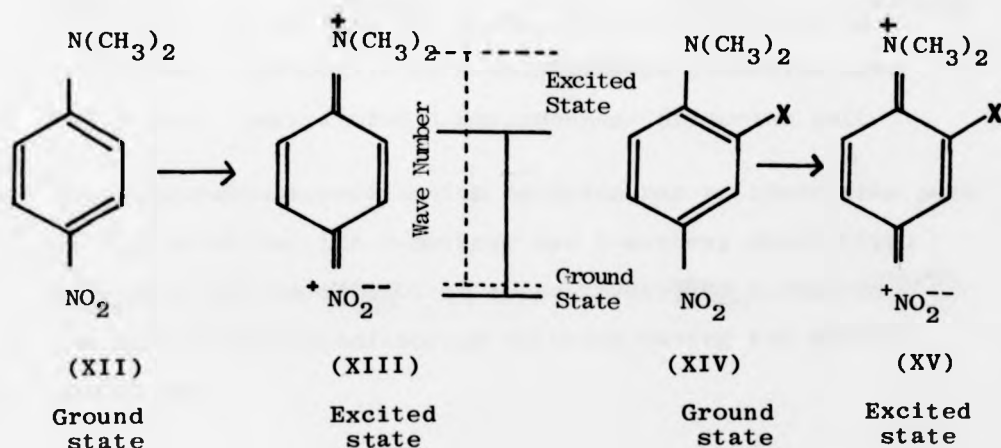
———X   equivalent to bulky alkyl or alkoxy group

————   unsubstituted 4-N, N -dimethylnitrobenzene

--------   substituted 4-N,N -dimethylnitrobenzene

Similarly the red shift observed in the substituted para-aminoarenediazonium salts suggests that their ground state is essentially quinoidal as indicated by structure (XVI)

(XVI)   (XVII)   (XVIII)   (XIX)

Ground state   Excited State   Ground state   Excited state
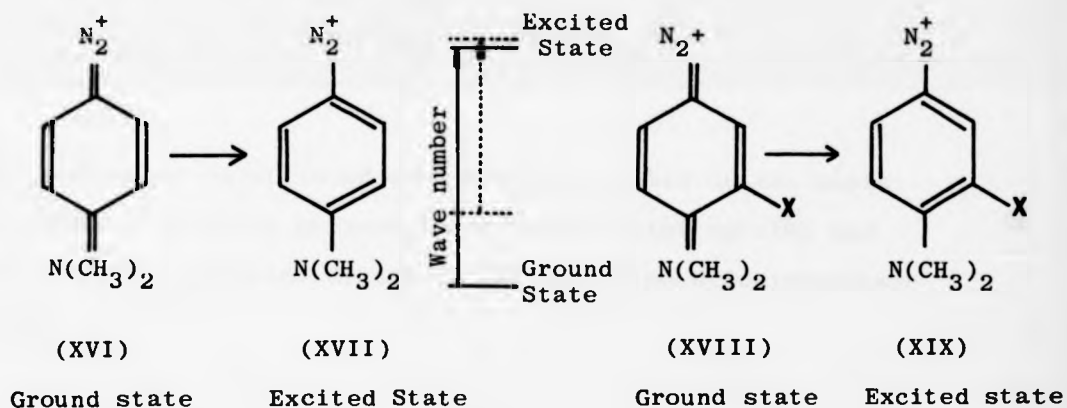
———X   equivalent to bulky alkyl or alkoxy group

————   unsubstituted 4-aminobenzene diazonium salt

---------   substituted 4-aminobenzene diazonium salt

4-morpholinobenzenediazonium chloride has an absorption peak at 380 nm whilst its 2-methoxy and 3-methoxy derivatives absorb at 365 nm and 407 nm respectively, 2,5-dimethoxy-4-morpholinobenzenediazonium chloride having its maximum at 397 nm.

Anderson and Steedly[24] have also proposed quinoidal structures of the type

(XX)
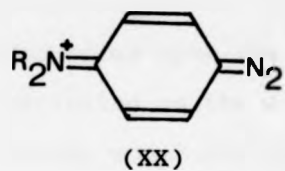
for para-amino substituted arenediazonium salts on the basis of marked similarity between their ultra-violet spectra and those of para-phenylenediazoime (XXI) and diphenylquinomethane (XXII).

(XXI)

(XXII)
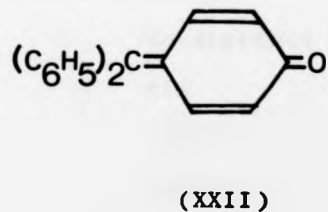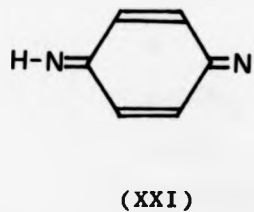
1.6. THERMOLYSIS OF ARENEDIAZONIUM SALTS

There are many similarities in the thermal and photochemical decomposition of arenediazonium salts: in particular, they both proceed either by an ionic or a radical mechanism (or both simultaneously) depending upon the reaction conditions. Previous research has concentrated on the thermal reaction and, since this provides a useful model for the photochemical reaction, a survey of the former follows.

Probably the most well-known property of arenediazonium salts is their thermal instability and some typical decomposition temperatures[6] are given below.

benzenediazonium salt	dec. T (^{O}C)
p-NO_2	98
p-Cl	120-121
H	no distinct dp
p-OCH_3	119
p-NH_2	157-159
p-$(CH_3)_2$N	146-148

As a general rule, the more thermally stable a particular diazonium salt (according to its decomposition temperature), the more it is photo-labile. Thermolysis of dry arenediazonium salts usually results in decomposition with some portion of the stabilising anion being substituted into the benzene ring. The Schiemann[25] reaction is a classical example and provides a useful route to fluoro-compounds, e.g.

$$Ar - N_2^+BF_4 \longrightarrow ArF + N_2 + BF_3 \qquad (8)$$
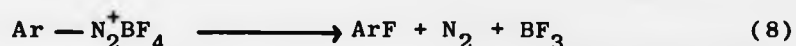
which may be inaccessible by alternative pathways.

Gremillion et.al.[26] have examined the stabilising effect of a large number of MCl_x^{n-} counter ions. Their findings indicate increased stability according to the metal present in the following order.

$$Fe < Sb < Bi < Hg < Sn \propto Zn < Cd$$

Waters[27] and colleagues have suggested a radical mechanism for the thermal decomposition of arenediazonium salts in solution, based on product analysis, whilst Hodgson[28,29] strongly refuted the formation of free radicals in proposing his scheme for the Sandmeyer reaction. Current evidence indicates that the thermal decomposition includes both ionic and radical pathways, depending upon reaction conditions. Heterolysis of arenediazonium cations gives rise to an arylcation[30]

$$Ar - N_2^+ \longrightarrow Ar^+ + N_2 \qquad (9)$$
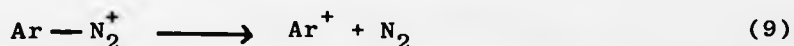
and nitrogen gas, whilst the homolytic cleavage of arenediazonium salts

$$Ar - N_2^+X^- \longrightarrow Ar^{\cdot} + N_2 + {}^{\cdot}X \qquad (10)$$
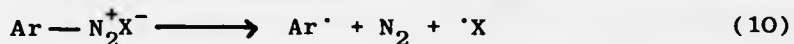
gives two neutral radicals. Evidence for the intermediacy of a phenyl cation in the thermolysis of arenediazonium salts is considerable. In addition to the characterisation of phenols derived from solvolysis, kinetic measurements

have shown the independence of solvolysis rate on added anions, at both low[31,32] and high concentrations.[33] Exceptions have been reported,[37] as with tetra-azotised para-phenylenediamine, which shows essentially second-order kinetics. Furthermore, the effect of substituents on the rate is inconsistent with a nucleophilic attack of solvent, but fits well when correlated with the first-order release of nitrogen.[34]

The mechanism by which arenediazonium salts decompose is known to be strongly solvent-dependent.[35] In water, a carbonium ion mechanism operates in which phenol is the principal product. This is believed to result from a two-step process, _i.e._ a rate-determining step (9) during which nitrogen is lost to give the aryl cation, followed by rapid solvolysis (11) to give phenol

$$Ar^+ + H_2O \longrightarrow ArOH + H^+ \tag{11}$$
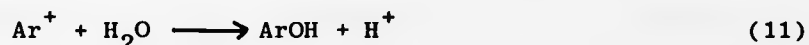
In alcoholic solvents, a radical mechanism preponderates (12,13). However, the reaction

$$Ar-N_2^+Cl^- + RCH_2OH \longrightarrow ArH + HCl + C_2H_4O \tag{12}$$
$$\longrightarrow Ar-O-CH_2R + HCl + N_2 \tag{13}$$

is considerably more complex than the overall stoichiometry suggests. Decomposition of benzenediazonium bisulphate in methanol yields primarily anisole[36] (70%) and

$$Ar-N_2^+HSO_4^- + CH_3OH \longrightarrow Ar-O-CH_3 + N_2 + H_2SO_4 \tag{14}$$
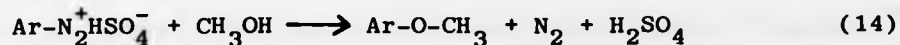
a small amount of reduction product, _i.e._ benzene (5%).

Further complications arise when negative groups are substituted into the ortho-position of the benzene ring, favouring formation of reduction products, but they have a reduced effect when situated in the meta- and para-positions. Strongly electron-withdrawing groups like NO_2 promote the formation of reduction products in any position.[37]

Variation of the alcohol appears to have little effect on the rate of thermal decomposition,[4,5] e.g. for benzenediazonium chloride.

	$10^{-5} k_{dec}(293 \text{ K})/s^{-1}$	$10^{-5} k_{dec}(303 \text{ K})/s^{-1}$
Methanol	26.0	123.2
Ethanol	26.0	123.2
Propan-1-ol		119.7
Butan-1-ol		115.1

Although altering the alcohols may have little effect on the overall *rate* of reaction, it exerts quite a strong influence on the type of products formed. Methanol typically yields a much higher proportion of the corresponding aryl ether than its alkanol analogues. As a general trend, increasing the molecular weight of the alcohol leads to increased amounts of reduction products. The pathway of thermal decomposition of arenediazonium salts in alcohols has been fairly well established,[40] anisole[41] being the principal product formed when benzenediazonium chloride is decomposed in methanol indicating a heterolytic cleavage of the C-N bond. Benzene, however, may be formed when conditions

are made favourable for radical chains by removal of dissolved oxygen.[42] Reduction products have been observed, however, when the chain reaction initiated by aryl radical formation has been completely suppressed. De Tar and Kosuge[43] have proposed a hydride transfer mechanism to account for the formation of reduction products after heterolysis of the C–N bond.

$$Ar^+ + CH_3OH \longrightarrow ArH + CH_2OH^+ \tag{15}$$

Thermolysis in water or acidified solution is less complicated, with nitrogen, phenol and ArX being formed.

$$2 ArN_2^+ \xrightarrow[OH^-]{X^-} ArOH + ArX + 2N_2 \tag{16}$$
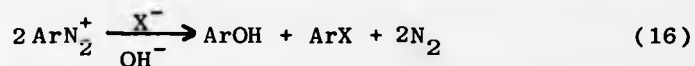
where X is derived from the stabilising anion or added acid. The rate of thermal decomposition is independent of pH[44] and the acid used. However, the ratio of phenol to substituted benzene (ArOH/ArX)[44] is variable and depends upon the initial concentration of arenediazonium salt, e.g.

$[H_2O]/[ArN_2^+Cl]$	$10^{-5}k/s^{-1}$	% yield phenol
2.36	26.2	24.3
3.11	26.8	30.0
11.89	25.2	40.0
158.6	21.2	88.0
1268.0	19.2	95.2

Substituent groups on the benzene ring of arenediazonium salts influence the rate of thermal decomposition. Electron-withdrawing species will draw the positive charge on the diazo group towards the ring (inductive effect) making the ring more positive (hence making the movement of positive charge from the N_2^+ group to the ring more difficult): conversely, electron donating groups will tend to make benzene ring more negative. Resonance effects are particularly important when ortho- and para- substituents are being considered. Alkyl[45] groups in the meta-position promote thermal decomposition, but suppress it when substituted in ortho- or para-positions.

Schulte-Frohlinde[46] has reported thermal decomposition rates for a variety of mono-substituted arenediazonium salts. Reasonable correlation between thermal decay rates and the Hammett σ constants was found, but 4-methoxybenzenediazonium fluoroborate deviated considerably from the remainder of the data.

substituent group	$k_{dec}(323K)/min^{-1}$
p-CH$_3$O	6.5×10^{-6}
p-Cl	2.35×10^{-4}
p-Br	4.90×10^{-4}
pNO$_2$	5.15×10^{-4}
H	8.54×10^{-2}
p-CH$_3$	8.60×10^{-3}

The exceptional stability of the 4-methoxy salt may be accounted for by quinoidal resonance strengthening the C-N bond by increasing its double bond character (17).

$$CH_3O-\!\!\!\!\!\bigcirc\!\!\!\!\!-\overset{+}{N}\!\!\equiv\!\!N \longleftrightarrow CH_3\overset{+}{O}=\!\!\bigcirc\!\!=\overset{+}{N}=\overset{-}{N} \qquad (17)$$

(XXIII)   (XXIV)
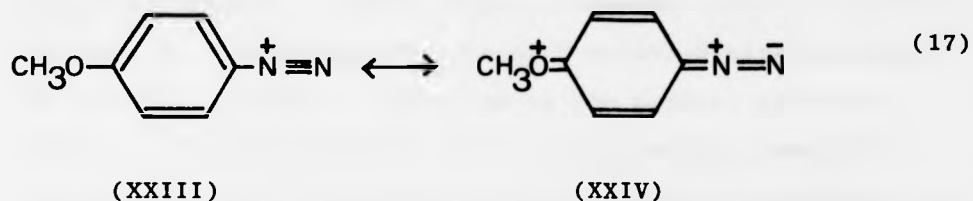
2-hydroxyarenediazonium[47] salts do not yield the typical
phenolic products derived from thermolysis in aqueous
solution, e.g. 2-hydroxybenzenediazonium chloride undergoes
a Favorskii[48] type rearrangement.

$$\bigcirc\!\!\!\!-\overset{OH}{\underset{\overset{+}{N_2}\bar{C}l}{}} + H_2O \longrightarrow \bigcirc\!\!\!\!-\overset{H}{\underset{}{}}COOH + N_2 + HCl \qquad (18)$$

(XXV)   (XXVI)
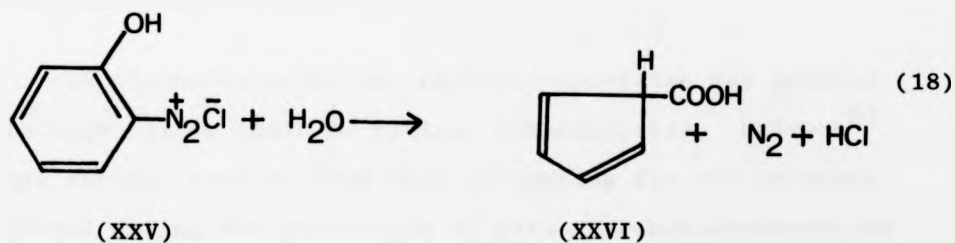
Recently Bunnett[49] et.al. have suggested that ArH and ArOCH$_3$
are derived from a common intermediate, i.e. an 'activated'
diazonium ion [symbolized $(ArN_2^+)^*$] in a mechanism of the
following type:

$$ArN_2^+ \underset{k_2}{\overset{k_1}{\rightleftharpoons}} (ArN_2^+)^* \underset{k\,(ionic)}{\overset{k\,(radical)}{<}} \begin{array}{l} Ar\cdot \rightarrow ArH \\ \\ Ar^+ \rightarrow ArOCH_3 \end{array} \qquad (19)$$
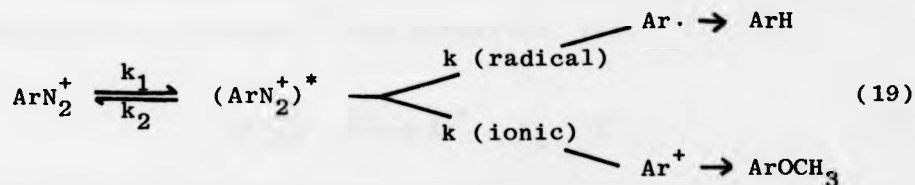
In reaction (19) the product ratio $ArH/ArOCH_3$ is reduced when oxygen is present.[49] When oxygen is absent and other radical scavengers, like sodium nitrite or 2-methyl-2-nitrosopropane are present, a similar reduction in the product ratio is observed. Oxygen probably acts by suppressing propagation of reaction (20) from which reduction products are formed (21).

$$\cdot CH_2OH + ArN_2^+ \longrightarrow Ar\cdot + N_2 + CH_2OH^+ \qquad (20)$$

$$Ar\cdot + CH_3OH \longrightarrow ArH + \cdot CH_2OH \qquad (21)$$
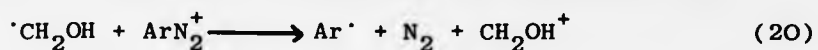
1.7. PHOTOLYSIS OF ARENEDIAZONIUM SALTS

In alcoholic solution, photodecomposition may proceed through either ionic or radical intermediates. Calvert[50] has invoked both of them when accounting for the products formed during the photolysis of para-nitrobenzenediazonium hexachlorostannate. Magnetic susceptibility measurements carried out by Boudreaux and Boulet[51] also indicated that radical intermediates are formed in the photolysis of arenediazonium salts in aqueous solution.

Photodecomposition in aqueous solvents (like the thermolysis) proceeds *via* carbonium[30] ion formation, *viz*.

$$ArN_2^+X^- \xrightarrow{\ h\nu\ } Ar^+ + N_2 + X^- \qquad (22)$$
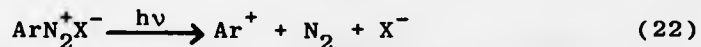
followed by rapid solvolysis to give the corresponding phenol,

$$Ar^+ + OH^- \longrightarrow ArOH \qquad (23)$$
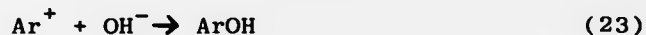
and additionally some substituted benzene may be formed.

$$Ar^+ + X^- \longrightarrow ArX \qquad (24)$$
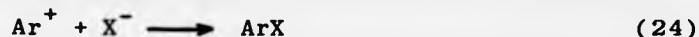
The percentage of phenol formed during the photolysis of arenediazonium salts is very sensitive to the presence of added anions at the time of carbonium ion formation, <u>e.g.</u>

Added anion	% phenol
F⁻	0.0
Cl⁻	24.0 ± 5
Br⁻	70.0 ± 5
I⁻	85.0 ± 5

(Data from the photolysis of $p\text{-}O_2NC_6H_5N_2^+$ in DMSO).[52]

Favorskii-type rearrangements have been reported in the photo-decomposition of the atypical[53] 2-hydroxybenzenediazonium salts (<u>cf</u>. the thermal decomposition). 1,2-quinols may be formed when ionisation of the hydroxyl group is prevented by the addition of acid, *viz*.

$$\qquad (25)$$

(70%) (12%)
(XXVII) (XXVIII) (XXIX)
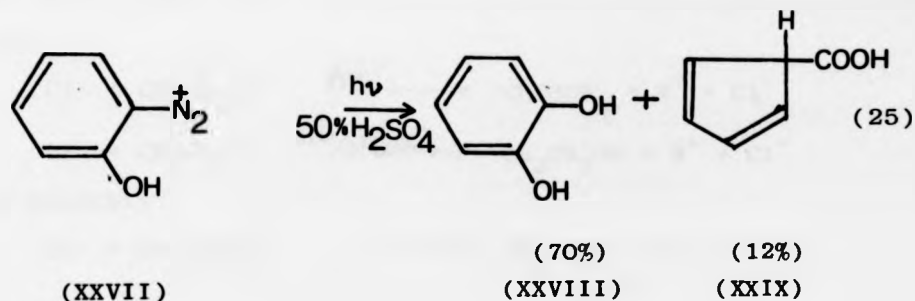
Süs $\underline{et.al}$.[54] have examined the unusual photodecomposition of the 2-hydroxyarenediazonium salts in considerable detail.

The variety of products observed from the photolysis of para-nitrobenzenediazonium hexachlorostannate[50] in deaerated methanol clearly indicates the co-existence of two parallel reaction schemes. One is the radical pathway which may be summarised by the following reactions:

$$O_2NC_6H_4N_2^+ \tfrac{1}{2}SnCl_6^{2-} \xrightarrow{h\nu} O_2NC_6H_4\cdot + N_2 + Cl\cdot \text{ or } SnCl_5\cdot \quad (26)$$

$$O_2NC_6H_4\cdot + CH_3CH_2OH \longrightarrow C_6H_5NO_2 + CH_3\dot{C}HOH \quad (27)$$

$$O_2NC_6H_4\cdot + CH_3CH_2OH \longrightarrow C_6H_5NO_2 + \cdot CH_2CH_2OH \quad (28)$$

$$O_2NC_6H_4\cdot + \cdot CHOHCH_3 \longrightarrow O_2NC_6H_4CHOHCH_3 \quad (29)$$

$$O_2NC_6H_4\cdot + \cdot CH_2CH_2OH \longrightarrow O_2NC_6H_4CH_2CH_2OH \quad (30)$$

$$2[\cdot CHOHCH_3] \longrightarrow CH_3CHOHCHOHCH_3 \quad (31)$$

$$2[\cdot CHOHCH_3] \longrightarrow CH_3CH_2OH + CH_3CHO \quad (32)$$

$$\cdot CHOHCH_3 + O_2NC_6H_4 \longrightarrow CH_3CHO + C_6H_5NO_2 \quad (33)$$

$$\cdot CH_2CH_2OH + O_2NC_6H_4\cdot \longrightarrow CH_2{\downarrow} = CHOH + C_6H_5NO_2 \quad (34)$$
$$CH_3CHO$$
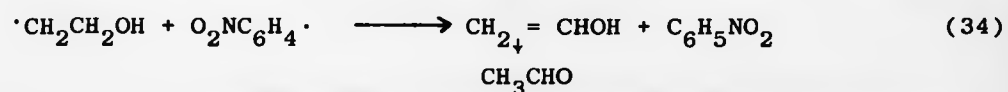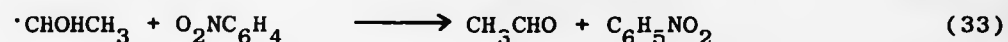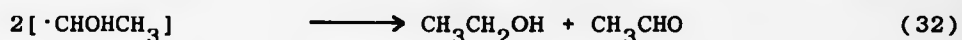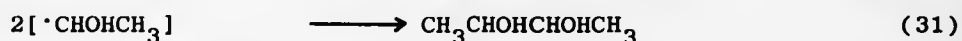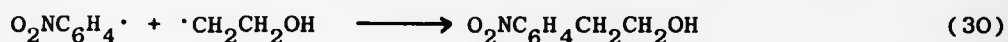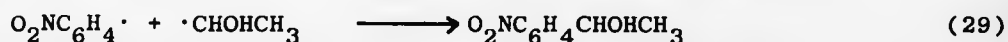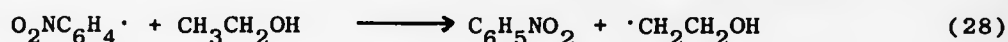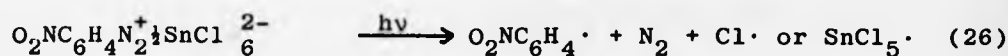
The only likely reactions of the highly reactive atomic chlorine are:

$$Cl\cdot + CH_3CH_2OH \longrightarrow \cdot CHOHCH_3 + H^+ + Cl^- \quad (35)$$

$$Cl\cdot + CH_3CH_2OH \longrightarrow \cdot CH_2CH_2OH + H^+ + Cl^- \quad (36)$$

and possibly

$$Cl\cdot + CH_3CH_2OH \longrightarrow CH_3CH_2O\cdot + H^+ + Cl^- \quad (37)$$
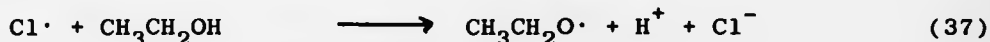
The ionic pathway (<u>i.e.</u>carbonium ion formation) also leads to the formation of a small amount of phenetole (5.0%).

$$O_2NC_6H_4N_2^+ \tfrac{1}{2}SnCl_6^{2-} \xrightarrow{\;h\nu\;} O_2NC_6H_4^+ + N_2 + \tfrac{1}{2}SnCl_6^{2-} \qquad (38)$$

$$O_2NC_6H_4^+ + CH_3CH_2OH \longrightarrow [O_2NC_6H_4\overset{\overset{\displaystyle H}{|}}{O}CH_2CH_3]^+ \qquad (39)$$
$$\downarrow$$
$$O_2NC_6H_4OCH_2CH_3 + H^+$$
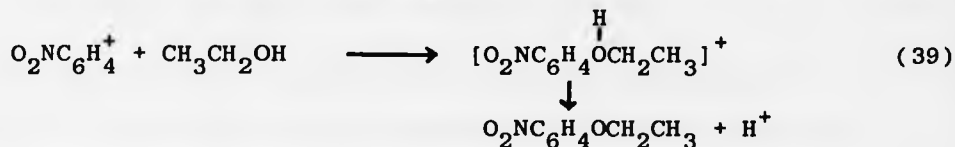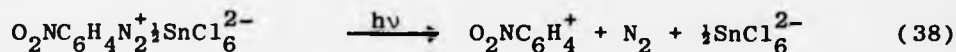
Calvert rejected the possibility of (26) initiating a chain reaction on account of the efficiency of (29). Hydroxymethyl radicals[55] are, however, known to initiate chain reactions when arenediazonium salts undergo thermal decomposition.

$$C_6H_5N_2^+ + R_2\overset{\cdot}{C}OH \longrightarrow C_6H_5\cdot + N_2 + R_2\overset{+}{C}OH \qquad (40)$$

$$C_6H_5\cdot + R_2CHOH \longrightarrow C_6H_6 + R_2\overset{\cdot}{C}OH \qquad (41)$$

$$C_6H_5N_2^+ + R_2\overset{\cdot}{C}OH \longrightarrow C_6H_5N_2\cdot + R_2\overset{+}{C}OH \qquad (42)$$

$$C_6H_5N_2\cdot \longrightarrow C_6H_5\cdot + N_2 \qquad (43)$$
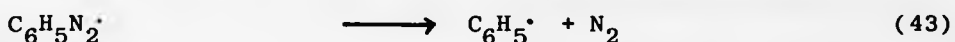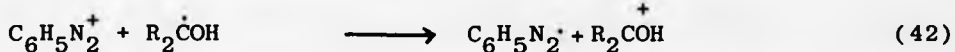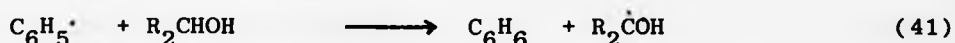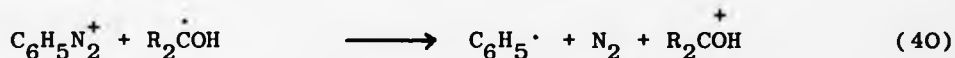
Reduction products have been characterised from the photolysis of several arenediazonium salts in aerated methanol where, according to Calvert,[50] ether-like products are expected.

<u>Photodecomposition of p-XC$_6$H$_4$N$_2$HSO$_4$ in aerated methanol.</u>

X	%XC$_6$H$_5$	%XC$_6$H$_4$OCH$_3$
CH$_3$	12	85
NO$_2$	82	4
CH$_3$O	31	57

(Data from De Tar <u>et.al.</u>)[43]

The formation of reduction products where photodecomposition occurs predominately *via* carbonium ion formation may possibly be explained by the hydride transfer mechanism proposed by De Tar.[43]

$$O_2NC_6H_4^+ + CH_3OH \longrightarrow O_2NC_6H_5 + CH_2OH^+ \tag{44}$$
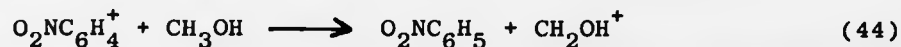
The photolysis of arenediazonium in solution can be spectrally sensitized by the presence of a suitable dye and activator. Yamase[56] et.al. have reported the spectrally sensitized photolysis of 4-diazodiphenylamine sulphate using methylene blue and either para-toluenesulphonate or 1,4-diazobicyclo-2,2,2-octane (DABCO) as an activator. The reactions related to the sensitization are outlined in the scheme below:

$$MB^+ + h\nu \longrightarrow (MB^+)^* \tag{45}$$

$$(MB^+)^* + DABCO \longrightarrow (MB\cdot \ldots \cdot DABCO) \rightarrow MB\cdot + \cdot DABCO \tag{46}$$

$$MB\cdot + 4DS \longrightarrow MB^+ + N_2 + \text{4-diphenylamino radical} \tag{47}$$
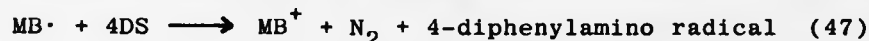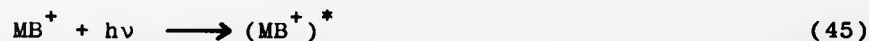
where

MB^+	=	methylene blue ground state
$(MB^+)^*$	=	methylene blue triplet state
$MB\cdot$	=	unprotonated semi-methylene blue
$(MB\cdot \ldots \cdot DABCO)$	=	a radical pair of unprotonated semi-methylene blue and half-oxidised activator

Photodecomposition only occurs when the system is irradiated with red light (absorbed only by the methylene blue). Radicals formed from the spectrally sensitized photodecomposition of 4-diazodiphenylamine have been used to initiate polymer formation[57] in an aqueous solution of acrylamide. Dye-sensitized photopolymerisation is extremely sensitive to both oxygen and the pH of the medium.[58]

The thermal and photodecomposition of arenediazonium salts have many features in common and this has led to the suggestion that the products are derived from the same intermediate. However, increased isotopic rearrangement (50) and enhanced selectivity of the photochemical transient for added anions[59] has led to its rejection.

$$\text{Ar-}\overset{+}{\text{N}}{}^{15}\!\equiv\!\text{N} \xrightarrow{\ h\nu\ } \text{D}^* \tag{48}$$

$$\text{D}^* \longrightarrow \text{Ar}\!-\!\overset{+}{\text{N}}{}^{15}\!\equiv\!\text{N} \tag{49}$$

$$\text{D}^* \longrightarrow \text{Ar}\!-\!\overset{+}{\text{N}}\!\equiv\!\text{N}^{15} \tag{50}$$

$$\text{D}^* + \text{H}_2\text{O} \longrightarrow \text{ArOH} + \text{H}^+ + \text{N}_2 \tag{51}$$

$$\text{D}^* + \text{Cl} \longrightarrow \text{ArCl} + \text{N}_2 \tag{52}$$
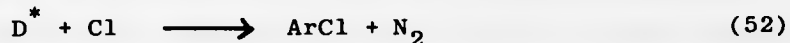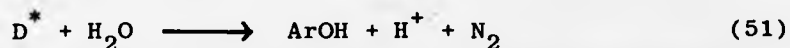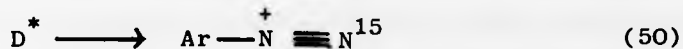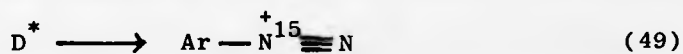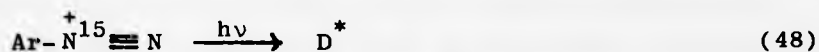
where D^* is a state of unestablished multiplicity.

1.8. DIAZONIUM SALTS AS REPROGRAPHIC AGENTS

Reprographic systems[60] based on arenediazonium salts may be conveniently divided into a number of discrete stages, initially one of coating the photolabile compound on to a

suitable support, irradiation (with decomposition of the arenediazonium salt) and, finally, one of image development. A further subdivision of moist and dry processes may be applied.

In moist processes, a paper is sensitised with an aqueous solution of the arenediazonium salt. The paper may then be exposed to near ultra-violet light from a mercury vapour lamp. Upon irradiation, arenediazonium salt in areas not covered by opaque lines is photodecomposed. A permanent image can then be fixed by addition of an alkaline solution of a suitable coupler giving an azo dye copy of the original print.

In dry or two-component[61] systems, a polymer film is used as a support for both a solvent-soluble arenediazonium salt and coupler (kept at a slightly acid pH to prevent pre-coupling). A preliminary precoating of the polymer film with a binding agent of 'filler' is frequently employed. Following irradiation, image development is effected by exposure to ammonia vapour.

Mono-substituted diazonium salts have limited application in such reprographic processes because of their thermal instability, which leads to sensitised papers with a very poor shelf life. Additionally, they absorb in the ultra-violet region of 220 to 330 nm which is outside the spectral range of most conventional light sources. Introduction of electron donating groups like alkyl amino and aryl mercapto into either para- or ortho-positions with respect to the diazonium group induce a red shift of the absorption maxima, and unlike the simple salts which are colourless, these are invariably yellow or orange-yellow in colour.

These substituent groups also achieve enhanced light absorption because the extended conjugation results in an increase in the extinction coefficient (or oscillator strength) of the transition. Similarly, the increased double bond character of the C-N leads to increased thermal stability and hence an increased shelf life of the coated papers. Typically arenediazonium salts used in reprographic processes absorb in the region 360-420 nm, and this range may be extended further into the red by lengthening the system of conjugated double bonds, e.g. by replacing benzene with naphthalene.

Two salts commonly used in reprographic papers marketed by Ozalid Ltd. are 2,5-dialkoxy derivatives of 4-morpholino and 4-tolylthiobenzenediazonium salts.
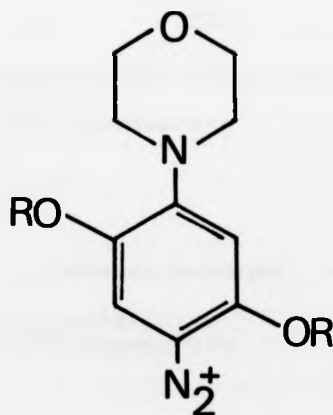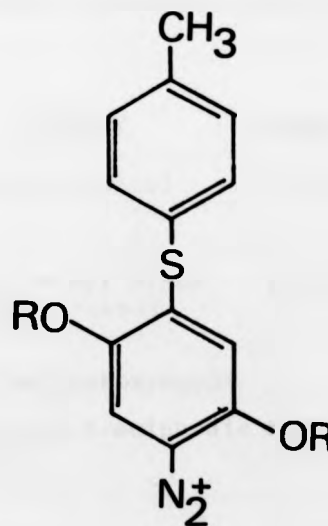
(XXX)   (XXXI)

4-morpholinobenzenediazonium tetrafluoroborate has what is termed high light sensitivity and moderate coupling activity which makes it a suitable choice for two-component or dry processes, 4-tolylthiobenzenediazonium tetrachlorozincate has a similar light sensitivity but a many-fold increase in the coupling activity which makes it suitable for moist processes only.

Decomposition using mercury vapour lamps utilises the emission lines at 365 and 405 nm and consequently only 30% of the total emitted radiation can be matched to the absorption spectra of arenediazonium salts.

The actual chromophore is the —N = N— link in the resultant azo dye, but the final colour is largely dependent on the type of coupler used, e.g.

Salt	Coupler	Image colour
4-morpholinobenzenediazonium tetrafluoroborate	phloroglucinol	red/brown
	monomethyl ether of resorcinol	yellow/brown
2,5-diethoxy-4-morpholino benzenediazonium tetrafluoroborate	2,3-dihydroxynaph-thalene-6-sulphonic acid	blue

Only the essential features of the moist (one-component) and dry (two-component) systems have been considered, the many variations and refinements having been reviewed by Pinot de Moira.[62]

Diazonium salt-based reprographic systems have replaced the much older ferricyanide papers (blue prints) principally because of the increased shelf life of the sensitised papers, and the distinct advantage of positive imaging which makes them a considerably more marketable product for the copying of large architectural and engineering drawings. Until recently dyeline papers have been able to hold a considerable proportion of the market because of their relatively inexpensive nature and the variety of coloured prints which may be produced. However, the decline in recent years is probably due to the widespread use of xerography which has now reached such a high level of sophistication that multi-coloured prints can be produced. Whilst the use of dyeline papers for routine office copying has contracted, however, dyeline processes have expanded in other areas.

A considerable quantity of literature and documentation is now stored on microfilm. Dyeline systems offer certain distinct advantages over the silver halide process in the production of microfilm. Apart from the economic considerations, azo dye molecules have only 1/300th the size of silver halide ion aggregates; consequently it is much easier to achieve the high degree of resolution required for satisfactory microfilming.

The production of lithographic plates for printing is another area where diazonium salts have found extensive application. Originally, ammonium dichromate gelatin plates were used, but these are extremely sensitive to changes in pH,

temperature and humidity and deteriorate rapidly due to a dark
reaction which gives the plates a working life of only a few
days. Zahn, in 1934, patented a lithographic printing system
utilising the condensation product between formaldehyde and
diazotised diphenylamine type compounds. In essence, exposed
areas form a decomposition product which is firmly attached
to a metal plate giving an ink receptive surface. Unexposed
areas are easily removed by washing away the highly ionic
condensation product with water.

Highly complex printed circuitry and the very delicate
components of many instruments are now produced by utilising
the photochemical properties of diazonium salts. Exposure
of light through a negative copy of the desired circuit hardens
a photosensitive layer and forms a protective coating over
copper areas where connections are required; unsensitised
compound may easily be removed from unexposed areas. Obviously,
as more intricate circuitry is demanded to handle the
miniaturisation of electrical components, this is a field
which may show considerable expansion.

1.9. AIM OF THIS WORK

Despite the extensive exploitation of arenediazonium salts
as the basis of an inexpensive and reliable reprographic
process, few fundamental studies of their photochemistry have
been made. In the present work we have endeavoured not only

to rectify this situation but also to resolve the many dis-
crepancies existing between previously published studies
concerning this problem.

Tsunoda and Yamaoka[63,64] and Schulte-Frohlinde and Blume,[65]
have reported photodecomposition yields of simple arenediazonium
salts in aqueous acid, and additionally Barraclough et.al.[66]
and Baltazzi et.al.[67] have determined quantum yields in
polymer films, but little else has been reported. We have
attempted to resolve discrepancies between their work and
ours whilst at the same time providing additional data for
some of the structurally more complex arenediazonium salts
used as reprographic agents. Of particular interest has
been the solvent dependence of the photodecomposition and the
influence of substituent groups.

Most of the mechanisms proposed for the photodecomposition
of arenediazonium salts have been based on quantum yields and
product analysis. A more direct approach has been considered
here, where the reactive intermediates have been trapped in
a variety of matrices at 77 K. Both ultra-violet and esr
spectroscopy have been used to aid identification of the
intermediates formed.

Although of a less quantitative nature, the latter part
of this work has been directed towards establishing the
electronic configuration of the aryl cation, thereby
complementing the several theoretical studies directed to
this topic, several of which indicate that $C_6H_5^+$ may exist
as a ground state triplet.

CHAPTER II

EXPERIMENTAL AND THEORETICAL STUDIES OF

INTERMEDIATES FORMED IN THE DECOMPOSITION

OF ARENEDIAZONIUM SALTS

2.1. <u>INTERMEDIATES IN THE DECOMPOSITION OF ARENEDIAZONIUM SALTS</u>

Aryl cations are rare as reaction intermediates and it is only in the decomposition of arenediazonium salts where substantial evidence for their existence can be found. Aryl compounds with leaving groups other than nitrogen could conceivably form aryl cations. Diaryliodanium cations (ArI^+Ar)[68] and arylmercuric cations $(ArHg^+)$,[69] are both potential sources, but their decomposition products suggest radical intermediates. Electrochemical oxidation of alkyl iodides[70] in acetonitrile leads to products derived from alkyl cations, but in similar oxidations of aryliodides the Ar-I bond remains intact.

Nucleophilic substitution of the diazonium group of an arenediazonium cation probably proceeds by a rate determining loss of nitrogen to form a strongly electrophilic intermediate generally regarded as a free aryl cation.

$$\text{(XXXII)} \xrightarrow[\text{(slow)}]{k_1} \text{(XXXIII)} \xrightarrow[\substack{\text{(fast)} \\ Nu^-}]{k_2} \text{(XXXIV)} \qquad (53)$$
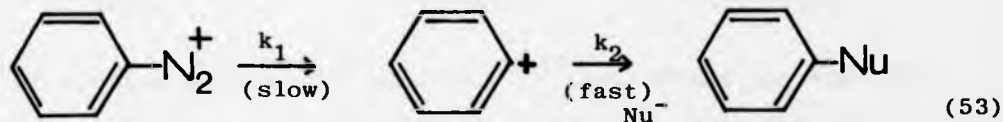
where $k_2 >>> k_1$

The validity of the S_N1 nature of the reaction is primarily
kinetic, being based on the insensitivity of the observed
rate of decomposition to added halide ions.[32] Verification
is limited to product analysis, but at relatively low solvent
concentrations some doubt is cast on this simple kinetic
interpretation[44].

A modification of this view with respect to the cationic intermediate
has been proposed to account for the increased rate of
decomposition observed when meta-substituents are present.
Resonance interaction with meta-substituents has led to the
suggestion[71] that the intermediate formed is a diradical
cation formed by an electronic rearrangement of the π system.

(54)

(XXXV)   (XXXVI)   (XXXVII)
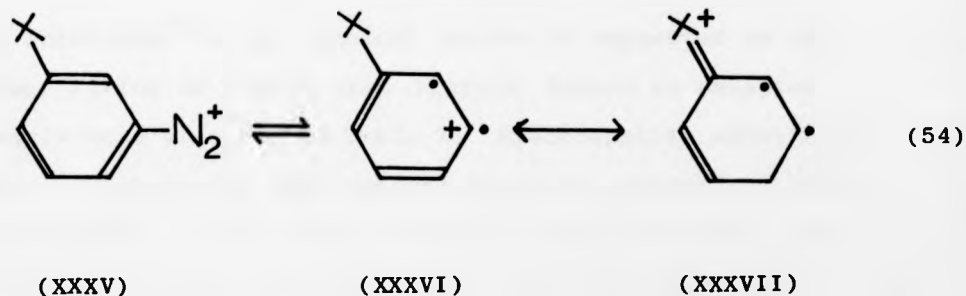
The concept was further modified[72,73] to account for the high
reactivity and apparently high selectivity of the intermediate
generated from the diazonium ion. Whilst maintaining the loss
of nitrogen as the rate determining step, the aryl cation
formed was postulated to exist in equilibrium with the
diradical cation shown below.

$$(55)$$

(XXXVIII)   (XXXIX)   (XL)   (XLI)

(XLII)
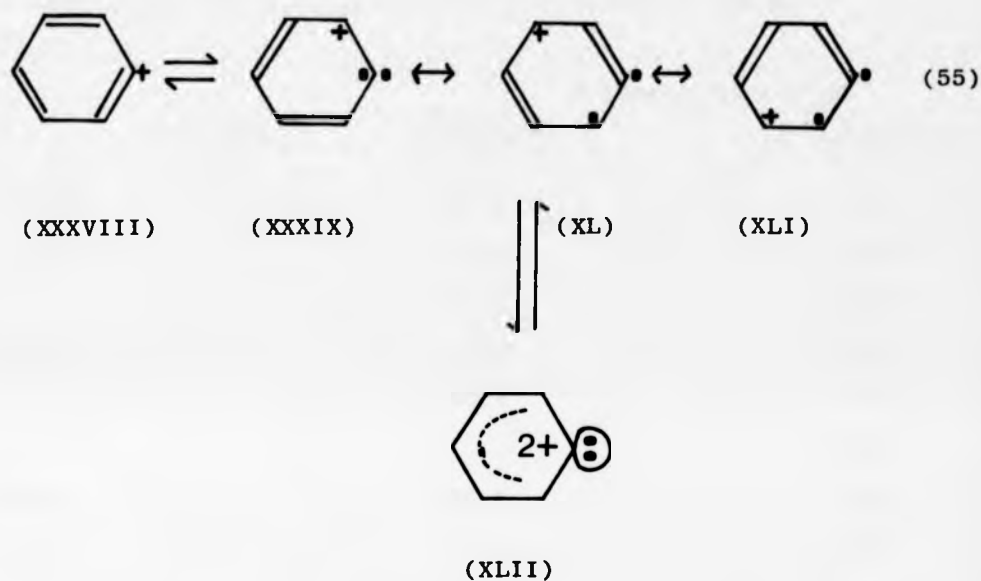
The existence[74] of a diradical cation is suggested by the
isomer ratios of substituted biaryls formed in selected
phenylations as shown in Table 1. Electrophilic substitution
(e.g. attack by a phenyl cation) would be expected to occur
predominantly at the para-position in methoxybenzene, the
meta-position in nitrobenzene, and the ortho- plus para-
positions in bromobenzene.

TABLE 1

RATIO OF ISOMERS FORMED IN THE PHENYLATION OF C_6H_5X

		% isomer formed	
	position	$C_6H_5N_2^+BF_4^-$	$(C_6H_5CO_2)_2$
PhOCH$_3$	o	57.5	69.8
	m	10.0	15.8
	p	32.5	15.8
PhNO$_2$	o	19.6	63.2
	m	80.4	9.7
	p	-	27.1
PhBr	o	56.1	56.2
	m	19.8	27.3
	p	24.1	16.5

However, in each case an appreciable fraction of other isomers is formed. Comparison with data from the decomposition of benzoyl peroxide which yields phenyl radicals, where ortho/para substitution may be expected to dominate, would suggest that the phenyl cation has some radical properties. The degree of positional selectivity of the phenyl cations has been attributed to the "carbenoid" form of the diradical (structure XLII). The point is further illustrated by the data given in Table 2. It is significant that in all cases the isomer distributions have been based on total yields of less than 4% for biaryl formation, with over 90% of the reaction leading to fluorobenzene,[75] and consequently the results should be viewed with considerable caution.

TABLE 2

ISOMER DISTRIBUTIONS FOR THE PHENYLATION OF TOLUENE

Phenylating agent	Proposed intermediate	o	m	p
Ph_3Bi[76]	radical	57.0	27.0	16.0
$(PhCO_2)_2$[76]	radical	66.5	19.3	14.2
$C_6H_5N_2^+BF_4^-$[77]	radical	57.4	20.0	22.3
$C_6H_5N_2^+BF_4^-$[77]	catonic	47.1	27.2	25.4
$C_6H_5N_2^+BF_4^-$[77]	catonic	47.3	21.1	31.6

Taft's[78] original report of enhanced resonance effects of meta-substitution in radical reactivities (ascribed to the formation of isoequivalent quinoidal structures) was extended by Taft[71] to the solvolysis of substituted arenediazonium ions. The effect of meta-substitution on the rate of thermal solvolysis of arenediazonium ions is indicated by the decrease in free energy of activation estimated from -2.303 RT [log k/ko-σ^op], of OCH_3 7.11 kJ mol^{-1}, OH 6.28 kJ mol^{-1}, C_6H_5 3.34 kJ mol^{-1}, CH_3 2.09 kJ mol^{-1} and Cl 0.83 kJ mol^{-1}. A transition state with a degree of radical cation character can be visualised in terms of the generally accepted mechanism for the thermal decomposition of arenediazonium ions, i.e. it may be regarded as a state where one of the π electrons has fallen into the vacant sp^2 hybrid orbital. Energetically this demotion is favoured by the fact that the valence state ionisation potential of a pure π electron in benzene is 11.16 eV, i.e. considerably

lower than that of a σ orbital which is 15.62 eV.[79]

Objections to the existence of the free phenyl cation have been raised on account of the extremely high energy requirements[80] implied in the generation of such a species ($\Delta H_f^o 298 = 1130 \pm 16 kJ\ mol^{-1}$) A scheme involving a process of lower energy is one in which the aryl cation (in any configuration) is entirely bypassed. Nucleophilic substitution could occur by a rate-determining attack of a nucleophile leading to an adduct with subsequent loss of nitrogen to form products.

$$\text{(56)}$$

(XLIII)   (XLIV)   (XLV)
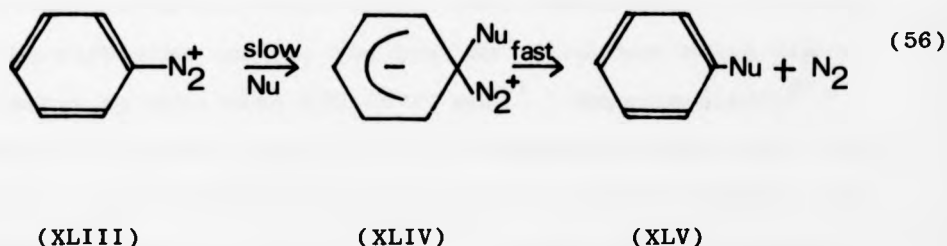
Some evidence for this postulate can be found from kinetic data, but has been rejected in favour of the cation intermediate. Thus the reaction of the para-phenylene-bis diazonium[81] ion with chloride ion to form the para-chlorobenzenediazonium ion is roughly bimolecular. Formation of para-bromonitrobenzene from the para-nitrobenzenediazonium ion in aqueous solution has been shown to be dependent on the concentration of added bromide ions[82]. The bimolecular process is particularly favoured in these ions because of the strong electron withdrawing substituents present   e.g.

$$(57)$$

(XLVI)   (XLVII)
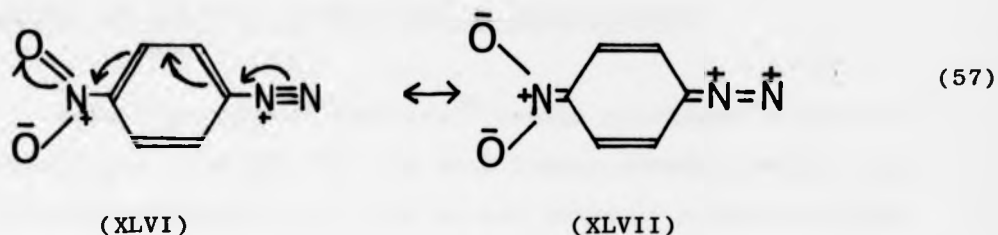
Singlet phenyl cation might seem a highly unlikely species[83] because the electron deficiency is localised in an orbital of relative high s character (sp^2) since it is better to give vacant orbitals maximum p character. Molecular orbital calculations on the vinyl cation have shown that it is linear at the carbonium centre, the bent sp^2 structure being higher in energy by more than 125.58 kJ mol^{-1}. Experimentally[84] 1-cyclooctenyl and 2-cis-2-butyl triflates solvolyze 10^5 times faster than 1-cyclopentenyl triflate, presumably because they can yield linear carbonium ions. It would seem that phenyl cation must also be approximately linear at C_1 - a circumstance not readily acceptable to the conventional view of aromatic chemistry.

Expanding Taft's[71] original proposal, the existence of an equilibrium between structures (XXXIX) and (XLII) would account for all the properties of a phenyl cation. Preliminary[85] molecular orbital calculations indicate the order of stabilities to be (XXXIX), (XXXXII), (XXXVIII), the triplet diradical cation being the ground state. A more detailed discussion of subsequent molecular orbital calculations follows in the next chapter.

2.2. MOLECULAR ORBITAL CALCULATIONS ON ARYL CATIONS

Molecular orbital theories[86] assign electrons in pairs to
orbitals ψ which are written as a linear combination of a set
of basic functions, $\phi\mu$. The $\phi\mu$ are normally centred on the
atoms, so expansion of (58) is often

$$\psi_1 = \sum_\mu C_{\mu i} \phi\mu \tag{58}$$

described as the linear combinations of atomic orbital (LCAO)
approximation. Large basic sets ($\phi\mu$) in theory lead to more
accurate molecular orbitals, but the increased complexity of
the calculations involved makes the use of a minimal basis
set easier to apply and interpret, i.e. one which consists
of the least number of atomic orbitals. If a large number
of ϕ functions are used, the basis set is usually described
as extended.

The simplest semiempirical methods are the extended Hückel
theories which are developments of the original π electron MO
theory due to Hückel. A semiempirical treatment, where the main
features of electron interaction are taken into account is the
complete neglect of differential overlap (CNDO).
One deficiency of CNDO is the neglect of one-centred exchange
integrals, i.e. the additional interatomic stabilisation due
to electrons with parallel spins occupying different atomic
orbitals. If contributions from these integrals are taken
into account, the scheme is described as the intermediate
neglect of differential overlap or INDO. For most closed

shell diamagnetic molecules CNDO and INDO methods give similar results; however, INDO gives a much superior description of electron spin density in radicals. The most intricate of all the methods is the *ab initio* treatment with Slater type exponential orbitals (STO).

Calculations involving STO are very time-consuming, hence Slater type functions are usually replaced with a linear combination of Gaussian functions. The resulting set of basis functions, with N Gaussian functions per STO function is referred to as STO-N.G.

Calculations on the phenyl cation of the differing MO levels of complexity have been performed by a number of workers. The stability of the phenyl cation has been described by Gleiter et.al.[87], using extended Hückel theory.

In discussing the electronic configuration of the phenyl cation, the various states are given in terms of the atomic orbitals a_1, a_2 and b_1 (Fig. 5).

A quantitative assessment as to the possible existence of the phenyl cation with a σ,π structure as originally proposed by Taft[71] has been published by Evleth and Horowitz[88]. They performed INDO type MO calculations on the phenyl cation using benzene geometry. Their results indicate that the lowest singlet and triplet states of the phenyl cation have σ structures $^1A_1$ and $^3B_2$ respectively (see Fig. 5). Additionally the triplet INDO phenyl cation is placed 3.5 eV above the singlet state. Its electronic structure is such that the positive charge is delocalised and both unpaired electrons reside in the σ system.

Figure (5)

Orbitals and states of the phenyl cation
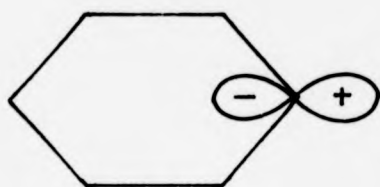
a_1

(XLVIII)
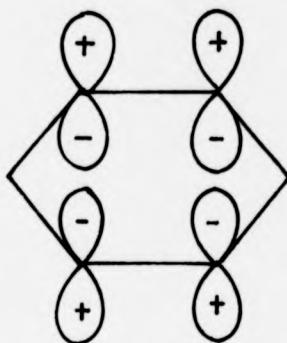
a_2

(IL)
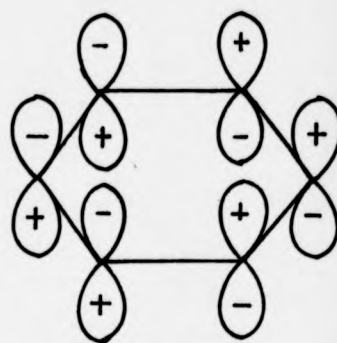
b_1

(L)

$^1A_1(a_2^2 a_1^2)$ σ singlet

(LI)

$^3B_2(a_2 b_1 a_1^2)$ σ triplet

(LII)
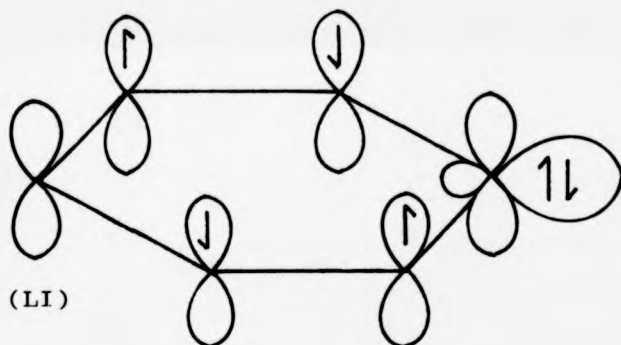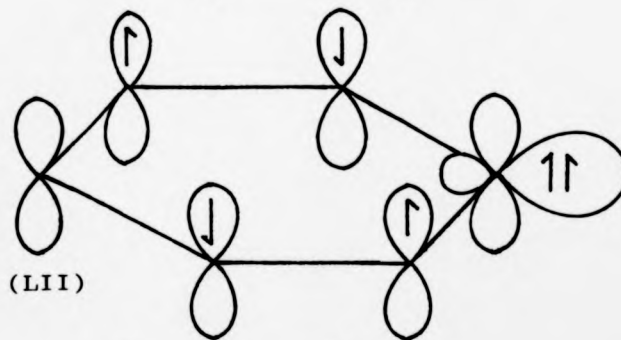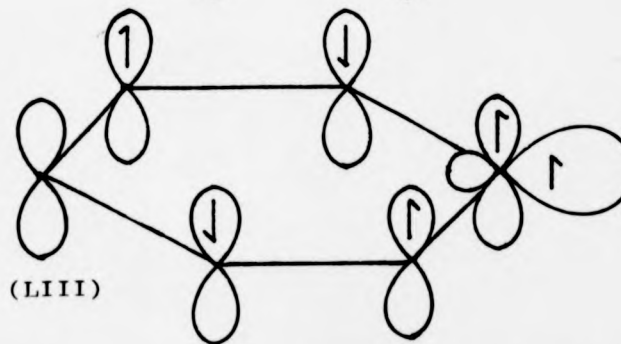
$^3A_2(a_2 b_1 a_1)$ σ π triplet

(LIII)

Figure (6)

Geometries and charge distributions of the singlet

phenyl cation as calculated by the INDO method[89]

GEOMETRIES

(LV)

(LVII)

(LIV)

CHARGE
DISTRIBUTION

(LVI)
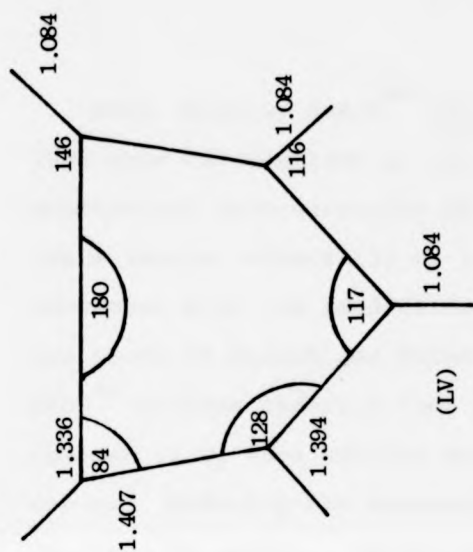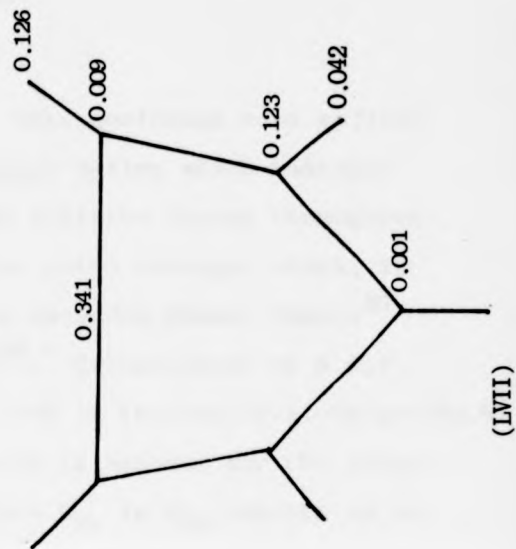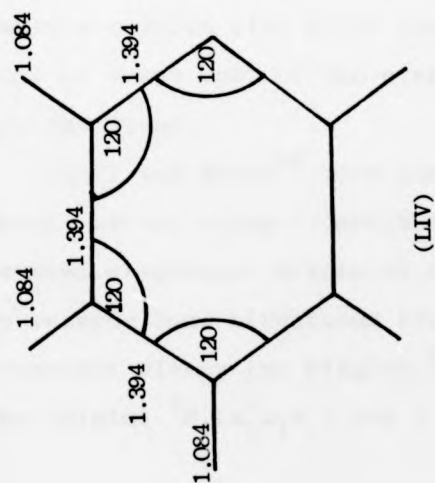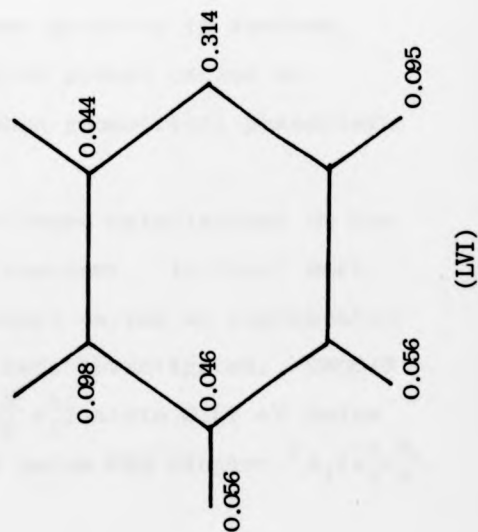
More recently Swain[89] et.al. have performed more refined
INDO type calculations on the phenyl cation which indicate
substantial delocalisation of the positive charge throughout
the molecule, especially on to the ortho hydrogen atoms, in
agreement with the predictions of extended Hückel theory[87]
and those of Evleth and Horowitz[88]. Calculations by S.C.F.
INDO[89] methods indicate that ca. 30% of the positive charge (Fig.6)
resides at C_1 when benzene geometry is assumed for the phenyl
cation. Reducing the symmetry from C_{2v} to D_{3h} results in an
increase in energy. Variation of the geometrical parameters
subject to maintaining C_{2v} symmetry leads to a singlet phenyl
cation some 4.05 eV lower in energy, compared with 1.76 eV
when the benzene geometry is optimized. Inspection of the
structure (LV), which is the singlet phenyl cation of lowest
energy, clearly shows that the C_2-C_1-C_6 bonds are linear
(hence the pentagonal shape) and considerably shorter than
the corresponding values when benzene geometry is assumed.
Swain's results also place the triplet phenyl cation at
6.29 eV above that of the singlet when geometrical parameters
are optimized.

Jaffé and Koser[90] have also performed calculations on the
phenyl cation using a CNDO/S type treatment. In their work,
several electronic states of the phenyl cation as represented
by valence bond structures (Fig.7) were investigated. CNDO/S
treatment places the singlet $^1A_1$ (a_2^2 b_1^2) state 0.87 eV below
the triplet $^3B_1$($a_2^2 b_1 a_1$) and 1.56 eV below the singlet $^1A_1$($a_2^2 a_1^2$).

Figure (7)

Preferred valence bond structure of the phenyl cation as determined by the CNDO method[90]

$a_2^2 a_1^2$ (I)

$a_2^2 b_1 a_1$ (II)

$a_2^2 b_1^2$ (III)

ENERGY

I   II   III

PREFERRED STRUCTURE

$^1A_1(a_2^2 b_1^2)$

$^3B_1(a_2^2 b_1 a_1)$

$^1A_1(a_2^2 a_1^2)$

(LVIII)

(LIX)

(LX)

I

II
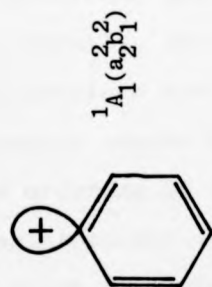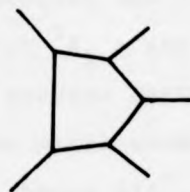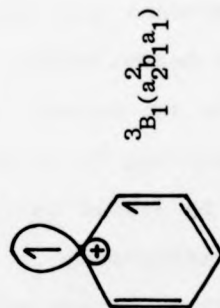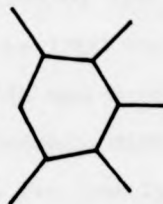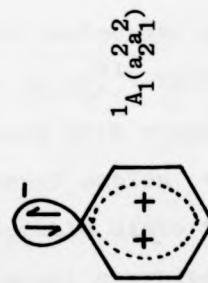
III
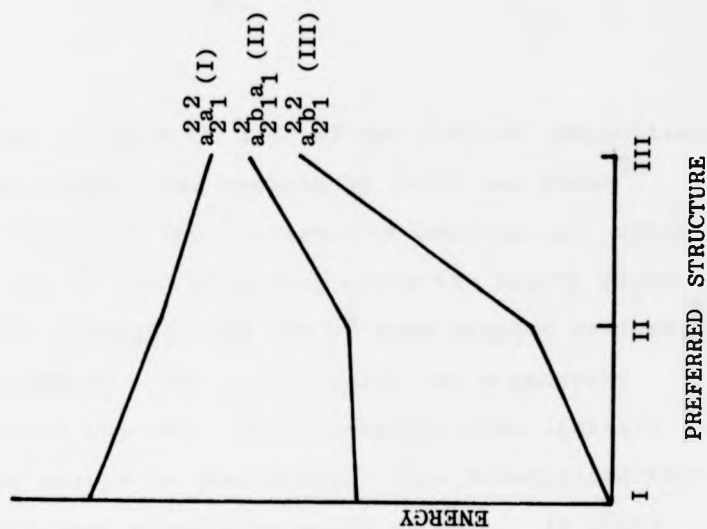
Slightly differing energies of 3.47 eV and 7.67 eV respectively
were obtained when CNDO/2 was applied by Jaffé and Koser[90].
When the energy levels of the different geometries are compared,
it appears that the π^6 type singlet prefers the highly distorted
geometry (_i.e._ the pentagon) and the π^4 type singlet prefers
a benzene-type geometry. The σ, π triplet has a geometry
intermediate between the two. Their findings also indicate
that the positive charge is considerably more delocalised than
any of the valence bond structures would suggest. It would
appear that the conformational preference of the phenyl cation
is related to the degree of hybridisation of the vacant C_1
σ orbital, maximum s character being adopted when the σ orbital
contains two electrons, but tending towards maximum p character
as electrons are successively removed.

Finally, the more sophisticated _ab initio_ molecular orbital
calculations have been carried out by Pople et.al[91]. Their
findings concur with those of previous workers with respect to
the ordering of the energy levels of the phenyl cation, the
singlet phenyl cation $^1A_1$ undergoing considerable distortion
in order to maximise the charge on to the vacant p orbital from
the σ framework.

However, Pople et.al.[91] arrived at different geometries for
the singlet and triplet states of the phenly cation. The
singlet $^1A_1$ state (unlike the INDO version of Swain[89] or the
CNDO version derived by Jaffé and Koser[90]) is not linear about
C_1 but still shows a considerably distorted geometry, the angle
at C_1 being 144°. Both the two low-lying triplets $^3B_1$ and $^3A_2$

were calculated by Pople[91] to have structures closely resembling that of benzene. Furthermore, Pople[91] has considered the π charge distribution and π spin densities (Fig.8). In the π^6 type phenyl cation there is a strong polarisation of electrons towards C_1 where a considerable excess accumulates (0.200 electron) in order to stabilise the positive charge. In the triplet $^3B_1$ state, the number of π electrons is 5; the odd electron has been primarily removed from C_1 (44%) as opposed to the $^3A_2$ triplet state when the unpaired electron is removed from the C_2 and C_5 carbon atoms (32%). If the π spin densities are examined, an excess of spin in the $^3B_1$ triplet at C_1, C_2 and C_4 suggests that the unpaired electron spends most of its time at these positions. However, in the $^3A_2$ triplet, the unpaired electron resides predominantly at C_3. Hence Pople's[91] findings are in direct contradiction to Taft's[71] original proposal since π donor substituents would exercise greatest stabilisation at otho- and para-positions to C_1 in the $^3B_1$ state, some agreement is evident when the $^3A_2$ state is considered, but it must be remembered that the positive charge is located at C_2 and C_5. Pople's[91] calculations place the singlet state 1.18 eV below the lowest triplet $^3B_1$ phenyl cation.

Evleth and Horowitz[88] have found that the 4-aminophenyl cation has a near degeneracy of singlet $^1A_1$ and triplet $^3A_2$ states in agreement with Pople's[91] predictions regarding the effectiveness of π donor substituents in stabilising the phenyl cation. Pople[92] has considered the stabilising effect gained

Figure (8)

Π charges and Π spin densities (in brackets) of the
phenyl cation as determined by an <u>ab initio</u> method[91]

0.934   0.988

0.937   1.200   Singlet $^1A_1$

(LX1)

0.929   0.876
(-0.388)   (+0.360)

0.828 (+0.561)   (+0.447) 0.561   Triplet $^3B_1$

(LXII)

0.821   0.681
(+0.538)   (+0.163)

0.987 (-0.478)   (+0.075) 1.008   Triplet $^3A_2$
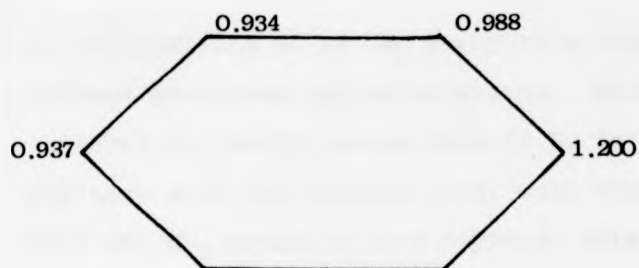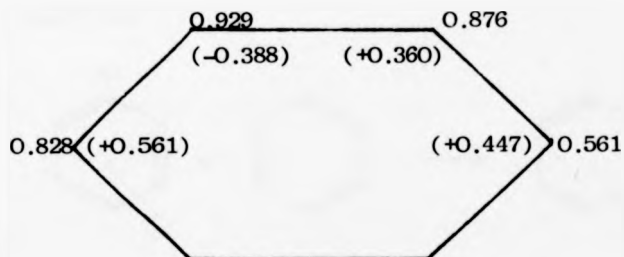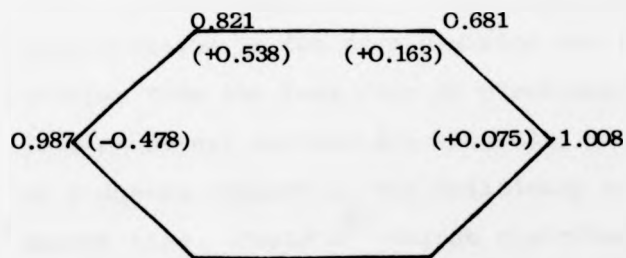
(LXIII)

by the addition of an NH_2 group to a singlet phenyl cation in various positions and orientations. Maximum stabilisation is achieved by the NH_2 group when it is in a para-position and coplanar with the benzene ring, with some degree of stabilisation when the NH_2 group is in a coplanar orientation in both meta- and ortho-positions.

Pople[93] has also extended his *ab initio* calculations to cover the first row species Li, BeH, BH_2, CH_3 NH_2, OH and F. The effect of the various groups was measured by the theoretical reaction:-

$$\text{(structures)} \qquad (59)$$
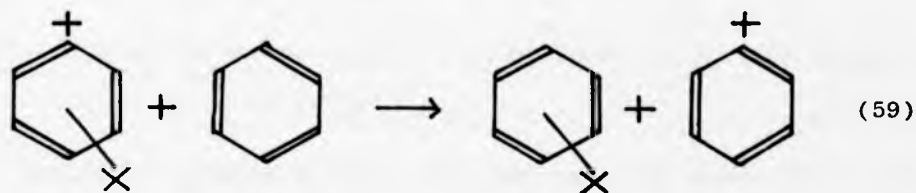
The *singlet* phenyl cation is effectively stabilised both by NH_2 and OH groups, but destabilised by fluorine. All substituents were found to have an ortho, meta,para ordering with respect to their stabilising effect, except NH_2 which affords maximum stabilisation in the para-position due to substantial π effects arising from the lone pair of electrons on the nitrogen atom. Triplet phenyl cations are naturally more readily stabilised by π donors because of the deficiency of π electrons in the phenyl ring. Pople's[91] charge distributions also predict π donors are most effective in stabilising the triplet phenyl cation when situated in the ortho- and para-positions. A π

acceptor, as might be expected, has no stabilising effect since the phenyl ring is already deficient in electrons. Such a substitution would be least effective at a meta-position where spin density is at its highest. The stabilising effects of NH_2 and OH groups in both the ortho- and para-positions are maximised when they are in coplanar configurations.

Finally, Pople[93] has compared the total energies of singlet and triplet $X-C_6H_4^+$: the predictions may be summarised thus:

(i) para-NH_2 exerts *net* triplet stabilisation (cf. the singlet level) of 103.81 kJ mol^{-1}

(ii) para-OH exerts *net* triplet stabilisation (cf. the singlet level) of 31.81 kJ mol^{-1}

It should be noted that these figures refer to small differences between two large total energies with a large inherent possible error. One factor of this work has been to test the validity of Pople's[93] predictions on these two substituents.

2.3. THEORY AND PRACTICE OF ELECTRON SPIN RESONANCE SPECTROSCOPY

The theory and practice of esr spectroscopy is well documented in numerous texts.[94,95,96] Only a brief review is intended here, with the emphasis on the use of esr in the detection and characterisation of triplet states of organic molecules.

An electron both travels around a nucleus (and consequently has orbital angular momentum) and also spins about its own axis (and has spin momentum). The spinning charge can be visualised

as a magnetic dipole, i.e. it functions as a small bar magnet.
Whilst the total electron magnetic dipole is a combination
of the two effects, more than 99% is usually derived from
spin rather than orbital motion. Electron spin is characterised
by the quantum number s, whose only value is $s = \pm\frac{1}{2}$, and the
spatial quantisation of electron spin, by the magnetic quantum
number M_s whose values are also $\pm\frac{1}{2}$.

If the magnetic dipole is placed in an external magnetic
field, it will orientate itself in a given direction of minimal
energy. The electrons will align themselves with their spins
either parallel or anti-parallel to the applied field since no
intermediate alignment is possible. Electrons aligned parallel
will have less energy than the zero field value, and conversely
electrons aligned anti-parallel to the external field will have
more energy. Interaction of a single electron with an applied
field may be represented by the formula

$$E = \pm(M_s g\beta)H \qquad (60)$$

where E = energy of interaction, g is the spectroscopic splitting
factor, H the applied field and β the Bohr magneton. The
spectroscopic splitting factor or 'g-value' is a measure of
the individual spin and orbital motions of an electron as
compared with its total angular momentum, and has a value of
2.0023 for a completely free spin.

The two possible orientations give rise to two differing
energies (Zeeman levels) of the unpaired electron, $+\frac{1}{2}g\beta H$ and
$-\frac{1}{2}g\beta H$, the energy difference being

$$E_2 - E_1 = g\beta H \tag{61}$$

(the two states being degenerate in the absence of an applied field). If the two energy levels are E_1 and E_2, then the energy required to produce a transition is

$$E_2 - E_1 = h\nu = g\beta H \tag{62}$$

where $h\nu$ is a quantum of energy with frequency ν and h is Planck's constant. The microwave frequency ν thus depends upon H, and the proportionality constant between them is given by

$$\gamma = \frac{\nu}{H} = \frac{g\beta}{H} \tag{63}$$

Most spectrometers operate in the X band region, where $\nu = 9.27 \times 10^9$ Hz and $H \simeq 330$ mT; for technical reasons ν is usually kept constant and the magnetic field increased until the resonance condition is reached.

In most cases, the distribution of electrons between the two energy states is given by the Maxwell-Boltzmann expression in which the ratio of the number in the upper state to that in the lower state is given by

$$\frac{N_2}{N_1} = \exp(\frac{-h\nu}{kT}) \tag{64}$$

where k is the Boltzmann constant and T the absolute temperature. Evidently greater sensitivity is achieved both by working at high resonant frequencies, i.e. high $h\nu$, and at low temperatures.

If the absorption of radiation is to continue, there must be some process which allows electrons in the upper level to dissipate energy and return to the ground state (otherwise the two levels would equalise and there would be no net absorption of energy). The ways in which electrons may lose their excess energy are termed relaxation processes. Excess energy may be lost in returning to the ground state by either spin-lattice or spin-spin relaxation. According to the Maxwell-Boltzmann expression, an imbalance exists between N_2 and N_1 of only 1% of the unpaired electrons (at 300 K) since the phenomenon of esr is dependent on promotion of electrons from N_1, the processes of relaxation must be extremely efficient.

Spin-lattice relaxation involves the transfer of energy from the spin system to the lattice by either direct or Raman processes. The direct process is important only at very low temperatures, i.e. ca. 4 K, because lattice vibrational modes are around 10^{13} Hz, rather than 10^{10} Hz as required for direct transfer. In the Raman or indirect process, a phonon is inelastically scattered as an electron flips its spin.

If there is a strong interaction between the unpaired electrons and the lattice, it will have a short relaxation time with a consequent large spread of energies resulting in a broad esr signal.

Spin-spin relaxation is a mechanism, whereby spins exchange energy amongst themselves; such interactions do not directly assist electrons in returning to the lower level, but do make

the system as a whole more conducive to spin-lattice relaxation. Since such interactions are dependent on the concentration of magnetic dipoles, they can be removed by dilution of the sample.

In addition to the applied magnetic field, other small permanent local fields may be present arising from magnetic nuclei in the molecule and occasionally from other unpaired electrons. The interaction of an unpaired electron with other magnetic nuclei is termed nuclear hyperfine interaction which is observed as fine structure in an esr spectrum. Frequently an unpaired electron is sensitive to the magnetic dipoles of neighbouring protons within the molecule. A proton with a nuclear spin of $I = \frac{1}{2}$ can have two possible orientations of its magnetic dipole corresponding to $M_I = +\frac{1}{2}$ or $-\frac{1}{2}$ with respect to the unpaired electron. Since $(2I + 1)$ orientations are possible $(2nI + 1)$ lines are observed where n = number of equivalent protons. Neutrons also possess a magnetic moment by virtue of their substructure. N^{14} nuclei have a nuclear spin of 1 and upon interaction with an unpaired electron give rise to three lines of equal intensity.

2.4. DETECTION OF TRIPLETS STATES BY ESR SPECTROSCOPY

Considering the case of $S = 1$, M_S will have values of +1, 0 or -1, and according to the selection rule $\Delta M_S = \pm 1$, two transitions are possible and will occur superimposed on each

other (Fig.9). However, ions possessing more than one unpaired
electron always have a zero field splitting between the various
spin levels, which gives rise to two lines (Fig. 10).

Zero field splitting, when detected, will be highly
anisotropic, necessitating strict orientation of the sample
within the cavity. Orientation will determine the level of
zero field splitting between $M_S = 0$ and the $M_S = \pm 1$ levels.
One method of overcoming the highly anisotropic effect is to
use the so-called forbidden transition, $\Delta M_S = 2$. To observe
the $\Delta M_S = 2$ transitions, it is necessary to orientate the
orbital momentum vectors by making the microwave field within
the cavity parallel to the D.C. applied magnetic field. (This
is achieved in the case of our resonant cavity which is of
the TE_{102} variety). This enables the $\Delta M_S = 2$ transitions to
be detected without crystal anisotropy affecting the spectrum.
As may be seen in Fig. 10, the $\Delta M_S = \pm 1$ transition will give
two anisotropic lines whilst the $\Delta M_S = 2$ transition will occur
at half the average field position of the two $\Delta M_S = \pm 1$ transitions,
that is $g \simeq 4$ for a comparatively free spin.

Systems where more than one unpaired electron is present are
frequently encountered. Transition metal ions with incompletely
filled d orbitals may accommodate up to five unpaired electrons,
giving a total spin of $5/2$. Organic molecules may also possess
more than one unpaired electron, biradicals and the triplet
state being notable examples.

Figure (9)

$\Delta M_S = 1$ transitions in the absence of zero field splitting.

Figure (10)

$\Delta M_S = 1$ transitions with zero field splitting
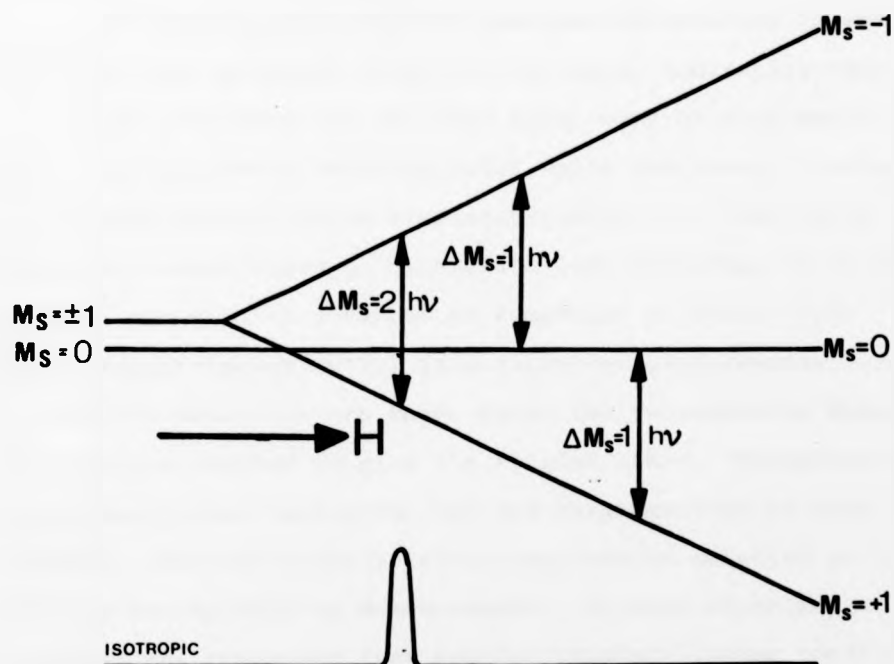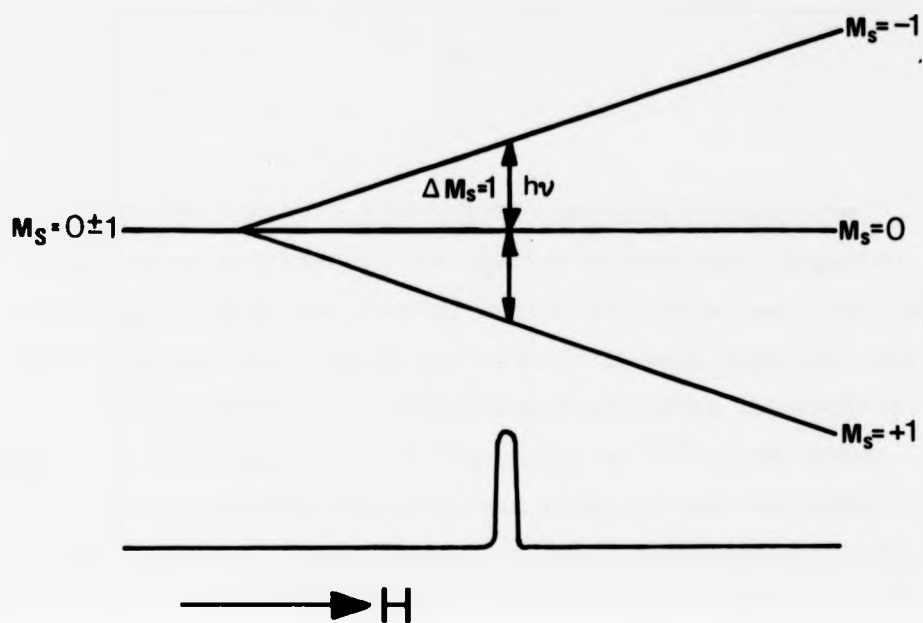
Molecules containing more than one unpaired electron experience an additional contribution to the local magnetic field, i.e. simply the dipolar magnetic field of one electron exerted at the position of the other. In many respects, the situation is analogous to anisotropic hyperfine interaction, but since the electron magnetic moment is 10^3 times larger than nuclear magnetic moments, the local electronic field is correspondingly more intense and may dominate the entire spectrum.

In biradicals, the electron-electron interaction is weak and these have g-values close to free spin, indicating that any coupling between the unpaired spins must be very small, since the spin-orbit coupling would split the energy levels giving effective g values displaced from $g \simeq 2$. The first systematic experiments on biradicals were performed by Jarrett et.al.[97] who studied a number of compounds of which 4,4-methylenebistriphenylmethyl is a representative example.

Certain molecules are known where the two unpaired spins are strongly coupled to give the triplet state. Phosphorescent compounds are one such group and the paramagnetism of such molecules excited to the triplet state can be detected by magnetic susceptibility measurements. Initial experiments to detect any resonance from excited triplets (under conditions where $10^{14} - 10^{15}$ unpaired spins were present) failed. It might be reasonably concluded that some factor must be entering which results in the signals being broadened beyond detection.

Consideration of the behaviour of the triplet energy levels in any non-crystalline solid material will show that this may be expected. It has already been said that there will be significant spin-orbit interaction if the electrons couple to give a resultant spin of $S = 1$. This interaction will split the three levels of the triplet state even in zero magnetic field, and in any molecule without spherical symmetry, the effect of this splitting on the spectrum will vary with the angle between the applied magnetic field and the molecular axis. This variation in splitting between the levels on application of a magnetic field arises from the two competing axes of quantitisation, i.e. that of the magnetic field and the molecular axis of symmetry (which subtend an angle θ).

Consequently, it is not surprising that in the case of rigid solutions containing randomly orientated triplets, θ may take any one of a large number of values, and the resulting spectrum will comprise a series of overlapping lines (arising from $\Delta M_S = 1$ transitions), and the overall signal will be too broad to detect.

Following the acceptance of extensive line broadening in randomly orientated molecules, Hutchinson and Mangum[98] performed a series of experiments on *orientated* molecules, demonstrating the usefulness of esr spectroscopy as a diagnostic aid in the analysis of triplet states. They observed $\Delta M_S = 1$ transitions in the esr of phosphorescent naphthalene in a single crystal of durene. Alignment of the triplets was desirable because the external field for such resonance varied over 200 mT.

Van der Waals and de Groot[99] observed that $\Delta M_S = 2$ transitions could be detected in randomly orientated samples. By removing the necessity of using single crystals, they considerably increased the number of species which could be examined.

In esr spectroscopy, triplet states are characterised by two parameters, referred to as D and E (Fig. 11). D may be regarded as the energy difference between $M_S = 0$ and the mean separation of the $M_S = \pm1$ levels in the absence of an external magnetic field, (i.e. it is a measure of the dipole-dipole interaction of the two unpaired electrons). The second parameter E is a measure of the separation between $M_S = +1$ and $M_S = -1$ at zero field.

The D parameter may be determined in triplet molecules having threefold or higher axes of symmetry from the position of the $\Delta M_S = 2$ transition since theory predicts that it should occur at half the average field positions of the two $\Delta M_S = 1$ transitions. However, with lower symmetry, and the introduction of a second parameter inducing overlapping of absorptions, such a ready assignment of the $\Delta M_S = 2$ transition is not always possible. The detection of $\Delta M_S = 1$ transitions in randomly orientated molecules combines the flexibility of the half field technique with several of those from single crystal analysis.

The esr spectra of excited triplets like naphthalene[100] and ground state triplets of transition metal ion complexes are well known, but few organic ground state triplets have been reported.

Figure (11)

Energy levels and transitions as a function of magnetic field for a ground state triplet
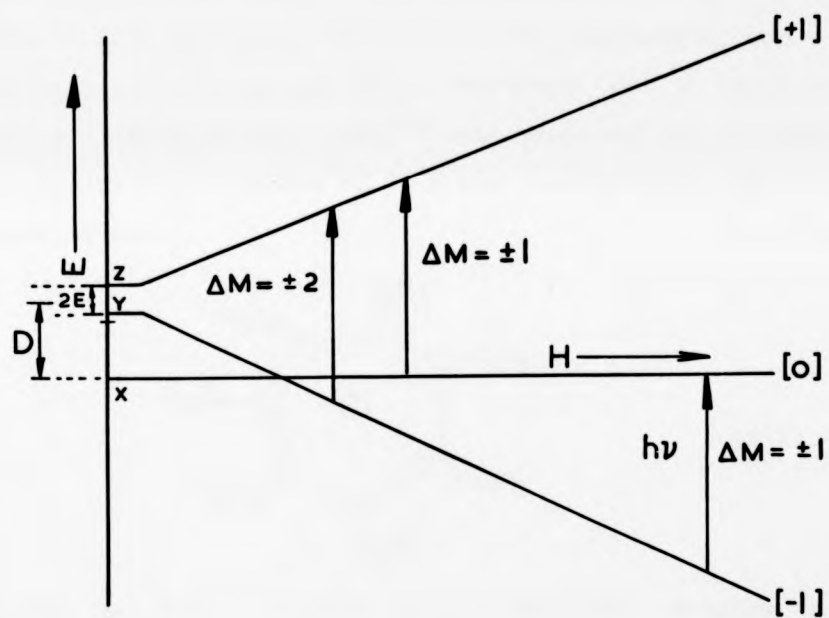
Tetraphenylcyclobutadiene[101] and the pentaphenylcyclopentadienyl cation[102] are both potential triplets, but are too unstable to isolate. Breslow and Chang[103] have prepared the heptaphenyl-cycloheptatrienyl anion, a derivative of the eight π-electron cycloheptatrienyl anion. The heptaphenylcycloheptatrienyl anion (LXIV), however, was found to be diamagnetic and consequently Breslow and Chang concluded that it was a singlet species. Breslow and Chang[104] have prepared the pentaphenyl-cyclopentadienyl cation at 77 K and demonstrated that it is a ground state
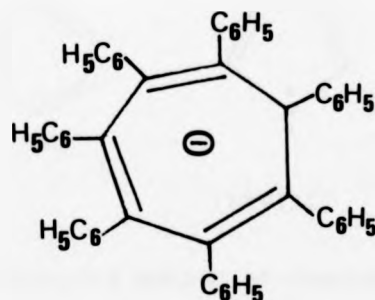
(LXIV)

triplet but did not record its esr spectrum. Breslow, Chang and Wasserman[105] have reported the esr spectrum of the pentachlorocyclopentadienyl cation (LXV) in which the $\Delta M_S = 1$ and $\Delta M_S = 2$ transitions were observed.
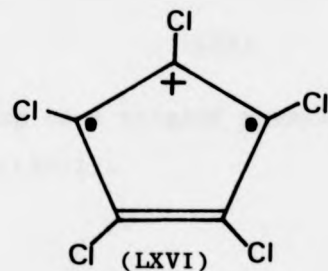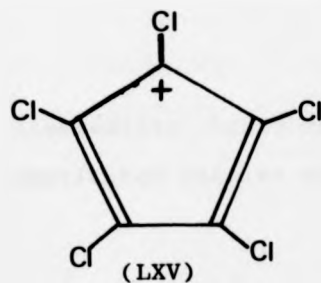
(66)

Wasserman et.al.[105] have also confirmed the existence of several other substituted cyclopentadienyl cations as ground state triplets from their highly characteristic esr spectra. Recently[106] the unsubstituted cyclopentadienyl has been reported to be a ground state triplet from esr data. Dibenzocyclopentadienylidene[107] (biphenylenemethylene) (LXVII), cyclopentadienylidene (LXVIII) and indenylidine (LXIX) are also reported to be ground state triplets.
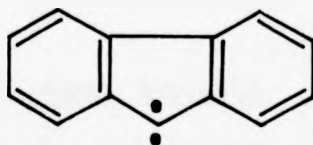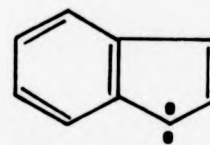
(LXVII)   (LXVIII)   (LXIX)

The only substantial series of organic ground state triplets are those derived from irradiated benzene 1,4-diazooxides[108] (LXX).   The

(LXX)

intermediate (LXXI) may be regarded as a triplet phenyl cation substituted with an oxygen anion (LXXII).

(66)

(LXXXI)   (LXXII)
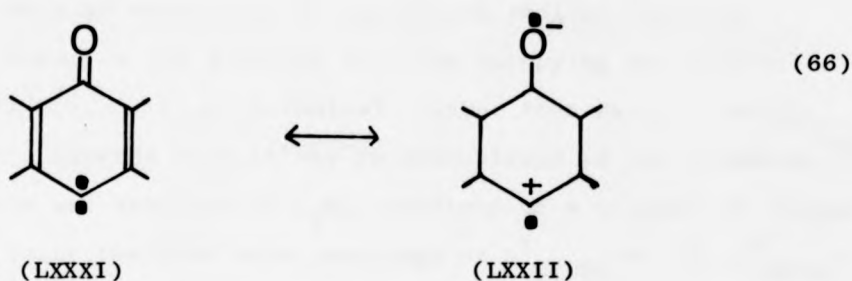
Structure (LXII) which has five π ring electrons is very
similar to the (π,σ) type triplet phenyl cation originally
proposed by Taft[71].

2.5. PHENYL RADICALS

The phenyl radical may be generated by a number of methods
at 77 K, <u>e.g</u>. Tanei[109] has observed its esr spectrum from the
ultra-violet irradiation of benzene. Similar esr spectra have
been recorded from photolysing iodobenzene adsorbed on silica
gel,[110] and the reaction of a sodium atom with

$$ArI + Na \longrightarrow Ar \cdot + NaI \qquad (67)$$
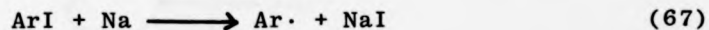
iodobenzene on a rotating cryostat[111]. Phenyl radicals have
also been detected by esr in photolytic and radiolytic
solution systems[112] by decarboxylation of the parent
carboxylic acid, <u>i.e</u>.,

$$ArCO_2^- + SO_4^{\cdot -} \longrightarrow Ar \cdot + SO_4^{2-} + CO_2 \qquad (68)$$
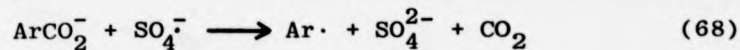
The high reactivity of the phenyl radical has been attributed to the unpaired electron occupying an sp -hybrid orbital [113] (_i.e._. σ-radical) rather than earlier models which suggested that it may be delocalised in the π system.[114]

The esr spectrum of $C_6H_5\cdot$ consists of a triplet of triplets when fully resolved with couplings of $a^H_{ortho} \sim 1.8$, $a^H_{meta} \sim 0.6$ and $a^H_{para} \sim 0.3$ mT for the ring protons. Slight variations in the coupling constants and resolution occur depending on the matrix used to trap the radical (Table 3).

Spin-trapping techniques[117] have also demonstrated the formation of phenyl radicals in solution. An intermediate[118] formed during the dye-sensitized photolysis of para-dialkylaminobenzenediazonium salts has been trapped using the stable nitrone 2-methyl-2-nitrosopropane[119]. The spin
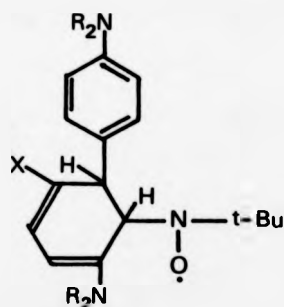
(LXXIII)

where X = H or Cl

adduct (LXXIII) exhibits an esr spectrum consisting of 3 × 2 lines _viz_. a main triplet arising from the N^{14} nucleus of the nitroxide group with a secondary smaller doublet splitting

TABLE 3

PROTON HYPERFINE COUPLING CONSTANTS FOR PHENYL RADICAL/mT

	Matrix	Ortho	Meta	Para
A_{ISO}	xenon	1.74	0.59	0.19
	C_6D_6	1.81	0.64	0.30
	silica gel[110]	1.71	0.65	
	water[116]	1.81	0.64	
A_x	xenon	2.19	0.66	0.20
	C_6D_6	2.12	0.66	
A_y	xenon	1.54	0.61	0.25
A_z	xenon	1.49	0.50	0.12
A_y, A_z	C_6D_6	1.69	0.64	

Data from Bennett and Mile[115]

originating from the single proton. Spin adducts have not
been observed from 2,5-dialkoxy-substituted arenediazonium
salts presumably because of steric hindrance at the reactive
site. The technique has also been used by Janzen et.al.[120]
to determine rate constants for hydrogen abstraction (from
methanol, ethanol and 2-propanol) by the phenyl radical.

Norman [121] et.al. have generated phenyl radicals in solution
by the one-electron reduction of arenediazonium salts with
titanium (III) ions. Only esr spectra corresponding to
solvent-derived radicals were observed, the

$$Ti^{III} + ArN_2^+ \longrightarrow Ti^{IV} + Ar\cdot + N_2 \qquad (69)$$

phenyl radical evading detection. This failure to detect
phenyl radicals was attributed to their highly reactive nature.
Phenoxyl radicals[122] have also been detected in the photolysis
of arenediazonium salts in solution, *viz*.

$$ArN_2^+ \longrightarrow Ar^+ + N_2 \qquad (70)$$

$$Ar^+ + H_2O \longrightarrow ArOH_2^+ \longrightarrow ArOH + H^+$$
$$\updownarrow$$
$$ArO^- + H^+ \qquad (71)$$

$$ArN_2^+ + ArO^- \longrightarrow Ar\cdot + ArO\cdot + N_2 \qquad (72)$$

2.6. SPECTRA OF TRANSIENT INTERMEDIATES

While many elaborate mechanisms have been formulated to account for the products formed from the photodecomposition of arenediazonium salts, these have been primarily based on product analysis.

Few workers have attempted direct observation of the reactive intermediates, although Porter and Ward[123] have detected phenyl radical absorption in the gas phase flash photolysis of benzene and halogenated benzenes. A rigorous analysis of their results indicates that the ground state electronic configuration of the phenyl radical is $(\pi^6 n)$ rather than $(\pi^5 n^2)$, while optical absorption of the phenyl radical is taken as arising from a $n \leftarrow \pi$ transition (Fig. 12). Cercek and Kongshaug[124] claim to have observed optical absorptions of phenyl and hydroxyphenyl in solution, using pulse radiolysis, the radicals being generated by the dissociative attachment of the hydrated electron, e^-_{aq}, to iodobenzene and para-bromophenol (Fig. 13). Their spectra are not in good agreement with those of Porter and Ward.

Calvert et.al.[50] attempted to record the ultra-violet spectrum of phenyl radical during the photolysis of para-dimethylaminobenzenediazonium tetrachlorozincate in an EPA glass at 77 K (Fig. 14). No interpretation of their resultant spectrum is offered other than that it probably arises from a short-lived species whose lifetime is very temperature-dependent.

Figure (12)

Electronic configuration of the phenyl radical.

Figure (13)

Optical absorption spectrum (by pulse radiolysis) of
a) $C_6H_5\cdot$ and b) $HOC_6H_4\cdot$

Figure (14)

Ultra-violet spectrum of the intermediate formed during
the photolysis of 4-N,N-dimethylbenzenediazonium
tetrachlorozincate in an EPA glass at 77 K.
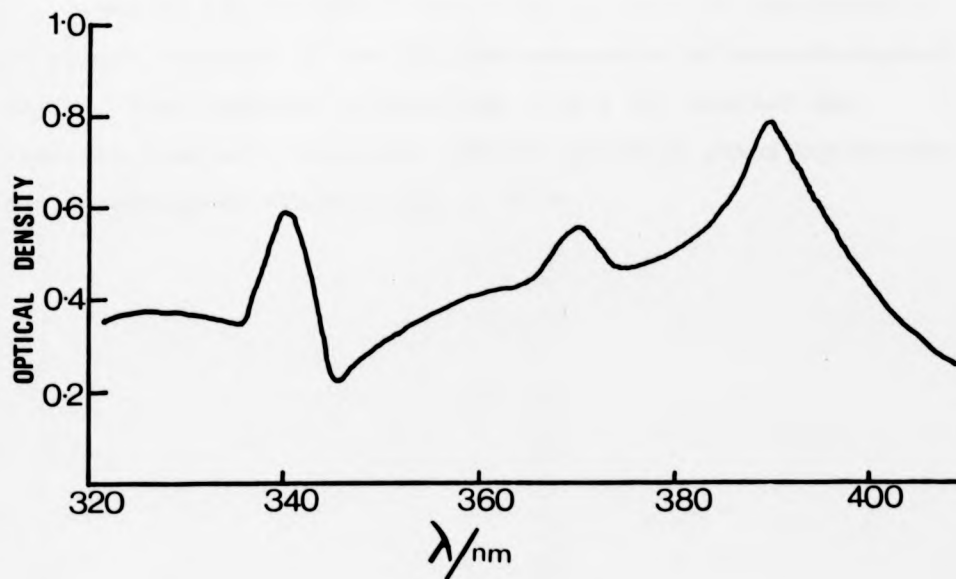
Böttcher et.al.[125] have presented evidence for the formation
of aryl cations as intermediates in the solution flash
photolysis of para-substituted arenediazonium salts in aqueous
solution. Their results are summarised in Table 4.

TABLE 4

Substituent group	λ_{max} intermediate	$\tau/\mu s$	
NEt$_2$	500	153.0	(at pH = 2)
OMe	420	65.0	
Cl	450	23.6	
NO$_2$	420	16.7	
H	400	1070.0	(ethylene glycol)

Sukagari and Kikuchi[18] have also claimed the intermediacy
of phenyl radicals in the photodecomposition of arenediazonium
salts. They observed a broad ($\Delta H \sim 2.5$ mT) singlet esr
spectrum from an irradiated (259 nm) methanol glass containing
benzenediazonium fluoroborate at 77 K.

CHAPTER III

MATERIALS AND METHODS

3.1. DESIGN AND OPERATION OF ESR SPECTROMETERS

The esr spectrometer at Warwick University, which has
been used for a large proportion of this work, is a con-
ventional X-band instrument supplied by Decca Radar Ltd.,
Model X-1.

Energy is supplied to a cavity (in which the sample under
observation is placed) through a rectangular wave guide, from
a source known as a klystron which emits monochromatic micro-
wave radiation ca. 9270.387 MHz. Microwave energy is passed
into the sample cavity through a small hole referred to as an
iris and is then fed to the detector,a crystal diode, *via* a
T-shaped bridge. A general purpose cavity operating in a TE_{102}
mode has been employed throughout this work. The original
copper-plated glass windows of the cavity were replaced by
more robust gold-plated ceramic ones. Two tuning controls
and a third coupling control are fitted to the cavity enabling
the microwave bridge to be tuned to produce zero current in
the crystal detector. Subjecting the cavity to a uniformly
varying magnetic field will remove the degeneracy of the spin
states of an unpaired electron, typically 330 mT for organic
radicals with relatively free spin. The net absorption of
microwave energy involved with an electron 'flipping its spin'
results in an unbalanced microwave bridge; this imbalance is
detected as a rise in current at the crystal diode. A seven
inch electromagnet with the poles 7.0 cm apart, giving a
maximum field of 600 mT (Newport Instruments, Ltd.) was used

in conjunction with the Decca esr spectrometer. 100 kHz
modulation of the magnetic field was used for phase sensitive
detection to produce a d.c. output signal applied to a pen
recorder, the modulated signal appearing on the first derivative
of the absorption curve. Spectra were recorded on a Hewlett-
Packard X-Y recorder using a sweep time and modulation
amplitude that gave maximum resolution. Spectra were also
recorded using Varian E-3, Varian E-109 and Bruker ER-200 tt
esr spectrometers.

The g-values were determined by calibrating the magnetic
field with standards of known g value and coupling constants.
Dilute solutions of Fremy's salt (potassium peroxylamine
disulphonate) display an esr spectrum of three lines of equal
intensity with a separation of 1.307 mT. A solution of
α,α'-diphenyl-β-picrylhydrazyl in benzene exhibits a five-
line spectrum with the lines in the intensity ratio of 1:3:5:3:1,
and was used as the second standard to calculate unknown g-values
from equation (73):

$$g_u = \frac{g_1 g_2 (X_1 + X_2)}{g_1 X_1 + g_2 X_2} \tag{73}$$

g_1 and g_2 are the respective g-values of standards and X_1 and
X_2 are field differences from the g_u position. Manganese (II)
sulphate, which has an esr spectrum comprising six lines of
approximately equal intensity separated by 9.80 mT was
occasionally used as a third standard. Calibration of the
entire magnetic field was accomplished using a finely powered

sample of 2% $[Cr(NH_3)_5Cl]Cl_2$[126] diluted in $[Co(NH_3)_5Cl]Cl_2$
prepared by co-crystallisation. The complex gives a total
of nine well-resolved lines at various intervals ranging
from 134.4 mT to 514.0 mT.

The original variable temperature probe supplied by Decca
Radar Ltd. was very cumbersome and frequently damaged during
use. This was replaced by a much simpler version based on the
original Decca design, but not incorporating the heating element
or thermocouple. Whilst the modified device could be used at
77 K for some time, loss of microwave power due to water con-
densing in the cavity was an occasional problem. Spectra were
recorded from samples at 77 K using a finger dewar on both
the Varian and Bruker esr spectrometers.

The simple goniometer designed for operation with a finger
dewar and Varian esr spectrometer was used for the single crystal
studies (Fig. 15). A small amount of silicone grease was used
to hold the crystal in place. Orientations were determined by
reference to the steel needle placed in the cork.

Samples were irradiated in a quartz dewer through a pyrex
filter with a HBO 200 W Wotan high pressure mercury vapour lamp.

Low-temperature glasses were prepared in an esr tube shown
in Fig. 16, with the sample placed in one of the side arms. All
glasses were degassed using a freeze-pump-thaw cycle (three
times) on a standard vacuum line operating at 1.3×10^{-4} Nm^{-2}.
Once degassed, the sample tube was sealed off using the stopcock
(G) and the sample gently shaken into the spectrosil tube.

Figure (15)

The goniometer

Key:-

(a) quartz rod

(b) protractor

(c) glass bush

(d) reference needle

(e) cork

(f) transparent quartz

(g) liquid nitrogen

(h) crystal
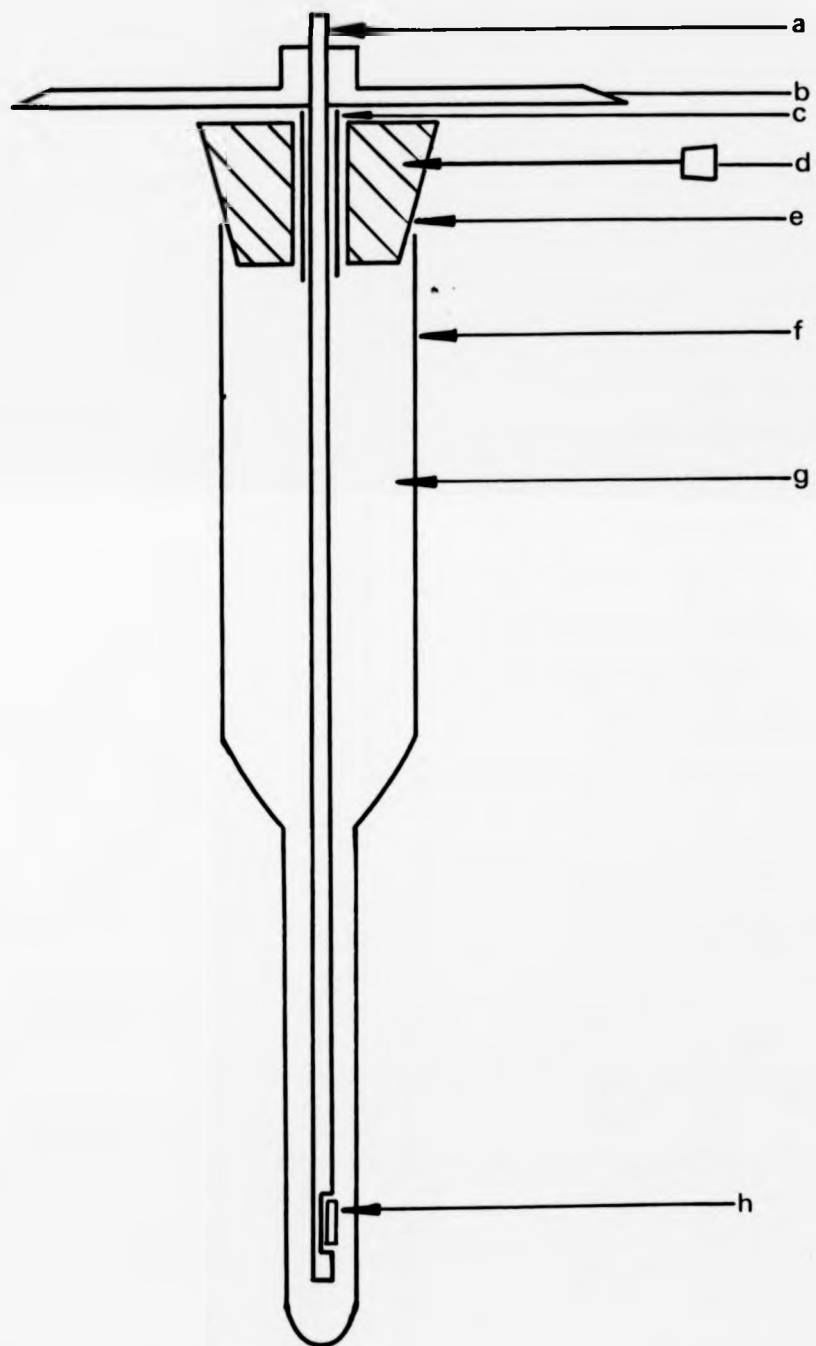
Figure (16)

ESR sample Tube

Key:-

B) sample bulbs

C) B10 cone (at a right angle to drawing)

G) greaseless stopcock

S) 'Spectrosil' sample tube

g) graded seal

o) 'Viton-A' 'O' ring
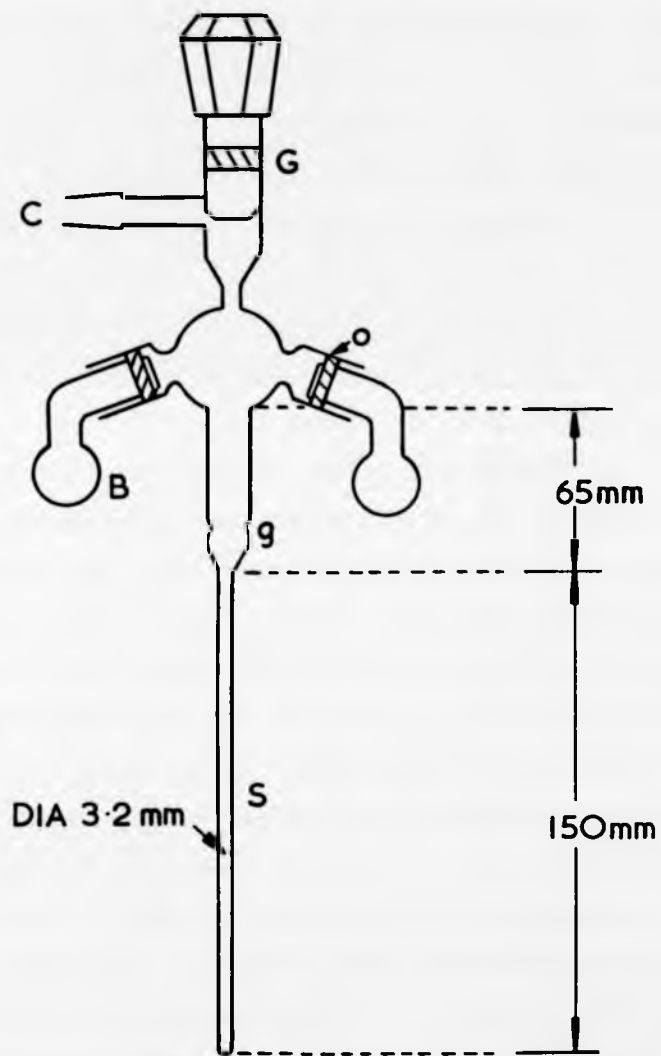
Spectrosil tubing (3.2 × 150 mm) with one end sealed was used for polymer films containing arenediazonium salts. The polymer film was inserted into the esr tube by either cutting a strip of film ca. 8 × 2 mm and coiling it into a cylindrical roll or cutting the film into small pieces which could then be lightly packed into an esr tube by gentle shaking.

3.2. THE OPTICAL BENCH

The optical bench (Fig. 17) consisted of a suitably housed high-pressure mercury vapour lamp, Wotan type HBO 200 W, connected to a power supply unit type S.C.T. 104 (supplied by K.S.M. Electronics Ltd., Potters Bar, Hertfordshire), giving a stabilised current to within ±0.1%. Two quartz plano-convex lenses were positioned directly in front of the lamp to give a parallel light beam which was focused by a third quartz lens. Narrow band Balzer metal interference filters were used to obtain monochromatic light of an appropriate wavelength. A Bausch and Lomb monochromator adjusted to give a bandwidth of 5.0 nm was used to evaluate any effects of vibrational energy on quantum yields. Solutions were photolysed in a cylindrical quartz cell (volume 20.0 cm ^{3}) placed in the water bath through which tap water was continually circulated to maintain a constant temperature.

Quantum yields are given in terms of reactant disappearance which may be defined as:-

Figure 17

The optical bench

Key:-

C)   cooling tower

M)   mercury vapour lamp

A)   adjustment screws (for aligning lamp)

P)   quartz plano-convex lenses

F)   quartz focusing lens

S)   shutter

B)   Balzer filter

W)   water bath

L)   light shield

T)   Teflon seals
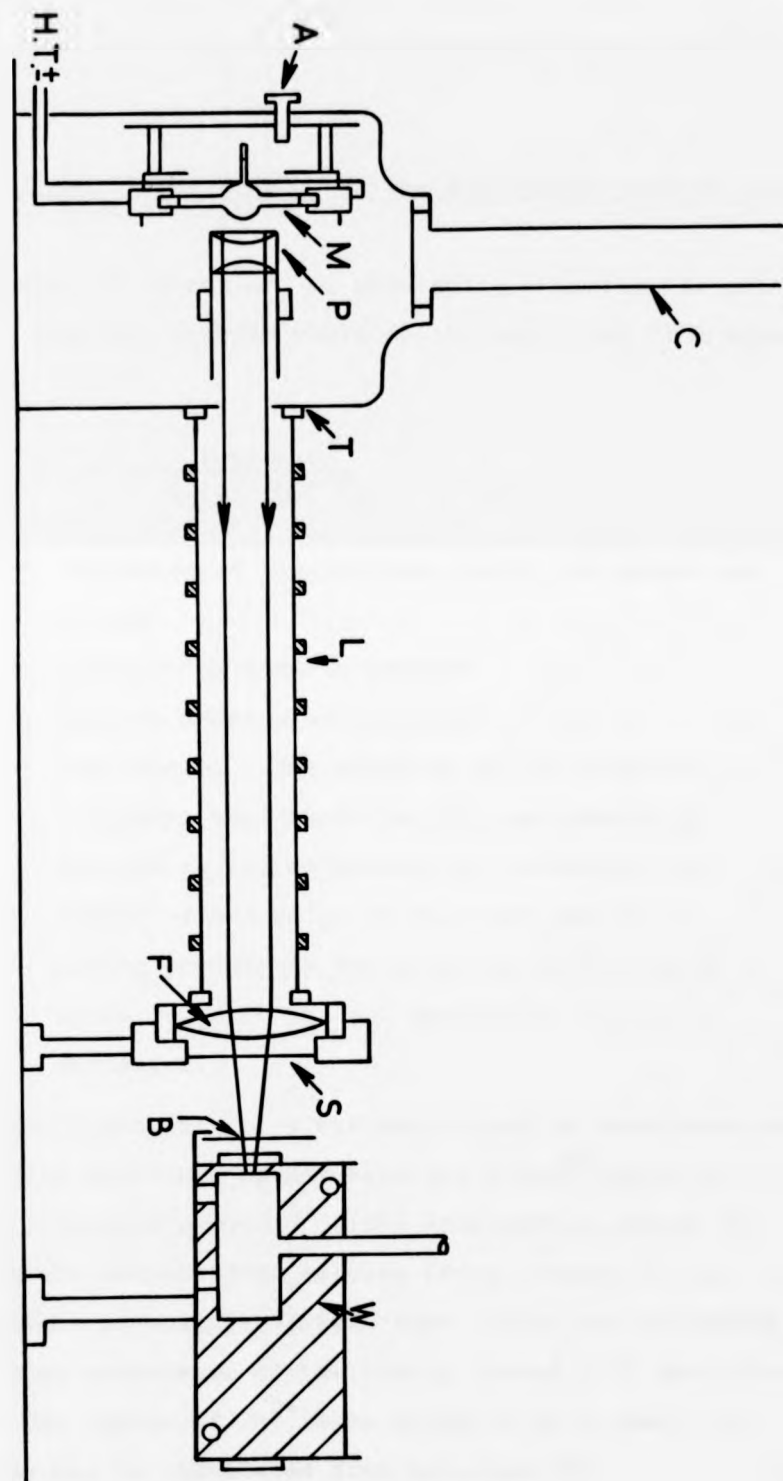
$\phi=\dfrac{\text{number of molecules undergoing the particular process concerned}}{\text{number of quanta absorbed}}$

$$(74)$$

If the number of molecules, n, undergoing a particular process is known, then the quantum yield can be estimated from equation (75).

$$\phi = \frac{n_{reactant}}{I_0 t(1-10^{-OD})} \qquad (75)$$

I_O = intensity of the incident light, in quanta per second

t = irradiation time in seconds

OD = optical density of solution

$(1-10^{-OD})$= fraction of light absorbed by the reactant (assuming that there is only one absorbing species at the wavelength of investigation.

$n_{reactant}$= number of molecules of reactant destroyed during photolysis for a period sufficiently short to leave the net absorbance virtually unchanged.

The incident light intensity was determined in accordance with the procedure described by Hatchard and Parker[127] employing a potassium trisoxalatoferrate (III) actinometer, which is based upon the proportional release (with respect to the incident light intensity) of Fe^{2+} ions, which are estimated from the high absorbance of the easily formed 1:10 phenathroline complex. The number of Fe^{2+} ions produced as a result of irradiation may be calculated from equation (76).

$$n_{Fe}^{2+} = \frac{6.023 \times 10^{20} \times V_1 V_3 \times O.D.}{V_2 l \varepsilon} \qquad (76)$$

where

V_1 = the volume of actinometer solution irradiated (cm^3)

V_2 = the volume of aliquot taken for analysis (cm^3)

V_3 = the final volume to which the aliquot V_2 is diluted (cm^3)

O.D. = the measured optical density of the solution at 510 nm after the addition of 0.1% 1:10 phenanthroline and buffer

ε = the experimental value of the molar extinction coefficient of the Fe^{2+} complex as determined from the slope of a calibration plot (i.e. 1×10^4 M^{-1} cm^{-1}).

Optical measurements and spectra were recorded using a Cary Model 14 spectrophotometer and either 1.0 cm quartz cells or standard circular actinometry cell with a path length of 5.0 cm.

3.3. LOW-TEMPERATURE ULTRA-VIOLET CELL

The low-temperature ultra-violet cell illustrated in Fig. (18) was designed for use with a Cary 14 spectrophotometer. The apparatus consists of two sections connected by a B2 joint, allowing access to the copper block cell. The two small B14 joints in the lower section enable a thermocouple to be fitted

Figure (18)

The low temperature ultra-violet cell

Key:-

a) connection to vacumm line

b) tap

c) silvered surface

d) B2 joint

e) glass-to-metal seal.

f) copper block assembly

g) quartz windows

h) sealing wax

i) thermocouple
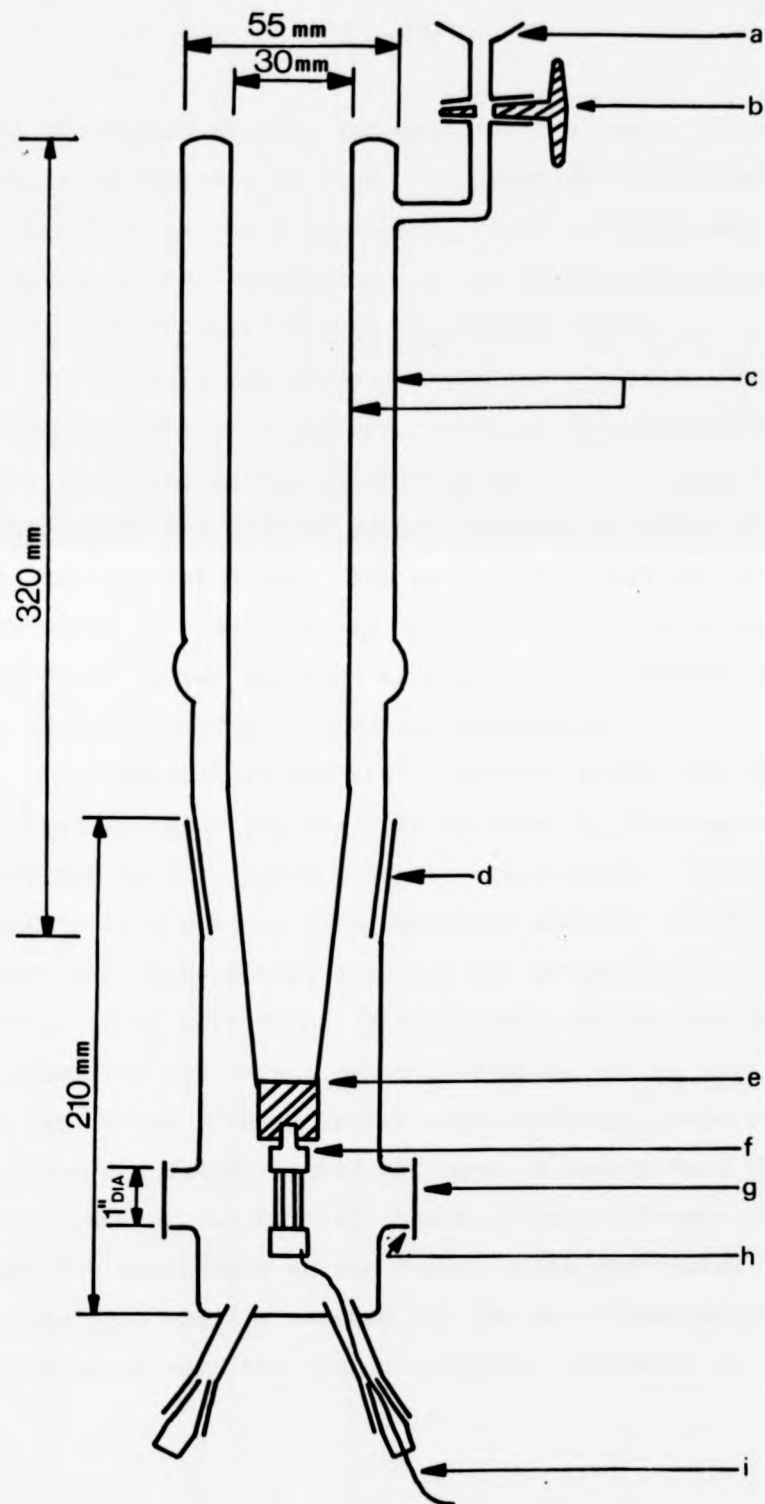
into the copper block. Temperatures 2-3° above 77K were frequently achieved on test. In practice, the thermocouple was not employed on a day-to-day basis as this made the apparatus rather cumbersome and the connections to the electric thermometer masked the optical train.

In practice its operation was quite satisfactory for recording spectra in polymer films, but a low temperature glass of either E.P.A. or MTHF could not be created in the cavity (Fig. 19) without either cracking of glass or solvent loss during evacuation. The rubber 'O' rings were a refine-ment added at a later stage to alleviate the problem; also a 'teflon' spacer was used in place of the original brass one, but with little improvement in performance.

Low-temperature spectra in polymer films have been obtained by inserting the film between the two quartz windows which are held in place with the brass stays. The copper block is then screwed into the upper section, a dummy washer (soft lead) and thermal conductivity grease being used at the joint. After attachment of the lower section, the whole system is evacuated to prevent water condensing on the cold surfaces, the tap marked A being in the open position. Once the system has been evacuated, liquid nitrogen is poured into the inner dewar. During the initial stages, liquid nitrogen loss is quite heavy but diminishes as the copper block approaches 77K. Fifteen minutes were usually allowed for the equilibration of the copper block with the liquid nitrogen. Although of little

Figure (19)

Detail of cooper block assembly

Key:-

a)   brass washer

b)   quartz windows

c)   brass stays

d)   'O' ring

e)   cavity for thermocouple
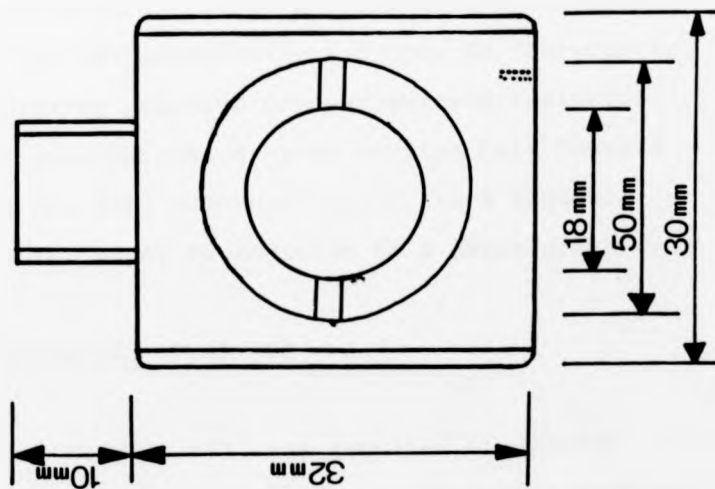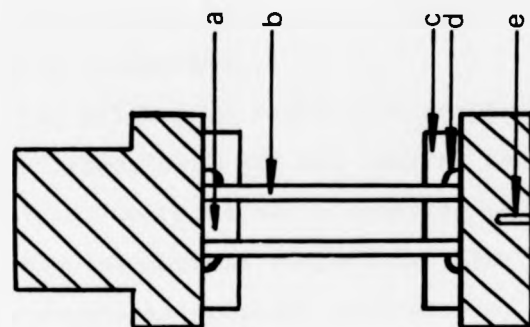
consequence, the evacuation trap was left open to the vacuum line during the cooling period to ensure a reasonable vacuum. Samples were irradiated through the quartz windows and spectra recorded at appropriate intervals.

The apparatus was allowed to reach room temperature by letting the liquid nitrogen boil off and leaving the apparatus to stand for a couple of hours before attempting to separate the two sections. When at ambient temperature, the system was introduced to atmospheric pressure very slowly, as the insides of the outer quartz windows occasionally become dirty with atmospheric dust.

3.4. THE X-RAY DIFFRACTOMETER

Data for the structure of 4-morpholinobenzenediazonium tetrafluoroborate was collected using a Syntex P2 four-circle diffractometer employing graphite monochromatised radiation. The diffractometer was controlled by an On-line Data General Nova computer, and all data recorded on a 7 track magnetic tape (for computer analysis) in addition to a paper print-out.

3.5. THE LASER FLASH PHOTOLYSIS APPARATUS

The ruby laser (Model K 347) was supplied by Applied Photophysics Ltd. 50 ns output pulses were frequency-doubled with an ammonium dihydrogen phosphate crystal to yield 347 nm radiation. The monitoring source was a pulsed 250 W xenon lamp. In the K 347 equipment, a colinear arrangement of the

laser and analysing beams was employed from the monochromator/
photomultiplier tube detection system. Signals were stored in
a Tetronix model 7623 storage oscilloscope equipped with 7B50
and 7A14A amplifiers. Traces were photographed on polaroid
negative film and enlarged for analysis, which was performed
using a least-squares computer program. The physical arrange-
ment of the various components in the system is shown in (Fig.
20).

3.6. SYNOPSIS OF SYNTHETIC ROUTES TO ARENEDIAZONIUM SALTS

Simple arenediazonium salts are conveniently prepared by
diazotisation of the purified parent amine, most of which are
commercially available. Structurally more complex diazonium
salts frequently require a synthesis involving several stages
which may be summarised as insertion, etherification, reduction
and finally diazotisation.

Nucleophiles like morpholine, pyrrolidine, piperidine and
thiocresol may be readily inserted into the aromatic ring with
gentle boiling in alcoholic solvents.

(77)
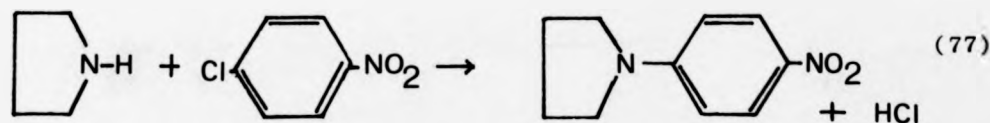
Similarly, 4-N,N-dialkyl nitroaromatics may be obtained *via*

Figure (20)

The laser flash photolysis apparatus

Photo-
Multiplier

Power
Supply

High Intensity
Monochromator

Filter

Oscilloscope

Absorption
Cell

Power
Supply

Xenon
Arc

Pulsing
Unit

Beam
Splitter

Filter

Frequency
Doubler

Filters

Trigger
Photutube

Q-Switched
Ruby Laser

$$CH_3CH_2Br + H_2N-\underset{\text{}}{\bigcirc}-NO_2 \rightarrow (CH_3CH_2)_2N-\underset{\text{}}{\bigcirc}-NO_2 + 2HBr \quad (78)$$
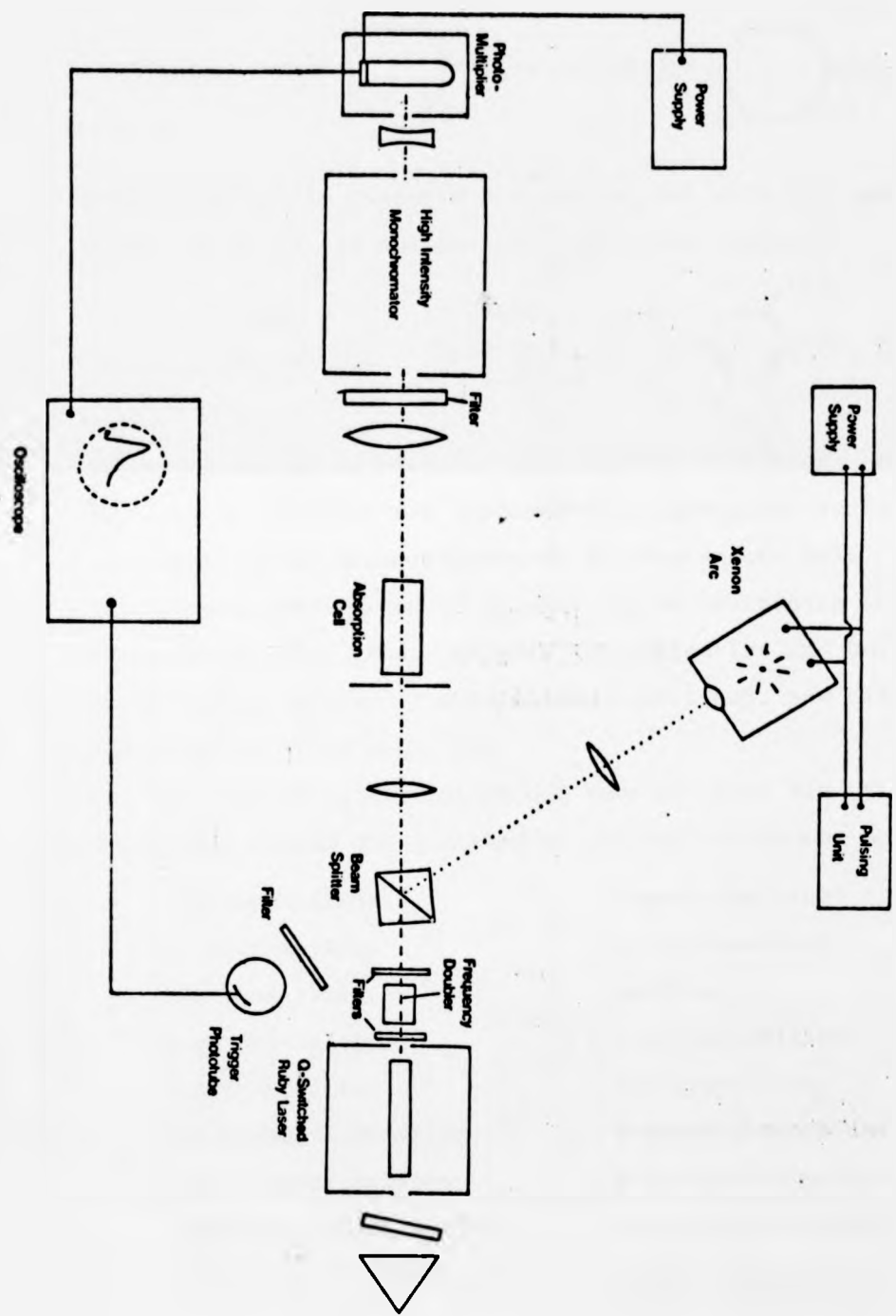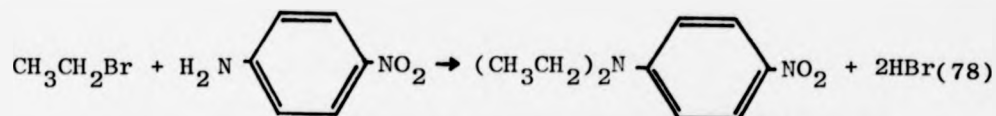
Etherification is conveniently carried out with the appropriate alkyl halide in dry acetone over potassium carbonate.

$$\underset{\text{OH}}{\overset{\text{OH}}{\bigcirc}}-NO_2 + CH_3I \xrightarrow[\text{Acetone}]{K_2CO_3} \underset{\text{OCH}_3}{\overset{\text{OCH}_3}{\bigcirc}}-NO_2 + 2HI \quad (79)$$
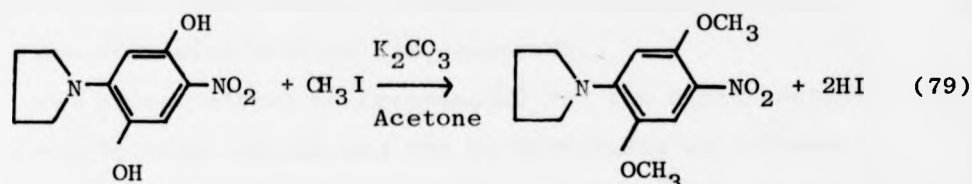
Reduction may be carried out by a variety of methods; classically Sn + HCl or Zn + HCl are employed with subsequent isolation of the amine as the chlorozincate or chlorostannate salt. However, the extreme sensitivity of aromatic amine containing strong electron-donating groups to both auto-oxidation and heat necessitates the use of much milder conditions, and catalytic reduction is to be preferred.

The following list of amines have all been diazotised by the direct method and isolated as tetrafluoroborate salts:-

4-methylaniline	3-methylaniline
4-chloroaniline	3-chloroaniline
4-bromoaniline	aniline
4-methoxyaniline	3-methoxyaniline
4-nitroaniline	3-nitroaniline
4-N,N-dimethylaniline	4-morpholinoaniline
4-N,N-diethylaniline	4-pyrrolidinoaniline
4-N,N-di-n-propylaniline	4-piperidinoaniline
4-N,N-di-n-butylaniline	2,5-di-n-propoxy-4-piperidinoaniline

All the amines were purified by either recrystallisation or vacuum distillation before diazotisation. However, in those instances where aryl-amines form insoluble oils before crystallising, heating the arylamine in an acidic solution with decolourising charcoal is preferable.

The direct method is recommended for the diazotisation of strongly basic amines and may be summarised as follows:-

Amine (0.15 mol) is dissolved (by gentle heating if necessary) in 10 M hydrochloric acid (50 cm^3) and diluted with water (100 cm^3). After dissolution, the solution is cooled to 0-5° C in an ice salt bath with stirring. (On cooling the hydrochloride salt of the amine frequently precipitates). A fresh solution of sodium nitrite (11.5 g) in water (80 cm^3) is then added at a rate which does not cause any appreciable increase in temperature. When addition of the sodium nitrite solution is complete, the reactant solution is stirred for a further five minutes. Precipitation is effected by the addition of an equimolar solution of 40% tetrafluoroboric acid; if desired, the tetrachlorozincate may be isolated by adding an equimolar quantity of zinc chloride in a saturated solution.

All the salts were recrystallised at least once (and in some cases several times). In the case of colourless diazonium salts, purification was continued until no pink/purple colouration was evident. Materials were then dried overnight in a dessicator.

Tetrafluoroborate salts are readily recrystallised by first dissolving them in acetone and then reprecipitating by the drop-wise addition of ether. Zinc chloride double salts may be purified by dissolving in water and then adding 0.1X g of sodium chloride where X is equivalent to the volume of water in cm^3 required to initially dissolve the salt.

Samples were stored in a refrigerator in dark bottles in quantities of 10 g or less as a precaution against the explosive nature of certain salts.

The following arenediazonium salts were gifts from Mr. P. Pinot de Moira of Ozalid Ltd.:-

4-tolylthio	BF_4^-
2,5-dimethoxy-4-tolylthio	BF_4^- ,$\frac{1}{2}ZnCl^{2-}$
2,5-diethoxy-4-tolylthio	BF_4^- ,$\frac{1}{2}ZnCl_4^{2-}$,PF_6^-
2,5-dimethoxy-4-morpholino	BF_4^-
2,5-diethoxy-4-morpholino	BF_4^- ,$\frac{1}{2}ZnCl_4^{2-}$,PF_6^- ,CNS^-
2,5-di-n-propoxy-4-morpholino	BF_4^-
2,5-di-n-butoxy-4-morpholino	BF_4^-
3-methyl-4-morpholino	BF_4^-
3-methyl-4-pyrrolodino	BF_4^-
3-methoxy-4-morpholino	BF_4^-
4-morpholinonaphthyl	PF_6^-
2,5-diethoxy-N,N-dibenzyl	BF_4^-
4-benzamido	$\frac{1}{2}ZnCl_4^{2-}$
2,4-bis-tolylthio-5-methoxy	BF_4^-

Gifts of 'Epikote', "Quilon S', Melanex' film and 2,5-di-n-propoxy-4-piperidinonitrobenzene were also received with thanks from Ozalid Ltd.

The following arenediazonium salts were prepared during the course of this work and their synthesis is described in detail:-

    4-amino

    2-morpholino

    2-morpholino-5-chloro

    2,5-di-n-propoxy-4-piperidino

    1,4(4'-diazophenyl)piperazine

    2,4-diazophenylmorpholine

All the salts were isolated as tetrafluoroborates and diazotised by the direct method unless otherwise stated.

4-AMINOBENZENEDIAZONIUM TETRAFLUOROBORATE

The compound may be prepared by two methods; the first involves protecting one of the amino groups and the second utilises 1 equivalent of sodium nitrite.

Method 1

(80)

(81)

(82)
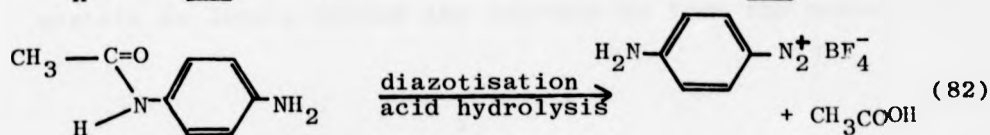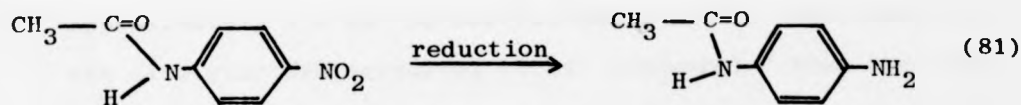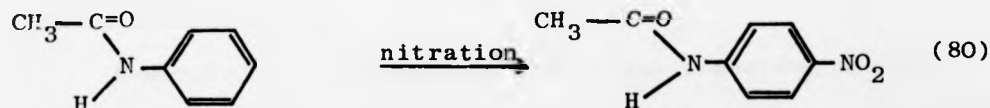
This method[128] involves several reprecipitations using sodium chloride before a pure sample can be obtained.

Method 2

Para-phenylenediamine(1.69 g) is diazotised by the direct method in water (8.0 cm^3) and concentrated HCl (4.0 cm^3) with NaNO$_2$ (1.12 g) to give 4-aminobenzenediazonium tetrafluoroborate upon addition of 40% tetrafluoroboric acid (1.91 g $\equiv$ 58.8% based on amine).

2-MORPHOLINO-NITROBENZENE

2-Chloronitrobenzene (25 g) was refluxed with morpholine (50 cm^3) and ethanol (25 cm^3) for 3 hours. The solution changed from a pale greenish-yellow to a deep red colour. On cooling, a dark red solid formed, which was separated and dissolved in acetone, and then filtered, to leave a white solid of morpholine hydrochloride. The acetone extracts yielded 26.4 g of 2-morpholinonitrobenzene. This was recrystallised from ethanol as bright orange-red prisms (m.p. 45° C) (22.34 g = 69.03%). (Found:C=57.15, H=5.71, N=13.06;Calc.,C=57.69,H=5.76,N=13.44).

2-MORPHOLINO-ANILINE

2-Morpholino-nitrobenzene (10 g) was dissolved in ethyl acetate (200 cm^3) which had been purged previously with nitrogen. Approximately 3.0 cm^3 of settled Raney nickel were added for the catalytic hydrogenation (2 bar pressure). When the ethyl acetate no longer showed any colouration from the parent nitro

compound, the hydrogenation was taken as being complete.
Following removal of the Raney nickel by filtration through
celite, the ethyl acetate was removed under reduced pressure
without heating, leaving large white crystals of 2-morpholinoaniline
(m.p. = 37°C) (8.9 g ≡ 93.68%).

(Found:C=67.45, H = 7.89, N = 15.57;Calc.,C=67.38, H = 7.91,N=15.71).

2-MORPHOLINO-5-CHLORONITROBENZENE

2,5-Dichloronitrobenzene (25 g) was refluxed with morpholine
(50 cm^3) and ethanol (25 cm^3) for 3 hours during which time a
bright yellow solid formed in the reaction vessel. On cooling,
2-morpholino-5-chloronitrobenzene was extracted into acetone to
separate it from any morpholine hydrochloride which may have
formed. The acetone was removed under reduced pressure and the
bright yellow product recrystallised from alcohol. (m.p. = 54°C)
(16.47 g ≡ 52.12%).

(Found:C=49.36,H=4.58,N=11.52;Calc.,C=49.49,H=4.56,N=11.54).

2-MORPHOLINO-5-CHLOROANILINE

2-Morpholino-5-chloronitrobenzene (10 g) was dissolved in
ethyl acetate (200 cm^3) and 3.0 cm^3 of settled Raney nickel
added. The catalytic hydrogenation was carried out at 2 bar
pressure until the original greenish-yellow colour had disappeared.
Subsequent separation of the catalyst and removal of the ethyl
acetate gave small transparent prisms of the amine. (m.p.42°C)
(8.32 g ≡ 94.97%).

(Found:C=55.93, H=6.34, N=13.02;Calc., C=56.20,H=6.55,N=13.11).

2-MORPHOLINO-5-CHLOROBENZENEDIAZONIUM TETRAFLUOROBORATE

2-Morpholino-5-chloroanilinie (4.15g) was dissolved in ethanol (25 cm^3) containing 6.0 cm^3 40% tetrafluoroboric acid, and cooled to below 5°C. Amyl nitrite (3.0 g) was then added with stirring at a rate which did not cause any rise in temperature. A dark orange precipitate soon formed which was filtered from the reaction mixture (4.93 g ≡ 66.70%). (Found:C =42.57,H=4.17,N=13.68; Calc.,C=38.56,H=3.56,N=13.49). Purity as determined by nitrometer method, 96.76%.

1,4-bis-(4'-NITROPHENYL)-PIPERAZINE[128]

$$2O_2N-\!\!\!\bigcirc\!\!\!-Cl \; + \; H-N\!\!\!\bigcirc\!\!\!N-H \xrightarrow{MgO} O_2N-\!\!\!\bigcirc\!\!\!-N\!\!\!\bigcirc\!\!\!N-\!\!\!\bigcirc\!\!\!-NO_2 \; (83)$$

$$+ \; 2HCl$$
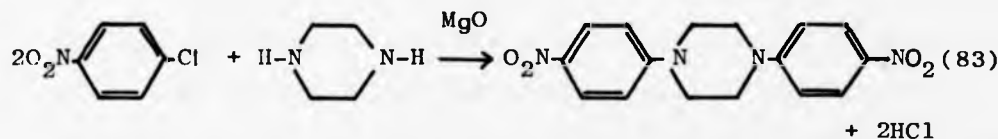
4-Chloronitrobenzene (78.75g), piperazine (21.50g) and MgO (5.0g) were heated in a mixed solvent comprising diethyl digol (72.5 cm) and methoxyethanol (87.5 cm^3) adjusted to reflux at 110°C (by the addition of distilled water, ca. 50 cm^3) for four days. On cooling, 20 g of an orange-brown solid were filtered from the reaction mixture (m.p. 188°C).

Alternatively,[129] the compound may be prepared by heating 4-chloronitrobenzene (6.3g) with piperazine (4.0g) at 150°C in the solid state. Any nitrophenylpiperazine (i.e. the mono-substituted compound) which may have formed being removed by washing the product with boiling ethanol. The compound was recrystallised from nitrobenzene. On cooling, 3.6 g of an orange coloured powder was collected (m.p.248°C)(3.6 g ≡ 54.8%) (Found:C=58.09,H=4.81, N.=16.54; Calc.,C=58.53,H=4.91,N=17.06).

1,4-bis-(4'-AMINOPHENYL) PIPERAZINE

1,4-bis-(4'nitrophenyl) piperazine (3.0 g) was suspended in methanol (15 cm^3) and heated to reflux on a steam bath. A solution of stannous chloride (21 g) in concentrated HCl(21.0 cm^3) which had previously been heated to 80°C were then added to the reaction mixture. After heating for 3 hours, during which time the reaction mixture changed from orange to yellow and eventually became colourless, when cooled on ice and allowed to stand overnight, small white needle-like crystals of the stannic chloride salt of the amine formed. The free amine was obtained by dissolving the salt in distilled water (10 cm^3) and adding this dropwise with vigorous stirring to 5M NaOH (25 cm^3). After heating for 40 minutes, a white solid formed which was filtered off and extracted with warm dimethylformamide in which the product crystallised as the solvent cooled. (m.p. 218°C) (1.4 g ≡ 54%)

(Found:C=71.44, H=7.48, N=20.79;Calc.,C=71.61,H=7.57,N=20.87).

1,4-bis-(4-DIAZOPHENYL)-PIPERAZINE TETRAFLUOROBORATE SALT

1,4-bis-(4'-aminophenyl)piperazine (0.86g) was dissolved in concentrated HCl (2 cm^3) in distilled water (3.5 cm^3) and the solution cooled to below 5°C. A solution of NaNO$_2$(0.5 g) in water (3.5 cm^3) was then added at a rate which did not produce any appreciable rise in temperature. Initially the diazotisation mixture went a pale green colour, but when addition of the NaNO$_2$ was complete, the colour changed to a dark brown-yellow. Addition of tetrafluoroboric acid gave a bright

1,4-bis-(4'-AMINOPHENYL) PIPERAZINE

1,4-bis-(4'nitrophenyl) piperazine (3.0 g) was suspended in methanol (15 cm^3) and heated to reflux on a steam bath. A solution of stannous chloride (21 g) in concentrated HCl(21.0 cm^3) which had previously been heated to 80°C were then added to the reaction mixture. After heating for 3 hours, during which time the reaction mixture changed from orange to yellow and eventually became colourless, when cooled on ice and allowed to stand overnight, small white needle-like crystals of the stannic chloride salt of the amine formed. The free amine was obtained by dissolving the salt in distilled water (10 cm^3) and adding this dropwise with vigorous stirring to 5M NaOH (25 cm^3). After heating for 40 minutes, a white solid formed which was filtered off and extracted with warm dimethylformamide in which the product crystallised as the solvent cooled. (m.p. 218°C) (1.4 g $\equiv$ 54%)

(Found: C=71.44, H=7.48, N=20.79; Calc., C=71.61, H=7.57, N=20.87).

1,4-bis-(4-DIAZOPHENYL)-PIPERAZINE TETRAFLUOROBORATE SALT

1,4-bis-(4'-aminophenyl)piperazine (0.86g) was dissolved in concentrated HCl (2 cm^3) in distilled water (3.5 cm^3) and the solution cooled to below 5°C. A solution of NaNO$_2$(0.5 g) in water (3.5 cm^3) was then added at a rate which did not produce any appreciable rise in temperature. Initially the diazotisation mixture went a pale green colour, but when addition of the NaNO$_2$ was complete, the colour changed to a dark brown-yellow. Addition of tetrafluoroboric acid gave a bright

yellow precipitate but this turned to a brownish colour when
the diazonium salt was collected by filtration (1.37g ≡ 92.9%).
(Found: C=40.57,H=3.45,N=18,12; Calc.,C=41.24,H=3.46,N=18.04).
Purity as determined by nitrometer method, 84.35%.

2,4-DINITROPHENYLMORPHOLINE

2,4-Dinitrochlorobenzene (24.1g) was added in small
portions to morpholine (50g) dissolved in ethanol (50 cm^3)
with cooling (as the initial reaction was rather vigorous).
After gentle refluxing overnight and allowing to cool, the
dark-yellow deposit which formed was dissolved in acetone to
remove morpholine hydrochloride which may have been present.
The crude product was separated by removal of the acetone
under reduced pressure, and recrystallised from methylated
spirit (m.p. = 19^OC) (26.38 g ≡ 86.9%).
(Found:C = 47.49, H=4.38, N=16.62; Calc.,C=47.43,H=4.38,N=16.60).

3-AMINO-6-MORPHOLINO-ANILINIUMSULPHATE

This was prepared from the parent nitro compound (10 g) by
catalytic hydrogenation (Raney nickel, 2 bar). Following
filtration of the catalyst, the ethyl acetate was cooled to
0^OC and concentrated sulphuric acid added with stirring until
a white precipitate of amine sulphate salt formed. The
instability of the free amine prevented its isolation. (m.p.
imprecise; ca. 210^OC) (7.68 g ≡ 48.03%).
(Found: C=32.94,H=5.18, N=10.72; Calc., C=31.00,H=4.42,N=10.84).

$$\left[H_3\overset{+}{N} - \underset{\underset{N^+H_3}{\big|}}{\bigcirc} - N\underset{}{\bigcirc}O \right] SO_4{}^{2-}$$

(LXXIV)
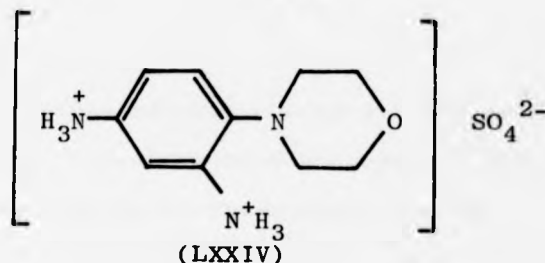
1-MORPHOLINO-BENZENE-2,4-di-DIAZONIUM TETRAFLUOROBORATE

3-Amino-6-morpholino-anilinum-sulphate (5.0g) was dissolved in glacial acetic acid (10 cm^3) and cooled on ice. A solution of nitrosyl/sulphuric acid was prepared by dissolving sodium nitrite (2.10 g) in concentrated sulphuric acid (21.0 cm^3), stirring for 15 minutes, and then cooling to below 5°C. The amine solution was then added dropwise with stirring to the nitrosyl/sulphuric acid at a rate which did not cause the temperature to rise above 10°C. When addition was complete, the mixture was stirred for a further 10 minutes. Methanol was added to the viscous mixture to precipitate the salt, which came out of solution as a yellow powder. On filtering, the salt rapidly turned brown and decomposed; consequently further attempts to isolate this salt were not made due to the risk of explosion.

The syntheses of the following salts were attempted:-
1,3-dimorpholino-5-hydroxybenzenediazonium tetrafluoroborate and
1,3-dimorpholino-5-methoxybenzenediazonium tetrafluoroborate,but satisfactory yields of the respective precursor nitro compounds could not be obtained.

1,3-DICHLORO-2-NITROPHENOL[130]

3,5-Dichlorophenol (8.0g) was nitrated using a solution of sodium nitrate (6.0g) in H$_2$O(90 cm^3) at 100°C by the gradual

addition of dilute sulphuric acid 1:5 (24 cm^3) over a period of two hours.   1,3-dichloro-6-nitrophenol was removed from the reaction mixture by steam distillation.   1,3-dichloro-2-nitrophenol was extracted from the tarry residue with hot dilute hydrochloric acid.   The crude orange-purple product was purified on an alumina column before being recrystallised from water. (m.p. 151°C) (1.57 g $\equiv$ 15.3%).

1,3-DIMORPHOLINO-2-NITROPHENOL

Attempts to condense morpholine with 1,3-dichloro-2-nitrophenol using methods analogous to similar condensations, gave an intractable tarry residue which could not be purified. This is ascribed to the formation of an internal salt (LXXVI).

(80)
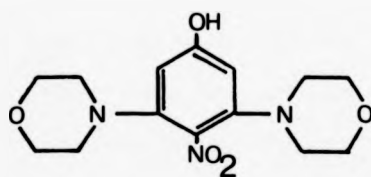
(LXXV)   (LXXVI)
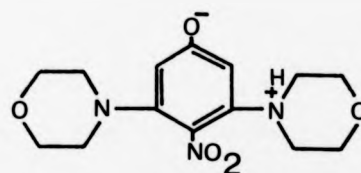
1,3-DICHLORO-2-NITROANISOLE[131]

1,3-Dichloro-2-nitrobenzene (0.75 g)was heated with methyl iodide (0.6 g)over potassium carbonate in dry acetone for 48 hours. 0.80 g of a crude straw-coloured product was extracted from the mixture and recrystallised from dilute methanol. (m.p. 69-70°C) (0.66 g $\equiv$ 82.50%).

CHAPTER IV

X-RAY DIFFRACTION STUDIES

4.1. THE STRUCTURE OF 4-MORPHOLINOBENZENEDIAZONIUM TERAFLUOROBORATE

The thermal decomposition rate constants, ultra-violet and infra-red spectra of para-dialkylaminobenzenediazonium salts are sufficiently well-differentiated from those of simple analogues, to suggest that their electronic ground state should be represented as a quinoidal type structure (see sections 1.4, 1.5 and 1.6).

We have attempted to determine the electronic ground state geometry (and hence the character of the ring) of a 4-dialkylaminobenzenediazonium salt (by following the approach of Mak and Trotter[132] in determining quinoidal character in 4-N,N-dimethylnitrobenzene by X-ray crystallography). Both preliminary and more refined structural studies of 4-N,N-dimethylbenzenediazonium tetrachlorozincate have appeared in the Russian literature,[133,134] and a refined structure of the benzenediazonium cation is available[8] for comparison. However the accuracy of the Russian work is questionable as the authors report severe deterioration of the crystal used, on being exposed to X-rays.

Block-shaped crystals of 4-morpholinobenzenediazonium tetrafluoroborate (prepared by the direct method) were grown from an ethanol/water mixture.

Data were collected on a Syntex-P2, four-circle diffractometer, with a graphite monochromator. The crystal was held at 173K using the LT-1 attachment to minimise the chance of radiation-induced decomposition. Reflections from the $\theta-2\theta$ scan mode were taken at a rate of 1° to 29.5° min^{-1} depending upon the intensity of a 2 second prescan, over the

range $2\theta_{\alpha 1}$-0.9 to $2\theta_{\alpha 2}$+0.9 to a $2\theta_{max}$ of 50°. Background counts were taken for a quarter of the scan time at the end of each reflection. Three high intensity reflections were chosen as standards, and these did not show any significant variation during the data collection. A total of 2466 reflections were collected (including 10 very intense ones taken at low power). For the purpose of analysis, 1674 unique reflections with $I/\sigma(I)$ > 3.0 were used. The data was corrected for Lorentz and polarisation effects, but not for absorption.

The structure was solved by the direct method using the computer program 'Multan'[135] running in the X-Ray-76 system.[136]

Systematic absences in the data of KOL, $(1 \neq 2n)$ and OKO, $(K \neq 2n)$ indicate space group $P2_1/C$, i.e. monoclinic. The crystal was found to contain 4 molecules per unit cell, the dimensions of which are given below with standard deviations in parentheses,

$$a = 13.675(4)\overset{o}{A}, \quad b = 10.686(4)\overset{o}{A}, \quad c = 8.982(2)\overset{o}{A},$$
$$\beta = 106.72(2)^{o}, \quad u = 1257.0(9)\overset{o}{A}^{3}, \quad \lambda = (Mo\text{-}K_{\alpha}) = 0.71069 \overset{o}{A}$$

Refinement of the structure was by the least squares method on a Burroughs B6700C computer. Refinement, with anisotropic temperature factors, gave an R value of 0.084. When the hydrogen atoms were inserted into the calculated positions, a final value of R = 0.065 was obtained.

The final atomic co-ordinates (Courtesy of Dr.T.J.Greenough) are given in Table 5, bond lengths and angles in Table 6, with equations in Table 7.

TABLE 5

FINAL ATOMIC CO-ORDINATES

ATOM	X	Y	Z
C(1)	25514(5)	19867(7)	13125(9)
C(2)	19404(5)	12083(7)	2190(9)
C(3)	22047(5)	-720(7)	947(8)
C(4)	31258(5)	-5202(7)	11410(8)
C(5)	37423(5)	2473(7)	22387(8)
C(6)	34505(5)	14934(7)	22968(8)
C(7)	19296(7)	-20683(8)	-13584(12)
C(8)	11234(8)	-28939(10)	-20629(13)
C(9)	-340(7)	-12552(10)	-28618(13)
C(10)	7067(8)	-3790(10)	-21783(15)
O	3010(4)	-24090(5)	-32723(6)
N(1)	45770(5)	28977(7)	42526(8)
N(2)	40770(5)	22741(6)	33870(7)
N(3)	15857(5)	-8383(6)	-9635(8)
B	33703(7)	51293(9)	11646(11)
F(1)	40224(3)	42194(4)	8758(5)
F(2)	37887(4)	62916(4)	11634(7)
F(3)	24359(3)	50567(5)	444(7)
F(4)	32193(5)	48592(5)	25845(6)
H(1)	23701(45)	28392(58)	14110(67)
H(2)	13479(45)	15718(58)	-4407(68)
H(4)	33537(42)	-13594(54)	11202(64)
H(5)	43659(44)	-1020(57)	29949(67)
H(71)	22293(54)	-19798(70)	-24788(83)
H(72)	24291(54)	-24077(71)	-4945(83)
H(81)	8384(56)	-29881(74)	-8527(86)
H(82)	13712(57)	-37216(73)	-25378(86)
H(91)	-5771(58)	-9358(75)	-36973(88)
H(92)	-3185(58)	-13300(73)	-16665(88)
H(101)	4149(60)	3535(79)	-17129(91)
H(102)	8394(59)	-815(77)	-33462(92)

TABLE 6

BOND LENGTHS(Å) AND ANGLES(°) WITH STANDARD DEVIATIONS IN PARENTHESES

N(1)	–	N(2)	1.1001(9)
N(2)	–	C(6)	1.3806(9)
C(6)	–	C(1)	1.3950(10)
C(1)	–	C(2)	1.3720(10)
C(2)	–	C(3)	1.4276(11)
C(3)	–	C(4)	1.4206(10)
C(4)	–	C(5)	1.3700(10)
C(5)	–	C(6)	1.3953(11)
C(1)	–	H(1)	0.955 (6)
C(2)	–	H(2)	0.939 (6)
C(4)	–	H(4)	0.951 (6)
C(5)	–	H(5)	0.997 (5)
C(3)	–	N(3)	1.3519(9)
N(3)	–	C(7)	1.4733(12)
C(7)	–	C(8)	1.4116(13)
C(8)	–	O	1.4179(11)
O	–	C(9)	1.4011(13)
C(9)	–	C(10)	1.3864(15)
C(10)	–	N(3)	1.4566(12)
C(7)	–	H(71)	1.194 (8)
C(7)	–	H(72)	0.946 (7)
C(8)	–	H(81)	1.260 (9)
C(8)	–	H(82)	1.078 (8)
C(9)	–	H(91)	0.954 (7)
C(9)	–	H(92)	1.245 (9)
C(10)	–	H(101)	1.021 (9)
C(10)	–	H(102)	1.159 (9)
B	–	F(1)	1.393 (1)
B	–	F(2)	1.368 (1)
B	–	F(3)	1.383 (1)
B	–	F(4)	1.380 (1)

TABLE 6 (Continued)

```
H(101)  -  C(10)  -  C(9)    112.20(5)
H(101)  -  C(10)  -  N(3)    106.70(4)
H(101)  -  C(10)  -  H(101)110.00(6)
H(102)  -  C(10)  -  C(9)     94.00(4)
H(102)  -  C(10)  -  N(3)    117.40(4)
F(1)  - B - F(2)             110.09(8)
F(1)  - B - F(3)             109.42(7)
F(1)  - B - F(4)             107.47(7)
F(2)  - B - F(3)             110.47(7)
F(2)  - B - F(4)             111.38(7)
F(3)  - B - F(4)             107.94(8)
N(1)  - N(2) - C(6)          179.82(8)
N(2)  - C(6) - C(1)          118.37(7)
N(2)  - C(6) - C(5)          118.52(6)
C(1)  - C(6) - C(5)          123.11(6)
C(6)  - C(1) - C(2)          117.96(7)
C(1)  - C(2) - C(3)          121.42(6)
C(2)  - C(3) - C(4)          117.88(6)
C(2)  - C(3) - N(3)          120.94(6)
C(4)  - C(3) - N(3)          121.17(7)
C(3)  - C(4) - C(5)          121.28(7)
C(4)  - C(5) - C(6)          118.35(6)
H(1)  - C(1) - C(6)          120.40(3)
H(1)  - C(1) - C(2)          121.60(3)
H(2)  - C(2) - C(1)          116.00(4)
H(2)  - C(2) - C(3)          122.60(4)
H(4)  - C(4) - C(3)          122.50(3)
```

TABLE 6 (Continued)

H(4)	- C(4)	- C(5)		116.20(3)
H(5)	- C(5)	- C(4)		119.60(4)
H(5)	- C(5)	- C(6)		122.00(4)
C(3)	- N(3)	- C(7)		122.08(6)
C(3)	- N(3)	- C(10)		122.50(6)
C(7)	- N(3)	- C(10)		111.85(7)
N(3)	- C(7)	- C(8)		113.78(8)
C(7)	- C(8)	- O		117.39(9)
C(8)	- O	- C(9)		111.55(7)
O	- C(9)	- C(10)		117.28(9)
C(9)	- C(10)	- N(3)		116.39(9)
H(71)	- C(7)	- N(3)		110.00(4)
H(71)	- C(7)	- C(8)		94.9 (3)
H(71)	- C(7)	- H(72)		112.30(6)
H(72)	- C(7)	- N(3)		110.50(5)
H(72)	- C(7)	- C(8)		114.50(5)
H(81)	- C(8)	- C(7)		93.40(3)
H(81)	- C(8)	- O		108.40(3)
H(81)	- C(8)	- H(82)		119.10(6)
H(82)	- C(8)	- C(7)		113.30(4)
H(82)	- C(8)	- O		105.50(4)
H(91)	- C(9)	- O		110.30(5)
H(91)	- C(9)	- C(10)		114.35(5)
H(91)	- C(9)	- H(92)		109.60(6)
H(92)	- C(9)	- O		112.20(4)
H(92)	- C(9)	- C(10)		92.80(3)

TABLE 7

EQUATIONS FOR LEAST SQUARES OF PLANES (IN ORTHOGONAL
ANGSTROM SPACE. X//a. Y ⊥ a IN ac PLANE, Z ORTHOGONAL

1.   O715X + 0.255Y - 0.651Z = 2.063

Deviations ($\overset{o}{A}$)

C(1)*	-0.004	O	0.010
C(2)*	0.000	H(1)	-0.020
C(3)*	0.002	H(2)	0.010
C(4)*	0.001	H(4)	0.010
C(5)*	-0.005	H(5)	-0.050
C(6)*	0.007	C(7)	0.270
N(1)	0.035	C(8)	-0.220
N(2)	0.020	C(9)	-0.310
N(3)	-0.025	C(10)	0.150

2.   0.643X + 0.228Y + 0.731Z = 2.106

Deviations ($\overset{o}{A}$)

N(3)*	-0.148	H(81)	-1.420
O*	0.174	H(82)	0.210
C(7)*	0.168	H(91)	0.100
C(8)*	-0.182	H(92)	-1.38
C(9)*	-0.166	H(101)	-0.290
C(10)*	0.155	H(102)	1.270
H(71)	1.340	C(3)	-0.250
H(72)	-0.160	C(6)	-0.530
H(81)	-1.42		

Dihedral angle between 1 and 2 ≡ 6.3°

* Atoms defining planes

As expected, the crystal contained 4-morpholinobenzene-
diazonium cations and tetrafluoroborate anions (Fig.21), the
packing of which is shown in Fig. (22). The cations are in
parallel planes with the anions in the spaces between planes.
In the cation, the planes of the two rings are not parallel
and subtend an angle of 6.3°. It is noticeable that in the
anion, the individual B-F distances and angles depart from
the mean ($1.381\overset{\circ}{A}$ and 109.46°) by more than the standard
deviations; this is presumably due to packing effects.

In Fig. (23) the significant parameters of other molecules
which are relevant to this study are shown (LXXVII)
benzenediazonium chloride,[8] (LXXVIII) 4-morpholinobenzenediazonium
tetrafluoroborate, (LXXIX) 4-N,N-dimethylbenzenediazonium
tetrachlorozincate,[134] (LXXX) 4-N,N-dimethylnitrobenzene[132] and
(LXXXI) nitrobenzene.[137] Comparison of the various structures
reveals the following:

(i)   That our structure of 4-morpholinobenzenediazonium
      tetrafluoroborate differs considerably from that of
      4-N,N-dimethylbenzenediazonium tetrachlorozincate with
      respect to certain bond lengths and angles

(ii) 4-N,N-dialkylbenzenediazonium salts would appear to
      resemble similarly substituted nitrobenzenes with
      respect to certain bond lengths and angles in the
      considerably distorted benzene ring.

When (LXXVII) and (LXXVIII) are compared, the effect of a
para-amino substituent, is one of lengthening C(1)-C(2) by
$0.02\overset{\circ}{A}$ and reducing C(2)-C(3) by $0.01\overset{\circ}{A}$. However, the more

Figure (21)

Computer simulation of the X-ray structure of

the 4-morpholinobenzenediazonium cation
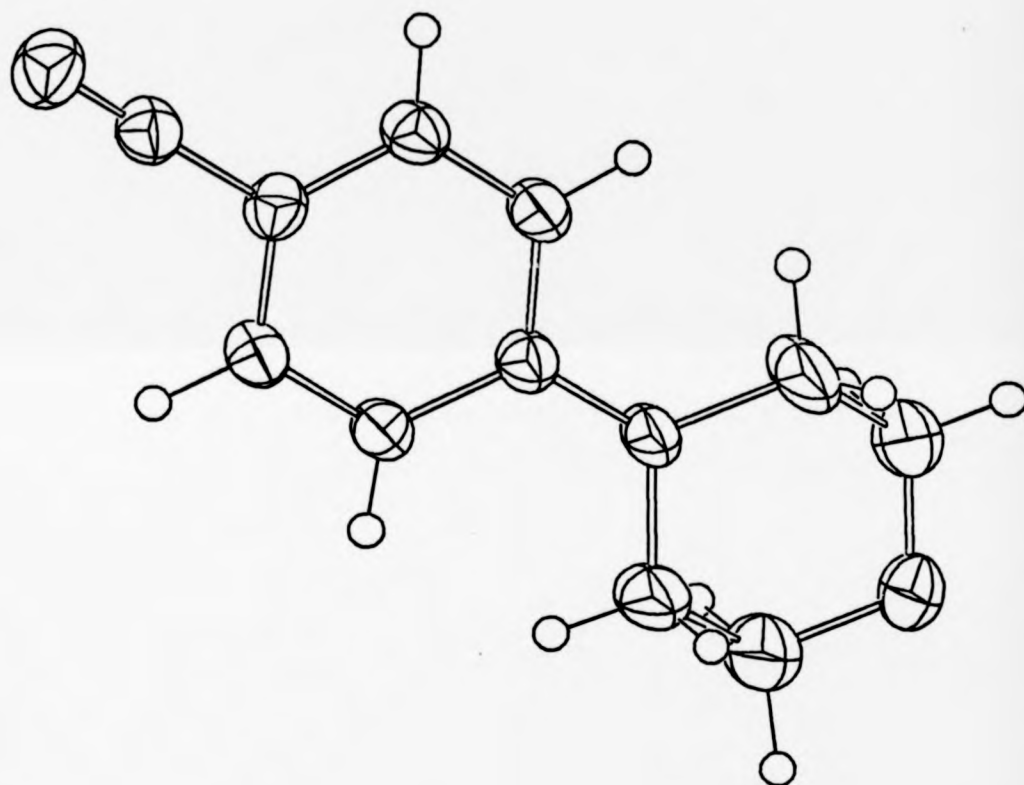
Figure (22)

Packing diagram for 4-morpholinobenzenediazoniom
cations in the ac plane.
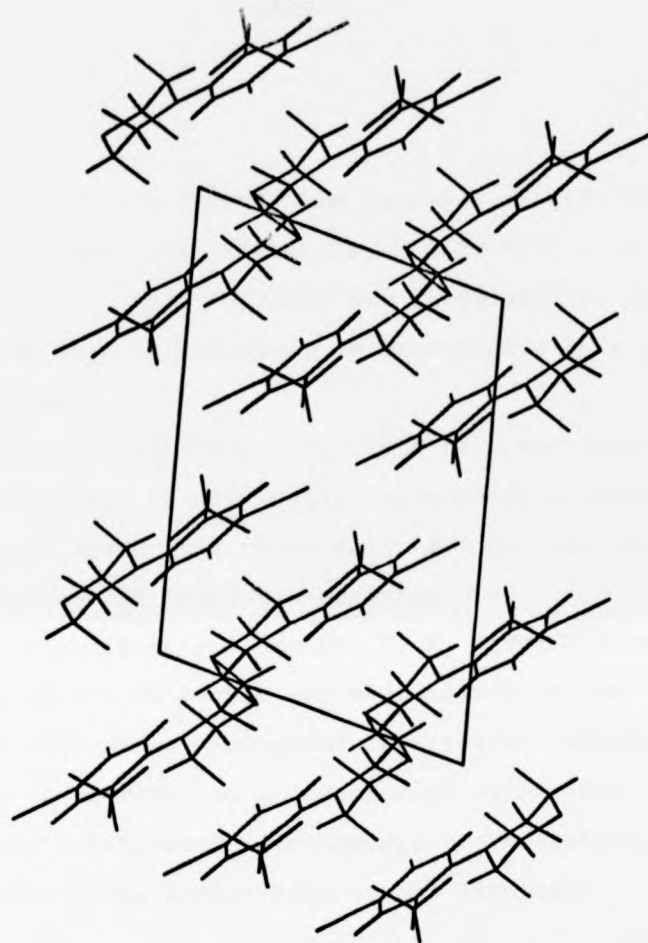
important effects, are firstly the increase in C(3)-C(4) by 0.05Å and secondly the reduction of C(3)-C(4)-C(5) from 121.7^O to 117.83^O. These effects are quite similar to those observed when nitrobenzene is substituted by a para-alkylamino group.

Although our crystallographic data have not confirmed the quinoidal nature of para-dialkylaminobenzenediazonium salts they have shown that these salts are considerably distorted from normal benzene geometries.

Ab initio calculations (by Dr. D. M. Hirst[138]) are at present in progress to verify our conclusions on the variation of bond order throughout the system. Simple MO methods fail to predict the geometries of either the 4-dialkylamino substituted nitrobenzene or benzenediazonium cation; clearly quite subtle effects are important.

Figure (23)

Bond lengths and angles in structures related to

4-morpholinobenzenediazonium tetrafluroborate

Cl

N
1.097

124.8
117.6
1.385
119.8
121.7
1.383
1.376

1.426
1.363
1.367
121
121
125
116

(LXXVII)

O 1.208
N 124
O 119

(LXXXI)

F 1.383
F 1.368
B 1.393
F 1.380
F

N
1.100

N
1.381

1.395
123.1
117.
1.395
117.6
1.372

180

1.370
128.28 121
117.8
1.428
1.352
(1.00)H
118.3
(0.95)H (142)
H(0.94)
H(0.95)

(1.19)H
(0.95)H
(126)H
(1.08)H
1.418
O 111.5 1.401
N 111.8
1.386
H(1.16)
H(0.95)
H(1.02)
H(0.95)

(LXXVIII)

½ZnCl$_4^{2-}$

N
1.17

N
1.48

171
1.41
130
110
115
1.44
1.43
121
118
125
1.43
1.41
1.45
1.39
1.53

CH$_3$
N
CH$_3$

(LXXIX)

O 121.4
N 1.25
O 119.3

1.405
1.400
119.6
121.0
117
119.8
121.2
121.5
1.375
1.435
1.358

118.2
121.0
N
CH$_3$
CH$_3$

(LXXX)

CHAPTER V

PHOTODECOMPOSITION QUANTUM YIELDS OF ARENEDIAZONIUM SALTS

5.1. QUANTUM YIELDS DETERMINED IN 0.05 mol dm^{-3} AQUEOUS SULPHURIC ACID

Throughout this work triply-distilled water has been used, and glass apparatus cleaned by soaking in chromic acid.

Visible and near ultra-violet spectra were recorded in an aqueous solution of 0.05 mol dm^{-3} sulphuric acid using 1.0 cm quartz cells. Typical spectra of para-substituted arenediazonium salts are shown in Fig. 24 , which clearly illustrates the extreme sensitivity of the $^1A_1$-$^1A_1$ band to the presence of electron-donating and -withdrawing groups.

Extinction coefficients were determined by making two separate weighings and then diluting with 0.05 mol dm^{-3} sulphuric acid to give a final range of concentrations having optical densities from 0.0 to 1.0 in a 1.0 cm cell. Table 8 summarises values from previously published work of λ_{max} and the corresponding extinction coefficient. Whilst values of λ_{max} are in good agreement, values of ε_{max} are however subject to some degree of variation. Discrepancies are maximal with those salts which have the highest thermal decomposition rates, e.g. 3-methyl and 3-methoxy derivatives.

Quantum yields for simple meta- and para-substituted arenediazonium salts were determined at 313 nm (using a Balzer R-UV No.16 filter). Photolysis was carried out in a cylindrical quartz cell (2.5 cm × 5.0 cm depth) fitted with an exit tube, equipped with a narrow bore 'Teflon' tap. Determinations were made from 20.0 cm^3 of 0.05 mol dm^{-3} sulphuric acid

Figure (24)

Ultra-violet spectra of arenediazonium salts

Figure showing optical density versus λ/nm spectra for p-NO₂, p-Cl, p-OCH₃, p-N(CH₃)₂, and 2,5-diethoxy-4-morpholino derivatives.
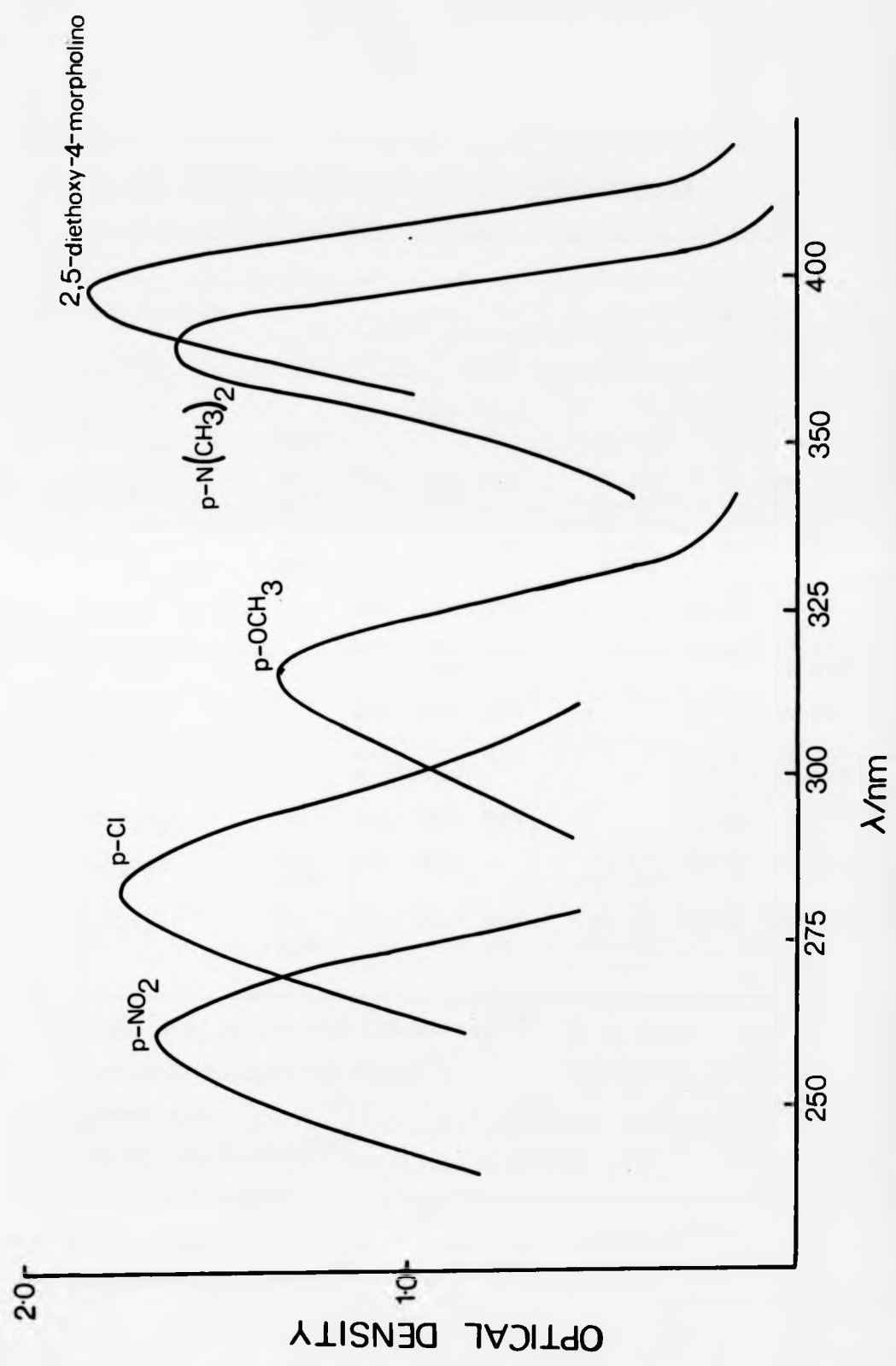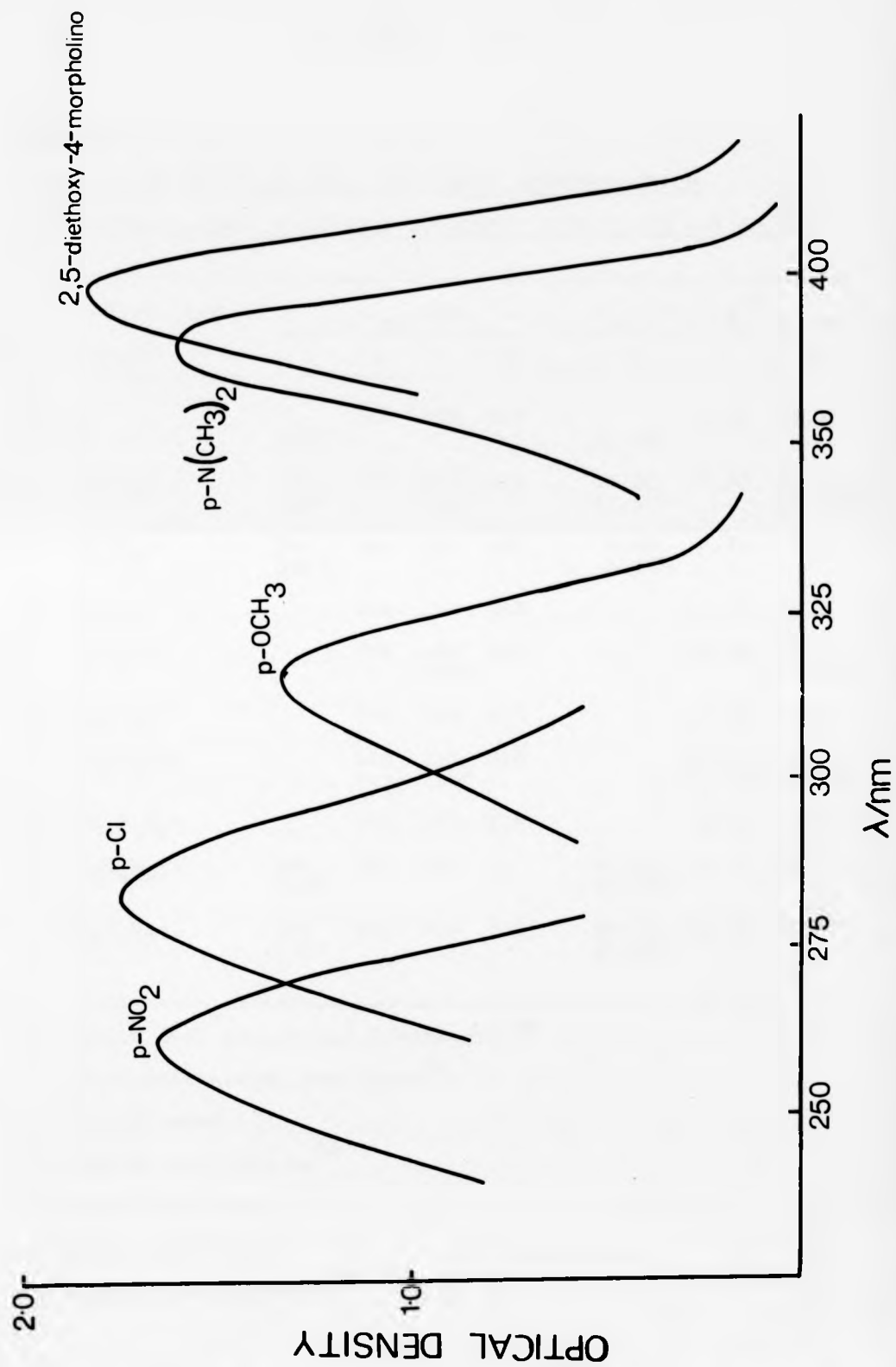
TABLE 8

ULTRA-VIOLET SPECTRAL DATA FOR SIMPLE ARENEDIAZONIUM
TETRAFLUOROBORATES IN AQUEOUS SULPHURIC ACID (0.05 mol dm^{-3})

Benzenediazonium cation	λ_{max}/nm				$\varepsilon_{max} \times 10^{-3}$ (M^{-1} cm^{-1})		
	a	b	c	d	a	b	c
$C_6H_5N_2^+$	262^e	263	262	264	12.50^e	13.20	11.50
$4\text{-}ClC_6H_4N_2^+$	284 280^e	282	283 281^g	283	17.30 17.90^e	17.70	16.60 15.67^g
$3\text{-}ClC_6H_4N_2^+$	267 265^e	266	267	266	9.40 9.83^e	9.34	9.40
$4\text{-}BrC_6H_4N_2^+$		293	293	293		18.00	18.12
$4\text{-}CH_3C_6H_4N_2^+$		278	278 293^g	279		13.95	13.91 15.07^g
$3\text{-}CH_3C_6H_4N_2^+$		270	269	270		11.20	10.30
$4\text{-}CH_3OC_6H_4N_2^+$		314 313^f	313 315^g	315		25.80 24.55^f	24.70 19.19^g
$3\text{-}CH_3OC_6H_4N_2^+$		275	272	275		6.16	7.75
$4\text{-}O_2NC_6H_4N_2^+$	260 260^e	261	262	–	15.75 17.09^e	15.10	15.60
$3\text{-}O_2NC_6H_4N_2^+$	232 233^e	233	233	232	20.10 21.00^e	20.80	20.30

a = Ozalid Ltd. Analytical laboratory[128]

b = Schulte-Frohlinde and Blume[46]

c = Present work

d = Tsunoda and Yamaoka[64]

e = Lewis and Hanson[139]

f = Evleth and Cox[20]

g = Sukigara and Kikuchi[18]

approximately 10^{-5} mol dm^{-3} in the arenediazonium salt under investigation. All samples were argon flushed for 10 minutes prior to photolysis. Irradiation times were of a duration which allowed the optical density of the solution to be recorded 15 to 20 times, during the course of the photolysis. Optical density verses time plots, were analysed using a computer program 'Actin' (See Appendix I) which corrects for the increased transmission of light as the solute is photodecomposed.

Photolysis of para- and meta-nitrobenzenediazonium tetrafluoroborates gave an increase in optical density at the irradiating wavelength. The phenolic products formed in both cases rapidly decreased the amount of light which is transmitted through the solution (known as the product "inner filter effect"). Values of ϕ for these two salts have been calculated from initial rate constants (for the photodecomposition) and are the average of three separate determinations.

Quantum yields for simple meta- and para-substituted arenediazonium salts are given in Table 9 together with any previously published data. Slight discrepancies between various sets of data are inevitable unless an accurate filter or monochromator is employed for selecting the desired irradiation wavelength. However our values of ϕ are in good agreement with those reported by Schulte-Frohlinde[65] (with the exception of the meta-methoxy derivative) whilst the data of Tsunoda and Yamaoko[64] are inconsistent with either set of

TABLE 9

PHOTODECOMPOSITION QUANTUM YIELDS (313 nm) FOR SIMPLE
META- AND PARA-SUBSTITUTED ARENEDIAZONIUM TETRAFLUOROBORATES
IN ARGON-BUBBLED 0.05 mol dm^{-3} SULPHURIC ACID

Benzenediazonium cation	ϕ at λ = 313 nm			%N$_2$[a]
	Tsunoda	Schulte-Frohlinde	This work	
$C_6H_5N_2^+$	0.38	0.52	0.48*	-
$4\text{-}ClC_6H_4N_2^+$	0.29	0.41	0.42	96.7
$3\text{-}ClC_6H_4N_2^+$	0.41	0.35	0.36	99.4
$4\text{-}BrC_6H_4N_2^+$	0.35	0.38	0.40	-
$4\text{-}CH_3C_6H_4N_2^+$	0.23	0.61	0.57	-
$3\text{-}CH_3C_6H_4N_2^+$	0.35	0.55	0.52	-
$4\text{-}CH_3OC_6H_4N_2^+$	0.52	0.38	0.39	-
$3\text{-}CH_3OC_6H_4N_2^+$	0.24	1.00	0.64	-
$4\text{-}O_2NC_6H_4N_2^+$	-	0.21	0.17	98.6
$3\text{-}O_2NC_6H_4N_2^+$	0.17	0.17	0.22	101.8

(a) % N$_2$ Determined by Nitrometer method

*   mean of two determinations

results. Correlation between φ and the Hammett σ constants
derived by Brown and Okamoto[140] was reasonably good, (Fig. 27
page 128) yielding a ρ value of -0.516 ± 0.005 with r = 0.56.
Values of φ for the meta-methoxy and para-methoxy salts have
not been included in the calculation of the regression line.
Alkoxy groups are well-known for their ability to donate
electrons, e.g. the Hammett σ constant for para-methoxy is
-0.27, while the corresponding value for meta-methoxy is +0.13.
Slight distortion of the aromatic ring in arenediazonium salts
combined with the generally abnormal behaviour of the meta-
methoxy group probably accounts for the anomalous values of
φ recorded for these salts.

Para-aminobenzenediazonium salts are frequently employed
as the light-sensitive component of commercial 'diazo type'
reprographic papers. Photodecomposition of these compounds
is the initial step in the image formation process. The speed
of such systems is dependent upon the quantum yield of the
particular arenediazonium salt used to sensitise the reprographic
paper. Consequently the quantum yields of para-aminobenzenediazonium
salts are of considerable interest because of (a) their economic
importance to the reprographic industry and (b) they provide a
suitable model for the study of substituents capable of forming
quinoidal type structures, e.g.
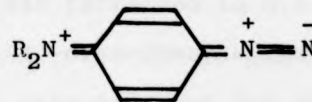
(LXXXII)   (LXXXIII)

A series of 4-N,N-dialkylbenzenediazonium salts have been studied to determine the influence of the various groups on the quantum yield. The quantum yields are given in Table 10 together with other currently available data. Our values of ϕ for 4-N,N-dialkyl analogues are fairly similar (ϕ average 0.54) although the value for the 4-amino salt is slightly higher ($\phi = 0.73$). Lowered values of ϕ for the series of 4-N,N-dialkylbenzenediazonium salts suggests some contribution of quinoidal (LXXXIII) forms to their excited state. The relatively high values of ϕ (compared to simpler salts) for 4-N,N-dialkylbenzenediazonium salts makes this group of compounds particularly suitable for commercial 'diazo type' reprographic papers.

Quantum yields for a number of more complex arenediazonium salts have also been determined in dilute sulphuric acid. Many of these salts are marketed by Ozalid Ltd in commercial 'diazo type' reprographic papers. In all cases the irradiation and monitoring wavelengths were 380 nm, a combination of a Balzer R-UV No.13 filter and a 10% neutral density filter being used in the optical train. The results are given in Table 11 and the spectral changes observed in a typical photolysis are shown in Fig. 25 .

Reproducible values of ϕ for 4-morpholino and 4-pyrrolidino salts, substituted in the 3-position, were only obtained when the concentration of sulphuric acid was increased to 0.5 mol dm^{-3}. The values of ϕ reported for 1-4-bis-(4'-diazophenyl)-piperazine have been calculated from an initial rate constant for the photo-decomposition. The ultra-violet spectra recorded during the

TABLE 10

PHOTODECOMPOSITION QUANTUM YIELDS (380 nm) FOR 4-AMINO AND 4-N,N-DIALKYLAMINO SUBSTITUTED BENZENEDIAZONIUM TETRAFLUOROBORATES IN ARGON-BUBBLED 0.05 mol dm^{-3} SULPHURIC ACID

Benzenediazonium cation	λ_{max}/nm	$\epsilon_{max} \times 10^{-3}$ (M^{-1} cm^{-1})	$\epsilon_{380} \times 10^{-3}$ (M^{-1} cm^{-1})	ϕ_{380}nm
4-amino	354	26.90	1.50	0.73
	353[a]	37.40[a]		0.25[a]
4-N,N-dimethyl	378	38.20	38.00	0.48
	375[a]	38.90[a]		0.25[a]
	378[b]	36.10[b]		0.44[b]
				0.57[c]
				0.68[d]
4-N,N-diethyl	380	40.80		0.54
	380[a]	40.30[a]		0.25[a]
	378[b]	40.20[b]		0.44[b]
				0.50[c]
				0.64[d]
				0.41[e]
4-N,N-di-n-propyl	380	39.50		0.59
				0.60[d]
4-N,N-di-n-butyl	398	28.00	20.70	0.56
				0.68[d]

a = Kroupa[21]

b = Cox, Bushnell and Evleth[23] ϕ determined at 405 nm

c = Cox, Bushnell and Evleth[23] ϕ determined at 365 nm

d = Mizianty[141]

e = Breitenbach[142]

TABLE 11

PHOTODECOMPOSITION QUANTUM YIELDS (380 nm) FOR COMPLEX ARENEDIAZONIUM TETRAFLUOROBORATES IN ARGON-BUBBLED 0.05 mol dm^{-3} SULPHURIC ACID

Benzenediazonium Cation	Anion	λ_{max}/nm	$\varepsilon_{max} \times 10^{-3}$ (M^{-1}cm^{-1}) Ozalid Ltd This work		ϕ380	%N$_2$
4-piperidino	BF$_4^-$	382		44.70	0.44	
4-pyrrolidino	BF$_4^-$	380		39.40	0.49	
*4-pyrrolidino-3-methyl	BF$_4$	396		37.12	0.40 (0.41)[a]	
4-morpholino	½ZnCl$_4^{2-}$	380	41.70	38.85	0.60 0.40	101.4
*4-morpholino-3-methyl	BF$_4^-$	395		26.25	0.31 (0.33)[a]	
*4-morpholino-3-methoxy	BF$_4$	401		25.80	0.56 (0.59)[a]	
2-morpholino	BF$_4$	434		4.93	0.13 (0.38)[b]	95.71 (98.81)
2-morpholino-5-chloro	BF$_4$	455		5.42	0.08 (0.34)[b]	96.76 (101.4)
2,5-dimethoxy-4-morpholino	BF$_4^-$	397	28.60	27.60	0.27	98.2
2,5-diethoxy-4-morpholino	BF$_4^-$	397	27.00	25.6	0.33	98.1
2,5-diethoxy-4-morpholino	½ZnCl$_4^{2-}$	397	23.70	23.00	0.34	82.9
2,5-di-n-propoxy-4-morpholino	BF$_4^-$	397	26.50	24.40	0.50	100.2
2,5-di-n-butoxy-4-morpholino	BF$_4^-$	397	26.90	23.70	0.52	102.2
4-tolylthio	BF$_4^-$	368		22.30	0.24	
2,5-dimethoxy-4-tolylthio	½ZnCl$_4^{2-}$	395	17.40	17.85	0.38	96.1
2,5-diethoxy-4-tolylthio	½ZnCl$_4^{2-}$	395	15.90	15.90	0.46	94.2
2,4-bis-tolylthio-5-methoxy	BF$_4^-$	383		10.61	0.50	
1,4-bis-(4'-diazophenyl)-piperazine	BF$_4^-$	401		72.00	0.20 (0.60)[a]	84.35 (100.44)[c]
4-morpholinonaphthyl	BF$_4^-$	430		31.00	0.22 (0.43)[b]	

* = determined in 0.5 mol dm^{-3} sulphuric acid
a = ϕ at 401 nm
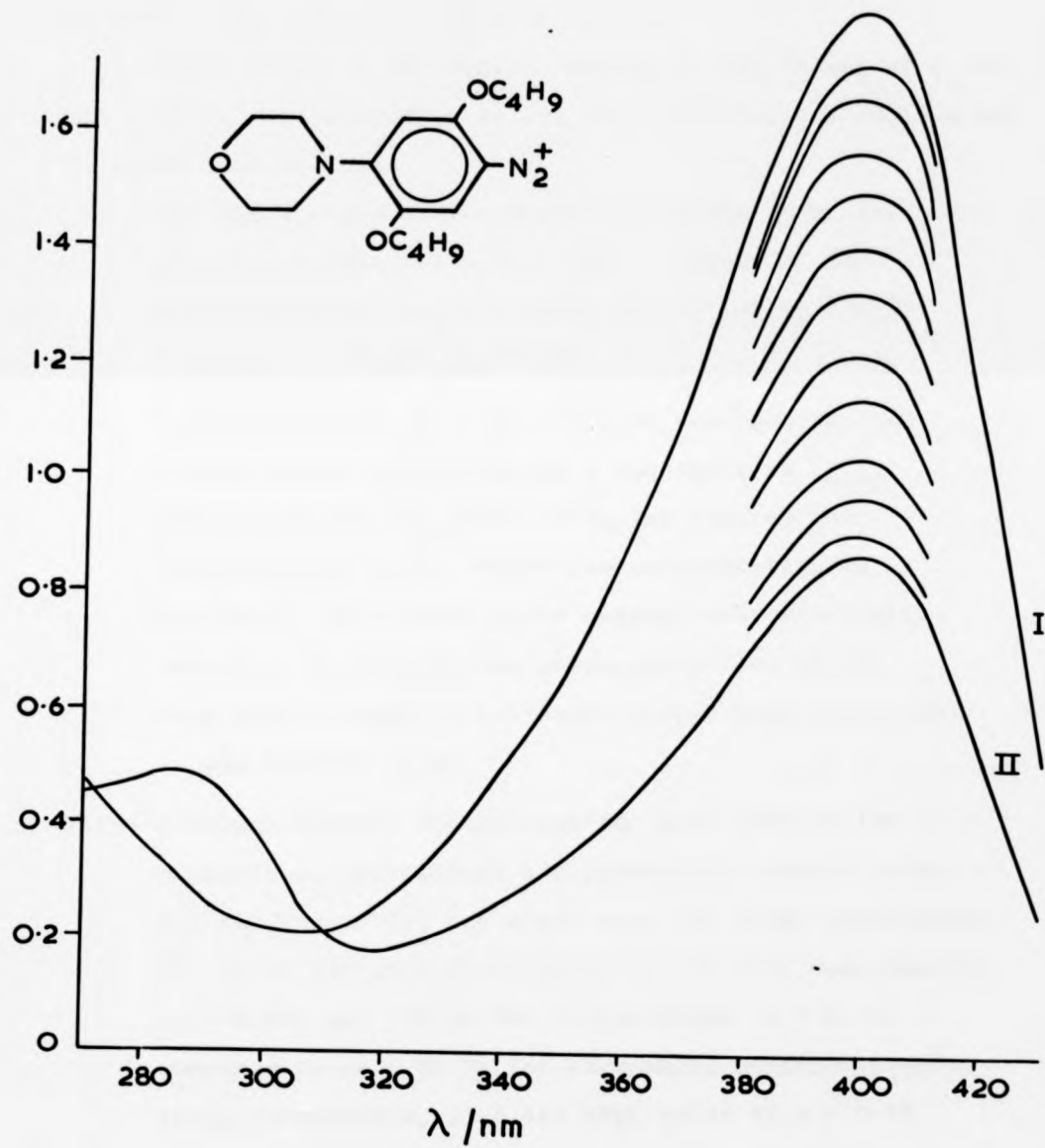b = ϕ at 439 nm
c = by element analysis

Figure (25)

Spectral changes observed during the 380 nm
photolysis of 2,5-di-n-butoxy-4-morpholinobenze-
diazonium tetrachlorozincate in argon-bubbled
0.5 mol dm^{-3} sulphuric acid

I = Initial spectrum   light intensity

1.082×10^{15} quanta s^{-1}

II = Final spectrum   Decrease in optical
density for successive
20s exposures

photolysis of this salt indicate that simultaneous heterolysis of both diazonium groups does not occur.

While there is no overall pattern in the values of ϕ for the complex arenediazonium salts, the following conclusions may be drawn from the data;

(i)   for the 2,5-dialkoxy-4-morpholino salts there is a gradual increase in ϕ with the +I effect of the substituent groups, viz. OCH_3 = 0.27 OC_2H_5 = 0.33 $n-OC_3H_7$ = 0.50 $n-C_4H_9$ = 0.52

(ii)   Substitution in the 3-position of 4-morpholino and 4-pyrrolidino salts induces a red shift in λ_{max}. Quantum yields for these salts are lowered when compared with their respective para-substituted analogue. Both these facts suggest that sterically twisting the para-dialkylamino group (out of the ring plane) leads to increased double bond character in the excited state.

(iii) Although Hammett σ constants for para-substituted morpholino, pyrrolidino and piperidino-benzoic acids are not available, one might note the large hypsochomic shifts of 114 nm 4-pyrrolidino (ϕ = 0.49), 4-morpholino (ϕ = 0.60) and 116 nm for 4-piperidino (ϕ = 0.44) compared to only 89 nm for para-amino benzenediazonium tetrafluoroborate, with its high value of ϕ = 0.73.

TABLE 12

EFFECT OF VARYING QUANTUM ENERGY ON THE PHOTODECOMPOSITION OF

(a) 2,5-DI-n-BUTOXY-4-MORPHOLINOBENEZNEDIAZONIUM
     TETRAFLUOROBORATE AND

(b) 4-N,N-DI-n-BUTYLAMINOBENZENEDIAZONIUM TETRAFLUOROBORATE IN
     0.05 mol dm^{-3} SULPHURIC ACID

| λ photolysis/nm	$\varepsilon \times 10^{-3}(M^{-1}cm^{-1})$	$\frac{d[A]}{dt}$ s^{-1}	ϕ	lamp output quanta s^{-1}
(a)				
340	6.65	4.637×10^{-4}	0.42	3.964×10^{14}
360	11.80	2.224×10^{-3}	0.44	10.139×10^{14}
380	19.70	3.043×10^{-3}	0.44	8.402×10^{14}
400	23.70	4.599×10^{-3}	0.48	9.584×10^{14}
420	13.30	2.315×10^{-3}	0.45	9.3115×10^{14}
(b)				
340	2.10	1.499×10^{-4}	0.43	3.964×10^{14}
360	8.40	1.938×10^{-3}	0.55	10.139×10^{14}
380	20.70	4.141×10^{-3}	0.58	8.402×10^{14}
400	29.00	6.864×10^{-3}	0.59	9.584×10^{14}
420	16.80	3.914×10^{-3}	0.60	9.3115×10^{14}

Figure (26)

Effect of varying quantum energy on ϕ_{dec} for

a) 2,5-di-n-butoxy-4-morpholinobenzenediazonium
   tetrafluoroborate
   and

b) 4-N,N-di-n-butylbenzenediazonium tetrafluoroborate
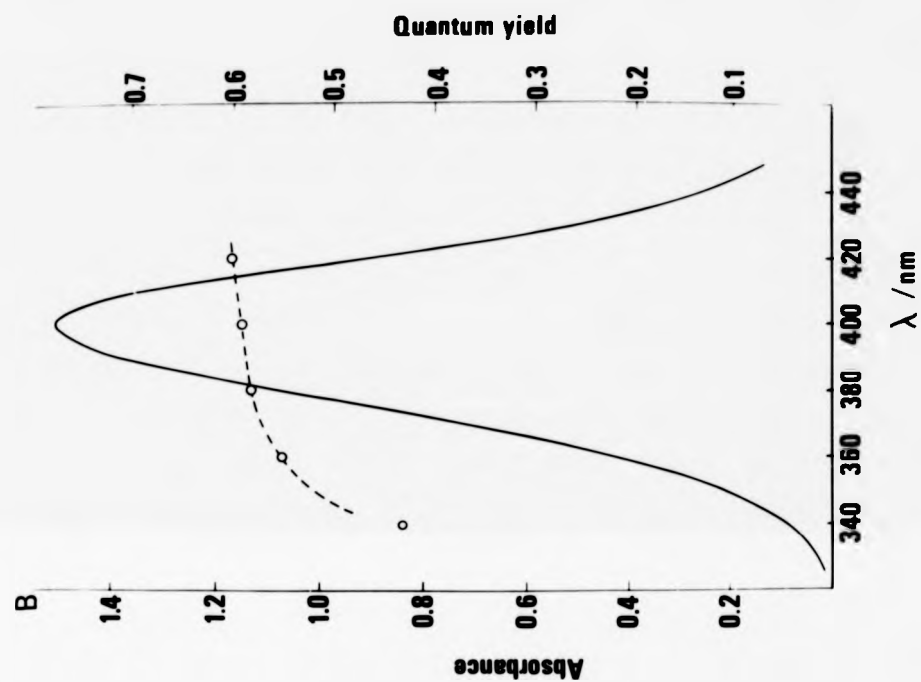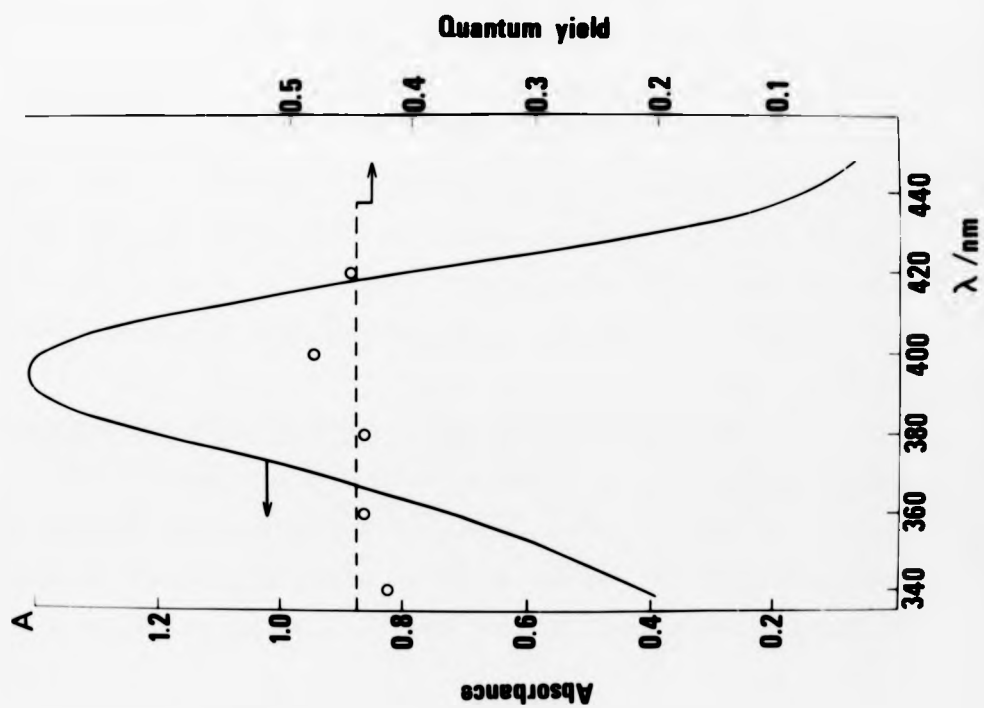
Quantum yields for 4-N,N-di-n-butyl and 2,5-di-n-butoxy-4-morpholinobenzenediazonium tetrafluoroborate have been determined at several wavelengths. A Bausch and Lomb monochromator adjusted to give a band width of 5.0 nm was used instead of Balzer interference filters. The results are given in Table 12 and graphically in Fig. (26). ϕ was found to be independent of the irradiating wavelength: these findings are indicative of efficient vibrational relaxation of the excited electronic state prior to photo-decomposition.

In summary, our findings indicate that ϕ may be increased by the presence of para-amino substituents. These substituents produce a resonant hybrid in which the quinoidal form plays an important part. Quinoidal forms of these hybrids may confer additional thermal stability (to the ground state) in these highly photolabile salts. Additional substituents may further red shift the absorption maxima (i.e. an increased con-tribution of quinoidal forms to the ground state) but these frequently have the effect of reducing ϕ (i.e. an increased contribution of quinoidal forms to the excited state).

5.2. QUANTUM YIELDS DETERMINED IN NON-AQUEOUS SOLVENTS

The thermal decomposition products of arenediazonium salts in alcohol are either an aryl-alkyl ether (formed by replace-ment of nitrogen by the alkoxyl group derived from the alcohol) or a reduction product (formed by replacement of nitrogen by

hydrogen). De Tar and Kosuge's[43] findings led them to conclude that both oxygen and acid minimized the free radical chain steps which lead to reduction products. It is therefore not unreasonable to suggest that the presence of acid and oxygen may have a similar effect on the photochemically derived products in alcoholic solution. The photodecomposition of the benzenediazonium cation was examined under a variety of conditions in ethanol to evaluate any such effects as evidenced by the quantum yield.

Quantum yields were determined by the same method used with aqueous acid solutions. The results are shown in Table 13 with approximately a ten-fold difference in rate being observed depending upon the conditions.

TABLE 13

PHOTODECOMPOSITION QUANTUM YIELDS (313 nm) FOR THE BENZENEDIAZONIUM CATION IN ETHANOL UNDER VARIOUS CONDITIONS

Conditions	ϕ
Acidified ethanol (aerated)	0.59
Ethanol (aerated)	0.94
Acidified ethanol (argon flushed)	2.34
Ethanol (argon flushed)	5.38

Inspection of the data in Table 13 indicates that acid-free solutions give appreciably higher values for ϕ than the corresponding acidic solutions. The higher values of ϕ in the absence of acid could be attributed to coupling of reactant with some product of photodecomposition. Calvert et.al.[50], however, do not report any such coupled product in their analysis following photolysis of the para-nitrobenzene-diazonium cation in ethanol, and we find no optical absorption of such a product on concluding irradiation. A radical chain reaction of the type proposed by Calvert et.al.[50] more satisfactorily accounts for the higher values of ϕ in the absence of acid. Furthermore Packer et.al.[145] have confirmed the existence of similar chain reactions in electron irradiated solutions of arenediazonium salts containing alcohols, viz.
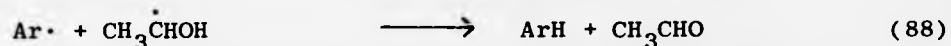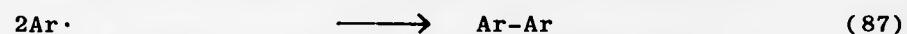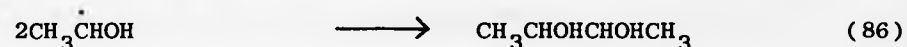
$$H_2O \rightsquigarrow H_2O^+ + e^- \xrightarrow{H_2O} OH\cdot + H_3O^+ + e^-_{aq} \tag{82}$$

$$ArN_2^+ + X^- + e^-_{aq} \longrightarrow Ar\cdot + N_2 + X^- \tag{83}$$

$$Ar\cdot + CH_3CH_2OH \longrightarrow ArH + CH_3\overset{\cdot}{C}HOH \tag{84}$$

$$CH_3\overset{\cdot}{C}HOH + ArN_2^+X^- \longrightarrow CH_3\overset{+}{C}HOH + Ar\cdot + N_2 + X^- \tag{85}$$

$$2CH_3\overset{\cdot}{C}HOH \longrightarrow CH_3CHOHCHOHCH_3 \tag{86}$$

$$2Ar\cdot \longrightarrow Ar\text{-}Ar \tag{87}$$

$$Ar\cdot + CH_3\overset{\cdot}{C}HOH \longrightarrow ArH + CH_3CHO \tag{88}$$

Oxygen acting as a radical scavenger (inhibiting propagation of the chain reaction) is the most likely cause of the considerably reduced value of ϕ in aerated solution.

Inspection of the data in Table 13 indicates that acid-free solutions give appreciably higher values for ϕ than the corresponding acidic solutions. The higher values of ϕ in the absence of acid could be attributed to coupling of reactant with some product of photodecomposition. Calvert et.al.[50], however, do not report any such coupled product in their analysis following photolysis of the para-nitrobenzene-diazonium cation in ethanol, and we find no optical absorption of such a product on concluding irradiation. A radical chain reaction of the type proposed by Calvert et.al.[50] more satisfactorily accounts for the higher values of ϕ in the absence of acid. Furthermore Packer et.al.[145] have confirmed the existence of similar chain reactions in electron irradiated solutions of arenediazonium salts containing alcohols, viz.
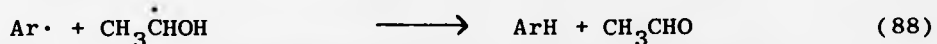
$$H_2O \longrightarrow\!\!\!\!\leadsto H_2O^+ + e^- \xrightarrow{\quad H_2O \quad} OH\cdot + H_3O^+ + e^-_{aq} \qquad (82)$$

$$ArN_2^+ + X^- + e^-_{aq} \longrightarrow Ar\cdot + N_2 + X^- \qquad (83)$$

$$Ar\cdot + CH_3CH_2OH \longrightarrow ArH + CH_3\overset{\centerdot}{C}HOH \qquad (84)$$

$$CH_3\overset{\centerdot}{C}HOH + ArN_2^+X^- \longrightarrow CH_3\overset{+}{C}HOH + Ar\cdot + N_2 + X^- \qquad (85)$$

$$2CH_3\overset{\centerdot}{C}HOH \longrightarrow CH_3CHOHCHOHCH_3 \qquad (86)$$

$$2Ar\cdot \longrightarrow Ar-Ar \qquad (87)$$

$$Ar\cdot + CH_3\overset{\centerdot}{C}HOH \longrightarrow ArH + CH_3CHO \qquad (88)$$

Oxygen acting as a radical scavenger (inhibiting propagation of the chain reaction) is the most likely cause of the considerably reduced value of ϕ in aerated solution.

Inspection of the data in Table 13 indicates that acid-free solutions give appreciably higher values for ϕ than the corresponding acidic solutions. The higher values of ϕ in the absence of acid could be attributed to coupling of reactant with some product of photodecomposition. Calvert et.al.[50], however, do not report any such coupled product in their analysis following photolysis of the para-nitrobenzene-diazonium cation in ethanol, and we find no optical absorption of such a product on concluding irradiation. A radical chain reaction of the type proposed by Calvert et.al.[50] more satisfactorily accounts for the higher values of ϕ in the absence of acid. Furthermore Packer et.al.[145] have confirmed the existence of similar chain reactions in electron irradiated solutions of arenediazonium salts containing alcohols, viz.
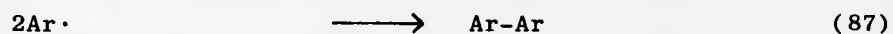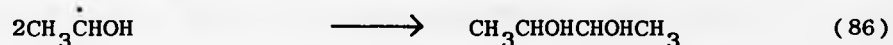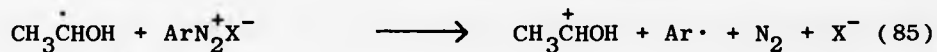
$$H_2O \longrightarrow\!\!\!\!\!\!\!\!\sqrt{\!\!\!\!\!\!\!\!\nearrow} H_2O^+ + e^- \xrightarrow{H_2O} OH\cdot + H_3O^+ + e^-_{aq} \tag{82}$$

$$ArN_2^+ + X^- + e^-_{aq} \longrightarrow Ar\cdot + N_2 + X^- \tag{83}$$

$$Ar\cdot + CH_3CH_2OH \longrightarrow ArH + CH_3\dot{C}HOH \tag{84}$$

$$CH_3\dot{C}HOH + ArN_2^+X^- \longrightarrow CH_3\overset{+}{C}HOH + Ar\cdot + N_2 + X^- \tag{85}$$

$$2CH_3\dot{C}HOH \longrightarrow CH_3CHOHCHOHCH_3 \tag{86}$$

$$2Ar\cdot \longrightarrow Ar-Ar \tag{87}$$

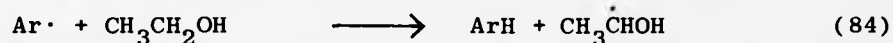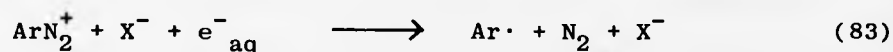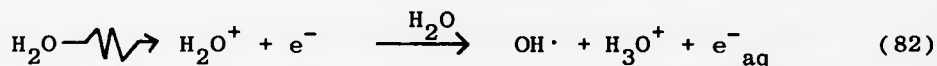$$Ar\cdot + CH_3\dot{C}HOH \longrightarrow ArH + CH_3CHO \tag{88}$$

Oxygen acting as a radical scavenger (inhibiting propagation of the chain reaction) is the most likely cause of the considerably reduced value of ϕ in aerated solution.

Reproducible values of ϕ could only be obtained from solutions where propagation of the radical chain reaction is minimal, i.e. in acidified or aerated solution.

Quantum yields for simple meta- and para-substituted arenediazonium salts have been determined in acidified ethanol under both aerated and deaerated conditions. Considerable loss of the arenediazonium salt occurred in neutral ethanol, due to thermal decomposition. Addition of sulphuric acid to aerated ethanolic solutions of the various arenediazonium salts reduced thermal decomposition to a negligible level. The quantum yields are given in Table 14. Many of those determined in acidified argon-bubbled ethanol approach or exceed unity, presumably because of insufficient acidification to suppress propagation of the chain reaction. Values of ϕ determined in the presence of oxygen were less than unity and reproducible. The values which gave good correlation between log ϕ and the appropriate Hammett σ constants were those determined in aerated acidified ethanol Fig. (27).

The data in Fig.(27) includes the corresponding determinations made in aqueous sulphuric acid, for comparison. The value of $\rho = -0.26 \pm 0.02$ (r = 0.98) is slightly lower than that of similar determinations in aqueous sulphuric acid where $\rho = 0.56 \pm 0.05$. Although the quantum yields in aerated acidified ethanol are higher in all cases, the two sets of data are sufficiently similar to suggest a common principal mechanism of carbonium ion formation under the conditions described.

TABLE 14

PHOTODECOMPOSITION QUANTUM YIELDS (313 nm) FOR SOME META- AND PARA-SUBSTITUTED ARENEDIAZONIUM TETRAFLUOROBORATES IN ETHANOL $(0.05 \text{ mol dm}^{-3})$ IN SULPHURIC ACID

Benzenediazonium cation	λ_{max}/nm	$\varepsilon_{max} \times 10^{-3}$ $(M^{-1}cm^{-1})$	$\varepsilon_{313} \times 10^{-3}$ $(M^{-1}cm^{-1})$	ϕ deaerated solution	ϕ aerated solution
$C_6H_5N_2^+$	259	11.80	1.60	0.72	0.58
$4\text{-}ClC_6H_4N_2^+$	280	12.25	1.50	1.74	0.49
$3\text{-}ClC_6H_4N_2^+$	262	8.80	1.80	0.82	0.45
$4\text{-}BrC_6H_4N_2^+$	290	15.85	4.65	0.42	0.46
$4\text{-}CH_3C_6H_4N_2^+$	275	14.10	1.66	0.58	0.60
$3\text{-}CH_3C_6H_4N_2^+$	265	10.60	2.43	0.97	0.59
$4\text{-}CH_3OC_6H_4N_2^+$	313	25.00	-	0.36	0.48
$3\text{-}CH_3OC_6H_4N_2^+$	275	6.65	1.28	0.35	0.58
$4\text{-}O_2NC_6H_4N_2^+$	258	15.60	3.12	0.50	0.34
$3\text{-}O_2NC_6H_4N_2^+$	237	19.20	1.26	0.46	0.37

Figure (27)

Hammett plots for

a) ⊘ quantum yields determined in (argon-flushed)
   0.05 mol dm^{-3} sulphuric acid

   and

b) ● quantum yield determined in aerated ethanol
   (0.05 mol dm^{-3} in sulphuric acid).
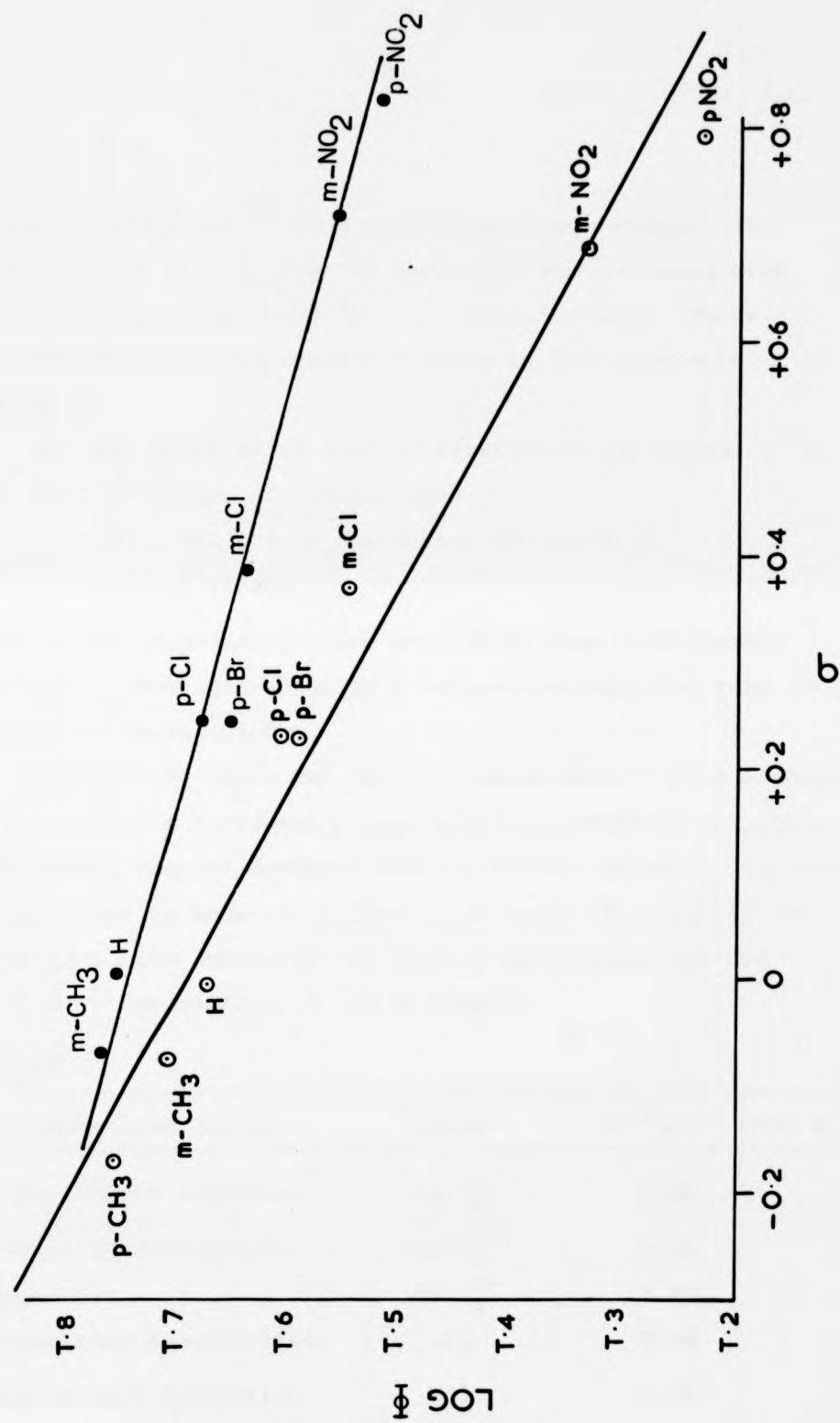
Mizianty et.al.[141] have determined photodecomposition quantum yields for a number of para-alkylaminobenzdiazonium salts in ethanol and 2 mol dm^{-3} hydrochloric acid. Their findings conflict with those presented in this work with respect to:

(i)   the sensitivity of ϕ to aeration of the medium

(ii) the effect of solvent upon ϕ

(iii) the stability of arenediazonium salts in
      neutral ethanol.

However their conclusions have been drawn from very limited data where a 20% difference in ϕ between solvents has been regarded as insignificant.

Commercially important arenediazonium salts with 4-morpholino or 4-tolylthio substituent groups were also observed to undergo considerable thermal decomposition in neutral ethanol. Thermal decomposition is known to follow first-order kinetics and the first-order rate constants for some of these reactions are given below for neutral, aerated ethanol.

TABLE 15

Benzenediazonium cation	Anion	$10^{-2}k/s^{-1}$ (291 K)
2,5-dimethoxy-4-tolylthio	$\frac{1}{2}ZnCl_4^{2-}$	1.06
2,5-diethoxy-4-tolylthio	$\frac{1}{2}ZnCl_4^{2-}$	1.45
4-morpholino	$\frac{1}{2}ZnCl_4^{2-}$	1.60
2,5-dimethoxy-4-morpholino	BF_4^-	0.90
2,5-diethoxy-4-morpholino	BF_4^-	1.75

TABLE 16

SPECTROSCOPIC AND QUANTUM YIELD DATA FOR THE 380 nm PHOTOLYSIS
OF COMMERCIALLY IMPORTANT ARENEDIAZONIUM SALTS IN AERATED
ACIDIFIED ETHANOL (0.05 mol dm^{-3} IN SULPHURIC ACID)

Benzenediazonium Salt		λ_{max}	$\epsilon_{max} \times 10^{-3}$	ϕ at
Cation	Anion		$(M^{-1}cm^{-1})$	λ 380 nm
4-morpholino	$\frac{1}{2}ZnCl_4^{2-}$	380	39.25	0.74[*] ± 0.03
2,5-dimethoxy-4-morpholino	BF_4^-	400	27.62	0.77
2,5-diethoxy-4-morpholino	BF_4^-	401	26.00	0.67
2,5-diethoxy-4-morpholino	$\frac{1}{2}ZnCl_4^{2-}$	402	26.97	0.72
2,5-di-n-propoxy-4-morpholino	BF_4^-	402	27.25	0.71
2,5-di-n-butoxy-4-morpholino	BF_4^-	403	28.87	0.70
2,5-dimethoxy-4-tolylthio	$\frac{1}{2}ZnCl_4^{2-}$	401	16.80	0.55[*] ± 0.02
2,5-diethoxy-4-tolylthio	$\frac{1}{2}ZnCl_4^{2-}$	401	15.00	0.54

*   Indicates the value of ϕ is the average of at least two
   determinations made on separate occasions.

Addition of sulphuric acid to aerated ethanolic solutions of these more complex arenediazonium salts completely suppressed thermal decomposition.

Although it is difficult to draw any rigorous conclusions from the data in Table 16 (because of the steric factors involved and the multiplicity of the substituents) some trends are evident,

(i)   the difference in ϕ between the morpholino and tolylthio salts and

(ii) the insensitivity of ϕ to substitution of alkoxy groups in the 2- and 5-positions. Finally the relative stability of the tolylthio salts (ϕ = 0.55) compared with the morpholino salts (ϕ average = 0.71) agrees with the qualitative observations of Bryan and Walker.[144]

Recently, Gokel and Cram[145] observed solubilisation of arenediazonium salts in chlorocarbon solvents by crown ether complexation. The formation of arenediazonium-crown ether complexes has been verified by nmr[145] and infra-red[145] spectroscopy. Izatt et.al.[146] in a detailed investigation of the solubilisation of arenediazonium salts with crown ethers found that complexation is extremely sensitive to both steric and electronic factors. Steric factors (i.e. the presence of alkyl or alkoxy substituents ortho to the diazonium group) effectively prevent entry of the diazonium group into the ring cavity of the crown ether. Additionally electronic factors

(such as the introduction of strong electron donating sub-
stituents like $-N(CH_3)_2$ para to the diazonium group) may
decrease the stability of the complex formed. This is
presumably due to the delocalisation of positive charge
away from the diazonium group. X-Ray crystallographic
data[147] indicates that complexation is effectively main-
tained via hydrogen bonding between the diazonium group
and available oxygen atoms in the crown ether ring
(structure LXXXIV).
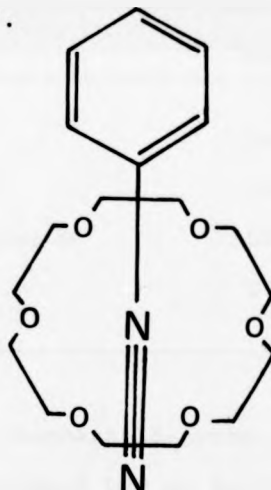
(LXXXIV)

Bartsch et.al.[148] have reported that such complexes
exhibit markedly enhanced thermal stability relative to the
corresponding uncomplexed arenediazonium salt; they con-
centrated on the thermal decomposition of tert-butylbenzenediazonium
tetrafluoroborate in 1,2-dichloroethane as this solvent eliminates
the potential problem of studying kinetics under heterogeneous
reaction conditions. In their work, several crown ethers were
examined in order to determine which were the most effective

in suppressing thermal decomposition. Their data is given below in Table 17.

TABLE 17

FIRST-ORDER RATE CONSTANTS FOR THE THERMAL DECOMPOSITION OF TERT-BUTYLBENZENEDIAZONIUM TETRAFLUOROBORATE IN 1,2-DICHLOROETHANE IN THE PRESENCE OF EQUIMOLAR CROWN ETHERS AT 323K

Crown ether	λ_{max}	$10^{-4}k/s^{-1}$(323K)
None	285	2.28
Dibenzo-18-crown-6	276	1.74
Dicyclohexyl-18-crown-6	280	1.42
18-Crown-6	276	1.36

15-Crown-5, N-tosylmonoaza-18-crown-6, hexathia-18-crown-6 and hexanthia-21-crown-6 had no influence upon the rate of thermal decomposition of tert-butylbenzendiazonium tetrafluoroborate 1,2-dichloroethane. As the results shown in Table 17 indicate, 18-crown-6 is the most effective macrocyclic polyether which suppresses thermal decomposition of arenediazonium salts in 1,2-dichloroethane. Bartsch et.al.[148] have also determined first-order rate constants for the thermal decomposition of tert-butylbenzenediazonium tetrafluoroborate in the presence of excess 18-crown-6. Their results are shown in Table 18.

TABLE 18

FIRST-ORDER RATE CONSTANTS FOR THE THERMAL DECOMPOSITION OF TERT-BUTYLBENZENEDIAZONIUM TETRAFLUOROBORATE IN 1,2-DICHLOROETHANE AT 323 K

$[18-crown-6]/[t-C(CH_3)_3C_6H_4N_2^+]$	λ_{max} nm	$10^{-4}k/s^{-1}$(323 K)
0.00	285.0	2.280
1.00	276.0	1.360
4.99	269.0	0.429
24.8	268.5	0.117
99.7	268.0	0.051

These results show that the rate constant for the thermal decomposition of tert-butylbenzenediazonium tetrafluoroborate in 1,2-dichloroethane may be reduced by a factor of 45 when a large excess of 18-crown-6 is present in the reaction mixture. The arenediazonium salt has an ultra-violet spectrum which exhibits a maximum at 285 nm in 1,2-dichloroethane; however, when the crown ether is present (at increasing concentrations), the diazonium ion chromophore is correspondingly blue-shifted.

Bartsch et.al.[149] have also found that complexation of arenediazonium ions with crown ethers of an appropriate size provides photochemical, as well as thermal stabilization. Additionally they reported decreased fluorobenzene yields

from the Schieman reaction (89) when the benzenediazonium ion

$$C_6H_5N_2^+ \ BF_4^- \ \xrightarrow{\ h\nu\ } \ C_6H_5F \ + \ N_2 \ + \ BF_3 \tag{89}$$
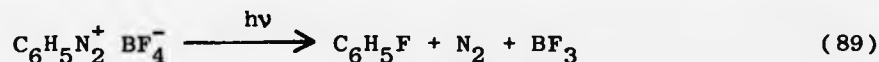
is in the form of a complex with 18-crown-6.

We have extended their work to include the photochemical decomposition of 4-morpholinobenzenediazonium tetrafluoroborate (a commercially useful arenediazonium salt) complexed with 18-crown-6 in dichloromethane, and the results are shown in Table 19.

TABLE 19

QUANTUM YIELDS FOR 4-MORPHOLINOBENZENEDIAZONIUM TETRAFLUOROBORATE DETERMINED IN DICHLOROMETHANE IN THE PRESENCE OF 18-CROWN-6

Conditions	λ nm	$\varepsilon \times 10^{-3}(M^{-1}cm^{-1})$	ϕ
4-morpholinobenzenediazonium tetrafluoroborate	383(λ max) 380(λ photolysis)	28.90 28.69	0.56
4-morpholinobenzenediazonium tetrafluoroborate + 100 mol dm^{-3} excess of 18-crown-6	359(λ max) 364(λ photolysis)	26.42 26.35	0.28

On 'crowning', a blue-shift of the absorption maximum of the arenediazonium salt was observed in accordance with the findings of Bartsch et.al.[148] The quantum yield for 4-morpholinobenzene-diazonium tetrafluoroborate in the absence of 18-crown-6 is 0.56, which is very close to the value in dilute sulphuric acid

of 0.60. In the presence of a 100 mol dm^{-3} excess of 18-crown-6, the quantum yield was reduced by a factor of 2, i.e. to 0.28. Our results would suggest some recombination of intermediates within the 'crown cage'.

However, several questions remain unanswered:

(a) the considerable blue-shift of λ_{max}. It is possible that the conjugation of the morpholino group is perturbed by bending within the crown cage, but this would appear unlikely when one considers the available data[150] for the uptake of metal ions, from which it would seem that only the $-N_2^+$ moiety is actually 'crowned'.

(b) Whether it is possible to find a concentration of crown ether which will usefully stabilise the arenediazonium salt against thermal decomposition but not reduce its photochemical sensitivity by as much as a factor of 2.

(c) The effect of other substituent groups on the arene-diazonium salt as regards (i) reducing the extent of photochemical recombination with the 'crown cage' and (ii) the degree of the wavelength shift on 'crowning'.

To conclude, crown ethers may have considerable potential for the solid state stabilization of thermally unstable arene-diazonium salts. However, crown ethers are of limited value in stabilizing arenediazonium salts in sensitised reprographic papers.

5.3. QUANTUM YIELDS DETERMINED IN CELLULOSE ACETATE FILM

Photodecomposition of simple mono-substituted arenediazonium salts in aqueous acid occurs via carbonium ion formation whilst in alcoholic solvents aryl radicals are generated. Product analysis and photodecomposition quantum yields have confirmed the existence of the two possible pathways. However, photo-decomposition of arenediazonium salts in a solid polymer support is less well understood. Few workers have attempted to resolve this situation, because of the difficulty associated with the isolation of photolysis products from a polymer film.

Previous work in this area is limited to that of Barraclough et.al.[66] and Baltazzi et.al.[67] in which the photo-decomposition quantum yields for a number of dialkylamino-benzenediazonium salts were reported.

Barraclough's[66] method involves mounting the polymer film in a spectrograph camera frame. Portions of the polymer film are then irradiated (through the shutter assembly) for differing periods of time (the final exposure being of sufficient duration to completely decompose the diazonium salt in the region of maximum absorption) and then coupling the remaining salt with 2-naphthol. Coupling reactions have been used for quantitive determinations of arenediazonium salts in solution and are known to be subject to some degree of error.[37] In Baltazzi's[67] method the photodecomposition is followed spectroscopically and a similar approach has been adopted in this work.

5.3. <u>QUANTUM YIELDS DETERMINED IN CELLULOSE ACETATE FILM</u>

Photodecomposition of simple mono-substituted arenediazonium salts in aqueous acid occurs via carbonium ion formation whilst in alcoholic solvents aryl radicals are generated. Product analysis and photodecomposition quantum yields have confirmed the existence of the two possible pathways. However, photodecomposition of arenediazonium salts in a solid polymer support is less well understood. Few workers have attempted to resolve this situation, because of the difficulty associated with the isolation of photolysis products from a polymer film.

Previous work in this area is limited to that of Barraclough et.al.[66] and Baltazzi et.al.[67] in which the photodecomposition quantum yields for a number of dialkylamino-benzenediazonium salts were reported.

Barraclough's[66] method involves mounting the polymer film in a spectrograph camera frame. Portions of the polymer film are then irradiated (through the shutter assembly) for differing periods of time (the final exposure being of sufficient duration to completely decompose the diazonium salt in the region of maximum absorption) and then coupling the remaining salt with 2-naphthol. Coupling reactions have been used for quantitive determinations of arenediazonium salts in solution and are known to be subject to some degree of error.[37] In Baltazzi's[67] method the photodecomposition is followed spectroscopically and a similar approach has been adopted in this work.

Films were cast from 10.0 cm^3 of an acetone solution of secondary cellulose acetate (acetic acid yield 53.4 %) containing the requisite quantity of arenediazonium salt drawn out with a threaded metal bar (25 threads per inch) supported between two parallel glass plates, Fig.(28). Films cast by this method were of high optical quality drying in less than two minutes, and having a reproducible thickness of 0.025 mm upon evaporation of the solvent. Films were exposed to the photolysis beam through a circular aperture with a radius of 0.36 cm, Fig.(29).

Quantum yields have been determined in cellulose acetate film for a number of simple mono-substituted arenediazonium salts (λ photolysis 313 nm) and for some of the more complex arenediazonium salts (λ photolysis 380 nm), the results are given in Table 20.

Photodecomposition quantum yields have been calculated from the ratio of the number of molecules of arenediazonium salt photodecomposed in time t, per unit area of film, to the number of light quanta absorbed over the same area in the same time.

$$\phi = \frac{\frac{(\Delta OD/t)}{\varepsilon} \times \frac{\pi \times r^2}{1000} \times 6.023 \times 10^{23}}{\text{number of quanta absorbed s}^{-1}} \tag{90}$$

where

ε = extinctinction coefficient of the arenediazonium salt at the exciting wavelength

r = radius of the aperture through which light was exposed to the film

Figure (28)

Metal bar and parallel glass plates used to prepare
cellulose acetate films

Figure (29)

Apparatus used to support cellulose acetate films during
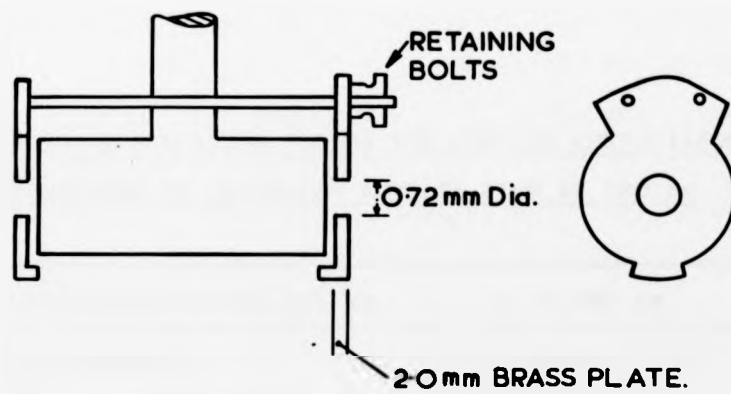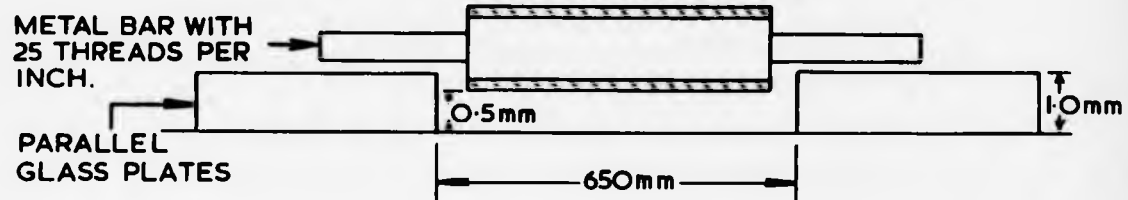quantum yield determinations

METAL BAR WITH
25 THREADS PER
INCH.

PARALLEL
GLASS PLATES

0·5mm

650mm

1·0mm

RETAINING
BOLTS

0·72 mm Dia.

2·0 mm BRASS PLATE.

TABLE 20

PHOTODECOMPOSITION QUANTUM YIELDS FOR SIMPLE META- AND PARA-
SUBSTITUTED BENZENEDIAZONIUM TETRAFLUOROBORATES IN CELLULOSE
ACETATE FILM AT 313 nm

Benzenediazonium cation	ϕ at 313 nm
$C_6H_5N_2^+$	0.26
$p-CH_3C_6H_4N_2^+$	*0.28 ± 0.056
$m-CH_3C_6H_4N_2^+$	0.29
$p-ClC_6H_4N_2^+$	0.30
$m-ClC_6H_4N_2^+$	*0.27 ± 0.054
$p-BrC_6H_4N_2^+$	0.28
$p-CH_3OC_6H_4N_2^+$	0.34
$m-CH_3OC_6H_4N_2^+$	0.36

* Average of at least two determinations made on separate
occasions.

TABLE 21

PHOTODECOMPOSITION QUANTUM YIELDS FOR COMPLEX ARENEDIAZONIUM
TETRAFLUOROBORATES IN CELLULOSE ACETATE FILM AT 380 nm

Benzenediazonium cation	ϕ at 380 nm
4-morpholino	0.30
2,5-diethoxy-4-morpholino	0.38
2,5-dinbutoxy-4-morpholino	0.28 (0.43)[67]
2,5-diethoxy-4-tolylthio	0.25
4-N,N-diethylamino	0.29 (0.25)[66]

TABLE 20

PHOTODECOMPOSITION QUANTUM YIELDS FOR SIMPLE META- AND PARA-SUBSTITUTED BENZENEDIAZONIUM TETRAFLUOROBORATES IN CELLULOSE ACETATE FILM AT 313 nm

Benzenediazonium cation	ϕ at 313 nm
$C_6H_5N_2^+$	0.26
$p-CH_3C_6H_4N_2^+$	*0.28 ± 0.056
$m-CH_3C_6H_4N_2^+$	0.29
$p-ClC_6H_4N_2^+$	0.30
$m-ClC_6H_4N_2^+$	*0.27 ± 0.054
$p-BrC_6H_4N_2^+$	0.28
$p-CH_3OC_6H_4N_2^+$	0.34
$m-CH_3OC_6H_4N_2^+$	0.36

* Average of at least two determinations made on separate occasions.

TABLE 21

PHOTODECOMPOSITION QUANTUM YIELDS FOR COMPLEX ARENEDIAZONIUM TETRAFLUOROBORATES IN CELLULOSE ACETATE FILM AT 380 nm

Benzenediazonium cation	ϕ at 380 nm
4-morpholino	0.30
2,5-diethoxy-4-morpholino	0.38
2,5-dinbutoxy-4-morpholino	0.28 (0.43)[67]
2,5-diethoxy-4-tolylthio	0.25
4-N,N-diethylamino	0.29 (0.25)[66]

Barraclough et.al.[66] reported little difference within
experimental error ($\pm$2.0 nm) of λ_{max} for arenediazonium salts
in solvents of differing polarity including a 7.5% (wt/vol)
solution of secondary cellulose acetate in acetone. ε_{max} also
appears to remain approximately constant in different solvents,
e.g. for para-diethylaminobenzenediazonium tetrafluoroborate

	λ_{max}nm	$\varepsilon_{max} \times 10^{-3}(M^{-1}cm^{-1})$
aqueous acid	380	40.80
acidified ethanol	380	40.10
cellulose acetate	380	40.30

Accordingly the values of ε used in the calculation of ϕ
for the various arenediazonium salts were those obtained from
the determination of ε_{max} in acidified ethanol, (Tables 14 and 16).

It is generally agreed that photolysis of arenediazonium
salts in solution follows first-order kinetics. In cellulose
acetate films, the logarithm of the decrease in absorbance
(after irradiation) with respect to time was linear in agreement
with the findings of Barraclough et.al. Tables 20 and 21
indicate that in cellulose acetate values of ϕ for the simple
mono-substituted arenediazonium salts are apparently independent of
the substituent group present (i.e. the Hammett ρ constant is
zero). This finding suggests that photodecomposition in
cellulose acetate films proceeds through a radical intermediate.
The possibility that the constancy of the quantum yield for the
various arenediazonium salts is an experimental artefact,

appears unlikely in view of the very different values for $\Delta(O.D.)/t$ measured for the different series of salts (which are compensated for in the calculation of ϕ by equally differing extinction coefficients).

Quantum yields for meta- and para-nitrobenzenediazonium tetrafluoroborate could not be determined inasmuch as their photolysis gave products which absorbed at the irradiation wavelength. The absorption spectra of the products formed could not be identified either as nitrobenzene, the most likely product, or para-nitrophenol. A similar attempt to match the photodecomposition products from benzenediazonium tetrafluoroborate (in cellulose acetate) with either benzene or phenol, were also unsuccessful.

CHAPTER VI

LOW TEMPERATURE ELECTRON SPIN RESONANCE
STUDIES OF IRRADIATED ARENEDIAZONIUM SALTS

6.1. SPECTRUM OF IRRADIATED 'DIAZO' FILM

Modern developments of 'Diazo type' reprographic systems employ a polymer film (in place of paper) as a support for the light-sensitive component. 'Melinex' (I.C.I. Ltd.) and 'Epikote' (Shell Ltd) are extensively used by Ozalid Ltd., for this purpose.

'Melanex' film coated with 2,5-di-n-butoxy-4-morpholino-benzenediazonium tetrafluoroborate was irradiated in situ with ultra-violet light (bare arc) at 77K. The esr spectrum (Fig. 30) consists of several well-defined features which are as follows:
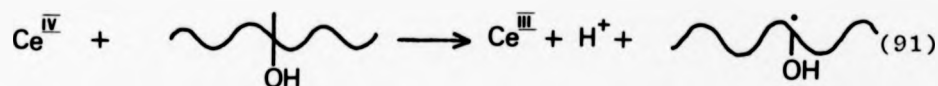
(i)   A structureless singlet centred near g=2 and
       similar to the one observed by Sukigara and
       Kikuchi from the photolysis of benzenediazonium
       tetrafluoroborate in a methanol glass at 77K.

(ii)   Three very broad singlets at field positions
       ca. 92.8, 163.0 and 437.0 mT. (These signals
       have been a principal area of investigation
       in this work).

(iii) At very high resolution, two small signals
       centred near g=2 and separated by 50.0 mT.

All signals were reproduced from a sample irradiated at 401 nm under similar conditions; however several minutes were required to generate detectable quantities of the paramagnetic species involved under these conditions. The intensities of

all the signals, are undiminished when the irradiating light
source is removed. All signals were absent when a similar
sample was irradiated at room temperature.

These signals may arise either from paramagnetic transients
formed from the photodecomposition of 2,5-di-n-butoxy-4-morpholino-
benzenediazonium tetrafluoroborate or from intermediates produced
during attack on the polymer support.

Any radials derived from oxidation of the polymer may be
conveniently prepared by sensitising the film with ammonium
ceric nitrate viz.

$$Ce^{\overline{IV}} \; + \; \diagdown\!\diagup\!\diagdown\!\diagup\!\diagdown\underset{OH}{|} \diagdown\!\diagup\!\diagdown\!\diagup \longrightarrow Ce^{\overline{III}} + H^+ + \; \diagdown\!\diagup\!\diagdown\!\diagup\underset{OH}{\overset{\bullet}{|}}\diagdown\!\diagup\!\diagdown \quad (91)$$

followed by irradiation at 77K. The polymer-derived radical
so obtained (Fig.31) has a g value of 2.0026. Clearly this
is not the species[151] responsible for the signals recorded in
the esr spectrum of irradiated 2,5-di-n-butoxy-4-morpholino-
benzenediazonium tetrafluoroborate at 77K. Moreover, as we
shall show later, the same wide field spectrum is produced
from aqueous glasses and powders of the arenediazonium salt.

Feature (iii) has been assigned to trapped hydrogen atoms
which are known to show this magnitude of coupling constart.
A detailed discussion of the assignment of features (i) and
(ii) follows in Sections 6.2 and 6.3. respectively.

Figure (30)

Esr spectrum of irradiated Melanex film coated with

2,5-di-n-butoxy-4-morpholinobenzenediazonium
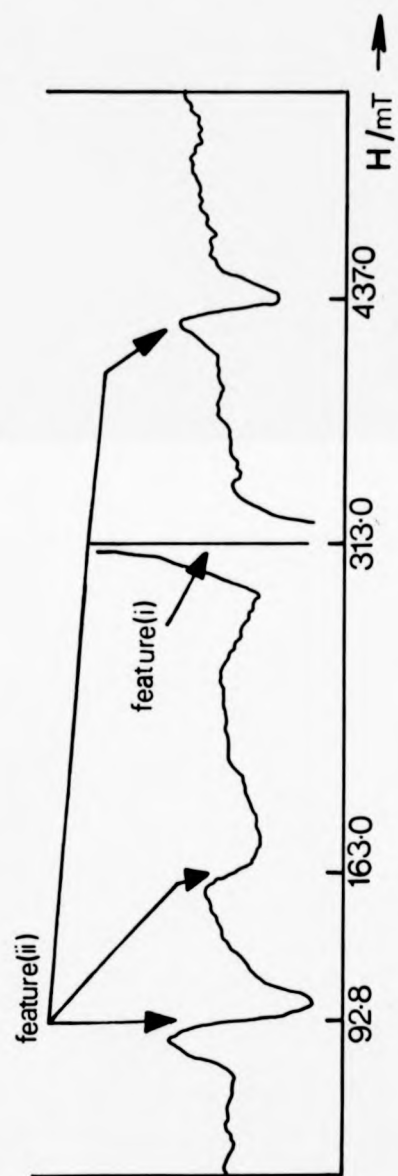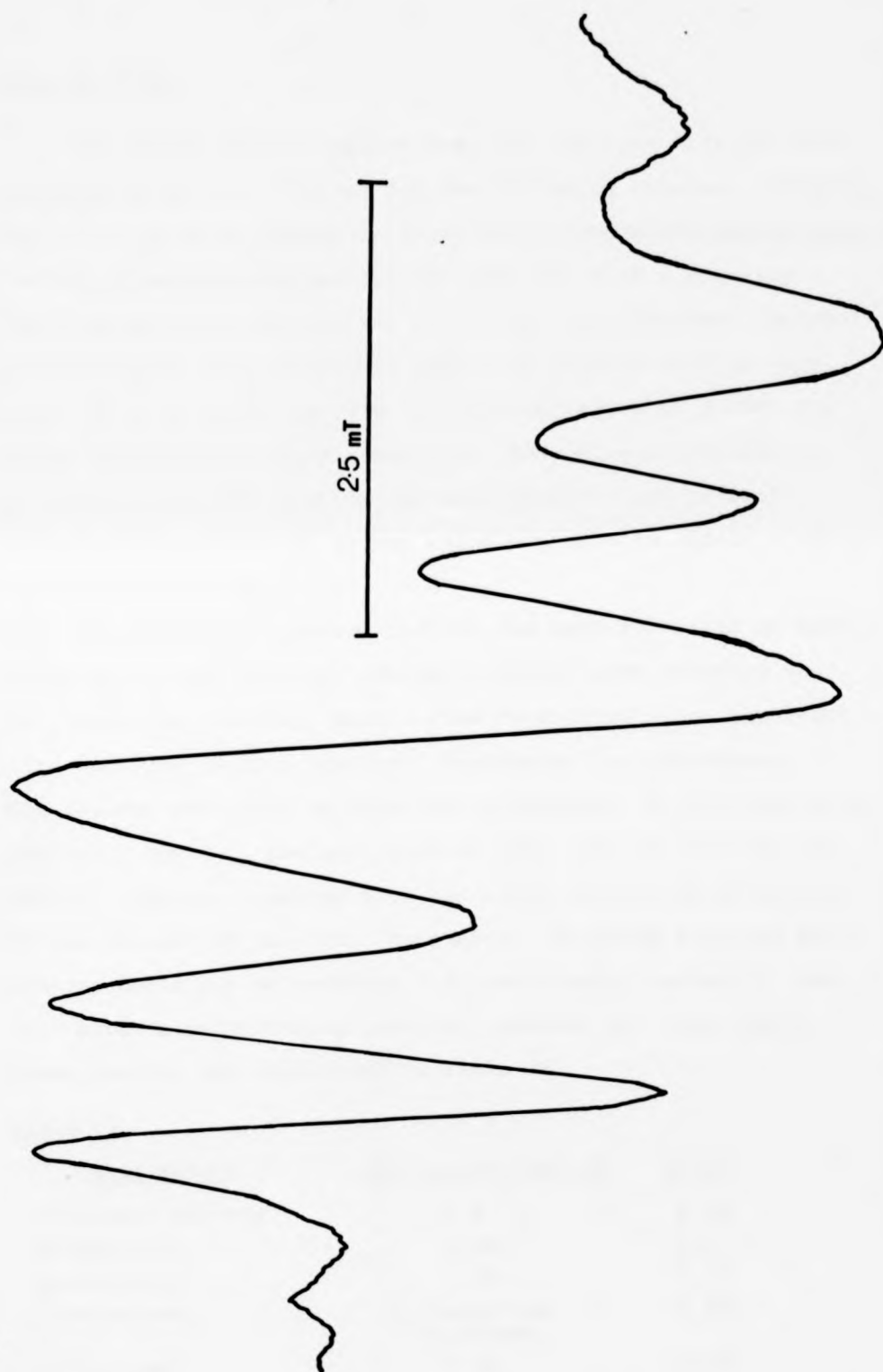
tetrafluoroborate at 77 K

feature(ii)

feature(i)

feature(iii)

H /mT

92·8   163·0   313·0   437·0

50 mT

Figure (31)

Esr spectrum of the polymer radical from cellulose

acetate film at 77 K

2.5 mT

6.2. ARYL RADICALS

The strong signal centred near g=2 (feature (i)) has been
assigned to an aryl radical for the following reasons. Firstly,
the spectrum is a singlet or (with other para-nitrogen substituted
salts), a weakly-resolved triplet (Fig.32) with a coupling
constant of ca.1.4 mT for two equivalent ring protons. Secondly,
our average g value of 2.0035 (Table 23 Section 6.3) is very
close to previously reported isotropic g values of 2.0030 for
methyl-substituted phenyl radicals. Some slight decrease in
g is expected since many of our aryl radicals are heavily
substituted with alkoxy groups which are able to induce a small
spin-orbit coupling.

The 4-morpholinophenyl radical has been generated in host
matrices of tert-butanol, methanol, deuteriated methanol and
on a silca gel surface, with a view to resolving the hyperfine
structure due to ring protons. Resolution in tert-butanol
(Fig.33) was poor with no hyperfine structure. In the remaining
matrices, however, the esr spectrum (Fig. 33) of this species
clearly displays coupling from the ortho protons as evidenced
by the triplet of ca. 1:2:1 intensity. Coupling from the meta
protons could not be resolved. In deuterated methanol, there
is a notable reduction in coupling constant and line width.
These results are summarised in Table 22.

TABLE 22

Host matrix	a^H ortho protons mT	ΔH mT
cellulose acetate	1.4	4.40
methanol-h_4	2.36	3.47
methanol-d_4	1.43	3.04
tert-butanol	no hyperfine structure	3.20
silica gel	1.55	3.15

Figure 32

a) 4-morpholinophenyl radical

b) 4-piperidinophenyl radical
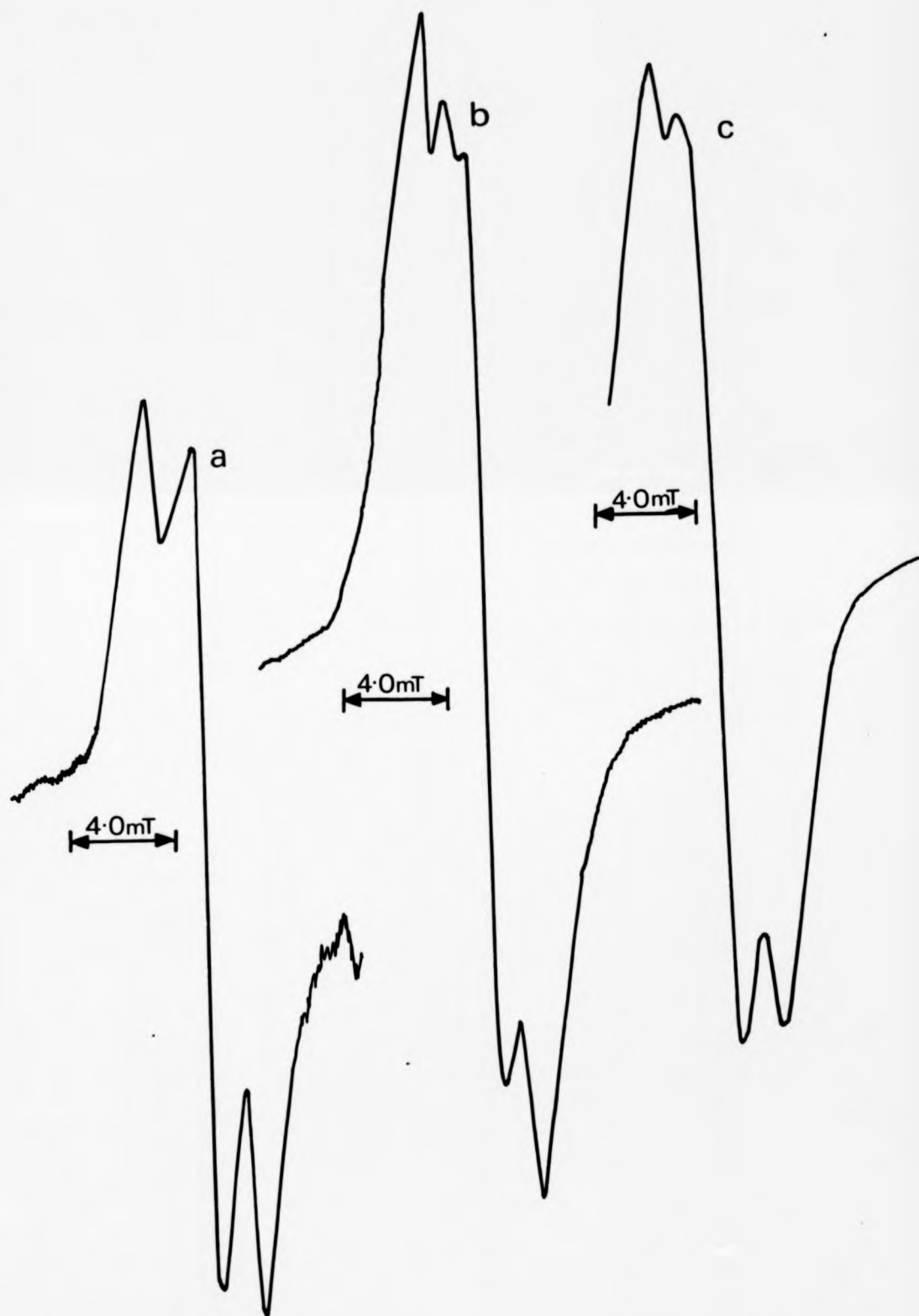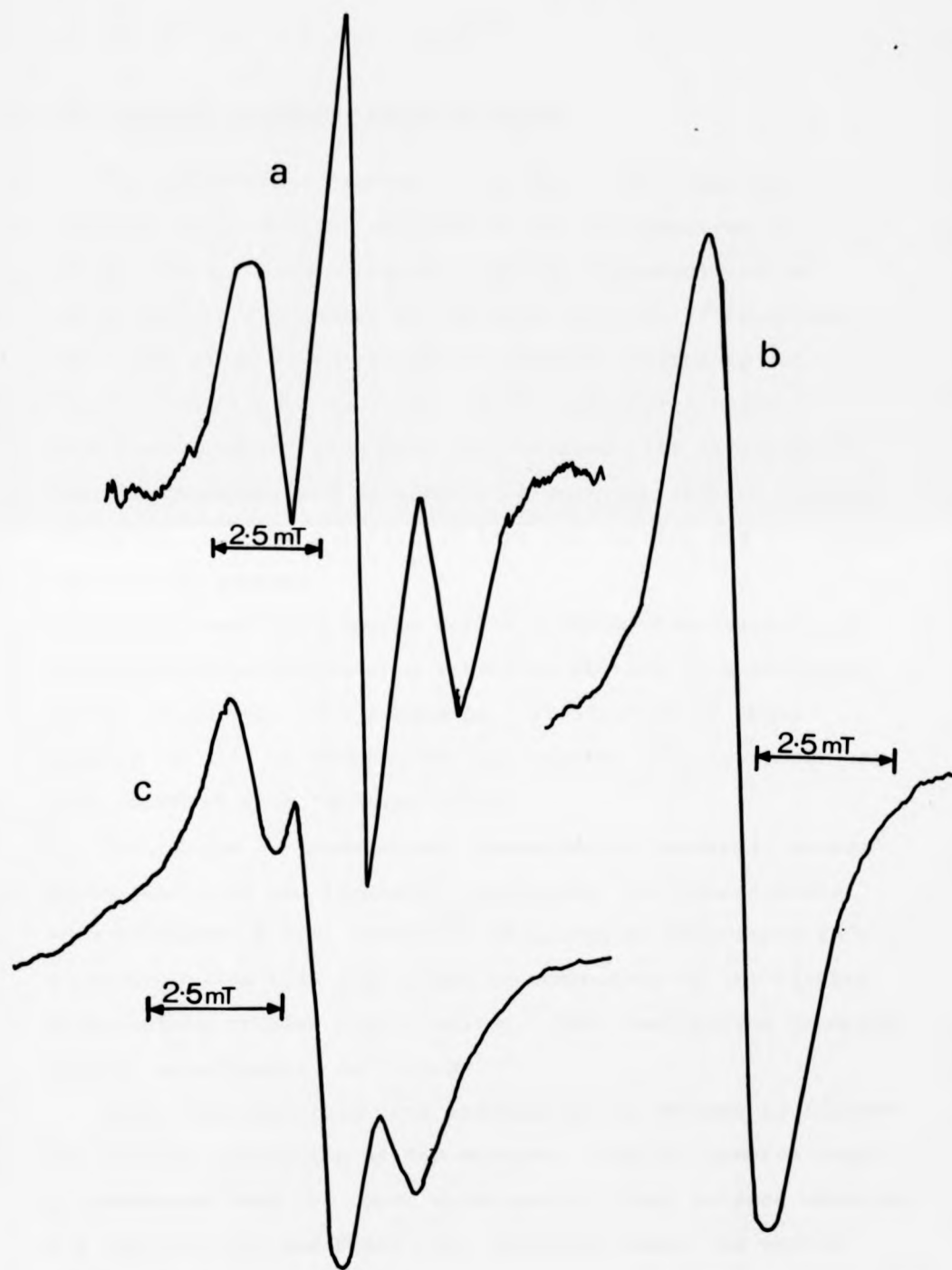
c) 4-pyrrolidinophenyl radical

Figure (33)

4-morpholinophenyl radical at 77 K in

a)   deuteriated methanol

b)   tert-butanol

c)   on the surface of SiO_2

6.3. ARYL CATIONS AS GROUND STATE TRIPLETS

The three broad signals at ca. 92.8, 163.0 and 437.0 mT
(feature (ii) Fig.30) observed in the esr spectrum of
irradiated 2,5-di-n-butoxy-4-morpholinobenzenediazonium
tetrafluoroborate coated on 'Melanex' film at 77 K provided
the first clues to establishing suitable conditions for
further investigations. Many of the commercial 'Diazo'
type reprographic films have been treated with lacquers and
certain couplers, and in order to reduce any effects of these
additives, most of our initial work was carried out in simpler
but related systems.

Preliminary experiments with 2,5-dialkoxy derivatives of
4-morpholinobenzenediazonium tetrafluoroborate in a cellulose
acetate film were very promising. Irradiation of these
samples in situ at 77 K yielded esr spectra closely resembling
that observed from 'Melanex' film.

The origin of these broad resonances at seemingly unusual
field positions was initially perplexing, but consultation
with Professor M.C.R. Symons[152] of Leicester University gave
a valuable lead that they might be components of the elusive
ground-state triplet phenyl cation. This realisation prompted
further experiments, as follows.

Other host matrices were examined in an attempt to improve
the overall resolution of the spectra. Similar spectra could
be generated from the above compounds in other polymer matrices,
e.g. polystyrene and Shell Ltd. 'Epikote' resin (an expoxy
polymer based on bis-phenol A). Comparable esr spectra were

also obtained from low temperature glasses of 2-phenylethanol, benzyl alcohol and 9.0 mol dm^{-3} aqueous lithium chloride containing 2,5-di-n-butoxy-4-morpholinobenzenediazonium tetrafluoroborate.

In an attempt to identify structural features which promote formation of Ar^+, a number of isomeric and structurally related salts were also examined. To this end, (i) a number of ortho isomers and (ii) the effect of other para-nitrogen bearing substituents like piperidine, pyrrolidine and N,N-dialkyl derivatives, have been investigated.

Shredded cellulose acetate film containing 2,5-di-n-butoxy-4-morpholinobenzenediazonium tetrafluoroborate was also studied to evaluate any effects arising from any possible preferential orientation of the arenediazonium salts in the polymer matrix.

All the data for this series of experiments have been summarised in Table 23 for comparison. An esr spectrum taken at 77K of an irradiated (shredded) cellulose acetate film containing 2,5-di-n-butoxy-4-morpholinobenzenediazonium tetrafluoroborate is shown in Fig. 34 and is representative of other spectra except for slight variations in the field positions.

To a first approximation there is no difference in peak positions or line shape between coiled and shredded samples of 2,5-di-n-butoxy-4-morpholinobenzenediazonium tetrafluoroborate in cellulose acetate film. This would suggest that arenediazonium salts have no preferred orientation within the system.

also obtained from low temperature glasses of 2-phenylethanol, benzyl alcohol and 9.0 mol dm^{-3} aqueous lithium chloride containing 2,5-di-n-butoxy-4-morpholinobenzenediazonium tetrafluoroborate.

In an attempt to identify structural features which promote formation of Ar^+, a number of isomeric and structurally related salts were also examined. To this end, (i) a number of ortho isomers and (ii) the effect of other para-nitrogen bearing substituents like piperidine, pyrrolidine and N,N-dialkyl derivatives, have been investigated.

Shredded cellulose acetate film containing 2,5-di-n-butoxy-4-morpholinobenzenediazonium tetrafluoroborate was also studied to evaluate any effects arising from any possible preferential orientation of the arenediazonium salts in the polymer matrix.

All the data for this series of experiments have been summarised in Table 23 for comparison. An esr spectrum taken at 77K of an irradiated (shredded) cellulose acetate film containing 2,5-di-n-butoxy-4-morpholinobenzenediazonium tetrafluoroborate is shown in Fig. 34 and is representative of other spectra except for slight variations in the field positions.

To a first approximation there is no difference in peak positions or line shape between coiled and shredded samples of 2,5-di-n-butoxy-4-morpholinobenzenediazonium tetrafluoroborate in cellulose acetate film. This would suggest that arenediazonium salts have no preferred orientation within the system.

Figure 34

Esr spectrum of 2,5-di-n-butoxy-4-morpholinobenzene-
diazonium tetrafluroborate in cellulose acetate film
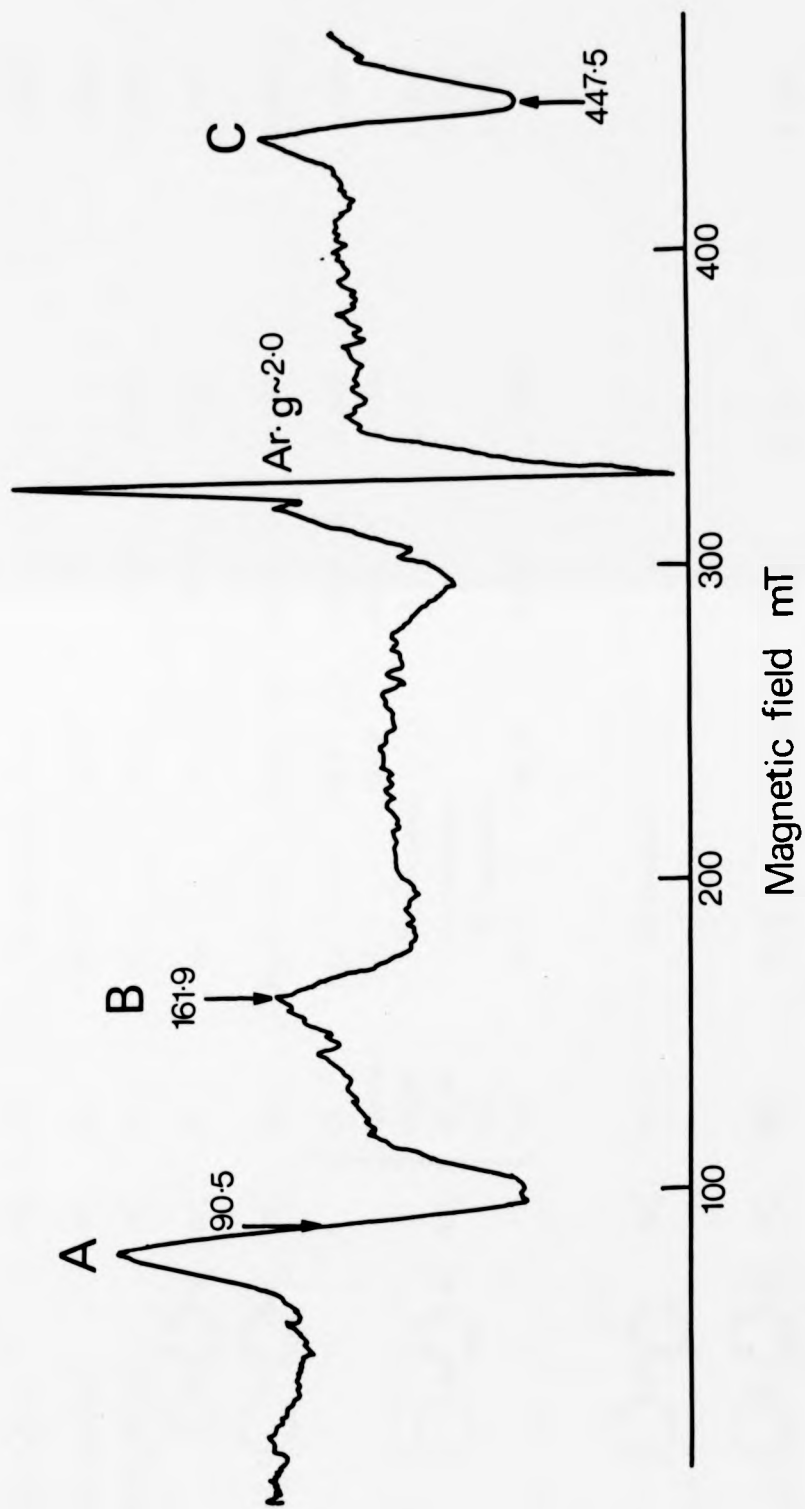at 77 K

152

A
90·5

B
161·9

Ar· g~2·0

C
447·5

Magnetic field mT
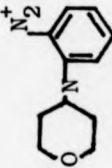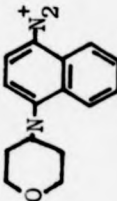
TABLE 23

Arenediazonium cation	Anion	Matrix	Field positions of peaks mT			D cm^{-1}	g-factor of Ar.
			A	B	C		
a) Monosubstituted ArN$_2^+$							
4-Me$_2$NC$_6$H$_4$N$_2^+$	BF$_4^-$	CA^c	No resonance				2.0036
4-(n-Bu)$_2$NC$_6$H$_4$N$_2^+$	BF$_4^-$	CA	100.0	166.0	$\underline{d}$		2.0009
4-(PhCH$_2$)$_2$NC$_6$H$_4$N$_2^+$	BF$_4^-$	CA	106.0	180.5	424.0	0.2087	2.0036
[pyrrolidinyl phenyldiazonium structure]	BF$_4^-$	CA	64.7	128.7	466.7	0.2675	2.0017
[piperidinyl phenyldiazonium structure]	BF$_4^-$	CA	66.3 ± 2.5	132.8 ± 3.6	4618.8 ± 3.0	0.2280	2.0020
[morpholinyl phenyldiazonium structure]	BF$_4^-$	CA	68.0 ± 1.1	126.7 ± 4.5	460.0 ± 5.0	0.2619	2.0040
		Epikote	91.6	166.2	447.8	0.2349	–
		CH$_3$OH	No resonance				2.0044
		CD$_3$OD	No resonance				2.0041
		SiO$_2$	No resonance				2.0043
		CA*	65.4	128.3	450.3	0.2227	–
[ortho-morpholinyl phenyldiazonium structure]	BF$_4^-$	CA	No resonance				
[morpholinyl naphthyldiazonium structure]	BF$_4^-$	CA	55.0	120.0	432.5	0.2499	2.0059

							Structure
2.0059	0.2499	432.5	120.0	55.0	CA	BF_4^-	C_6H_5, N–H, para N_2^+
2.0037	0.1902	403.0	169.0	124.0	CA	BF_4^-	cyclopentyl, N_2^+, Me
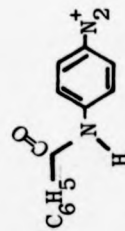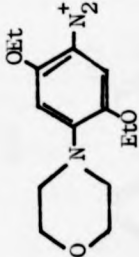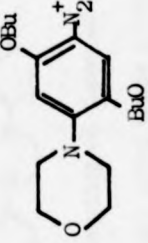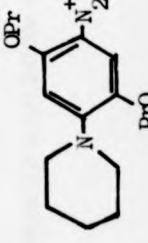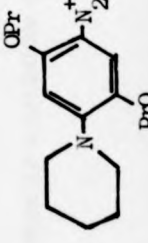
b) ArN_2^+ bearing two substituents

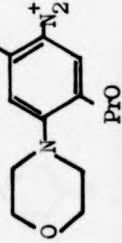|							Structure
–	0.2389	462.5	177.5	101.0	CA	BF_4^-	Cl, N_2^+, tetrahydropyranyl
no resonance	–		No resonance	No resonance	CA	BF_4^-	N_2^+, Me, tetrahydropyranyl
–	0.2178	425.0	169.5	94.0	CA	BF_4^-	N_2^+, Me, tetrahydropyranyl
–	0.2019	420.0	187.0	111.0	CA	BF_4^-	N_2^+, MeO, tetrahydropyranyl
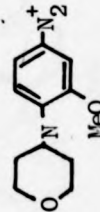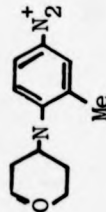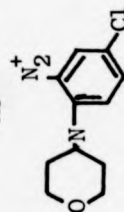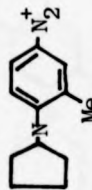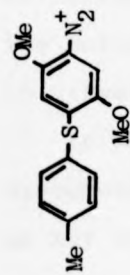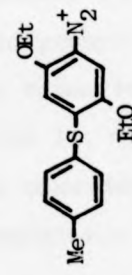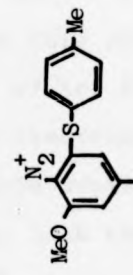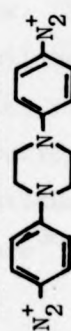
c) ArN_2^+ bearing three substituents

							Structure
2.0036	–	449.7	–	85.1	CA	BF_4^-	OMe, N_2^+, MeO, tetrahydropyranyl

Structure	Anion	Medium					g-value
OEt / EtO morpholine N_2^+	BF_4^-	CA	87.6	159.4	446.1	0.2355	2.0034
		SiO$_2$ (ε)	78.9	148.0	453.8	0.2490	-
		PhCH$_2$OH	No resonance				2.0042
		PhCH$_2$CH$_2$OH	85.1	158.8	450.8	0.2416	-
	PF_6^-	CA	85.6	159.8	449.1	0.2400	-
		MTHf [f]	93.0	154.5	442.8	0.2338	2.0041
		polystyrene-f	No resonance				2.0043
	½ZnCl$_4^{2-}$	CA-f	88.1	-	446.4		-
	CNS^-	CA	80.8	-	448.2		2.0036
			No resonance				2.0045
OPr / PrO morpholine N_2^+	BF_4^-	CA	80.0±11.0	165.1	4387±10.0	0.2303	2.0036
OBu / BuO morpholine N_2^+	BF_4^-	CA*	84.5	160.1	425.2	0.2205	2.0035
		CA	92.8±2.5	163.0±1.0	437.2	0.2279	2.0036
		MF [g]	80.4	146.0	452.9	0.2487	2.0047
		LiCl-H$_2$O	58.1	126.4	444.6	0.2590	-
		LiCl-D$_2$O	83.2	156.3	424.0	0.2238	-
OPr / PrO piperidine N_2^+	BF_4^-	CA	87.9	158.1	436.0	0.2304	2.0020

Structure	Counterion		CA	g-value
(OMe, N$_2^+$, MeO, S, Me)	$\frac{1}{2}$ZnCl$_4^{2-}$	No resonance	CA	2.0040
(OEt, N$_2^+$, EtO, S, Me)	BF$_4^-$	No resonance	CA	2.0043
	$\frac{1}{2}$ZnCl$_4^{2-}$	No resonance	CA	2.0045
	PF$_6^-$	No resonance	CA	2.0045
(Me, S, N$_2^+$, MeO, S, Me)	BF$_4^-$	No resonance	CA	2.0086
(d) Bis diazonium salt	2BF$_4^-$		CA	Weak singlet 165.0 1.9876

(a) Recording of these as follows: Peak A at crossover, B at upward peak, C at downwards peak.

(b) A nil entry means no measurement was made (c) CA = cellulose acetate (d) Peak too weak for accurate determination

(e) MTHF = 2 methyltetrahydrofuran (f) Weak resonances CA* = Shredded cellulose acetate (g) MF = 'Melanex' film i.e. basically a cellulose propionate.

Glassy samples would be expected to give a purely random orientation of the arenediazonium salts for comparison with cellulose acetate samples. Again, no difference in line shape was observed; however, our calibrated field positions indicate some overall broadening of the spectra which is not surprising when the vast differences in the host matrix are considered. When deuteriated 9 mol dm^{-3} LiCl was used as a glass, peak positions approached those observed in cellulose acetate film.

Contrary to expectations phenyl radicals were observed in both $LiCl-H_2O$ and $LiCl-D_2O$ glasses suggesting that even in highly aqueous conditions contributions from the homolytic cleavage of the $Ar-N_2^+$ bond cannot be neglected.

Additionally, we have observed well-resolved spectra from 4-N,N-dibenzylamino-3-ethoxybenzenediazonium and 4-benzamido-2,5-diethoxybenzenediazonium tetrafluoroborate, showing that formation of Ar^+ is not limited to those arenediazonium salts containing a cyclic amino substituents in the 4-position.

Contrary to our expectations, the 2-morpholino salts exhibited no resonance whatsoever (possibly due to the formation of an azo dye of unidentified internal salt). The results from 2,4-bis-tolylthio-5-methoxybenzenediazonium tetrafluoroborate were rather disappointing. The presence of two tolylthio groups in this particular salt had been expected to stimulate formation of Ar^+ in the triplet configuration.

In Chapter II, the electronic configuration of Ar^+ was discussed in considerable detail. Aryl cations have been invoked as key intermediates in both the thermolysis[30] and photolysis[30]

of arenediazonium salts, particularly in aqueous acidic
solution where the product is invariably ArOH. Taft[71]
originally suggested a triplet $(\pi)^5(sp^2)^1$ electronic
configuration for Ar^+ and this was later modified by
Abramovitch et.al.[75] Wasserman and Murray[108] have obtained
esr spectra which are characteristic of a triplet state from
the photolysis of 1,4-diazoxides (see Section 3.4) hitherto
evidence for the formation of the widely discussed charged
Ar^+ species has been based primarily on kinetic studies[32]
and product analyses.[43]

In this work the triplet state character of para-$R_2NC_6H_5^+$
has been demonstrated for a variety of para-amino groups by
means of esr spectroscopy. Analogous experiments with simpler
arenediazonium salts failed to provide esr spectra characteristic
of the triplet state. The apparent stability at 77 K of the
highly substituted aryl cation may be the result of several
effects, operating simultaneously, viz, (i) delocalisation
of the odd π electron on to substituent groups to give
contributions of the type $\cdot X-C_6H_4\cdot$ (ii) general steric effects
of the bulky substitutents, and (iii) 'locking' of the
important 4-amino group by the matrix into a conformation
maximising conjugation with the π system. A contribution
from $R_2\overset{+\cdot}{N}-C_6H_4\cdot$ cannot be neglected. However, the behaviour
of such a species is likely to be that of a bi-radical (i.e.
the interatomic distance separating the two unpaired electrons
is sufficiently large for them to remain independent of each

other). Consequently any resonance from $R_2^{+\cdot}N-C_6H_4\cdot$ would be expected[97] to occur at ca. g=2. Again (see later) the magnitude of the D parameter of our triplet suggests close proximity of the two electrons.

Resonance at the unusual field positions of ca. 80, 150 and 440 mT in the esr spectra of irradiated arenediazonium salts suggests a spin system other than $S=\frac{1}{2}$. These resonances are believed to be the first three of the four components expected of an S=1 system (or triplet state) expected from a phenyl cation with a $(\pi)^5(sp^2)^1$ type electronic configuration. Assignment of the individual peaks is in accordance with the procedure described by Wasserman et.al.[153] and is set out in Fig. 35 which also depicts a high field sweep for the very weak fourth component. An extremely weak signal has been detected at 587 mT. In Fig. 35 the double quantum transition denoted by dq was enhanced when the microwave power was reduced from 10 to 3 dB in agreement with the proposed assignment to this peak, the intensity of which is dependant on the square of the microwave power. Our assignment of the transitions is confirmed (Fig. 36) by the observation of H_{min} (a component of the $M_S=2$ transition) in a powder sample of 2,5-di-n-butoxy-4-morpholinobenzenediazonium tetrafluoroborate. In Fig. 37 the weak resonance observed at 577 mT provides additional evidence for the assignment of the high field Z(11) component.

Figure (35)

Assignment of the peaks:-

Line position (mT)	Assignment	Comments
80.5 } } 587.0 }	$H_{\underline{z}}$	Parallel features: 587 mT line extremely weak and broadened as expected. Low field component combined with $\Delta m = 2$ transition.
170.0 } } 446.7 }	$H_{\underline{x} + \underline{y}}$	Perpendicular features. Low field component combined with $\Delta m = 2$ transition.
305.0	dq	Intensity increased by increase of microwave power.
334.2	Ar·	Taken as free spin value for calculation
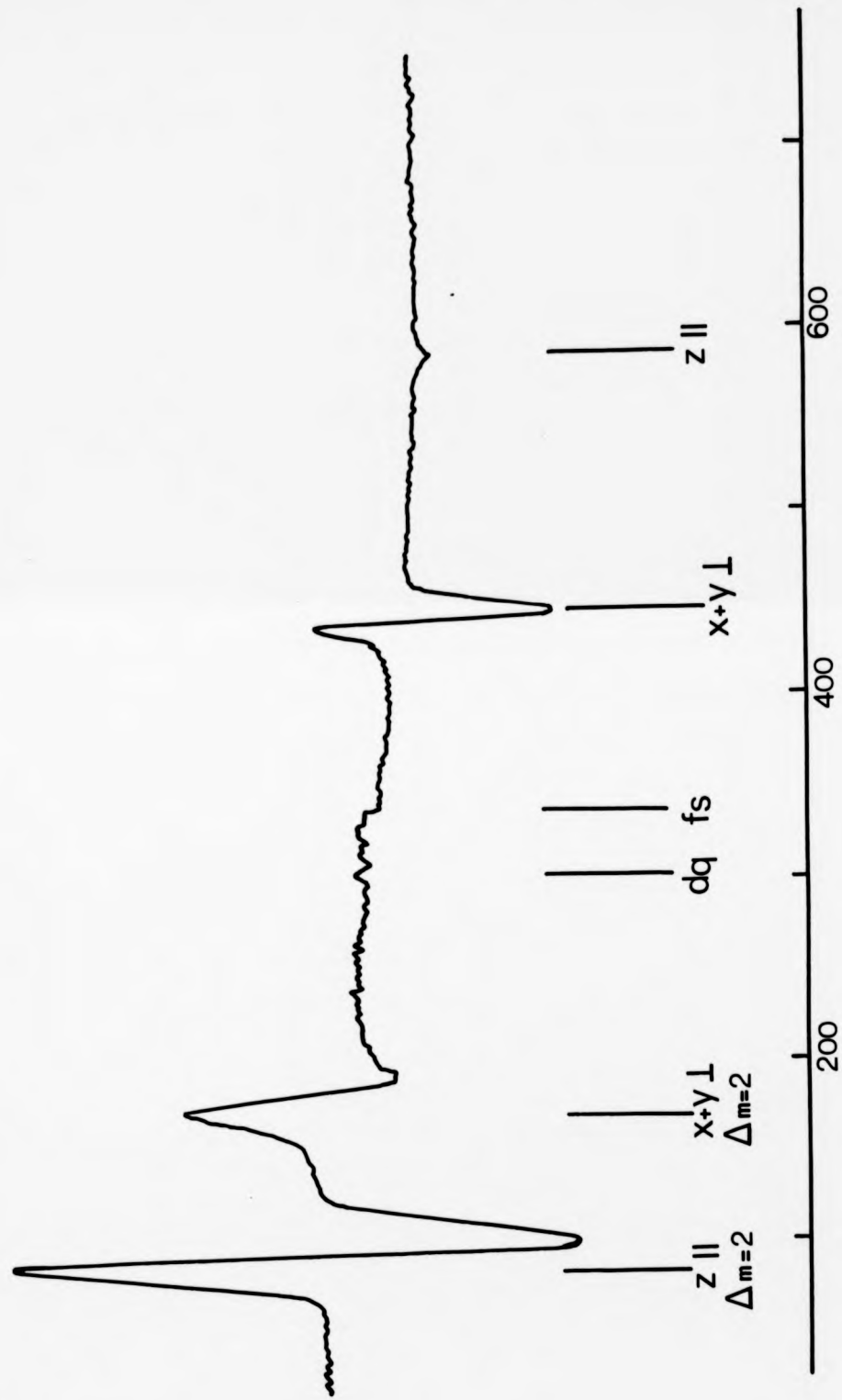
Magnetic field   mT

Figure (36)

Esr spectrum of an irradiated powder sample of

2,5-di-n-butoxy-4-morpholinobenzenediazonium

tetrafluoroborate at 77 K
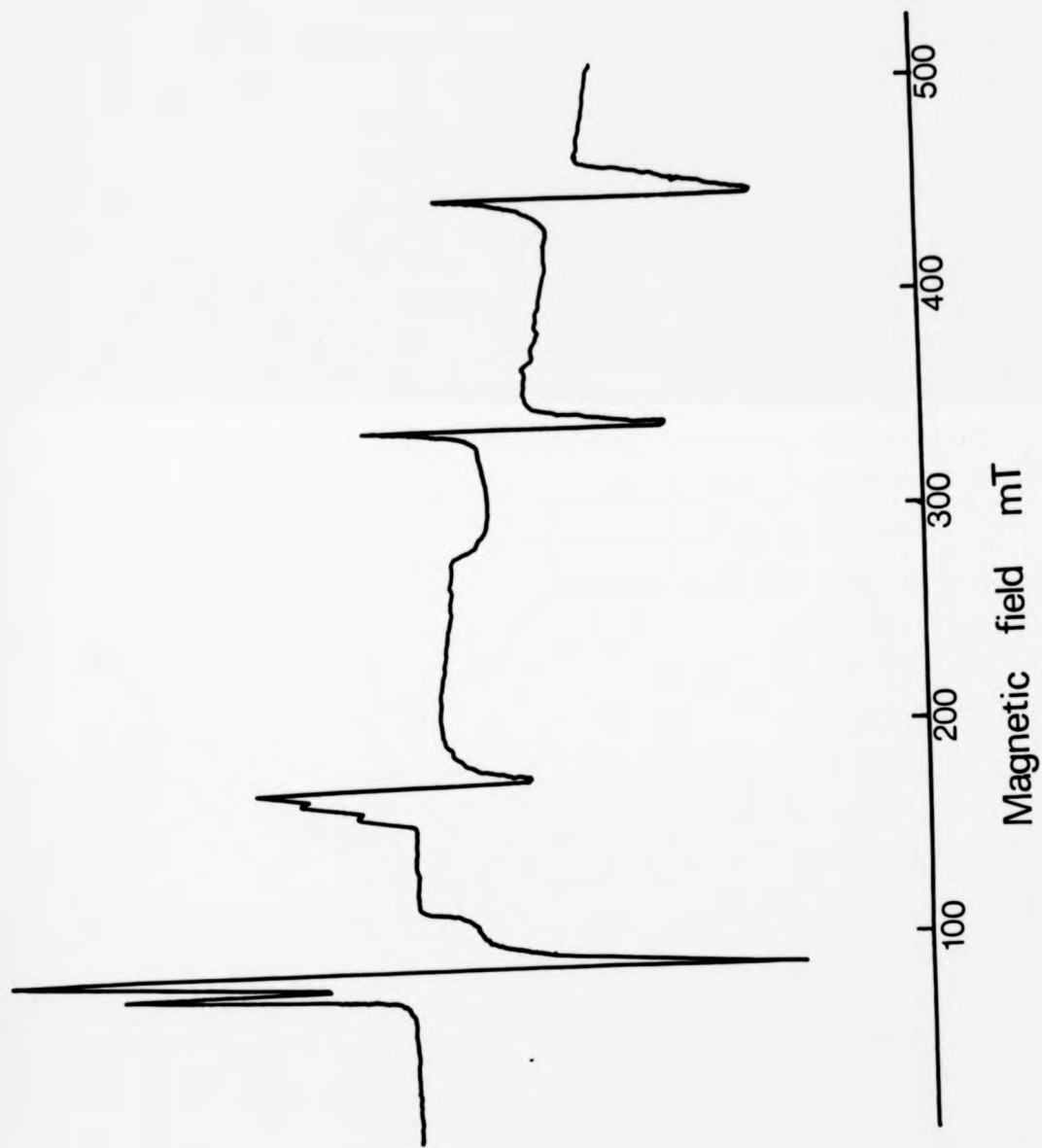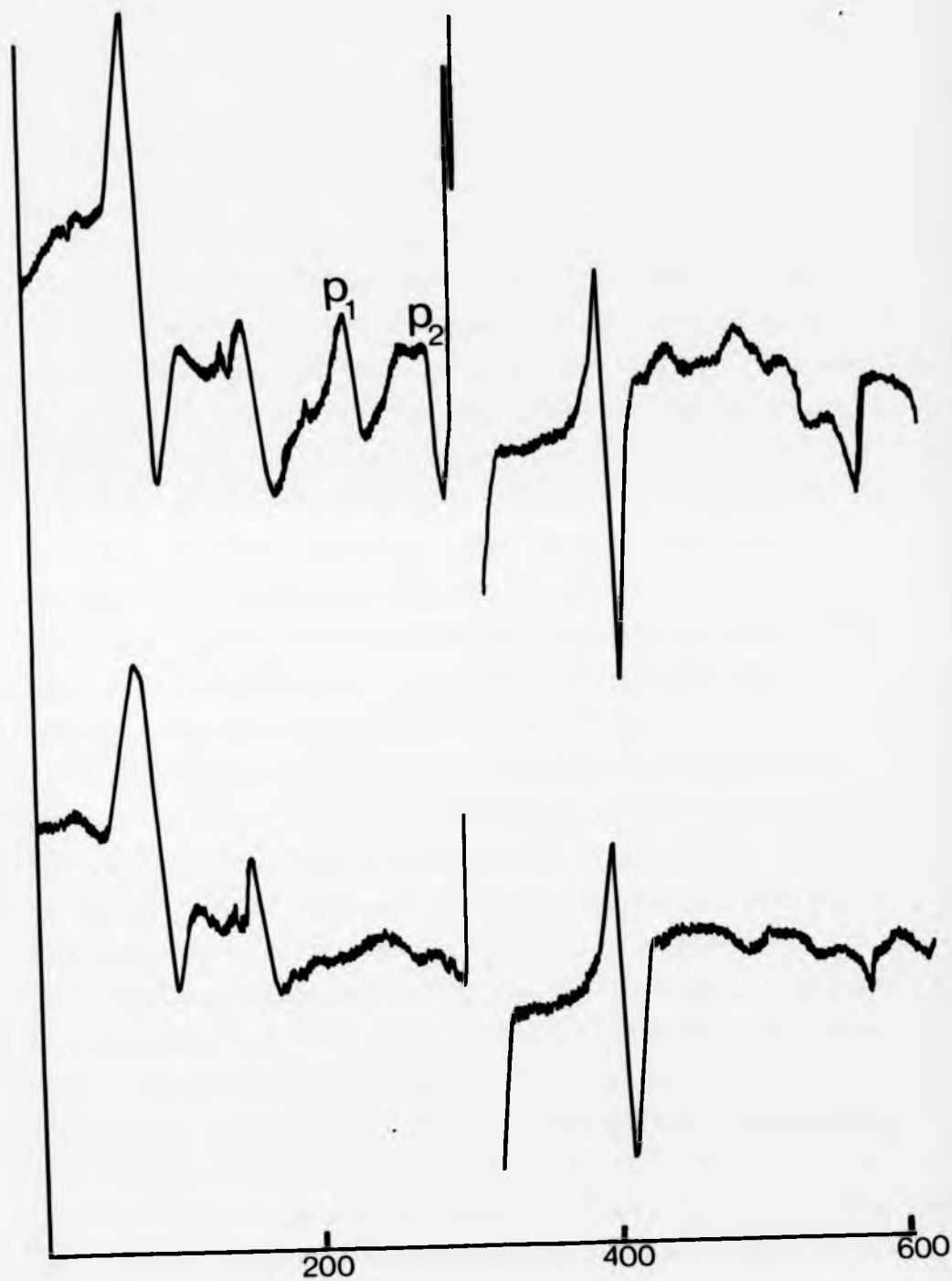
Magnetic field   mT

Figure (37)

Spectra of irradiated 2,5-di-n-butoxy-4-morpholino-
benzenediazonium tetrafluoroborate

a) Recorded at 103 K; peaks P_1 and P_2 are formed
    from decay of the triplet state

b) As above recorded at 77 K

Magnetic field mT

An average value of $D = 0.2234 \pm 0.0030$ cm^{-1} with
$E = \leq 0.004$ cm^{-1} has been calculated from the resonance
field positions given in Table 23: Appendix II contains a
detailed account of the procedure used to calculate D and E.
The value of $D = 0.2234 \pm 0.0030$ implies a spin separation of
2.27 $\overset{\text{o}}{\text{A}}$. Wasserman obtained a value of $D = 0.3179$ for structure
(LXXXI) and a calculation indicated that this implies a spin
density of 0.4 at C(1). By analogy, our value of D is
equivalent to a π spin density of 0.28 at C(1). Pople's[91]
calculation on the $^{3}B_{1}$ state of $C_{6}H_{5}^{+}$ places a large spin
density of ca. 0.5 at C(1) and our estimate is in fair agree-
ment. Additionally our experimental observations concur with
Pople's[92] calculations that para-amino substituents can
stabilise the aryl cation in the triplet state.

If the spectra in Fig. 37 are compared, the spectrum
recorded at 103 K displays two additional peaks (at $g = 2.63$ and
$g = 2.235$) denoted P_{1} and P_{2} arising from decomposition products
of the aryl cation. Controlled warming experiments have shown
that resonance arising from the aryl cation disappears at 125 K.
The resonance centred near $g = 2.35$ reaches its maximum intensity
at this temperature. Further warming to 150 K transforms this
singlet into a doublet (Fig.38) at the same field position.
The precise nature of the species is unknown but it is unlikely
to be that of a conventional organic radical by virtue of its
g-value. Similar spectra have been recorded from the decomposition
of 2,5-di-n-butoxy-4-morpholinobenzenediazonium tetrafluoroborate
in a glass of 2-phenylethanol.

Figure (38)

Esr spectra of secondary radicals derived from irradiated
2,5-di-n-butoxy-4-morpholinobenzenediazonium tetra-
flouroborate at temperatures upwards of 77 K

phenyl radical

125 K

131 K
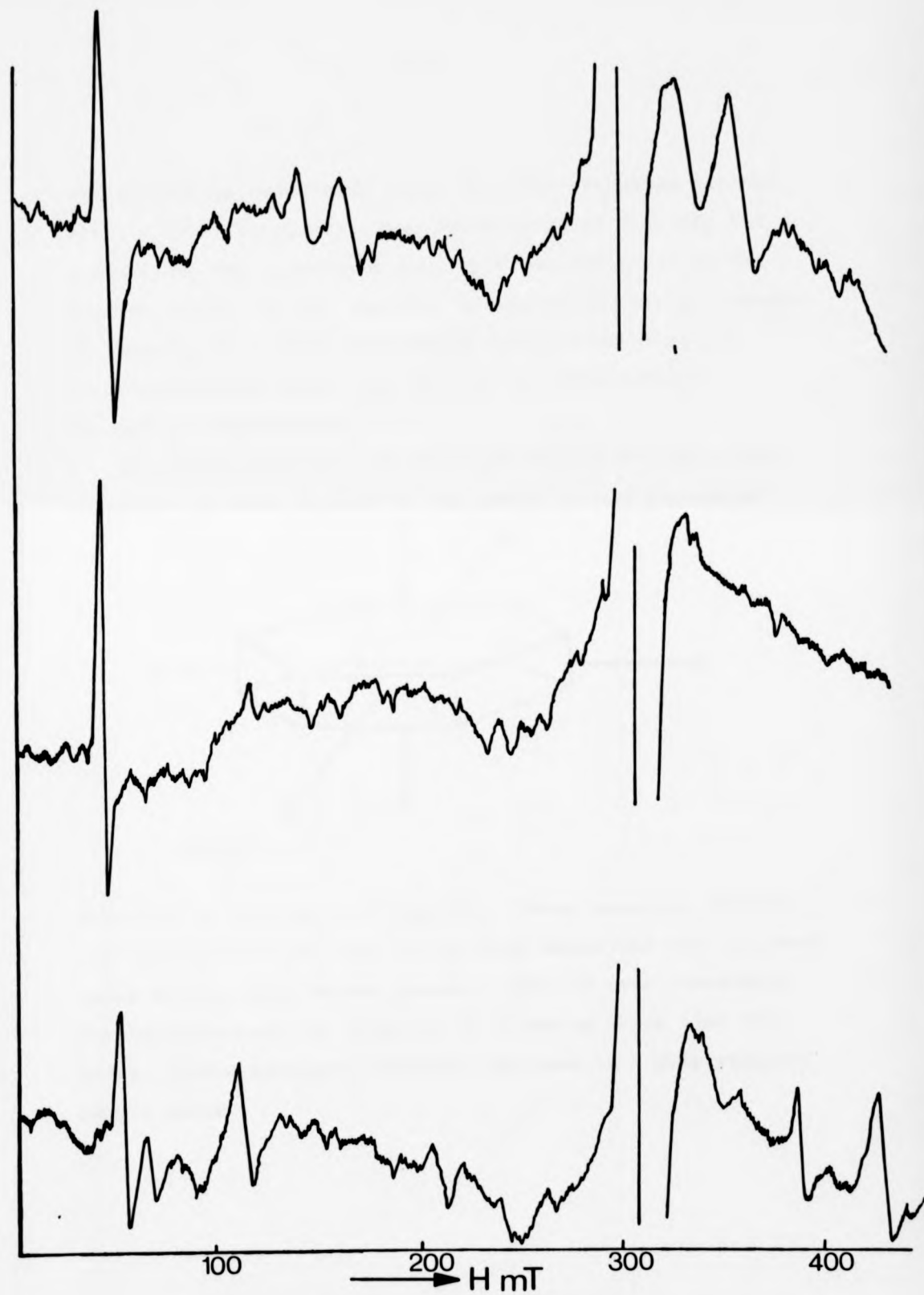
140 K

150 K

50 mT

150 K

15 mT
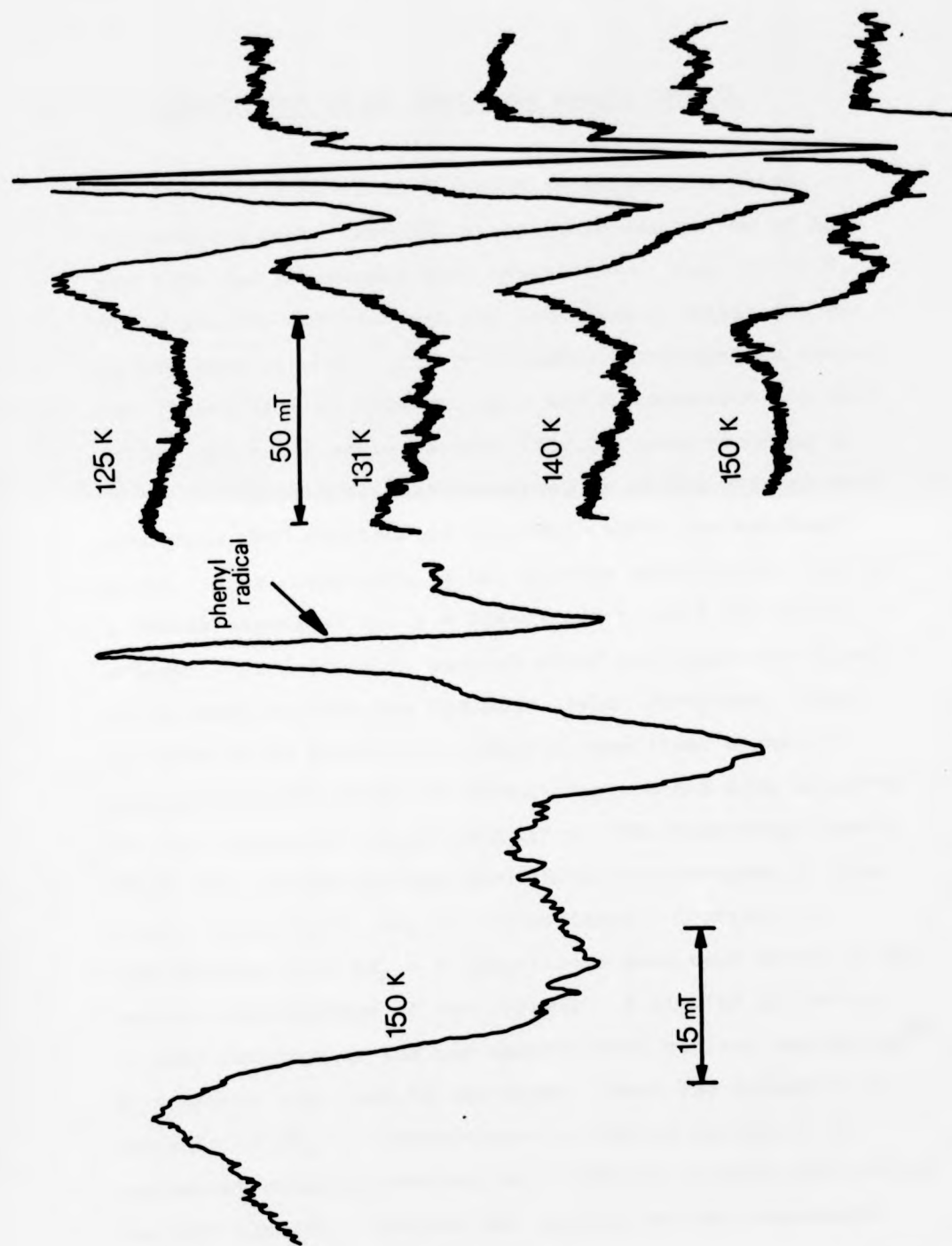
6.4. ESR OBSERVATIONS ON AN IRRADIATED SINGLE CRYSTAL

A single crystal of 4-morpholinobenzenediazonium tetrafluoroborate randomly situated in the bottom of an esr tube was irradiated with ultra-violet light at 77 K. While precise orientations for the crystal within the esr cavity were unknown, this preliminary investigation tested the feasibility of determining D and E parameters for each of the principal axes. Spectra (Fig.39) were recorded at 77 K, for three different orientations of the crystal each involving 360° rotation of the tube (about its vertical axis). From inspection of the spectra presented in Fig.39, a strong signal at ca. g $\propto$ 2(assigned to Ar·) is clearly evident. Additionally, several other well-resolved signals are present at both low and high-fields positions. When the spectra in Fig.39 are compared, the first signal is apparently independent of orientation and has been assigned to (the isotropic) $\Delta M_S = 2$ transition. The remaining signals which are orientation-dependent have been assigned to (the highly anisotropic) $\Delta M_S = 1$ transitions. Contrary to expectations four $\Delta M_S = 1$ transitions have been detected for certain orientations of the crystal. A similar situation to that observed in the esr spectra from excited napthalene[98] in a durene host, may be envisaged. Here the detection of two sets of $\Delta M_S = 1$ transitions is readily explained by napthalene molecules having two different orientations within the host crystal. However our spectra are not consistant with this view. Crystal structure determinations for several

Figure (39)

Esr spectra of a randomly situated single crystal of
4-morpholinobenzenediazonium tetrafluoroborate when
irradiated at 77 K and rotated in the cavity.

arenediazonium salts have shown that the diazonium cations
are all parallel planes. The observation of four $\Delta M_S = 1$
transitions may arise from the imperfect alignment of the
crystal within the esr cavity. Alternatively the phenomenon
of twinning (a problem frequently encountered X-ray in
crystallographic study) may account for this rather
unexpected observation.

Single crystals of 4-morpholinobenzenediazonium tetra-
fluoroborate were mounted in the cavity of the goniometer

(LXXXV)

described in Section 3.1 (Fig.15). Three separate crystals
were mounted one for each of the axes shown and held in place
using silcone high vacumn grease. Samples were irradiated
for approximately two hours at 77 K during which time the
bright yellow hexagonal crystals darkened to a deep reddish/
purple colour.

arenediazonium salts have shown that the diazonium cations
are all parallel planes. The observation of four $\Delta M_S = 1$
transitions may arise from the imperfect alignment of the
crystal within the esr cavity. Alternatively the phenomenon
of twinning (a problem frequently encountered X-ray in
crystallographic study) may account for this rather
unexpected observation.

Single crystals of 4-morpholinobenzenediazonium tetra-
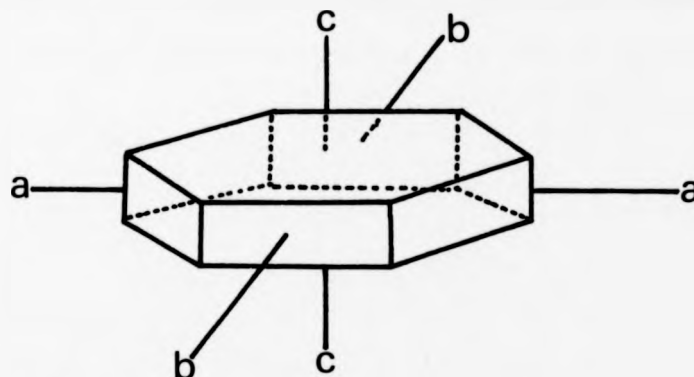fluoroborate were mounted in the cavity of the goniometer

(LXXXV)

described in Section 3.1 (Fig.15). Three separate crystals
were mounted one for each of the axes shown and held in place
using silcone high vacumn grease. Samples were irradiated
for approximately two hours at 77 K during which time the
bright yellow hexagonal crystals darkened to a deep reddish/
purple colour.

Figure (40)

Phenyl radical and trapped hydrogen atoms

from a single crystal of 4-morpholinobenzenediazonium

tetrafluoroborate at 77 K.

50 mT

4·0 mT
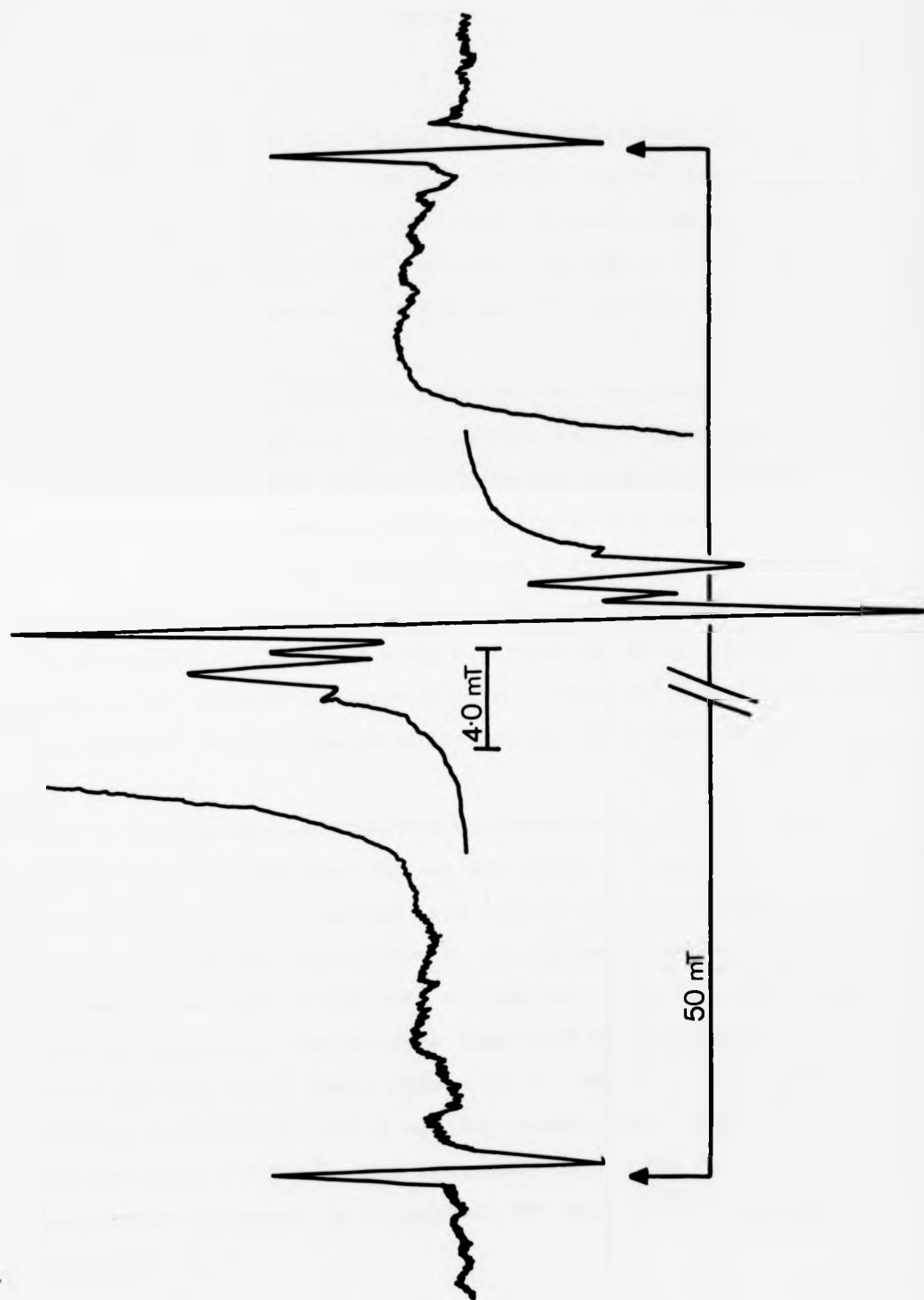
Spectra were run on a Varian E3 esr spectrometer
at Leicester University. For each of the crystal axes
shown, a phenyl radical was recorded. Ground-state triplet
spectra were recorded at 10° intervals through a rotation
of 180° whilst the magnetic field was scanned from 0 to
500 mT.

Strong resonance centered near g=2 was observed in all
esr spectra, from each of the principal axes. This was
assigned to the phenyl radical. Hydrogen atoms could also
be detected in esr spectra corresponding to the three
different orientations. Fig. 40 shows a typical esr spectrum
of the phenyl radical (taken from axis C and rotating through
the AB plane). A detailed single-crystal study of phenyl
radicals has already appeared in the literature[154] and
consequently further characterisation of these spectra was
not attempted.

The resonances now regarded as characteristic of the
triplet state of the aryl cation are shown in Fig.41, as
a series of spectra recorded from axis B while rotating
the crystal through the AC plane. In agreement with earlier
findings a maximum of four $\Delta M_S = 1$ and one $\Delta M_S = 2$ transitions
could be detected. The spectra displayed marked angular
variation for a very small change in θ. Spectrum (a) was
recorded with $\theta = 45^O$ and a similar spectrum was also
recorded when $\theta = 135^O$. The intensity of the $\Delta M_S = 1$
transitions decreased as θ approach 90° and their resolution
increased.

Figure (41)

Esr spectra from an irradiated single crystal of
4-morpholinobenzenediazonium tetrafluoroborate at
77 K for a 10° rotation about axis B in the AC
plane.

45

47·5

θ

50

52·5

55

Magnetic field mT
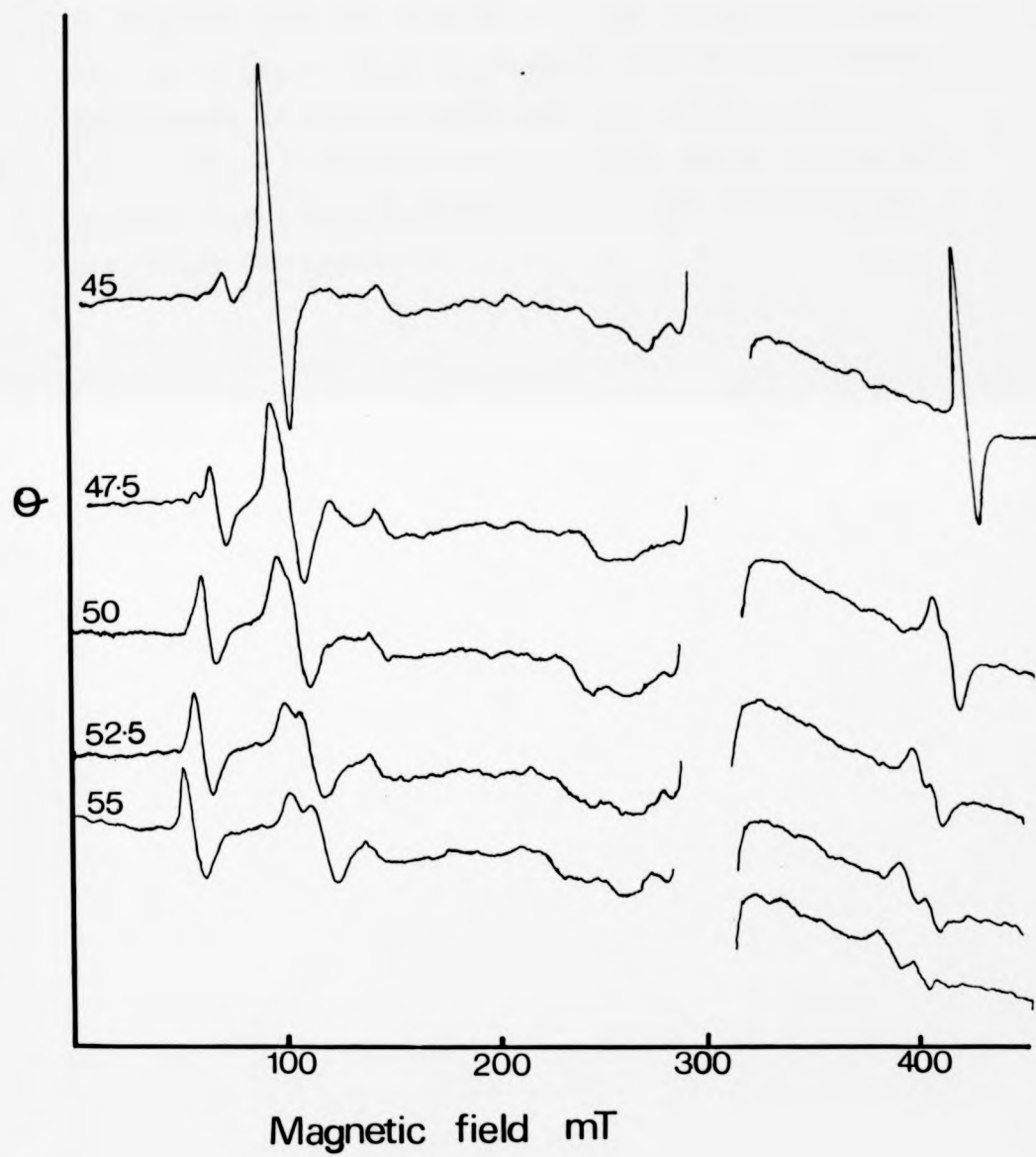
Attempts have been made to plot the variation in field position of $\Delta M_S = 1$ with θ. However this was not possible because none of the data sets contained sufficiently well-resolved $\Delta M_S = 1$ transitions for a total change in θ of 90°. In this respect the results from the single crystal study were rather disappointing.

CHAPTER VII

OPTICAL SPECTRA OF REACTIVE INTERMEDIATES
FORMED IN THE PHOTODECOMPOSITION OF
ARENEDIAZONIUM SALTS

## 7.1. INTERMEDIATES FORMED IN CELLULOSE ACETATE FILM AT 77 K

We have attempted to characterise further the intermediates formed at 77 K during the photolysis of arenediazonium salts in cellulose acetate film, by ultra-violet spectroscopy.

Initial experiments using a silvered pyrex dewar (with suitable provision for the optical train) yielded little information. Many of the spectra obtained were of poor quality from which only limited conclusions could be drawn. The inferior nature of the spectra obtained was attributed to ice crystals forming in the liquid nitrogen, combined with its tendency to bubble.

Two arenediazonium salts were examined using this system, namely 2,5-diethoxy-4-morpholino and 2,5-diethoxy-4-tolylthio-benzenediazonium tetrafluoroborate. At initial concentrations which gave optical densities of ca. 2.0 at their absorption maxima, neither of the salts gave an ultra-violet absorbing transient after photolysis at 77 K. However, at substantially higher concentrations (initial optical density at λ_{max} ca.30.0) the visible spectrum of 2,5-diethoxy-4-morpholinobenzenediazonium tetrafluoroborate displayed a new peak after photolysis, at 77 K Fig.(42). The new peak was very broad, ranging from 410 to 490 nm with λ_{max} 450 nm, and disappeared upon warming the sample to room temperature. No such feature was observed in the past-photolysis spectrum of 2,5-diethoxy-4-tolylthiobenzenediazonium tetra-fluoroborate at 77 K.

Figure (43)

Spectral changes observed during the photolysis of

2,5-diethoxy-4-morpholinobenzenediazonium tetrafluoroborate

at 77 K in cellulose acetate film.
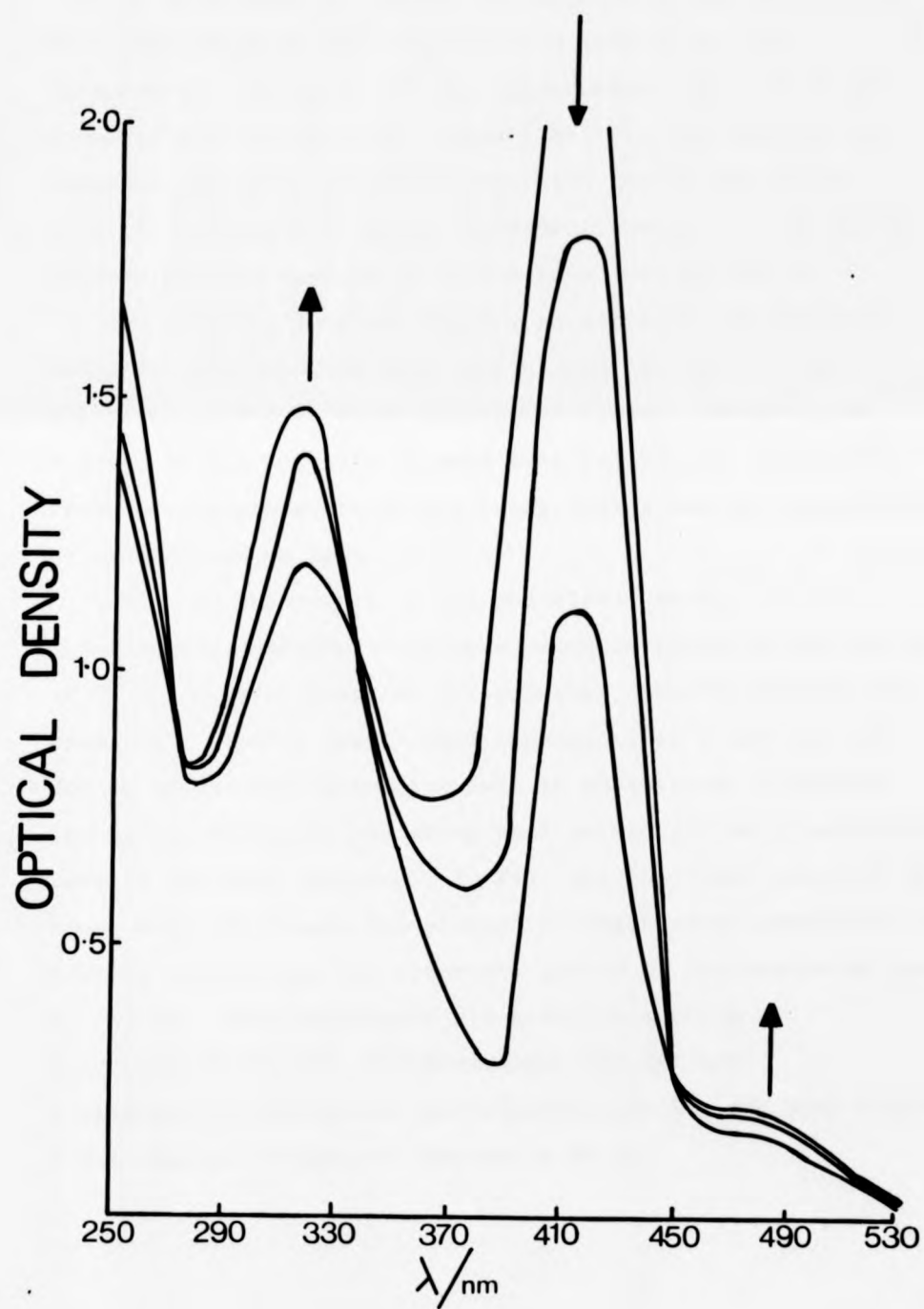
In an attempt to improve the quality of the spectra, a
more sophisticated low-temperature ultra-violet cell
(described in Section 3.3) was constructed, and used in all
subsequent investigations. Essentially it was designed to
alleviate the problems associated with having the sample
directly suspended in liquid nitrogen, and the use of quartz
windows enabled spectra to be recorded down to 230 nm.

As with the previous system, no ultra-violet absorbing
transient was detected when samples had initial optical
densities of 2.0 at their absorption maxima. However, as
before, it was possible to make some qualitative deductions
about the intermediate formed using higher initial concentrations
of arenediazonium salt.

Fig. 43 shows part of the photolytic decay of
2,5-diethoxy-4-morpholinobenzenediazonium hexafluorophosphate
at 77 K. Several features are apparent when the spectra are
examined. Firstly the gradual appearance of a new peak at
307 nm as the arenediazonium salt is photolysed. Secondly,
the broad and weakly absorbing peak at 410-490 nm is apparently
part of the same spectrum. In Fig. 44a the final spectrum is
shown when the sample was allowed to reach room temperature and
clearly illustrates the transient nature of the absorbing species
at 307 nm. Post-photolysis ultra-violet spectra of
4-morpholino Fig.44b, 4-N,N-dimethyl Fig.44c and
4-methoxybenzendiazonium tetrafluoroborate Fig.44d also display
a well-defined transient species at 77 K.

Figure (42)

Visible spectrum of the intermediate formed at 77 K
from irradiated 2,5-diethoxy-4-morpholinobenzene-
diazonium tetrafluoroborate in cellulose acetate film.
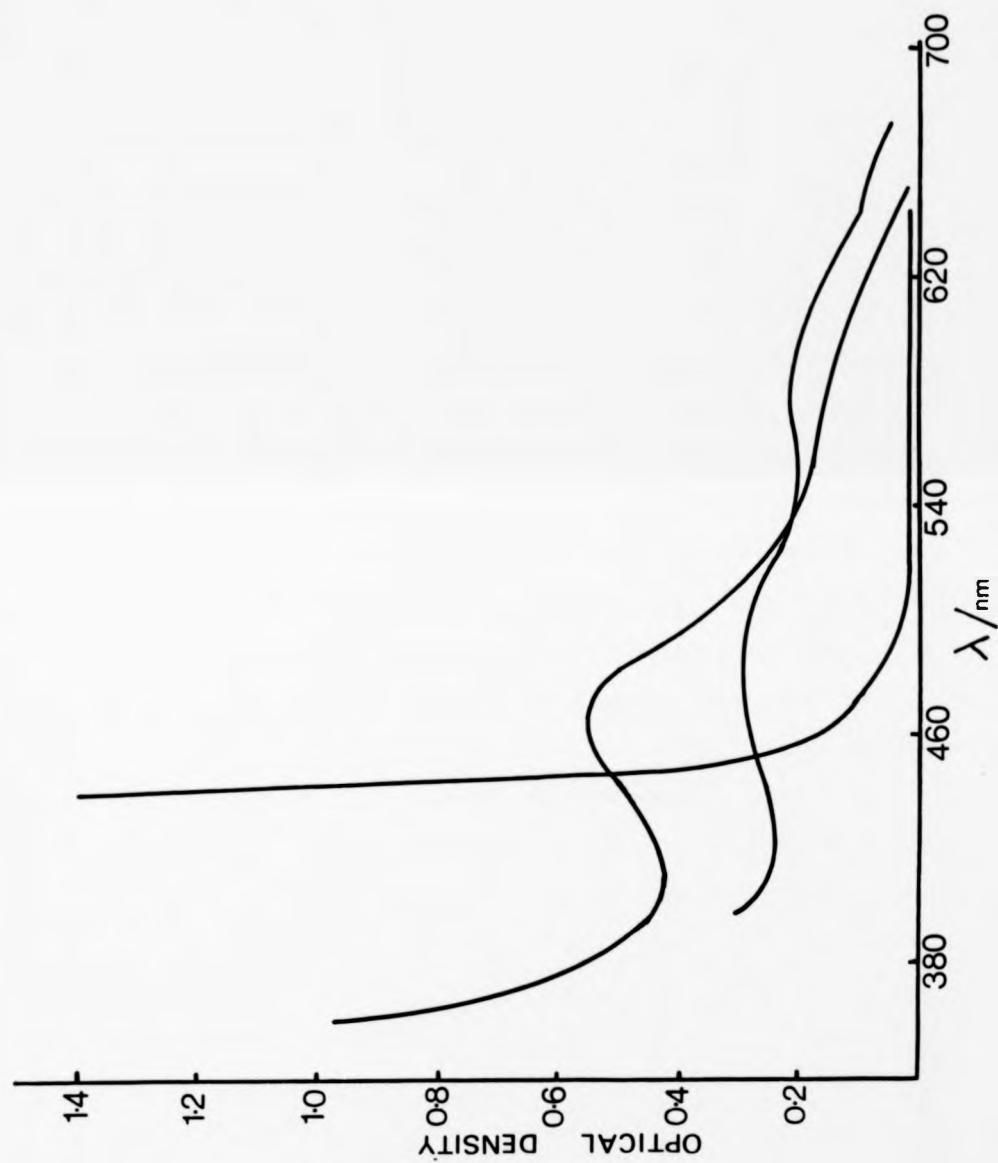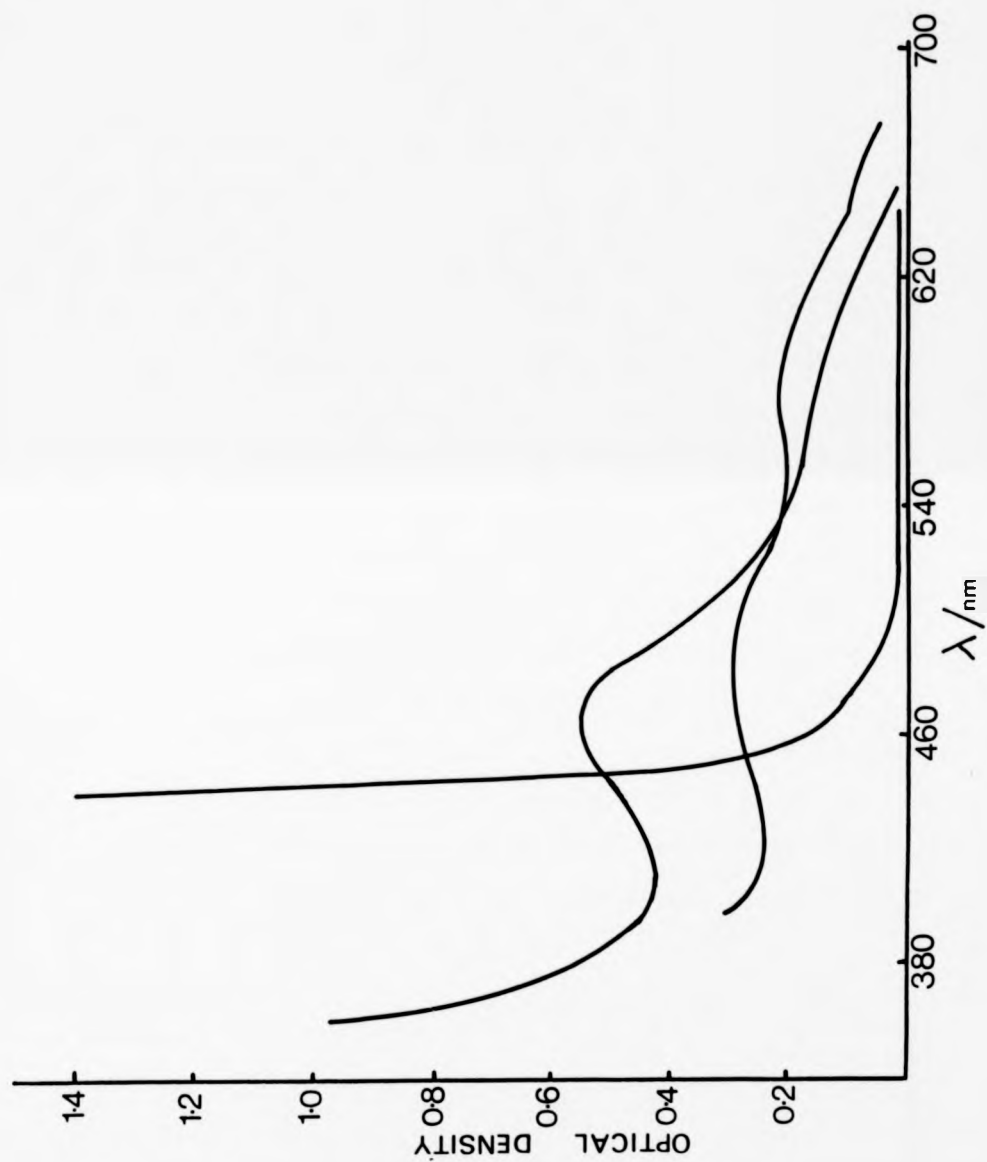
Figure (44)

Ultra-violet spectra of the intermediate formed during
the photolysis of

(a) 2,5-diethoxy-4-morpholinobenzenediazonium
     tetrafluoroborate

(b) 4-morpholinobenzenediazonium tetrafluoroborate

(c) 4-N,N-dimethylbenzenediazonium tetrafluoroborate

(d) 4-methoxybenzenediazonium tetrafluoroborate
     in cellulose acetate film at 77 K

where

     1 = initial spectrum at 77 K

     2 = spectrum of intermediate at 77 K

     3 = final spectrum at room temperature
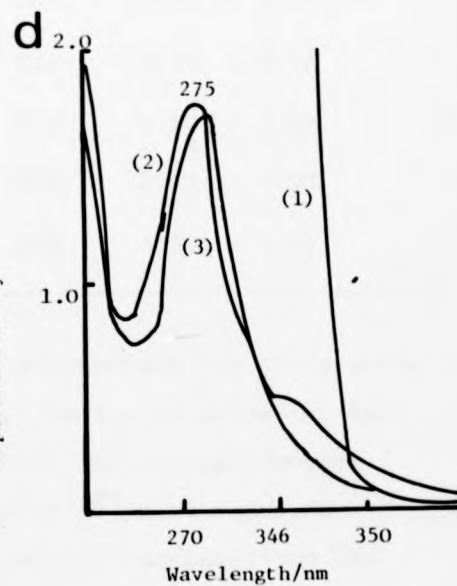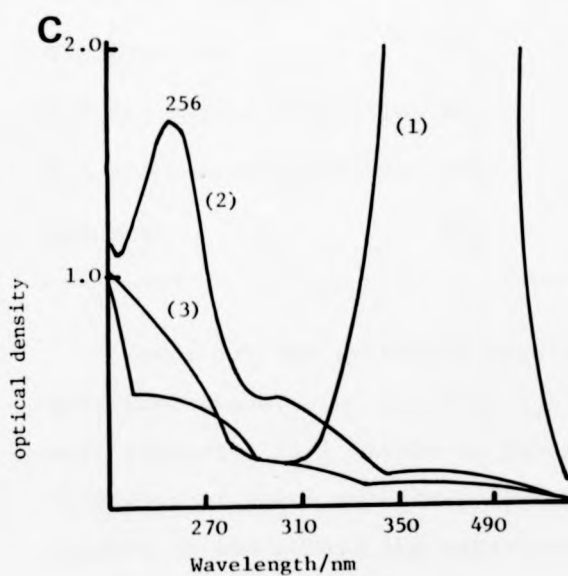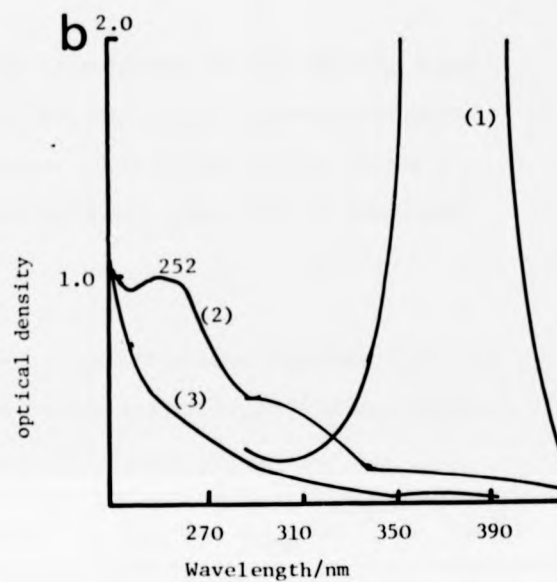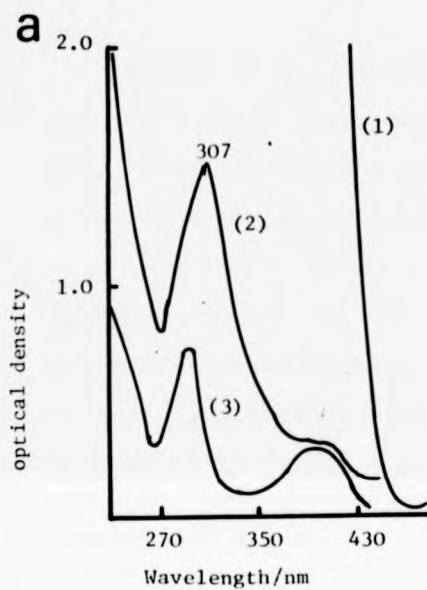
Values of ε_{max} determined from films incorporating high and low initial concentrations of the parent arenediazonium salt, were not in good agreement. Estimated extinctions given in Table 24 are averaged between these two situations.

TABLE 24

Extinction coefficients and λ_{max} of transient species formed in the photolysis of arenediazonium salts in cellulose acetate film at 77 K

Substituent group	Anion	λ_{max}nm	$\varepsilon_{max} \times 10^{-3}$ ($M^{-1}cm^{-1}$)
4-methoxy	BF_4^-	275	3.60 ± 0.80
4-N,N-dimethylamino	BF_4^-	256	2.64 ± 0.76
4-morpholino	BF_4^-	252	9.80 ± 2.35
2,5-diethoxy-4-morpholino	PF_6^-	307	5.70 ± 1.62
2,5-diethoxy-4-tolylthio	BF_4^-	312	3.97 ± 1.03
Hydrogen	BF_4^-	260	1.961 ± 0.49

There are two principal possible assignments for the species described above, i.e. firstly, the aryl cation or secondly, the aryl radical. Very little is known about the optical spectra of either of these species. Cercek et al.[124] have reported spectra of the phenyl and para-hydroxyphenyl radicals from the pulse radiolysis of aqueous solutions of iodobenzene and par-bromophenol. Böttcher et al.[125] have reported λ_{max} for various

claimed aryl cations, obtained by flash photolysis of aqueous solutions arenediazonium salts. However, as we shall show in the next section, the latter assignment is almost certainly erroneous.

Our spectra are probably those of the corresponding substituted phenyl radicals because, firstly the Hammett ρ value of almost zero for quantum yields determined in cellulose acetate indicates that photodecomposition occurs primarily through a radical intermediate, and secondly, the intensity of resonance from the phenyl radical in esr studies is several times greater than that of the corresponding aryl cation, (when the latter is observed at all). Particularly significant is the close agreement between the λ_{max} figures for the transient species from the 2,5-diethoxy-4-morpholino- and 2,5-diethoxy-4-tolythio-benzenediazonium salts: these suggest a species of common type, and yet while *both* of these salts produce esr spectra of $Ar\cdot$, only the former yields Ar^{+}.

7.2. INTERMEDIATES FORMED IN AQUEOUS MEDIA AT 300 K

Using the technique of ns laser-flash photolysis, it
has been attempted to detect aryl cation formation during
the photodecomposition of arenediazonium salts in aqueous
solution at room temperature.

Throughout this work 2.0 cm diameter cylindrical quartz
cells with a volume of 5.0 cm^3, have been used. All samples
were argon flushed prior to irradiation. Solutions of
arenediazonium salts were not 'flashed' more than three
times in order (i) to ensure complete absorption of the
exciting pulse from the laser and (ii) to reduce the effects
of photo-products.

We have been unable to detect any optically absorbing
transient species in the range 400-700 nm during the 347 nm
excitation of 4-nitro,4-N,N-dimethyl and 2,5-di-n-butoxy-
4-morpholinobenzenediazonium tetrafluoroborate in aqueous
solution at room temperature. These findings are in direct
contradiction to those reported by Becker et al.[125] using µs
methods. Consequently the possibility that their spectra
are derived from excitation of some product formed during
photodecomposition must be considered.

Para-nitrophenol, the most likely photolysis product,
does however give a transient species on flash photolysis,
under similar conditions as the parent arenediazonium salt.
The transient λ_{max} 420 nm had a half-life of 2.27 µs
($k_1 = 4.41 \times 10^{-5}$ s^{-1} for reaction with water) which is

somewhat shorter than that observed by Becker et al.[125] of
16.7 μs. Our value is probably more accurate since many
of the half-lives determined by Becker[125] approach the
duration of his exciting light pulse. The precise nature
of the transient is unknown but it is likely to be one of
the three structures given below:-
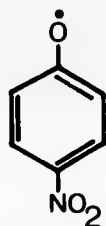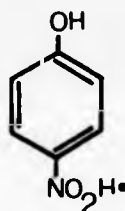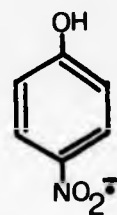
(LXXXVI)   (LXXXVII)   (LXXXVIII)

all of which absorb in the 400-450 nm region. This view is
supported by the observation that flash photolysis of
acidified 4-nitrophenol does not give any detectable transient
absorption, probably because little exists in the photo-
sensitive anionic form at low pH.

Obviously these preliminary findings cast serious doubt
on the credability of the assignments reported by Becker
et al.[125] for substituted aryl cations. It appears that all
his data may well refer to phenoxyl radicals, and in a private
communication Becker[155] has agreed with our assignment of
his transitions

CHAPTER VIII

CONCLUDING REMARKS

8.1. CONCLUDING REMARKS

One of the most widespread reprographic methods (excluding silver halide processes) is that based on arenediazonium salts sensitised to ultra-violet light. During the past fifty years 'diazo' type reprographic papers have been used for duplicating engineering/ architectural drawings and routine office copying.

This research was undertaken in conjunction with Ozalid U.K. Ltd to re-examine some of the shortcomings associated with 'diazo' type reprographic papers, namely background discolouration, fading and the deterioration of dyeline prints with ageing. Additionally, speed improvement, either by amplification or dye-sensitizing the photodecomposition of arenediazonium salt was considered. Obviously before these problems can be solved detailed knowledge of both the mechanisms involved in photodecomposition and formation of subsequent products, is required.

An initial literature search revealed few fundamental studies concerned with the photochemisty of arenediazonium salts. The ultimate object of this investigation has been to rectify this situation.

Contributions from quinoidal forms of arenediazonium salts (in their ground state) are frequently proposed when the properties of para-N,N-dialkyl derivatives are being examined. Nesterova et al.[133,134] have attempted to determine the importance of quinoidal forms to the ground state of these salts by X-ray crystallography. Their level

of refinement was rather low and hence inconclusive. In this work, a considerably superior structure for a para-N,N-dialkyl salt is presented. Bond lengths and angles in the structure strongly suggest that these salts should be represented as a resonant hybrid with a large contribution from quinoidal forms. However semi-empirical calculations have failed to verify this conclusion, and recourse will have to be made to *ab initio* methods.

Quantum yields determined in aqueous acid confirm and complement those made by Schulte-Frohlinde,[65] implying that the values reported by Tsunoda and Yamaoko[64] should be treated with caution. Substitution of strong electron-releasing groups in the benzene ring have been observed to increase ϕ. Quantum yields determined in aqueous acid indicate that whilst substitution of additional electron releasing groups may increase thermal stability, any further enhancement of ϕ is not realised. It was hoped that quantum yield determinations in ethanol would give some insight into the photodecomposition of arenediazonium salts in non-aqueous media, e.g. coated on cellulose. However the situation proved to be considerably more complex than originally envisaged. Under selected conditions the dichotomy of the homo and hetero-cleavages of the C-N bond could be resolved, thus aeration and acidification favour heterolytic cleavage whilst deaeration and the absence of acid promotes homolytic cleavage and subsequent propagation of the short radical chain reaction.

Quantum yields determined in cellulose acetate films at room temperature showed a marked insensitivity to substitution into the benzene ring, i.e. $\rho = 0$, from which it may infer that photodecomposition occurs predominately via homolysis of the C-N bond.

Low-temperature esr studies of irradiated arenediazonium salts have been exceptionally rewarding. The existence of Ar^+ as a ground state triplet has been a subject of considerable debate for some time. Spectra presented in this thesis provided the first unequivoal evidence for the formation of Ar^+ in the photodecomposition of arenediazonium salts. Additionally the fourth line of the triplet spectra[156] has confirmed its observation. Additionally esr spectra[156] compatible with Ar^+ formation have been obtained from arenediazonium salts bearing solely methoxy groups, further complementing the results in this work and the findings of Pople et al.[92,93].

Attempts to record the ultra-violet spectra of Ar^+ were on the whole disappointing. Ultra-violet spectra of substituted phenyl radicals are virtually unknown and whilst our spectra are probably those of substituted phenyl radicals, an unambiguous assignment at this stage is not possible. Becker et al.[125] have reported the ultra-violet spectra of substituted aryl cations, but their assignment of the spectra is doubtful when the findings presented in this work are considered.

At present the only satisfactory method of increasing
the speed of 'diazo' type reprographic papers is by improved
matching of the electronic absorption bands of the arenediazonium
salts with the emission lines of mercury vapour lamps used to
effect photodecomposition. Although much of this work has
been of a fundamental nature it is hoped that we have laid
the foundations for future work directed towards the utilisation
of arenediazonium salts as a complete reprographic material as
in contact printing.

APPENDIX I

COMPUTER PROGRAM ACTINOMETRY

4.1. COMPUTER PROGRAM ACTINOMETRY

In a photochemically induced decay to give non-absorbing products, the kinetic decay is normally taken to be zero-order in that the number of molecules decomposing per second is strictly related to the number of quanta absorbed, which in turn is related to the incident intensity of the lamp.

$$\text{i.e.} \quad -\frac{\Delta A}{\Delta t} = k \quad s^{-1} \tag{a_1}$$

where A = absorbance at the irradiation wavelength, i.e.

$$A = \log_{10} I_o / I_t \tag{a_2}$$

As a typical photochemical reaction proceeds, I_t increases, (i.e. the compound is photochemically decomposed) and hence the values of k decrease accordingly; consequently only the initial points (when I_t is low) are used to determine $\Delta A/\Delta t$. If I_t increases, the ratio I_a/I_o decreases, hence

$$-\frac{\Delta A}{\Delta t} = k(I_a/I_o) \tag{a_3}$$

rearrangement of

$$A = \log_{10} I_o / (I_o - I_a)$$

gives

$$10^A = \frac{I_o}{I_o - I_a}$$

i.e. $\qquad 10^{-A} = (I_o - I_a)/I_o = 1 - (I_a/I_o)$

i.e. $\qquad I_a/I_o = (1 - 10^{-A})$

Substituting into (a_3)

$$- \frac{dA}{dt} = k(1 - 10^{-A})$$

The computer program 'Actinometry' calculates 'instantaneous' values of k for a series of pairs of data points for A and t, allowing for the increase in transmitted light as photodecomposition proceeds. It then averages the values of k and recalculates a set of A's for each value of t, drawing a smooth curve (Fig. A1).

The kinetic equations leading to the program are as follows:

$$- \frac{dA}{dt} = k(1 - 10^{-A})$$

if $y = t$ and $x = A$

$$- \frac{dx}{(1-10^{-x})} = k \, dy$$

$$y = - \frac{1}{k} \int \frac{dx}{1-10^{-x}} + c$$

Figure A_1 Computer simulation using Actinometry
program of the photochemical decay of
an arenediazonium salt.
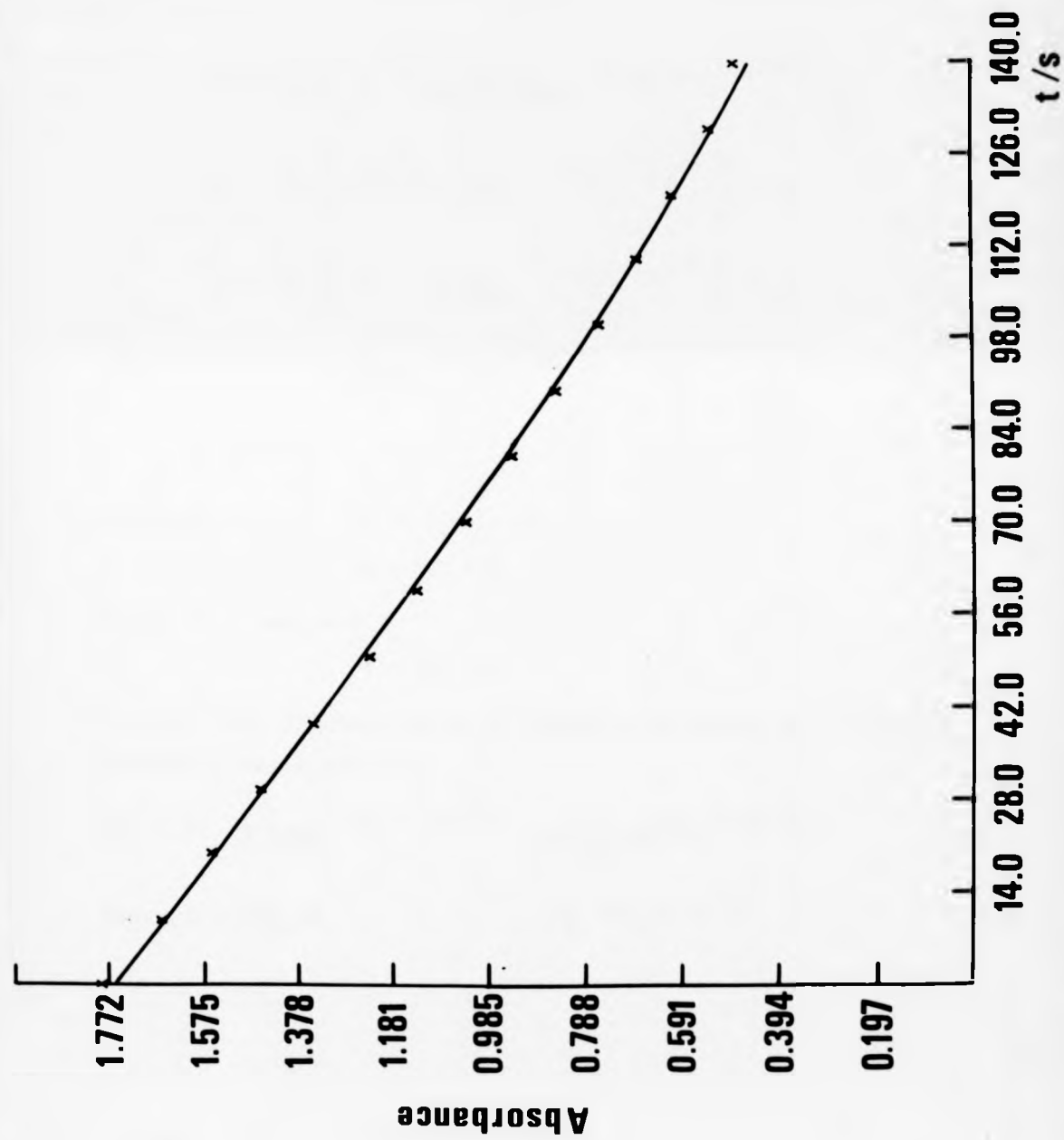
From the standard integral $\dfrac{dx}{a+be^{px}} = \dfrac{x}{a} - \dfrac{1}{ap} \log_e(a+be^{px})$

$$y = - \frac{1}{k} \left[\frac{x}{1} - \frac{1}{1.(-2.3026)} \log_e(1-e^{-2.3026x}) \right] + c$$

$$y = \frac{1}{k} \left[x + \frac{1}{2.3026} \log_e(1-10^{-x}) \right] + c$$

$$t = - \frac{1}{k} \left[A + \frac{1}{2.3026} \log_e(1-10^{-A}) \right] + c$$

Let $Y = A + \dfrac{1}{2.3026} \log_e(1-10^{-A})$

$t = \dfrac{1}{k}[Y] + c$

Multiply by k: $kt = -[Y] + kc$

$kc - kt = Y$

If $ck = c'$ and $-k = m$

$$Y = mt + c'$$

Now all that is required is to estimate Y, using least squares estimates for m and c'

Now $Y = \dfrac{1}{2.3026} \log_e(1-10^{-A}) \equiv \dfrac{1}{\log_e 10} \log_e(1-10^{-A})$

Where $L = \log_e 10$ $\equiv \dfrac{1}{L} \log_e(1-10^{-A})$

Now $\qquad 10^{-A} = \text{Exp}[\log_e(10^{-A})]$

$$= \text{Exp}[-A \log_e 10]$$

$$= \text{Exp}[-AL]$$

Therefore $\qquad Y = A + \log_e[1 - \text{Exp}(-AL)]/L$

which may be rearranged to

$$A = \log(e^{LY} + 1)/L$$

Hence our values of Y from the linear least squares regression can now be used to calculate values of A, and we can obtain our best estimate of k.

A listing of the computer program is as follows:

```
ACTINOMETRY;
"BEGIN"
"INTEGER"N;
"READ"N;
"PRINT"`` `P`ACTINOMETRY`L2``;
  "BEGIN"
  "REAL"A,B,C,D,F,G,H,K,L,M,P,DM,DC,DDY;
"REAL"LARGEA;
  "INTEGER"I;
"ARRAY"X,Y,AA,V,W[1:N];
  L:=LN(10);
LARGEA:=0;
  "FOR"I:=1"STEP"1"UNTIL"N"DO"
   "BEGIN"
"READ"X[I],AA[I];
"IF"AA[I]>LARGEA"THEN"LARGEA:=AA[I];
Y[I]:=AA[I]+LN(1-EXP(-AA[I]*L))/L;
  W[I]:=1/(Y[I]*Y[I]);
W[I]:=1;
   "END";
L1:
  A:=B:=D:=C:=G:=H:=0;
  "FOR"I:=1"STEP"1"UNTIL"N"DO"
   "BEGIN"
   H:=H+W[I];
   A:=A+W[I]*X[I];
   B:=B+W[I]*X[I]*Y[I];
   D:=D+W[I]*Y[I];
   F:=F+W[I]*X[I]*X[I];
   "END";
  P:=H*F-A*A;
  M:=(H*B-A*D)/P;
  C:=(F*D-A*B)/P;
  "FOR"I:=1"STEP"1"UNTIL"N"DO"
   "BEGIN"
   K:=M*X[I]+C-Y[I];
   K:=K*K;
   G:=G+W[I]*K;
   "END";
  DDY:=SQRT(G/(N-2));
  DM:=DDY*SQRT(H/P);
  DC:=DDY*SQRT(F/P);
  "PRINT"``S4`SLOPE = `,SAMELINE,FREEPOINT(4),M,``S10``,`ESD(SLOPE) = `,
  DM,``L2``;
  "PRINT"` INTERCEPT = `,SAMELINE,FREEPOINT(4),C,``S6``,
  `ESD(INTERCEPT) = `,DC,``L5``;
  "PRINT"`COMPARISON OF OBSERVED AND CALCULATED ABSORBANCES`L4``;
  "PRINT"``TIME     OBSERVED     CALCULATED      ABSORBANCE`L``;
  "PRINT"``S8`ABSORBANCE    ABSORBANCE      DIFFERENCE`L2``;
  "FOR"I:=1"STEP"1"UNTIL"N"DO"
```

```
    "BEGIN"
   K:=M*X[I]+C;
   K:=EXP(K*L)+1;
   V[I]:=LN(K)/L;
    "PRINT"FREEPOINT(4),X[I],SAMELINE,``S3``,AA[I],``S7``,V[I],SCALED(4),
``S7``,AA[I]-V[I],``L``;
    "END";
  PUNCH(5);
 WAY(0,0);
  SETORIGIN(0,0);
  MOVEPEN(0,600);
  SETORIGIN(600,0);
 MOVEPEN(0,0);DRAWLINE(0,2000);DRAWLINE(2000,2000);
 DRAWLINE(2000,0);DRAWLINE(0,0);MOVEPEN(0,0);
  "FOR"I:=1"STEP"1"UNTIL"10"DO"
   "BEGIN"
   MOVEPEN(200*I,50);
   DRAWLINE(200*I,0);MOVEPEN(200*I,2000);DRAWLINE(200*I,1950);
   MOVEPEN(50,200*I);
   DRAWLINE(0,200*I);MOVEPEN(2000,200*I);DRAWLINE(1950,200*I);
   "END";
  "BEGIN"
  "REAL"XS,YS,T,YY;
 YS:=LARGEA*1.1;
 YS:=2000/YS;
  XS:=ABS(X[N]-X[1]);
  XS:=XS/2000;MOVEPEN(0,XS*LN(EXP(C*L)+1)/L);
  "FOR"I:=1"STEP"1"UNTIL"2000"DO"
   "BEGIN"T:=I*XS;
   YY:=M*T+C;
   YY:=EXP(YY*L)+1;
   YY:=LN(YY)/L;YY:=YY*YS;
 DRAWLINE(T/XS,YY);
   "END";
  "FOR"I:=1"STEP"1"UNTIL"N"DO"
   "BEGIN"
 MOVEPEN(X[I]/XS,AA[I]*YS);
   CENCHARACTER(9);
   "END";
   "FOR"I:=1"STEP"1"UNTIL"9"DO"
   "BEGIN"
   MOVEPEN(-160,200*I);
   "PRINT"WAY(0,5),ALIGNED(1,3),200*I/YS;
   MOVEPEN(-75+I*200,-75);
   "PRINT"WAY(0,5),ALIGNED(3,3),200*I*XS;
   "END";
  MOVEPEN(-175,1200);
  "PRINT"WAY(1,5),`ABSORBANCE`;
  MOVEPEN(1200,-150);
  "PRINT"WAY(0,5),`TIME`;
  MOVEPEN(700,2200);
  "PRINT"WAY(0,7),`ACTINOMETRY`;
  MOVEPEN(0,0);
  "END";
 "COMMENT"INPUTS AS FOLLOWS: N(NUMBER OF OBSERVATIONS),
 TIME[1],ABSORBANCE[1],...TIME[N],ABSORBANCE[N];
  MOVEPEN(0,2500)
  "END";
 "END"OF PROGRAM;
```

APPENDIX II

ANALYSIS OF ESR TRIPLET STATE SPECTRA

A2 ANALYSIS OF ESR TRIPLET STATE SPECTRA

The complete Hamiltonian of a free atom which represents
the total energy of the system may be considered as the sum
of all the energy contributions

$$H = H_1 + H_2 + H_3 + H_4 + H_5 + H_6 + H_7 + H_8 \qquad (a_4)$$

H_1 which represents that part of the Hamiltonian which is
spin independent and is usually the most dominant term. H_5
represents small terms involving magnetic interactions between
electrons and H_8 is the term responsible for the diamagnetism.
Hence a spin Hamiltonian may be written as the sum of the
remaining terms,

$$H_5 = H_2 + H_3 + H_4 + H_6 + H_7 \qquad (a_5)$$

H_2 is that part of the potential energy which arises from
the electrostatic field of neighbouring atoms and is
frequently termed the crystal field.

H_3 refers to spin orbit coupling i.e. the interaction of
orbital angular momentum with electron spin.

H_4 the Zeeman term and is mainly responsible for the
paramagnetism.

H_6 is the term for interaction with nuclear spins and
arises from two causes, magnetic interaction with
the magnetic moment of the nucleus and secondly
electrostatic interaction with the electric
quadrupole moment of the nucleus.

H_7 is the nuclear contribution which is very small and
may be considered negligible.

A2 ANALYSIS OF ESR TRIPLET STATE SPECTRA

The complete Hamiltonian of a free atom which represents
the total energy of the system may be considered as the sum
of all the energy contributions

$$H = H_1 + H_2 + H_3 + H_4 + H_5 + H_6 + H_7 + H_8 \qquad (a_4)$$

H_1 which represents that part of the Hamiltonian which is
spin independent and is usually the most dominant term. H_5
represents small terms involving magnetic interactions between
electrons and H_8 is the term responsible for the diamagnetism.
Hence a spin Hamiltonian may be written as the sum of the
remaining terms,

$$H_5 = H_2 + H_3 + H_4 + H_6 + H_7 \qquad (a_5)$$

H_2 is that part of the potential energy which arises from
the electrostatic field of neighbouring atoms and is
frequently termed the crystal field.

H_3 refers to spin orbit coupling i.e. the interaction of
orbital angular momentum with electron spin.

H_4 the Zeeman term and is mainly responsible for the
paramagnetism.

H_6 is the term for interaction with nuclear spins and
arises from two causes, magnetic interaction with
the magnetic moment of the nucleus and secondly
electrostatic interaction with the electric
quadrupole moment of the nucleus.

H_7 is the nuclear contribution which is very small and
may be considered negligible.

The EPR spin Hamiltonian for a principal axis system can be written as

$$Hs = \beta(g_x S_x H_x + g_y S_y H_y + g_z S_z H_z) + D'S_z^2 + E'S_x^2 + F'S_y^2 \qquad (a_6)$$

by writing

$$E'S_x^2 + F'S_y^2 = \tfrac{1}{2}(E'+F')(S_x^2+S_y^2) + \tfrac{1}{2}(E'+F')(S_x^2-X_y^2) \qquad (a_7)$$

and using the relationship

$$S_x^2 + S_y^2 + S_z^2 = S(S+1) \qquad (a_8)$$

Upon substituting

$$E = \tfrac{1}{2}(E' + F') \qquad (a_9)$$

$$\text{and}$$

$$D = D' - \tfrac{1}{2}(E' + F') \qquad (a_{10})$$

and subtracting the constant term

$$[(\tfrac{1}{3})D + \tfrac{1}{2}(E' + F')]S(S+1) \qquad (a_{11})$$

We may write

$$Hs = \beta(g_x S_x H_x + g_y S_y H_y + g_z S_z H_z) + D(S_z^2 - \tfrac{1}{3}S[S+1]) + E(S_x^2 - S_y^2) \qquad (a_{12})$$

If the axis of quantization is z and H is parallel to z and S = 1 then we may write

$$Hs = g_z \beta H_z + D[S_z^2 - \tfrac{1}{3}S(S+1)] + E(S_x^2 - S_y^2) \qquad (a_{13})$$

In the case axial symmetry i.e. when X, Y directions are equivalent E = O and

$$g_x = g_y = g \qquad \qquad g_z = g$$

a_6 may be reduced to

$$Hs = \beta[g \quad SzHz + g \quad (SxHx + SyHy) + D(Sz^2 - \tfrac{1}{3}S(S+1)] \qquad (a_{14})$$

we may write

$$Hs = gz\beta HSz + D[Sz^2 - \tfrac{1}{3}S(S+1)] \qquad (a_{15})$$

Since the eigenvalues ε satisfy

$$H\psi = \varepsilon\psi \qquad (a_{16})$$

therefore

$$(H - \varepsilon I)\psi = 0 \qquad (a_{17})$$

where I is the identity operator

Hence solving a_{14} for the energy levels

$$| \quad \rangle, \quad \tfrac{1}{3} \quad D + (gz^2\beta^2 Hz^2 + E^2)^{\tfrac{1}{2}}$$

$$| 0 \rangle, \quad -\tfrac{2}{3} \quad D$$

$$|-1 \rangle, \quad \tfrac{1}{3} \quad D - (gz^2\beta^2 Hz^2 + E^2)^{\tfrac{1}{2}}$$

In zero magnetic field the levels are

$$| 1 \rangle, \quad \tfrac{1}{3} \quad D + E$$

$$| 0 \rangle, \quad -\tfrac{2}{3} \quad D$$

$$|-1 \rangle, \quad \tfrac{1}{3} \quad D - E$$

The energies of the three states as a function of the magnetic field for H parallel z are shown in (Fig. A2).

Figure A_2

Esr D and E parameters of a ground state
triplet at zero field.

$$|+1\rangle \quad \tfrac{1}{3}D+(g_z^2\beta^2H_z^2+E^2)^{\tfrac{1}{2}}$$

$$|0\rangle$$

$$|-1\rangle \quad \tfrac{1}{3}D-(g_z^2\beta^2H_z^2+E^2)^{\tfrac{1}{2}}$$

x

y

z

2E

$\tfrac{1}{3}D+E$

$\tfrac{1}{3}D-E$

$-\tfrac{2}{3}D$

FIELD

ENERGY
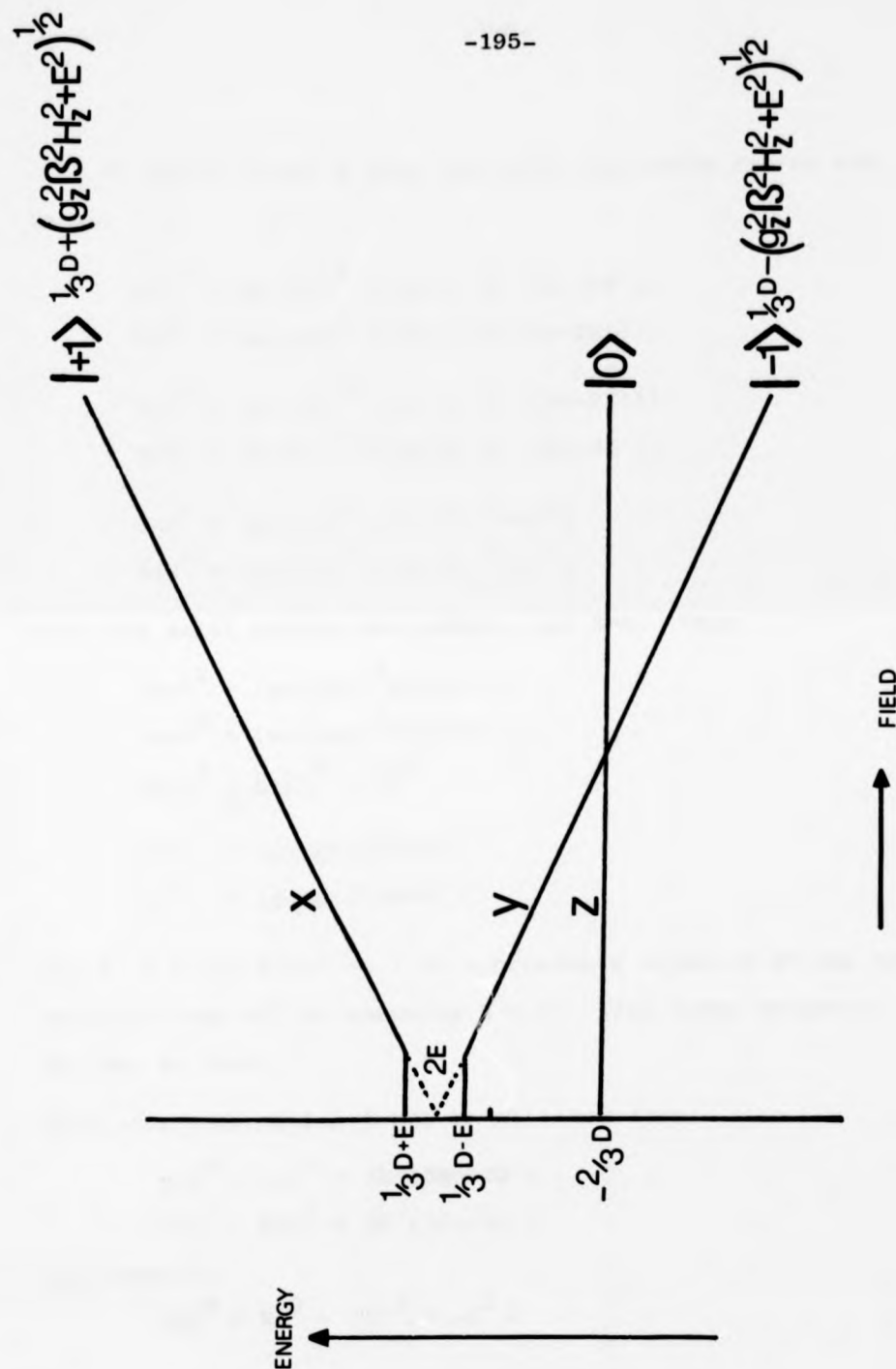
To obtain D and E when the axial resonance fields are known.

$$Hx1^2 = (ge/gx)^2 [(Ho-D'+E')(Ho+2E')]$$
$$Hx2^2 = (ge/gx)^2 [(Ho+D'-E)/Ho-2E')]$$
$$(a_{18})$$

$$Hy1^2 = (ge/gy)^2 [(Ho-D'-E')(Ho-2E')]$$
$$Hy2^2 = (ge/gy)^2 [(Ho+D'+E')/Ho+2E')]$$
$$(a_{19})$$

$$Hz1^2 = (ge/gz)^2 [(Ho-D')^2-E'^2]$$
$$Hz2^2 = (ge/gz)^2 [(Ho+D')^2-E'^2]$$
$$(a_{20})$$

With the axial fields determined, and E=O. Then

$$Hxy1^2 = (ge/gxy)^2 Ho(Ho-D')$$
$$Hxy2^2 = (ge/gxy)^2 Ho(Ho+D')$$
$$(a_{21})$$

$$\frac{Hxy2^2 - Hxy1^2}{Ho} = 2D'$$
$$(a_{22})$$

$$Hz1 = (ge/gz)(Ho-D')$$
$$Hz^2 = (ge/gz)(Ho+D')$$
$$(a_{23})$$

For E' $\neq$ O and E'/D' $\ll$ 1 an approximate value of D' may be obtained from Hz^2 by assuming E = O. With lower accuracy Hz1 may be used.

With this information E may be obtained from

$$Hy2^2 - Hx2^2 = 2E'(3Ho+2D')$$
$$Hx1^2 - Hy2^2 = 2E'(3Ho-2D')$$
$$(a_{24})$$

Additionally

$$Hdq^2 = Ho^2 - (D'^2/3 -E^2)$$
$$(a_{25})$$

Figure A_3

Esr spectrum of 2,5-di-n-butoxy-4-morpholino
benzenediazonium tetrafluroborate at 77 K in
$LiCl-D_2O$
bottom
Chromium standard use to calibrate magnetic field

Magnetic field mT

a

b

Magnetic field   mT

100   200   300   400
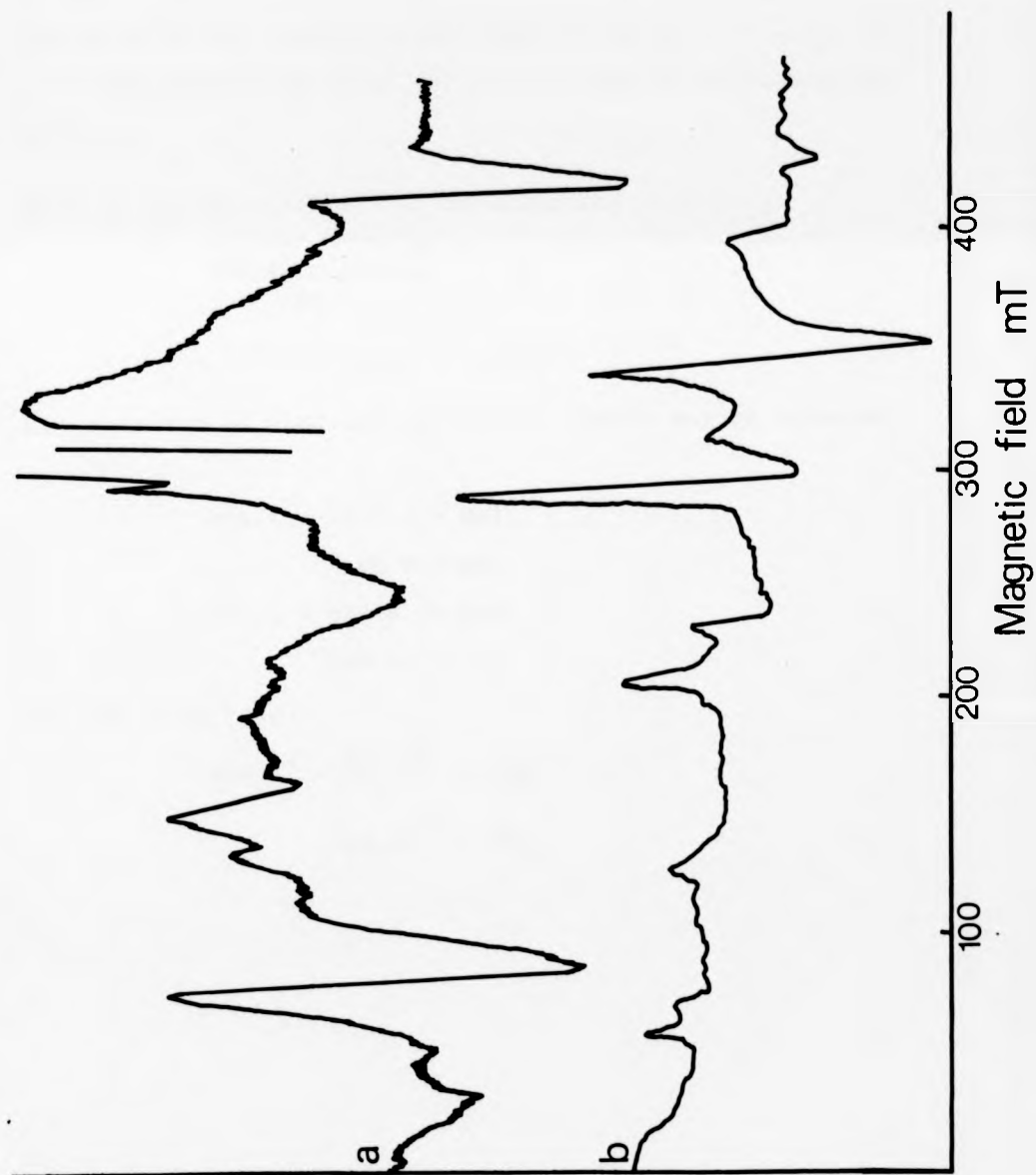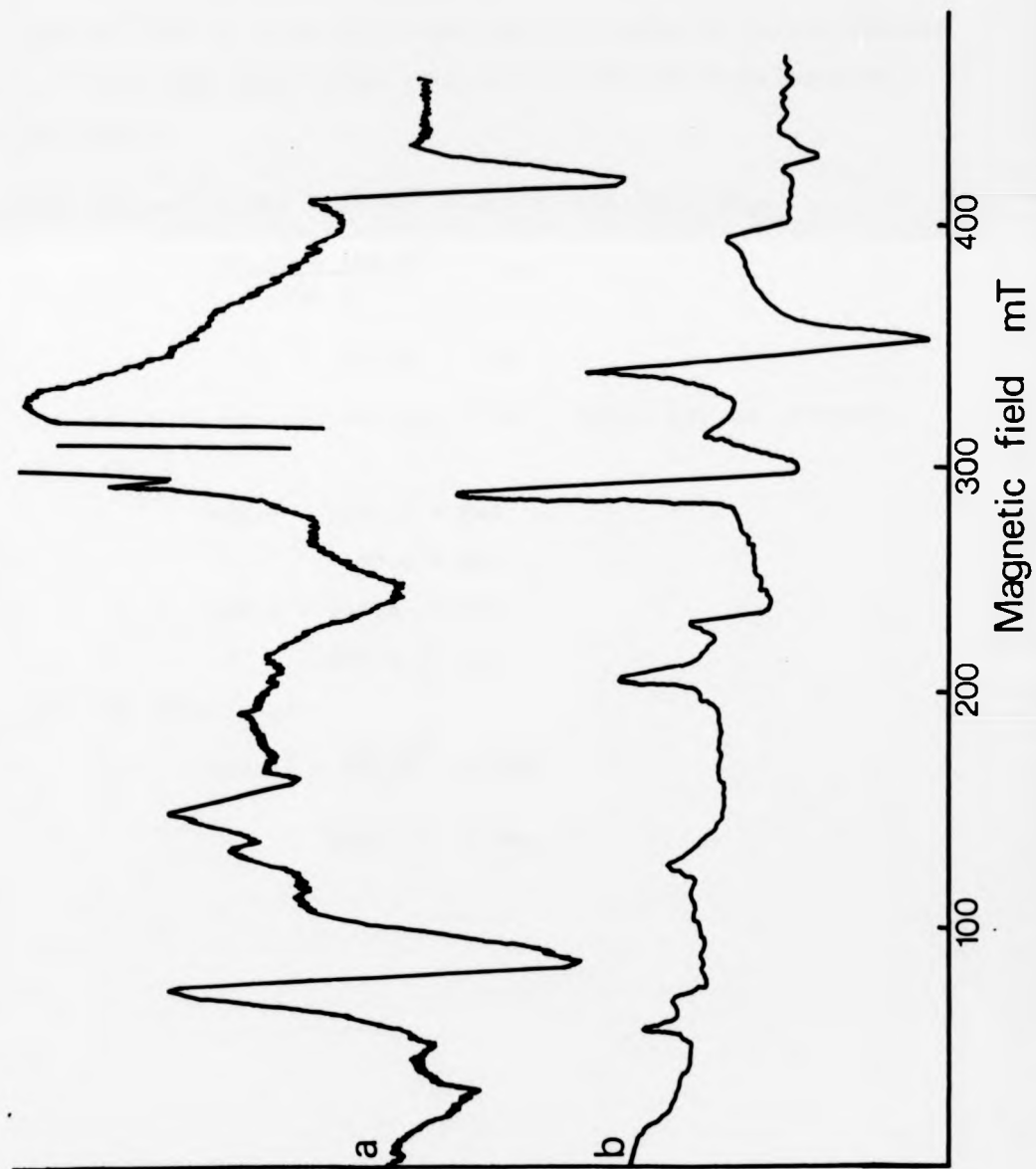
and

$$2D' = \frac{55640}{R^3} \qquad \text{(where R is given in } \overset{\text{o}}{A}) \qquad (a_{26})$$

D, for the aryl cation formed from photolysis of 2,5-di-n-butoxy-4-morpholinobenzenediazonium tetrafluoroborate in a LiCl-D_2O glass (Fig. A3) at 77 K may be calculated as follows:-

With Ho set at 328.1 mT and substituting into (a_{22})

$$\frac{425.9^2 - 159.7^2}{328.1} = 2D'$$

$$237.5 \quad = D'$$

and position of high and low field z lines may be obtained from (a_{23})

$$328.1 - 2375.5 = Hz1$$

$$90.6 = Hz1$$

$$328.1 + 237.5 = Hz2$$

$$565.5 = Hz2$$

and Hdq from (a_{25})

$$328.1^2 - \frac{237.5^2}{3} = Hdq$$

$$298.0 \quad = Hdq$$

The results are summarized below

Line	observed	calculated
$Hz1 + H_{min}$	83.2	90.6
$Hxy1 + \Delta M$	159.7	159.7
Hdq	298.8	290.0
Hy2	425.9	425.9
Hz 2	–	565.5

$D' = 237.5$ which gives 0.2219 cm^{-1}

REFERENCES

REFERENCES

1. P. Griess, Annalen, (1858), 106, 123.

2. R. M. Elofson, R.L. Edsberg and P.A. Mecherly, J. Electrochem Soc., (1950), 97, 166.

3. H. Zollinger and C. Wittwer, Helv. Chim. Acta., (1952), 35, 1209.

4. H. Zollinger, Helv. Chim. Acta., (1953), 36, 1730.

5. T. N. Polynova, N. G. Bokii and M. A. Porai-Koshits, J. Struct. Chem., (1965), 6, 841.

6. B. A. Porai-Koshits, Ross. Chem. Rev., (1970), 39, 283.

7. L. Klasinc and D. Schulte-Frohlinde, Z.Phys. Chem. (Frankfurt) (1968), 60, 1

8. C. Römming, Acta. Chem. Scand., (1963), 17, 1444.

9. E. S. Lewis and M. D. Johnson, J. Amer. Chem. Soc. (1959), 81, 2070.

10. A. E. Polansky and P. Schuster, Monatash., (1956), 96, 396

11. B. A. Porai-Koshits, Tetrahedron, (1960), 11, 30.

12. C. F. Goodeve and L. J. Wood, Proc. Royal Soc., (1938), A166, 342.

13. M. Aroney, R. J. W. LeFévre and R. L. Werner, J. Chem. Soc., (1955), p.276.

14. K. B. Whetsel, G. F. Hawkins and F. E. Johnson, J. Amer. Chem. Soc., (1956), 78, 3360.

15. K. Tabei and C. Ito, Bull. Chem. Soc. Japan., (1968), 41, 514.

16. M. Sukigara and S. Kitkuchi, Bull. Chem. Soc. Japan, (1967), 40, 1077.

17. L. A. Kazitsyna, O. A. Reutor and Z. F. Buchkovskii, Russ. J. Phys. Chem., (1960), 34, 404.

18. M. Sukigara and S. Kikuchi, Bull. Chem. Soc. Japan., (1967), 40, 461.

19. M. Sukigara and S. Kikuchi, Bull. Chem. Soc. Japan., (1967), 40, 1082.

20. E. M. Evleth and R. J. Cox, J. Phys. Chem., (1967), 71, 4082.

21. J. Kroupa, Chem. Listy., (1973), 67, 1035.

22. H. Böttcher, A. V. El'Cov and N. I. Ptiscev, J. Prakt. Chem., (1973), 315, 725.

23. R. J. Cox, P. Bushnell and E. M. Evleth. Tetrahedron letts., (1970), 3, 207.

24. L. C. Anderson and J. W. Steedly, J. Amer. Chem. Soc. (1954), 76, 5144.

25. A. I. Vogel, Practical organic chemistry, Longmans (1955).

26. A. F. Gremillion, H. B. Jonassen and R. J. O'Connor, J. Amer. Chem. Soc., (1959), 81, 6134.

27. W. A. Waters, J. Chem. Soc., (1937) p.113, p.2007, p.2014.

28. H. H. Hodgson, S. Birtwell and J. Walker, J. Chem. Soc. (1941), p.770.

29. H. H. Hodgson, J. Chem. Soc., (1948), p.348.

30. W. A. Waters, J. Chem., (1942), p.266.

31. D. F. DeTar and A. R. Ballentine, J. Amer. Chem. Soc., (1956), 78, 3916.

32. H. Pray, J. Phys. Chem., (1926), 30, 1417

33. J. S. P. Blumberg, Rec. Trav. Chem., (1930), 49, 259.

34. E. S. Lewis, L.D. Hartung and B. M. McKay, J. Amer. Chem. Soc., (1969), 91, 419.

35. N. Kamigata, M. Kobayshi and H. Minato, Bull. Chem. Soc. Japan., (1972), 45, 2047.

36. H. Hantzsch and E. Jochem. Chem. Ber., (1901), 35, 3337.

37. K. H. Saunders "The aromatic diazo-compounds and their technical applications" Edward Arnold and Co., (1936),(a)p.

38. W. A. Waters. Chem. Revs., (1937), 21, 169.

39. C. E. Waring and J. R. Abrams, J. Amer. Chem. Soc., (1941), 63, 2757.

40. D. F. DeTar and M. N. Toretzky, J. Amer. Chem. Soc., (1956), 78, 3925.

41. D. F. DeTar and M. N. Toretzky, J. Amer. Chem. Soc., (1956), 78, 3928.

42. D. F. DeTar and M. N. Toretzky, J. Amer. Chem. Soc., (1955), 77, 1745.

43. D. F. DeTar and T. Kosuge, J. Amer. Chem. Soc., (1958), 80, 6072.

44. M. L. Crossley, R. H. Kienle and C. H. Benbrook, J. Amer. Chem. Soc., (1940), 62, 1400

45. E. S. Lewis and E. B. Miller, J. Amer. Chem. Soc., (1953), 75, 429.

46. D. Schulte-Frohlinde and H. Blume, Z. Phys. Chem. (Frankfurt), (1968), 59, 299

47.　J. DeJonge, R. Dijkstra and P. B. Braun, Rec. Trav. Chim, (1949), 68, 430.

48.　R. O. C. Norman, "Principles of organic synthesis" Methuen, (1968), p.454.

49.　T. J. Broxton, J. F. Bunnett and C. H. Paik, J.C.S. Chem. Comm., (1970), p.1363.

50.　W. E. Lee, J. G. Calvert and E. M. Malmberg, J. Amer. Chem. Soc., (1961), 83, 1928.

51.　E. A. Boudreaux and E. Boulet, J. Amer. Chem. Soc., (1958), 80, 1588.

52.　M. D. Johnson, J. Chem. Soc., (1965), p.805.

53.　J. DeJonge and R. Dijkstra, Rec. Trav. Chim., (1948), 67, 328.

54.　O. Süs, Ann. Chem. (1953), 579,133.

55.　E. S. Lewis and D. J. Chalmers, J. Amer. Chem. Soc., (1971), 93, 3267.

56.　T. Yamase, T. I. Kawa, H. Kokado and E. Inoue, J. Photo. Sci. and Eng., (1973), 17, 28.

57.　T. Yamase, T. Somi, T. I. Kawa, H. Kokado and E. Inoue, J. Photo. Sci. and Eng., (1974), 18, 25.

58.　E. Inoue, H. Kokado, T. I. Kawa, T. Yamase and Y. Inoue, Bull. Chem. Soc. Japan., (1974), 47, 3181.

59.　E. S. Lewis, R. E. Holliday and L. D. Hartung, J. Amer. Chem. Soc., (1969), 91, 430.

60.　D. J. Brown, Chem. and Ind., (1944), April, p.146.

47. J. DeJonge, R. Dijkstra and P. B. Braun, Rec. Trav. Chim, (1949), 68, 430.

48. R. O. C. Norman, "Principles of organic synthesis" Methuen, (1968), p.454.

49. T. J. Broxton, J. F. Bunnett and C. H. Paik, J.C.S. Chem. Comm., (1970), p.1363.

50. W. E. Lee, J. G. Calvert and E. M. Malmberg, J. Amer. Chem. Soc., (1961), 83, 1928.

51. E. A. Boudreaux and E. Boulet, J. Amer. Chem. Soc., (1958), 80, 1588.

52. M. D. Johnson, J. Chem. Soc., (1965), p.805.

53. J. DeJonge and R. Dijkstra, Rec. Trav. Chim., (1948), 67, 328.

54. O. Süs, Ann. Chem. (1953), 579,133.

55. E. S. Lewis and D. J. Chalmers, J. Amer. Chem. Soc., (1971), 93, 3267.

56. T. Yamase, T. I. Kawa, H. Kokado and E. Inoue, J. Photo. Sci. and Eng., (1973), 17, 28.

57. T. Yamase, T. Somi, T. I. Kawa, H. Kokado and E. Inoue, J. Photo. Sci. and Eng., (1974), 18, 25.

58. E. Inoue, H. Kokado, T. I. Kawa, T. Yamase and Y. Inoue, Bull. Chem. Soc. Japan., (1974), 47, 3181.

59. E. S. Lewis, R. E. Holliday and L. D. Hartung, J. Amer. Chem. Soc., (1969), 91, 430.

60. D. J. Brown, Chem. and Ind., (1944), April, p.146.

47. J. DeJonge, R. Dijkstra and P. B. Braun, Rec. Trav. Chim, (1949), 68, 430.

48. R. O. C. Norman, "Principles of organic synthesis" Methuen, (1968), p.454.

49. T. J. Broxton, J. F. Bunnett and C. H. Paik, J.C.S. Chem. Comm., (1970), p.1363.

50. W. E. Lee, J. G. Calvert and E. M. Malmberg, J. Amer. Chem. Soc., (1961), 83, 1928.

51. E. A. Boudreaux and E. Boulet, J. Amer. Chem. Soc., (1958), 80, 1588.

52. M. D. Johnson, J. Chem. Soc., (1965), p.805.

53. J. DeJonge and R. Dijkstra, Rec. Trav. Chim., (1948), 67, 328.

54. O. Süs, Ann. Chem. (1953), 579,133.

55. E. S. Lewis and D. J. Chalmers, J. Amer. Chem. Soc., (1971), 93, 3267.

56. T. Yamase, T. I. Kawa, H. Kokado and E. Inoue, J. Photo. Sci. and Eng., (1973), 17, 28.

57. T. Yamase, T. Somi, T. I. Kawa, H. Kokado and E. Inoue, J. Photo. Sci. and Eng., (1974), 18, 25.

58. E. Inoue, H. Kokado, T. I. Kawa, T. Yamase and Y. Inoue, Bull. Chem. Soc. Japan., (1974), 47, 3181.

59. E. S. Lewis, R. E. Holliday and L. D. Hartung, J. Amer. Chem. Soc., (1969), 91, 430.

60. D. J. Brown, Chem. and Ind., (1944), April, p.146.

47. J. DeJonge, R. Dijkstra and P. B. Braun, Rec. Trav. Chim, (1949), 68, 430.

48. R. O. C. Norman, "Principles of organic synthesis" Methuen, (1968), p.454.

49. T. J. Broxton, J. F. Bunnett and C. H. Paik, J.C.S. Chem. Comm., (1970), p.1363.

50. W. E. Lee, J. G. Calvert and E. M. Malmberg, J. Amer. Chem. Soc., (1961), 83, 1928.

51. E. A. Boudreaux and E. Boulet, J. Amer. Chem. Soc., (1958), 80, 1588.

52. M. D. Johnson, J. Chem. Soc., (1965), p.805.

53. J. DeJonge and R. Dijkstra, Rec. Trav. Chim., (1948), 67, 328.

54. O. Süs, Ann. Chem. (1953), 579,133.

55. E. S. Lewis and D. J. Chalmers, J. Amer. Chem. Soc., (1971), 93, 3267.

56. T. Yamase, T. I. Kawa, H. Kokado and E. Inoue, J. Photo. Sci. and Eng., (1973), 17, 28.

57. T. Yamase, T. Somi, T. I. Kawa, H. Kokado and E. Inoue, J. Photo. Sci. and Eng., (1974), 18, 25.

58. E. Inoue, H. Kokado, T. I. Kawa, T. Yamase and Y. Inoue, Bull. Chem. Soc. Japan., (1974), 47, 3181.

59. E. S. Lewis, R. E. Holliday and L. D. Hartung, J. Amer. Chem. Soc., (1969), 91, 430.

60. D. J. Brown, Chem. and Ind., (1944), April, p.146.

61. P. Pinot de Moira, R. Lando and A. S. Tanebaum, J. Photo
     Sci., (1965), 13, 144.

62. P. Pinot de Moira, J. Photo. Sci., (1974), 22, 187.

63. T. Tsunoda and T. Yamaoko, Chiba Daigako Kogakubu Kenkyo
     Hokoko, (1968), 19, 129.

64. T. Tsunoda and T. Yamaoko, J. Soc. Sci. Photo. Japan,
     (1966), 29, 197.

65. D. Schulte-Frohlinde and H. Blume, Z. Phys. Chem. (Frankfurt)
     (1968), 59, 282.

66. R. Barraclough, F. Jones, D. Patterson and A. Tetlow,
     J. Soc. Dyers and Colourists, (1972), 88, 22.

67. E. S. Baltazzi, E. E. Dailey, P. Datta, H. Printy and
     W. J. Wagner, Photo. Sci. and Eng., (1974), 18, 123.

68. S. D. Ross, "Progress in Physical Organic Chemistry",
     Vol. I. Interscience, New York (1963).

69. J. H. Robson and G. F. Wright, Can. J. Chem., (1960), 38, 21.

70. L. L. Miller and A. K. Hoffmann, J. Amer. Chem. Soc., (1967),
     89 593.

71. R. W. Taft, J. Amer. Chem. Soc., (1961), 83, 3350.

72. R. A. Abramovitch and G. Tertzakian, Tetrahedron Lett.,
     (1963), p.1511.

73. R. A. Abramovitch and G. Tertzakian, Can. J. Chem., (1965),
     43, 940.

74. R. A. Abramovitch and J. G. Saha, Tetrahedron, (1965),
     21, (1965).

75. R. A. Abramovitch and J. G. Saha, Can. J. Chem., (1965), 43, 3269.

76. D. H. Hey, D. A. Shingleton and G. H. Williams. J. Chem. Soc., (1963), p.5612.

77. R. A. Abramovitch and F. Gadallah, J. Chem. Soc. (B), (1968), p.497.

78. R. W. Taft, I. R. Fox and I. C. Lewis, J. Amer. Chem. Soc., (1961), 83, 3349.

79. J. Hinze and J. H. Jaffe, J. Amer. Chem. Soc., (1962), 84, 540.

80. J. L. Beauchamp, Adv. Mass. Sepctrom., (1974), 6, 717.

81. E. S. Lewis and M. D. Johnson, J. Amer. Chem. Soc., (1960), 82, 5408.

82. E. S. Lewis and W. H. Hinds, J. Amer. Chem. Soc., (1952), 74, 304.

83. C. G. Swain, J. E. Sheats and K. G. Harbison, J. Amer. Chem. Soc., (1975), 97, 783.

84. W. D. Pfeifer, C. A. Bahn, P. R. Schleyer, S. Bocher, C. E. Harding, K. Hommell, M. Hancock and P.J. Stang, J. Amer. Chem. Soc., (1971), 93, 1513.

85. G. H. Williams, "Advances in free-radical chemistry", Vol. 2, Academic Press, London, (1967), p.116.

86. J. A. Pople, Acc. Chem. Res., (1970), p.217.

87. R. Gleiter, R. Hoffmann and W. D. Stohrer, Chem. Ber., (1972), 105, 8.

88. E. M. Evleth and P. M. Horowitz, J. Amer. Chem. Soc., (1971), 93, 5636.

89. C. G. Swain, J. E. Sheats, D. G. Gorensten and K.G. Harbison, J. Amer. Chem. Soc., (1975), 97, 791.

90. H. H. Jaffe and G. F. Koser, J. Org. Chem, (1975), 40, 3082.

91. J. D. Dill, P. R. Schleyer, J. S. Binkley, R. Seeger, J. A. Pople and E. Haselbach, J. Amer. Chem. Soc., (1976), 98, 5428.

92. J. D. Dill, P. R. Schleyer and J. A. Pople, Tetrahedron Letts, (1975), 33, 2857.

93. J. D. Dill, P. R. Schleyer and J. A. Pople, J. Amer. Chem. Soc., (1977), 99, 1.

94. J. E. Wertz and J. R. Bolton, "Electron Spin Resonance", McGraw-Hill, (1972).

95. P. B. Ayscough, "Electron Spin Resonance in Chemistry", Methuen, (1967).

96. D. J. E. Ingram, "Free Radicals as studied by Electron Spin Resonance", Butterworths, (1958).

97. S. H. Jarrett, G. J. Sloan and W. R. J. Vaughan, J. Chem. Phys., (1956), 25, 697.

98. C. A. Hutchinson and B. W. Mangum, J. Chem. Phys., (1958), 29, 952.

99. J. H. Van der Waals and M. S. de Groot, Mol. Phys., (1959), 2, 333.

100. H. H. Freedman, J. Amer. Chem. Soc., (1961), 83, 2195.

101. R. Breslow and H. Chang, J. Amer. Chem. Soc., (1961), 83, 3727.

102. R. Breslow and H. Chang, J. Amer. Chem. Soc., (1962), 84, 1484.

103. R. Breslow and H. Chang, J. Amer. Chem. Soc., (1963), 85, 2033.

104. R. Breslow, R. Hill and E. Wasserman, J. Amer. Chem. Soc., (1964), 86, 5349.

105. R. Breslow, R. Hill, H. Chang and E. Wasserman. J. Amer. Chem. Soc., (1967), 89, 1112.

106. M. Saunders, R. Breslow and E. Wasserman, J. Amer. Chem. Soc., (1973), 95, 3018.

107. E. Wasserman, L. Barash, A. Trozzolo and R.Murray, J. Amer. Chem. Soc., (1964), 86, 2304.

108. E. Wasserman and R. Murray, J. Amer. Chem. Soc., (1964), 86, 4203.

109. T. Tanei, Bull. Chem. Soc. Japan., (1967), 40, 2456.

110. S. Nagai, S. Ohnishi and I. Nitta, J. Phys. Chem., (1969), 73, 2438.

111. J. E. Bennett, B. Mile and A. Thomas, Chem. Comm., (1965), p.265.

112. H. Zemel and R. W. Fessenden, J. Phys. Chem., (1975), 79, 1419.

113. P. H. Kasai, P. A. Clark and E. B. Whipple, J. Amer. Chem. Soc., (1970), 92, 2640.

114. K. Morokuma, S. Ohnishi, T. Masoda and K. Fukui, Bull.
      Chem. Soc. Japan, (1963), 36, 1228.

115. J. E. Bennett and B. Mile, J. Phys. Chem., (1971),
      75, 3432.

116. J. E. Bennett, B. Mile and A. Thomas, Proc. Roy. Soc.
      (1966), A293, 246.

117. E. G. Janzen, Acc. Chem. Res., (1971), p.31.

118. T. Yamase, T.I.Kawa, H. Kokado and E. Inoue, Photo, Sci.
      and Eng., (1974), 18, 647.

119. R. J. Holman and M. J. Perkins, J. Chem. Soc.C., (1970),
      p.2195.

120. E. G. Janzen, D. E. Nutter and C. Anderson-Evans, J. Phys,
      Chem., (1975), 79, 1983.

121. B. Ashworth, B. C. Gilbert and R. O. C. Norman, J. Chem.
      Res., (1977), p.94.

122. P. J. Zandstra and E. M. Evleth, J. Amer. Chem. Soc.,
      (1964), 86, 2664.

123. G. Porter and B. Ward, Proc. Roy. Soc., (1965), A287, 457

124. B. Cercek and M. Kongshaug, J. Phys. Chem., (1970), 74, 4319

125. H. Böttcher, H. G. O. Becker, V.L. Ivanov and M. G. Kusmin,
      Chimia., (1973), 27, 437.

126. W. T. M. Andriessen, J. Mag. Res., (1976), 23, 339.

127. C. G. Hatchard and C. A. Parker, Proc. Roy. Soc., (1956),
      A235, 518.

128. Ozalid Ltd., Loughton, Essex, England.

129. E. Schering, Chem. Ber., (1891), 24, 3237.

130. H. H. Hodgson and J. Walker, J. Chem. Soc., (1935), p.530.

131. H. H. Hodgson and J. S. Wignal, J. Chem. Soc., (1927), p.2216.

132. T. C. W. Mak and J. Trotter, Acta. Cryst., (1965), 18, 68.

133. Ya. M. Nesterova, M. A. Porai-Koshits, A. V. Upadysheva and L. A. Kazitsyna, Zh. Strukt. Khim., (1966), 7, 129.

134. Ya. M. Nesterova and M. A. Porai-Koshits, Zh. Strukt. Khim., (1971), 12, 108.

135. M. M. Woolfson in, "Crystallographic Computing Techniques", Munksgaard, (1976).

136. J. M. Stewart, Technical Report TR-446, Computer Science Centre, University of Maryland, America.

137. J. Trotter, Acta. Cryst., (1959), 12, 884.

138. D. M. Hirst, Unpublished results, University of Warwick, Coventry, England.

139. E. S. Lewis and M. P. Hanson, J. Amer. Chem. Soc., (1967), 89, 6268.

140. H. C. Brown and Y. Okamato, J. Amer. Chem. Soc., (1958), 80, 4980.

141. M. F. Mizianty, E. A. Fitzgerald and G. H. Kimber, Photo. Sci. and Eng., (1971), 15, 331.

142. M. Breitenbach, K. H. Heckner and D. Jäkel, Z. phys. Chem., (Leipzig), (1970), 24, 377.

143. C. J. Heighway, J. E. Packer and R. K. Richardson, Tetrahedron Letts., (1974), $\underline{51}$, 4441.

144. P. R. Bryan and M. Walker, Chem. and Ind., (1974), December, p.948.

145. G. W. Gokel and D. J. Cram, J.C.S. Chem. Comm., (1973), p.481.

146. R. M. Izatt, J. D. Lamb, B.E. Rossiter, N. E. Izatt and J. Christensen, J.C.S. Chem. Comm., (1978), p.386.

147. B. L. Haymore, J. A. Ibers and D. W. Meek, Inorg. Chem., (1975), $\underline{14}$, 541.

148. R. A. Bartsch, H. Chen, N. F. Haddock and P. N. Juri, J. Amer. Chem. Soc., (1976), 98,6753.

149. R. A. Bartsch, N. F. Haddock and D. W. McCann, Tetrahedron Letts., (1977), $\underline{43}$, 3779.

150. H. K. Frensdorff, J. Amer. Chem. Soc. (1971), $\underline{93}$, 600.

151. Y. Ogiwara, N. Hon and H. Kubota, J. Applied Poly. Sci. (1974), $\underline{18}$, 2057.

152. M. C. R. Symons, Private communication, University of Leicester, Leicestershire, England.

153. E. Wasserman, L. C. Snyder and W. A. Yager, J. Chem. Phys., (1964), $\underline{41}$, 1763.

154. F. Barigelletti, G. Poggi and A. Breccia. J.C.S. Faraday Trans II (1974), $\underline{70}$, 1198.

155. H. G. Becker, private communication, Technisce Hochschule, Leuna-Merseburg, West Germany.

156. T.J. Kemp, Unpublished results, University of Warwick, England.